SYNTHESIS OF BRANCH-GUIDE DIRECTIONAL COUPLERS AND FILTER PROTOTYPES

by

L.F. LIND

A thesis presented for the degree of Doctor of Philosophy at the University of Leeds

September 1968

Acknowledgments

The author wishes to express his gratitude to Dr. R. Levy for his continual and experienced guidance, to Dr. J. Scanlan for his much valued advice and to Professor G.W. Carter for the use of the facilities of the Electrical Engineering Department.

The author is also indebted to the Ministry of Technology which supported this research.

List of Contents

Chapter 1.

Introduction.

1.1 Object of the Thesis.

The object of this thesis is the solution of the following problems using the theories of lumped and distributed network synthesis:

(1) Synthesis of equally terminated, lumped and distributed filters containing an even number of elements.

(2) Synthesis of symmetrical and asymmetrical branch-guide directional couplers.

1.2 The Philosophy of Circuit Theory.

In the past twenty years, network synthesis has been well developed for networks containing lumped elements. More recently, network synthesis techniques have been devised for networks containing distributed elements.

Network synthesis is in itself a basic discipline which may be applied to a large variety of physical problems. It consists fundamentally of three aspects, e.g.

(1) Realizability criteria,

(2) Approximation,

(3) Synthesis.

The existence of realizability criteria means that network theory has been brought to a stage of development well ahead of many other subjects, since it enables one to tell in ad-

vance whether a problem possesses a solution physically obtainable using elements of specified form. It is extremely valuable to know in advance whether a problem or class of problems does or does not possess a solution because of fundamental limitations.

Once it is established that a solution to a problem exists, then it is usually possible to approximate to the ideal as closely as one pleases. This is the branch of circuit theory classified above as part (2). Once a suitable approximating function has been determined, then, provided it satisfies the criteria of physical realizability, the third part of circuit theory consists in synthesizing the approximation function exactly. A large variety of synthesis techniques have been developed for this purpose; in general each different technique leads to a different network structure.

1.3 Lumped and Distributed Network Theory.

In Chapter 2 the fundamentals of lumped element network synthesis which are necessary in the later chapters are discussed. The development is restricted to two-port ladder structures (which contain reciprocal, linear, passive, and time invariant elements), as the ladder structure is the only structure used for synthesis purposes in this thesis.

The properties of a positive real driving-point impedance and the associated bounded real voltage reflection

coefficient are described in detail. Then, through the development of the network transfer matrix, the concept of network insertion loss is introduced.

This leads naturally to the introduction of Darlington's insertion-loss synthesis technique, for which both the theory and a numerical example are presented.

An extension of the insertion loss definition of a two-port to an n-port is given next, through the use of the scattering matrix. Its properties of symmetry, existence, and the unitary condition (for a lossless network) are derived, these properties being useful when the scattering matrix of a directional coupler is examined.

The last section in chapter 2 discusses a phase-magnitude relationship of an analytic function, which is also used to advantage in the directional coupler work.

In chapter 3 it is shown how lumped element network theory is extended by Richards' transformation to apply to distributed networks. An additional two port circuit element, a length of transmission line (unit element) is introduced here which has no counterpart in lumped circuit theory.

The properties of a cascade of unit elements terminated at either end by resistors (a distributed filter) are discussed in the last section of this chapter.

1.4 The Synthesis of Equally Terminated, Low-Pass Filters of Even Order.

In the conventional synthesis of doubly terminated lumped and distributed filters, Chebyshev polynomials of the first kind are used when an equiripple insertion loss specification is desired. A shortcoming of using Chebyshev polynomials of even degree in this insertion loss specification is that they yield filters having an unequal resistance ratio in the case of low-pass filters.

A modified low-pass equiripple polynomial of even degree has been found independently by the author (and by others) with the desirable property that its value at the origin may be shifted to any level below its passband ripple level, including zero (the condition necessary for equally terminated designs). The properties of this polynomial are examined in chapter 4, and then it is used to synthesize lumped and distributed equally terminated filters. The standard Darlington synthesis technique is employed for this purpose.

A computer program was written to perform this synthesis. It was found that for the higher degree filters a conformal transformation was necessary in the synthesis to preserve numerical accuracy. Use of this mapping function for the distributed case represents original work in that the mapping has thus far been developed and used only for lumped element

synthesis. Tables of element values are presented for a wide range of input specifications. The tables were used in the design of a coaxial low-pass filter. The measured VSWR frequency performance was found to agree quite closely with the theoretical performance. In the final section of chapter 4, a proof showing that the modified polynomial is optimal (under suitable restrictions) is given.

1.5 Branch-Guide Directional Couplers.

At the beginning of chapter 5 the definition of a directional coupler is stated. Then, through the use of scattering matrix properties which were developed in chapter 2, properties of perfect and nearly perfect symmetric directional couplers are discussed. Also a description is given of the decomposition of a four port directional coupler into two related two-port networks, through the use of an even and odd mode analysis.

The discussion then becomes more specialized by considering only one type of directional coupler, the branch-guide directional coupler. A brief history of the development of symmetric branch-guide directional couplers is presented, and the shortcomings of these design theories are examined in detail.

It is at this point that the original work contained in this thesis on branch-guide directional couplers is introduced.

A new design theory is presented, which allows for symmetric as well as asymmetric couplers.

First the general form of the approximation function is found. Then two specification functions, the Butterworth and Chebyshev approximations, are presented, both of which possess the required form.

A description of the complete synthesis process (which uses the Darlington synthesis technique) is given next, and illustrated by a numerical example.

Tables for both Butterworth and Chebyshev symmetrical and asymmetrical couplers are presented which should cover most cases of practical interest.

The asymmetric directional coupler requires an unequal output to input resistance ratio. In this respect it also may be regarded as an impedance transformer. It represents a new structure which has not yet been described in the literature. It is found that for similar input specifications the asymmetric coupler has a larger bandwidth than the symmetric coupler.

Several designs resulting from the new synthesis technique for both Butterworth and Chebyshev symmetrical couplers have been constructed both in X-band waveguide and in stripline. The experimental and theoretical results are described, and it is found that there is quite close agreement between the two.

It is found that the new synthesis technique for symmetrical couplers gives superior results compared with previous approximate methods both for the Butterworth and Chebyshev cases. The design of couplers having a bandwidth greater than one octave appears to be feasible.

Chapter 2.

Lumped element Network Synthesis.

2.1 Properties of the Driving-Point Impedance.

Consider a network composed of elements which are lumped, linear, bilateral, time invariant, and passive. The types of elements which fit this description are resistors, capacitors, and coils (having both self and mutual inductance). Kirchoff's equilibrium equations for the m +1 node network, on a nodal basis, may be written as

$$
\begin{aligned}
y_{11} V_1 + y_{12} V_2 + \dots + y_{1m} V_m &= I_1 , \\
y_{21} V_1 + y_{22} V_2 + \dots + y_{2m} V_m &= I_2 , \\
&\;\;\vdots \\
y_{m1} V_1 + y_{m2} V_2 + \dots + y_{mm} V_m &= I_m ,
\end{aligned}
\qquad (2.1)
$$

where y_{ii} is the admittance between node i and the common (datum) node, with all other nodes joined to datum, y_{ik} is the admittance between nodes i and k, and I_k is the input (source) current to node k. To simplify matters, all of the current sources are assumed to have the same sinusoidal time variation $I_k = I_k e^{jwt}$. More complicated waveforms may be expressed as a Fourier series and the principle of Superposition is then applied to obtain the total result. From the postulates of linearity and time invariance it is seen that the V_k must also have this e^{jwt} time variation so that it cancels out on both sides of the equation.

The nodes for this network are chosen so that the admittance y_{ik} has the form

$$y_{ik} = \sigma_{ik} + jwC_{ik} + \frac{1}{jwL_{ik}} \quad . \tag{2.2}$$

Mutual inductances are avoided by replacing each coil pair containing mutual inductance by a three-coil potentially equivalent Pi or T network.

Now it is convenient to introduce the generalized complex variable s defined by

$$s = \sigma + jw, \tag{2.3}$$

where σ and w are real variables. This complex variable s is the same as the Laplace transform variable s,

$$\text{i.e.} \quad L\left(f(t)\right) = F(s) \equiv \int_0^\infty f(t)e^{-st}\,dt, \tag{2.4}$$

where F(s) is the complex frequency transform of the time waveform f(t). This f(t) is assumed to have zero value for $t < o$.

Substituting (2.3) into (2.2), y_{ik} may be written as

$$y_{ik} = \sigma_{ik} + sC_{ik} + \frac{1}{sL_{ik}} \quad . \tag{2.5}$$

This apparently simple step is of great importance, since now y_{ik} is a real function of the complex variable s. Furthermore, it may be shown that y_{ik} and indeed any rational function R(s) is an analytic function of s (satisfies the Cauchy-Riemann equations) over the entire s-plane, excepting the points at which R(s) becomes infinite in value(commonly referred to as the poles of R(s)). Analytic function theory has been developed into a powerful mathematical tool, and certain results from this

theory will be used in the following work.

One immediate application of analytic function theory results from the uniqueness theorem, which states that two analytic functions which have identical values on an arbitrary finite line segment in the complex plane must have identical values over their entire region of analyticity (for rational functions, over the finite complex plane, excepting the pole points, of course) and thus be identical. This theorem leads to the principle of analytic continuation. In Eq.(2.2) y_{ik} is defined on the imaginary axis of the s-plane. By using the above theorem, it is seen that y_{ik} may now be defined uniquely over the entire finite s-plane (Eq.(2.5)) by a knowledge of its values on the imaginary axis, ie. $y_{ik}(jw)$ has been analytically continued into the s-plane.

In Eq.(2.1) all of the y_{ik} are now assumed to be functions of s. This equation may be solved for the voltages by using standard determinant methods to yield

$$\begin{aligned} V_1 &= \frac{\Delta_{11}}{\Delta} I_1 \quad \frac{\Delta_{21}}{\Delta} I_2 \quad \cdots \quad \frac{\Delta_{m1}}{\Delta} I_m \ , \\ V_2 &= \frac{\Delta_{12}}{\Delta} I_1 \quad \frac{\Delta_{22}}{\Delta} I_2 \quad \cdots \quad \frac{\Delta_{m2}}{\Delta} I_m \ , \\ &\text{----------} \\ V_m &= \frac{\Delta_{1m}}{\Delta} I_1 \quad \frac{\Delta_{2m}}{\Delta} I_2 \quad \cdots \quad \frac{\Delta_{mm}}{\Delta} I_m \ , \end{aligned} \tag{2.6}$$

where Δ is the determinant of the y matrix in Eq.(2.1) and Δ_{jk} is the corresponding cofactor of this determinant.

Now the open-circuit driving-point impedance for the first part of this network may be defined as

$$z_{11} \equiv \left. \frac{V_1}{I_1} \right| I_2 = I_3 = \ldots = I_m = 0 \ . \tag{2.7}$$

From Eq.(2.6) it is seen that

$$z_{11} = \frac{\Delta_{11}}{\Delta} \ , \tag{2.8}$$

where Δ_{11} and Δ are rational functions of s, and each consists of sums of products of the basic admittances given by Eq.(2.5). Thus z_{11} will have the form

$$z_{11} = \frac{a_o s^n + a_1 s^{n-1} + \ldots + a_n}{b_o s^d + b_1 s^{d-1} + \ldots + b_n} = \frac{N(s)}{D(s)} \ , \tag{2.9}$$

in which all of the a_i and b_i are real numbers.

The fundamental theorem of algebra states that a polynomial of degree n will have n (generally complex) roots. Since the a_i and b_i are real, any complex roots of N(s) or D(s) in Eq.(2.9) must occur in conjugate pairs.

Assuming that the network is initially quiescent, a unit impulse of current is now suddenly applied at the first port at t = o. The Laplace transform of this current is given by Eq.(2.4) as

$$I_1(s) = \int_0^\infty f(t) e^{-st} \, dt = 1. \tag{2.10}$$

Substituting this current into Eq.(2.7),

$$z_{11}(s) = V_1(s), \tag{2.11}$$

and hence,

$$V_1(t) = L^{-1}\left(z_{11}(s)\right) \quad . \tag{2.12}$$

Expanding Eq.(2.9) into partial fraction form gives

$$z_{11}(s) = \sum_{k=1}^{p} \frac{Ak}{s-s_k} + \sum_{k=1}^{a} \frac{Bk}{s^k} + \sum_{j=1}^{b_1} \sum_{k=2}^{b_2} \frac{C_{jk}}{(s-s_j)^k} . \tag{2.13}$$

By the use of standard inverse Laplace transforms, $V_1(t)$ is obtained from Eqs. (2.12) and (2.13) as

$$V_1(t) = \sum_{k=1}^{p} A_k e^{s_k t} + \sum_{k=1}^{a} \frac{B_k t^{k-1}}{(k-1)!} + \sum_{j=1}^{b_1} \sum_{k=2}^{b_2} \frac{C_{jk}}{(k-1)!} t^{k-1} e^{s_j t}. \tag{2.14}$$

Since the network is assumed not to contain any energy sources, $V_1(t)$ can only have a damped exponential or damped oscillatory exponential response, or, in extreme cases, have a steady d.c. or oscillatory response. Term by term inspection of Eq.(2.14) yields the conditions necessary for this sort of response:

1) If the pole is simple, its real part cannot be greater than zero.
2) A pole at the origin must be a simple pole.
3) If the pole is of multiple order, its real part is less than zero.

An analogous analysis may now be done for the short-circuit driving-point admittance $Y_{11}(s)$, whose poles are the zeros of $Z_{11}(s)$, and the same set of conditions are found to hold.

In conclusion, a necessary condition for S_σ to be a zero or pole of $Z_{11}(s)$ is that its real part is negative, or may be zero if the zero or pole is simple. In terms of the complex s-plane, the poles and zeros of $Z_{11}(s)$ are in the left half s-plane, and, if on the imaginary axis, must be simple. As it turns out, this is a necessary but not sufficient requirement if $Z_{11}(s)$ is to represent the open-circuit driving-point impedance of a passive network.

Intuitively, it is also known that

$$\text{Re}\left(Z_{11}(s)\right)_{s=jw} \geq 0 \quad \text{for } -\infty \leq w \leq \infty, \tag{2.15}$$

where Re stands for "the real part of".

If the real part of Z_{11} were negative at some frequency, it would imply that energy could be extracted from the passive network at that frequency, which is impossible (assuming the network is initially quiescent).

Now Z_{11} does not possess any poles in the right half s-plane, and thus is analytic (satisfies the Cauchy-Riemann equations) there. An important result from analytic function theory states that if a function is analytic over a region R of the complex plane and does not have a zero in R, its real part attains both its minimum and maximum value over R on the boundary of R. By using this result and Eq. (2.15), it follows that

$$\text{Re}\left(Z_{11}(s)\right) \geq 0, \quad \text{Re}\,(s) \geq 0\,. \tag{2.16}$$

A function which satisfies this condition is known as a positive function. It has also been shown that $Z_{11}(s)$ possesses real coefficients, such that when s is real $Z_{11}(s)$ is also purely real. This type of function is known as a real function. A function that possesses both of these properties is known as a positive real (p.r.) function. Thus it is necessary for $Z_{11}(s)$ to be a p.r. function. It can also be shown that the p.r. condition is sufficient for $Z_{11}(s)$ to represent the open-circuit driving-point impedance for a passive network. This fact is shown through the development of a general network realization technique (1), which has as its starting point a p.r. $Z_{11}(s)$.

2.2 The Voltage Reflection Coefficient.

The input impedance Z_{11}, however, is not a convenient function to specify in the work that follows. A useful function which is closely related to Z_{11}, the voltage reflection coefficient Γ, is therefore now examined. For the network in Fig.2.1, where all impedances have been normalized so that $Z_s=1\,\Omega$, Γ is defined by

$$\Gamma(s) \equiv \frac{Z(s) - Z_s}{Z(s) + Z_s} = \frac{Z(s) - 1}{Z(s) + 1} \quad , \tag{2.17}$$

where $Z(s)= Z_{11}(s)$. Eq. (2.17), in analytic function theory terms, may be viewed as a conformal mapping of the Z-plane into the Γ-plane. It is easily shown that the right half of the Z-plane becomes the region inside a circle of unit radius centered at the origin in the Γ-plane, and that the imaginary axis of the Z-plane transforms into the circle of unit radius in the Γ-plane.

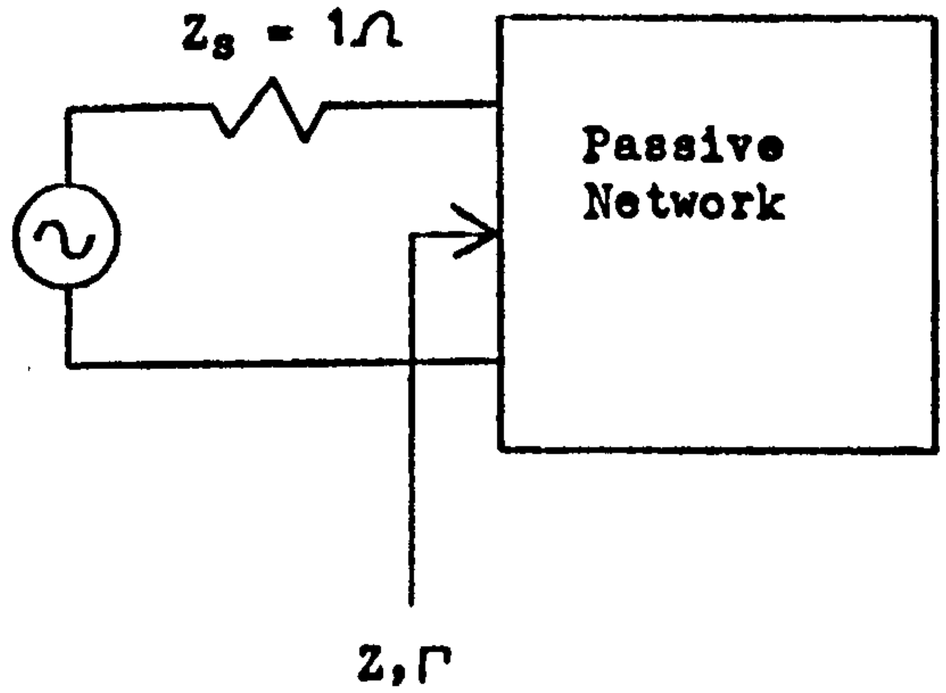

Fig. 2.1. Definition of the voltage reflection coefficient Γ.

Hence,

$$|\Gamma(s)| \leq 1 \quad \text{for Re}\{Z(s)\} \geq 0. \tag{2.18}$$

In the previous section it was seen that Z(s) must be a positive real function, and so, from Eqs.(2.16) and (2.18),

$$|\Gamma(s)| \leq 1 \quad \text{for } \sigma \geq 0. \tag{2.19}$$

Thus $|\Gamma(s)|$ is bounded (by unity) for values of s whose real part is equal to or greater than zero. It is easily shown from Eq.(2.17) that $\Gamma(s)$ is real when s is real (since Z(s) is real then). A function which possesses both of these properties is called a <u>bounded real</u> (b.r.) function. Conversely, if the bound in Eq.(2.18) holds for an arbitrary b.r. $\Gamma(s)$, then the Z(s) calculated from this $\Gamma(s)$ is necessarily p.r., and may be developed into a realizable passive network.

Another important result from analytic function theory is the maximum modulus theorem, which states that if a function of a complex variable is analytic over a region R, its absolute value (modulus) at any point of R is less than or equal to the maximum modulus over the boundary of R.

Now, given that:

$\Gamma(s)$ is analytic (does not have any poles) in the right half of the s-plane and is a real function of s, (2.20)

and the bound

$$|\Gamma(jw)| \leq 1, \quad -\infty \leq w \leq \infty, \tag{2.21}$$

then the associated Z(s) is a p.r. function.

To show this important conclusion, use of the maximum modulus theorem gives the result

$$|\Gamma(s)| \leq 1, \text{ for } \sigma \geq 0.$$

From this fact it follows that, for the associated Z(s),

$$\text{Re}\{Z(s)\} \geq 0, \text{ for } \sigma \geq 0,$$

and, from Eqs.(2.20) and (2.17),

$$\text{IM}\{Z(s)\} = 0, \text{ for } s = \sigma + j0.$$

Hence Z(s) is a p.r. function of s, and is realizable as a passive network.

The main purpose of the work thus far has been to establish the conditions (2.20) and (2.21) which $\Gamma(s)$ must satisfy to represent the voltage reflection coefficient of a passive network in Fig. 2.1. The fact that Eq.(2.21) must be satisfied is physically obvious, since the fraction of the incident power which is reflected at the input to the network at real frequencies cannot be greater than unity. The conditions (2.20) and (2.21) are the main goal of the work thus far and will be used in the development of the Darlington insertion loss technique in section 2.4.

2.3 Two-Terminal-Pair Network Parameters.

Two-terminal-pair networks will be used in this thesis, and so it is worthwhile discussing some basic properties of these networks. A two-terminal-pair network is illustrated schematically in Fig.2.2 as a box with two pairs of terminals. The network inside the box is assumed to be linear, reciprocal, time invariant, and passive but may be completely arbitrary in

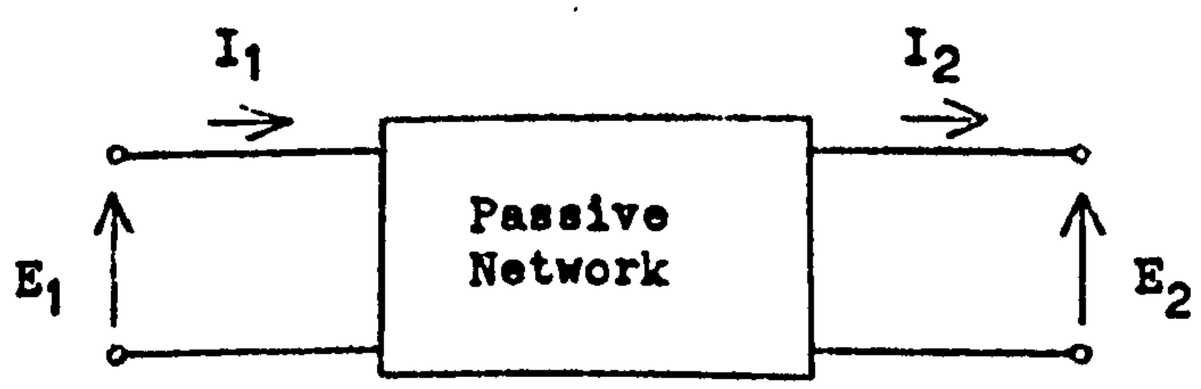

Fig. 2.2. Voltage and current definitions for a two-terminal-pair network.

all other respects. The external electrical behaviour of the network can thus be expressed by means of any two linear relations involving the variables V_1, I_1, V_2, I_2. Six pairs of such relations can be written expressing any two of these variables as functions of the other two. Only one of these six pairs, however, will be used extensively in this thesis.

This pair of linear relations expresses the variables at the input terminals V_1, I_1, as functions of the variables at the output terminals V_2, I_2,

$$\begin{pmatrix} V_1 \\ I_1 \end{pmatrix} = \begin{pmatrix} A & B \\ C & D \end{pmatrix} \begin{pmatrix} V_2 \\ I_2 \end{pmatrix} \quad . \tag{2.22}$$

The $\begin{pmatrix} A & B \\ C & D \end{pmatrix}$ matrix is commonly known as the transfer matrix. The entries in this matrix can be defined by

$$A = \left.\frac{V_1}{V_2}\right|_{I_2=0} \quad , \qquad B = \left.\frac{V_1}{I_2}\right|_{V_2=0} \quad ,$$

$$C = \left.\frac{I_1}{V_2}\right|_{I_2=0} \quad , \qquad D = \left.\frac{I_1}{I_2}\right|_{V_2=0} \quad . \tag{2.23}$$

It is seen that A and D are dimensionless transfer ratios, whereas B and C have, respectively, the dimensions of impedance and of admittance. These parameters are related to the open-circuit impedances and to the short-circuit admittances as follows:

$$Z_{11}=\frac{A}{C},\quad Z_{12}=Z_{21}=\frac{1}{C},\quad Z_{22}=\frac{D}{C},$$

$$Y_{11}=\frac{D}{B},\quad Y_{12}=Y_{21}=-\frac{1}{B},\quad Y_{22}=\frac{A}{B},$$

$$\det Y=\frac{1}{\det Z}=\frac{C}{B}, \tag{2.24}$$

where $$\begin{vmatrix} A & B \\ C & D \end{vmatrix} = AD-BC=1. \tag{2.25}$$

The last relation states that only three of the four circuit parameters are independent, as one would expect from the reciprocity theorem.

In the particular case of symmetrical networks, that is, of networks whose input and output terminals cannot be distinguished by means of external measurements, the parameters necessary to specify a two-terminal-pair network reduce to two. One has, in fact,

$$Y_{11}=Y_{22}\ ,\quad Z_{11}=Z_{22}\ ,\quad A=D. \tag{2.26}$$

Reciprocal impedance networks represent another special case in which the number of independent parameters is two. These networks are characterized by the properties

$$B=C,\ \det Y=\det Z=1,\ Y_{11}=Z_{22},\quad Z_{12}=-Y_{12},$$
$$Z_{11}=Y_{22}. \tag{2.27}$$

The transfer matrix is particularly useful for the analysis of cascaded networks, where the overall transfer matrix is given by the product of the individual matrices in the appropriate

order. The individual matrices used in this thesis are given in Fig.2.3.

In this thesis only lossless networks terminated at either end by resistors are considered, as shown in Fig.2.4. Let all impedances be normalized so that the source resistance is one ohm. This is consistent with the definition of the voltage reflection coefficient Γ considered in the previous section. In Fig.2.4 it is desired to express Γ as a function of A,B,C,D, and R_L. Combining the transfer matrices for R_L and the lossless network gives the result

$$\begin{pmatrix} A & B \\ C & D \end{pmatrix} \begin{pmatrix} 1 & 0 \\ \frac{1}{R_L} & 1 \end{pmatrix} = \begin{pmatrix} A+\frac{B}{R_L} & B \\ C+\frac{D}{R_L} & D \end{pmatrix} = \begin{pmatrix} \underline{A} & \underline{B} \\ \underline{C} & \underline{D} \end{pmatrix} .$$

From Eq.(2.24), $Z = Z_{11} = \underline{A}/\underline{C}$. Recall now that the definition of Γ was $\Gamma = \frac{Z-1}{Z+1}$.

Hence

$$\Gamma = \frac{\left(A - \frac{D}{R_L}\right)+\left(\frac{B}{R_L} - C\right)}{\left(A + \frac{D}{R_L}\right)+\left(\frac{B}{R_L} + C\right)} . \qquad (2.28)$$

This result is very important and will be used in the thesis to derive the transfer matrix for a lossless network from the voltage reflection coefficient.

In Fig.2.4, the relationship between V_s and V_L can be easily expressed in matrix form as

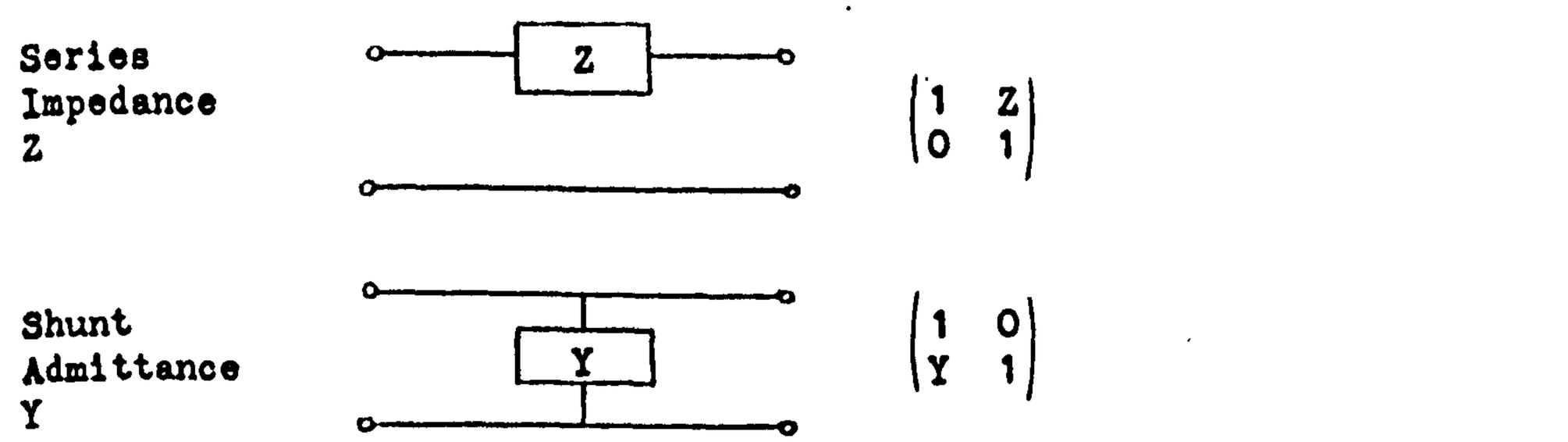

Fig. 2.3. Transfer matrices for several two port networks.

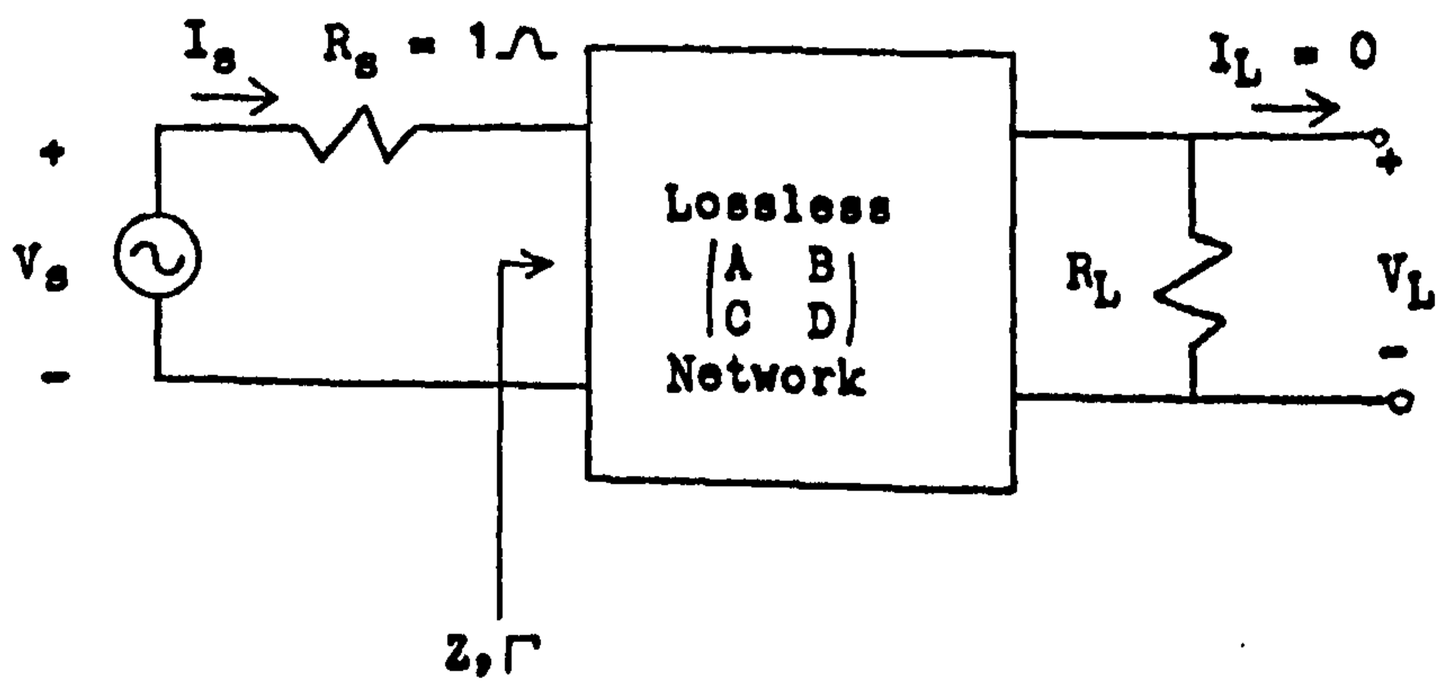

Fig. 2.4. Specific network configuration which is used in this thesis.

$$\begin{pmatrix} V_s \\ I_s \end{pmatrix} = \begin{pmatrix} 1 & 1 \\ 0 & 1 \end{pmatrix} \begin{pmatrix} A & B \\ C & D \end{pmatrix} \begin{pmatrix} 1 & 0 \\ G_L & 1 \end{pmatrix} \begin{pmatrix} V_L \\ 0 = I_L \end{pmatrix} \tag{2.29}$$

where $G_L = 1/R_L$.

By straightforward matrix multiplication,

$$\begin{pmatrix} V_s \\ I_s \end{pmatrix} = \begin{pmatrix} A + G_L B + C + G_L D & B + D \\ C + G_L D & D \end{pmatrix} \begin{pmatrix} V_L \\ 0 \end{pmatrix},$$

which gives

$$\frac{V_s}{V_L} = A + G_L B + C + G_L D. \tag{2.30}$$

The voltage insertion ratio is a function commonly used to describe the overall behaviour of a network when it is inserted between the source and the load. It is defined as the ratio of the voltage across the load resistance R_L when the network is removed and replaced by an ideal transformer to maximize power to the load, to the voltage across R_L when the transformer is removed and the network inserted. It may easily be shown that the ideal transformer

should have a $1:\sqrt{R_L}$ turns ratio to deliver maximum power to the load. Under this condition, let V_L' be the voltage across R_L.

To determine the ratio V_g/V_L', the ideal transformer transfer matrix (Fig.2.3) is used to obtain the result

$$\begin{pmatrix} V_S \\ I_S \end{pmatrix} = \begin{pmatrix} 1 & 1 \\ 0 & 1 \end{pmatrix} \begin{pmatrix} \sqrt{G_L} & 0 \\ 0 & \sqrt{R_L} \end{pmatrix} \begin{pmatrix} 1 & 0 \\ G_L & 1 \end{pmatrix} \begin{pmatrix} V_L' \\ 0 \end{pmatrix}$$

$$= \begin{pmatrix} 2\sqrt{G_L} & \sqrt{R_L} \\ \sqrt{G_L} & \sqrt{R_L} \end{pmatrix} \begin{pmatrix} V_L' \\ 0 \end{pmatrix} ,$$

or that

$$\frac{V_S}{V_L'} = 2\sqrt{G_L} . \tag{2.31}$$

Now the above definition of the voltage insertion ratio may be applied, giving

$$\frac{V_L'}{V_L} = \frac{1}{2}\left(\sqrt{R_L}A + \sqrt{G_L}D + \sqrt{G_L}B + \sqrt{R_L}C \right). \tag{2.32}$$

The square of the magnitude of the voltage insertion ratio is called the <u>insertion loss</u> of the network. This quantity may be regarded as the ratio of the maximum power Po that the generator can furnish to the load (with the ideal transformer connected between R_s and R_L), to the power P_L actually delivered to the load through the network; i.e.,

$$\frac{P_o}{P_L} = \left|\frac{V_L'}{V_L}\right|^2 = \frac{1}{4}\left|\sqrt{R_L}\ A + \sqrt{G_L}\ D + \sqrt{G_L}\ B + \sqrt{R_L}\ C\right|^2 . \tag{2.33}$$

The open-circuit impedance and short-circuit admittance for a lossless network are pure reactance functions, i.e. odd functions of frequency (2). From Eq.(2.24), it is seen that A and D must be even functions of frequency and that B and C are odd functions of frequency. By use of the reciprocity relation AD - BC = 1, Eq.(2.33) may be regrouped to form

$$\frac{P_o}{P_L} = 1 + \frac{1}{4}\left\{\left(\sqrt{R_L}\ A - \sqrt{G_L}\ D\right)^2 + \left(\sqrt{G_L}\ B' - \sqrt{R_L}\ C'\right)^2\right\} \tag{2.34}$$

on the imaginary axis, where $B' = -jB$ and $C' = -jC$. This definition may now be extended to the entire s-plane (using analytic continuation) by replacing w by s/j in Eq.(2.34).

If the network is symmetrical ($R_L = 1$ and $A = D$) then Eq.(2.34) may further be simplified to

$$\frac{P_o}{P_L} = 1 + \frac{1}{4}\left[B' - C'\right]^2 . \tag{2.35}$$

For an antimetrical network ($R_L = 1$ and $B = C$) Eq.(2.34) reduces to

$$\frac{P_o}{P_L} = 1 + \frac{1}{4}\left[A - D\right]^2 . \tag{2.36}$$

2.4 The Darlington Insertion-Loss Synthesis Technique.

2.4.1. Theory.

There are many different techniques for the realization of a driving-point impedance. In general, different techniques lead to different structures or arrangements of the elements. If the structural form of the network is known in advance, and the driving-point impedance satisfies certain realizability criteria for that structure, then a synthesis technique can hopefully be devised to obtain the element values in the structure from the input port driving-point impedance. This thesis is concerned only with the structure shown in Fig.2.4 (in which the lossless network is a cascade of simple networks) for which the insertion loss is specified. The synthesis technique which is used for this structure is called the Darlington insertion-loss method (3), a description of which now follows.

Since the ABCD network in Fig.2.4 is assumed lossless, the transmitted power to the load R_L is the difference between the available power and the reflected power. Therefore, in Fig.2.4, the insertion loss is given by

$$\frac{P_o}{P_L} = \frac{1}{1-|\Gamma(jw)|^2} \geq 1. \qquad (2.37)$$

In modern two-port filter design it is usually the insertion loss as a function of frequency which is the design specification.

In section 2.2 it was shown that $\Gamma(s)$ is a bounded real function, which implies that when s is real $\Gamma(s)$ is also real, and thus complex zeros or poles of $\Gamma(s)$ must occur in complex conjugate pairs. Consider a pair of complex zeros (or poles) of $\Gamma(s)$. Then $\Gamma(-s)$ contains images of these zeros about the imaginary axis, and the four zeros in $\Gamma(s)\,\Gamma(-s)$ have (quadrantal) symmetry about the real and imaginary axes. Multiplying these zeros together yields the factor

$$(s^2+as+b)\ (s^2-as+b)=$$

$$s^4+cs^2+d,$$

which is an <u>even</u> function of s^2, or of w^2 if $s=jw$. Similarly, a zero (or pole) of $\Gamma(s)$ on the real axis will give rise to a mirror image zero in $\Gamma(-s)$, resulting in $\Gamma(s)\,\Gamma(-s)$ having a factor

$$s^2-\sigma^2\ ,$$

which is again an even function of w^2. Thus, a necessary requirement on the numerator and denominator of $\Gamma(s)\,\Gamma(-s)$ is that they be even functions of w when $s=jw$. It follows that $|\Gamma(jw)|^2$ must be of the form

$$|\Gamma(jw)|^2=\frac{M(w^2)}{W(w^2)}\ \leq\ 1. \qquad (2.38)$$

From Eq.(2.37), the insertion loss when $s=jw$ is given by

$$\frac{P_o}{P_L}=\frac{1}{1-\frac{M(w^2)}{W(w^2)}}=\frac{W(w^2)}{W(w^2)-M(w^2)}\ \geq\ 1.$$

Letting $N(w^2) = W(w^2) - M(w^2)$, this equation may be rewritten as

$$\frac{P_o}{P_L} = 1 + \frac{M(w^2)}{N(w^2)} \geq 1, \tag{2.39}$$

where M and N have non-negative values on the w axis.

The next step in the Darlington synthesis method is to expand the definition of $|\Gamma(jw)|^2$ to the entire s-plane by analytic continuation (replacing jw by s). Eq.(2.38) may now be written

$$\Gamma(s)\,\Gamma(-s) = \frac{M(-s^2)}{M(-s^2) + N(-s^2)} . \tag{2.40}$$

How may Eq.(2.40) be factored to recover $\Gamma(s)$?

The roots of the denominator may be found from

$$M(x) + N(x) = 0, \tag{2.41}$$

where $x = -s^2$. Since Eq.(2.41) has real coefficients, complex zeros of this polynomial will be in complex conjugate pairs, a pair giving rise to a factor

$$x^2 \pm ax + b =$$

$$s4 \pm as^2 + b,$$

where $b > 0$.

This factor may be shown to represent a quartet of $\Gamma(s)\,\Gamma(-s)$ poles (having symmetry about the real and imaginary axes). Since $\Gamma(s)$ must be a bounded real function (Eq.(2.20)), the two lhp (left half plane) poles must be chosen for $\Gamma(s)$. Other factors of Eq.(2.41) will be of the form $(x \pm a)$, $a > 0$.

The factor $(x+a)$ results in two poles, at $s=\pm\sqrt{a}$. Again, since $\Gamma(s)$ must be bounded real, the lhp pole is chosen for $\Gamma(s)$. Finally, a factor $(x - a)$ implies that two poles of $\Gamma(s)\,\Gamma(-s)$ are on the imaginary axis of the s-plane. In turn, Eqs.(2.38) and (2.37) show that at these zero points $P_o/P_L = 0$, which, by the construction of P_o/P_L in Eq.(2.39) ($M(w^2)$ and $N(w^2)$ are non-negative), is impossible. Thus a factor $(x - a)$ will not appear in the factorization of Eq.(2.41). The imaginary axis is seen to be a "sorting" boundary for the denominator roots of Eq.(2.40), with the lhp zeros forming the denominator of $\Gamma(s)$.

The numerator roots are determined from

$$M(x) = 0, \tag{2.42}$$

where $x=-s^2$. Complex roots of Eq.(2.42) occur in complex conjugate pairs, a pair of which yields the quartet of roots

$$s^4 \pm as^2 + b, \quad b>0.$$

Either the lhp pair or the rhp pair may be chosen for $\Gamma(s)$, the other pair going to $\Gamma(-s)$. Factors of the form $(x+a)$, $a>0$, have roots at $s=\pm\sqrt{a}$, and either may be chosen for a zero of $\Gamma(s)$, with the other zero going again to $\Gamma(-s)$. Finally, factors with the form $(x - a)$ have roots at $s \pm j\sqrt{a}$. Since $M(w^2)\geq 0$, these roots must be of even multiplicity, ie. $(x - a)^{2k}$, where k is an integer. Then $\Gamma(s)$ and $\Gamma(-s)$ have the factors $(x - a)^k$.

Thus, in general, many different selections are possible for the zeros of $\Gamma(s)$, each leading to a different network

having the same insertion loss. If all of the zeros of $M(-s^2)$ are on the imaginary axis, however, it is seen that the factorization of $\Gamma(s)\,\Gamma(-s)$ in Eq.(2.40) is unique and only one network will emerge. Such will be the case for most of the networks considered in this thesis.

The final step in the Darlington technique is the realization of the lossless network from $\Gamma(s)$. Although many different methods may be used, the method used in this thesis is to recover the transfer matrix for the lossless network from Γ (Eq.2.28). Then elements are extracted from this transfer matrix according to the desired structure. The method is to premultiply (or postmultiply) the transfer matrix by the inverse matrix of the desired element and then require the resulting transfer matrix to be of lower degree. This requirement will determine the element value. It turns out that this requirement leads to two independent equations for the element value, which is very useful when estimating the inaccuracy (due to round-off errors, etc.) in the numerical calculations.

2.4.2. An Example of the Darlington Method: The Butterworth Specification.

A maximally flat function is one which has all of its zeros coincident at one frequency point, commonly referred to as the center frequency. A maximally flat function g which possesses n zeros at the center frequency ω_0 has the property

that g and its first n-1 derivatives are equal to zero at w_o. Thus, if a Taylor series expansion of g is made about w_o, the first term in the series will be $a_n(w-w_o)^n$, where

$$a_n = \frac{1}{n!}\left(\frac{d^n g}{dw^n}\right)\Bigg|_{w=w_o} .$$

It is now apparent why this function is called maximally flat. For values of w close to w_o, g has a value very close to zero. For larger (or smaller) values of w, however, g may become large. Thus a maximally flat function is an excellent approximation to zero at one frequency point or over a narrow frequency band. As the bandwidth about w_o is made larger, g becomes less effective in approximating zero over this band. Electrical Engineers commonly refer to the maximally flat approximation to zero as a Butterworth specification, named after the British scientist who first used this specification in the design of filters.

Consider the symmetrical structure shown in Fig.2.5. Analysis of the lossless network shows that A=D is a second degree even polynomial of s with constant term unity and that B and C are third degree odd polynomials in s. Also from the structure it can be seen that as $w\to\infty$ the insertion loss will have a sixth order pole at ∞ and that at $w=o$, $P_o/P_L=1$. From the insertion loss formula Eq.(2.35) it is observed that P_o/P_L-1 is the square of an odd polynomial $(B'-C')$ in w. A function which satisfies the above insertion loss conditions for this

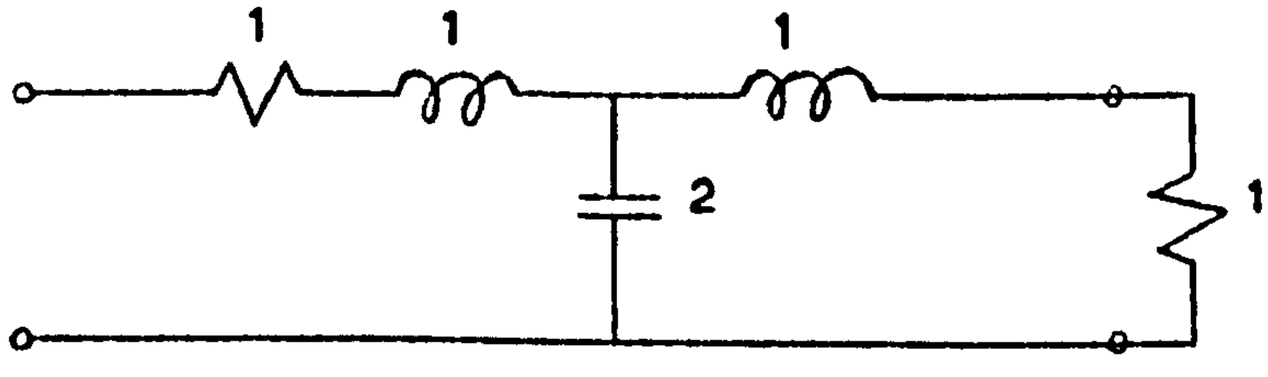

Fig. 2.5. Ladder network with Butterworth insertion loss specification.

structure is the Butterworth low-pass insertion loss function

$$\frac{P_o}{P_L} = 1 + w^6 ,$$

which has its 3dB point (the point at which $\frac{P_o}{P_L} = 2$, or

$10 \log_{10} \left(\frac{P_o}{P_L}\right) = 3.0$) at $w = 1$. Then, from the relation

$$\left|\Gamma(jw)\right|^2 = \frac{\frac{P_o}{P_L} - 1}{\frac{P_o}{P_L}} ,$$

(Eq.(2.37)), it is found that

$$\left|\Gamma(jw)\right|^2 = \frac{w^6}{1+w^6} .$$

Thus, in Eq.(2.40),

$$\Gamma(s) \times \Gamma(-s) = \frac{-s^6}{1-s^6} .$$

Since all of the zeros of the voltage reflection coefficient are on the imaginary axis, the factorization of $\Gamma(s)\cdot\Gamma(-s)$ will be unique, as stated earlier. In fact, for the numerator,

$$\text{Num}\left\{\Gamma(s)\right\} = s^3.$$

The roots of the denominator lie on the unit circle and are separated by $360^o/6 = 60^o$. By choosing the left-half plane roots and then multiplying the corresponding factors together, it turns out that

$$\Gamma(s) = \frac{s^3}{s^3 + 2s^2 + 2s + 1} . \qquad (2.43)$$

Recall that the definition of the voltage reflection coefficient is $\Gamma = \frac{(A-D)+(B-C)}{(A+D)+(B+C)}$. (2.28)

Hence, multiplying both numerator and denominator of Eq.(2.43) by two (so that the constant term in A = D is one), it is found that for the lossless network

$$\begin{pmatrix} A & B \\ C & D \end{pmatrix} = \begin{pmatrix} 2s^2+1 & 2s^3+2s \\ 2s & 2s^2+1 \end{pmatrix} .$$

Starting at the left-hand side of this network, a series coil will first be removed. The inverse matrix for a series coil is easily shown to be

$$\begin{pmatrix} 1 & -Ls \\ o & 1 \end{pmatrix} .$$

Therefore,

$$\begin{pmatrix} 1 & -Ls \\ o & 1 \end{pmatrix} \begin{pmatrix} 2s^2+1 & 2s^3+2s \\ 4s & 2s^2+1 \end{pmatrix} =$$

$$\begin{pmatrix} 2s^2 - 2Ls^2+1 & 2s^3 - 2Ls^3+2s - Ls \\ 2s & 2s^2+1 \end{pmatrix} = \begin{pmatrix} \underline{A} & \underline{B} \\ \underline{C} & \underline{D} \end{pmatrix} . \quad (2.44)$$

The requirement that this matrix be of lower degree results in two equations:

1) $\underline{A}$: $2s^2 - 2Ls^2 = 0$, from which $L = 1$.

2) $\underline{B}$: $2s^3 - 2Ls^3 = 0$, from which $L = 1$.

Thus the accuracy checking feature of this matrix decomposition method is brought to light. After L is removed, the transfer

matrix will be

$$\begin{pmatrix} 1 & s \\ 2s & 2s^2+1 \end{pmatrix} . \qquad (2.45)$$

Next a capacitor C_1 will be removed. The inverse matrix for a shunt C_1 is

$$\begin{pmatrix} 1 & o \\ -C_1 s & 1 \end{pmatrix} .$$

Therefore,

$$\begin{pmatrix} 1 & o \\ -sC_1 & 1 \end{pmatrix}\begin{pmatrix} 1 & s \\ 2s & 2s^2+1 \end{pmatrix}=\begin{pmatrix} 1 & s \\ 2s-sC_1 & 2s^2-C_1 s^2+1 \end{pmatrix} .$$

By inspection, $C_1 = 2$. Since the network is symmetrical ($A = D$), the final series coil has an inductance of 1 (henry). The final network with element values is shown in Fig.2.5. After removing all of the elements, the transfer matrix should be the unit matrix $\begin{pmatrix} 1 & o \\ o & 1 \end{pmatrix}$, which may be viewed as a 1:1 transformer. This transformer may be omitted from the cascade, if desired. The realization has thus been achieved.

The above method of determining the element values from Γ is not the "quickest" one (a continued fraction expansion of A/C results in the same element values), but it is a very straightforward method and gives accuracy information as the synthesis proceeds, and is useful in other types of networks to be discussed later.

2.5 The Scattering Matrix.

The extension of the insertion loss concept to an n-port network will now be considered. It is remembered that the insertion loss description of a two port network is meaningful when the network is terminated at either end by a finite non-zero impedance. If the network has an open or short-circuit on either end then some other description (such as the voltage or current insertion ratio) becomes more appropriate. This same fact holds true for an n-port description function. All of the n-port networks considered in this thesis are resistively terminated. Hence the scattering matrix description of the n-port will be developed with this restriction.

Consider the n-port shown in Fig.2.6.

Let (V) and (I) be $1 \times n$ column matrices defined by

$$(V) = \begin{pmatrix} V_1 \\ V_2 \\ \cdot \\ \cdot \\ V_n \end{pmatrix} , \quad (I) = \begin{pmatrix} I_1 \\ I_2 \\ \cdot \\ \cdot \\ I_n \end{pmatrix} , \tag{2.46}$$

and let (A), (B), (C), (D), and (X) be defined as $n \times n$ matrices. The most general linear relationship between (V) and (I) is given by

$$\Big((A)(V) + (B)(I)\Big) = (X)\Big((C)(V) + (D)(I)\Big) \quad . \tag{2.47}$$

Specialized forms of Eq.(2.47) may be derived. For instance, if

$$(B) = (C) = 1_n,$$
$$\text{and} \quad (A) = (D) = 0, \tag{2.48}$$

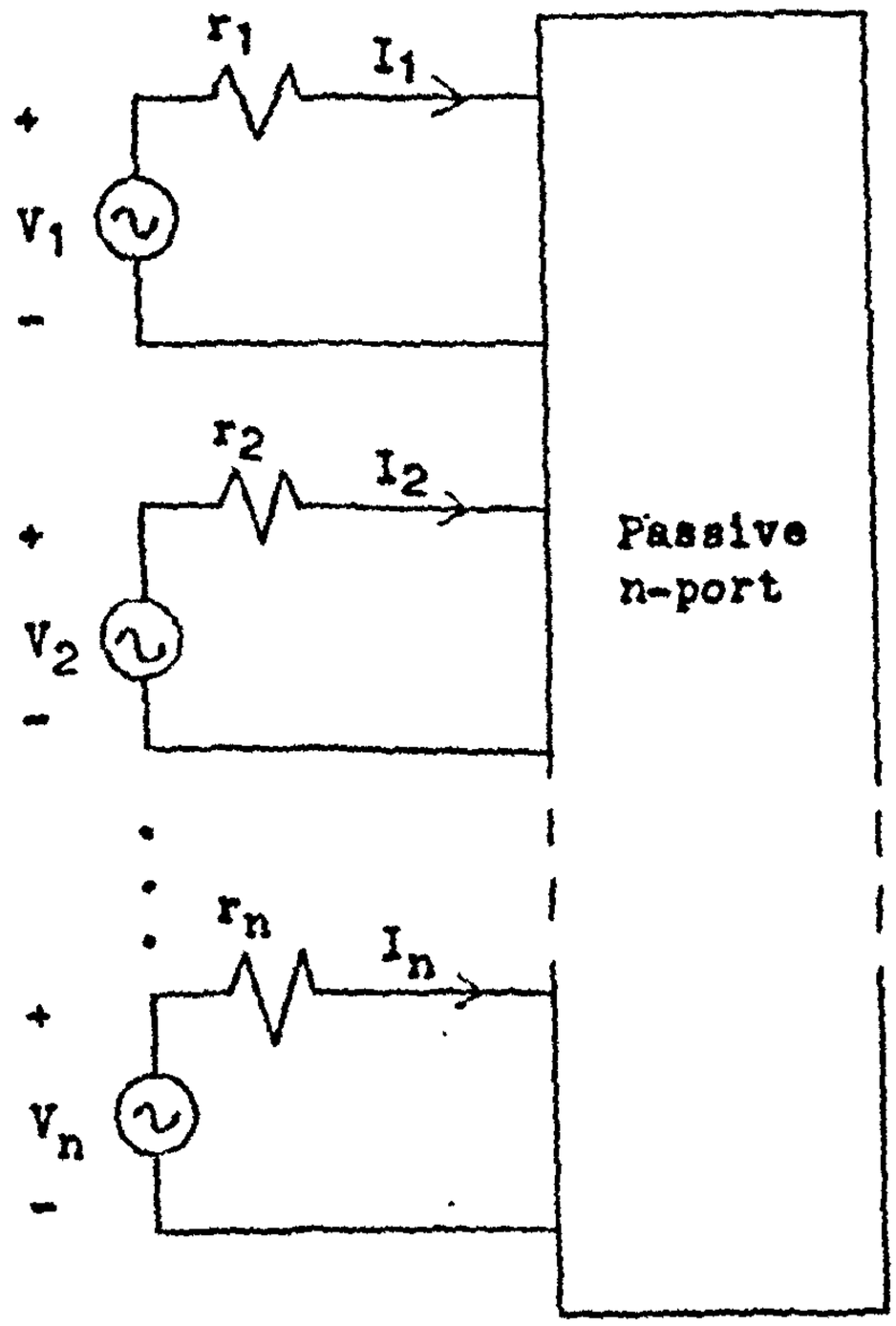

Fig. 2.6. Voltage and current definitions for a generalized n-port network.

where O is the null matrix (all entries are zero) and 1_n is the unit matrix of rank n (entries on the major diagonal are 1 and zero elsewhere), then (X) turns out to be the (Y) or short-circuit admittance matrix. On the other hand, if

$$(B) = (C) = O, \qquad (2.49)$$

$$\text{and} \quad (A) = (D) = 1_n,$$

then (X) is equivalent to the (Z) or open-circuit impedance matrix.

Now, to extend the concept of insertion loss to an n-port network, in Fig.2.6 let

$$|S_{jk}|^2 \equiv \frac{\text{power delivered to } r_j \text{ by } V_k \text{ with n-port inserted}}{\text{maximum power delivered to } r_j \text{ by } V_k \text{ with optimizing transformer inserted}}, \qquad (2.50)$$

where the (X) matrix in Fq.(2.47) is now defined as the (S) matrix, and S_{jk} is the entry of the jth row and kth column. By comparing Eqs.(2.50) and (2.33) it is seen that $|S_{jk}|^2 = 1/P_o/P_L$ for a 2-port, and so this is the connecting link between insertion loss and the (S) matrix (which is now called the scattering matrix) for an n-port.

The question now arises as to what definitions to give the (A), (B), (C), and (D) matrices so that definition (2.50) holds true for the n-port. To simplify matters, it is first assumed that (A), (B), (C), and (D) are diagonal matrices (all entries not on the major diagonals are zero). Further, let

$$(A) = (C) = \frac{1}{2}\left\{\text{diag } R_j^{\frac{1}{2}}\right\}^{-1} = \frac{1}{2}\left\{\text{diag } R_j^{-\frac{1}{2}}\right\}, \qquad (2.51)$$

and

$$(B) = -(D) = -\frac{1}{2}\left\{\text{diag } R_j^{\frac{1}{2}}\right\} ,$$

where $(\text{diag } R_j^{\frac{1}{2}})$ is a diagonal matrix of degree n and the R_j are real, positive numbers called the port normalizing numbers. With these definitions, first a restriction on the scattering matrix due to the passivity of the n-port will be derived, and then the quantities on the right side of Eq.(2.50) will be developed to verify the definition of the scattering matrix.

Let Eq.(2.47) be written in the form

$$(b) = (S)\ \ (a) . \tag{2.52}$$

Then from (2.51) and (2.47),

$$\begin{aligned} b_j &= \tfrac{1}{2}(R_j^{-\frac{1}{2}}\ V_j - R_j^{\frac{1}{2}}\ I_j), \\ \text{and} \qquad a_j &= \tfrac{1}{2}(R_j^{-\frac{1}{2}}\ V_j + R_j^{\frac{1}{2}}\ I_j). \end{aligned} \tag{2.53}$$

Solving for (V) and (I),

$$\begin{aligned} (V) &= (\text{diag } R_j^{\frac{1}{2}})\ \ \Big((a)+(b)\Big) , \\ (I) &= (\text{diag } R_j^{-\frac{1}{2}})\ \ \Big((a)-(b)\Big) . \end{aligned} \tag{2.54}$$

Now since V_j and I_j in Fig.2.6. are assumed to be sinusoidal time waveforms, the power entering the n-port through port j $= R_e\left(V_j {}^{*} I_j\right)$, where the asterisk indicates the complex conjugate. The total power entering the n-port is given by

$$P = \sum_{j=1}^{n} \left(R_e\ V_j^{*}\ I_j\right) = (\tilde{V})(I), \tag{2.55}$$

where the tilda means the transposed (making the column matrix into a row matrix) complex conjugate. From (2.54),

$$(\tilde{V}) = \left((\tilde{a}) + (\tilde{b})\right) \quad \left(\text{diag } R_j^{\frac{1}{2}}\right) \quad , \tag{2.56}$$

and hence

$$P = R_e \left((\tilde{V})(I)\right) = R_e \left(\left((\tilde{a}) + (\tilde{b})\right) \ (\text{diag } R_j^{\frac{1}{2}})(\text{diag } R_j^{-\frac{1}{2}}) \left((a)-(b)\right)\right)$$

$$= R_e \left(\left((\tilde{a})+(\tilde{b})\right) \left((a)-(b)\right)\right)$$

$$= (\tilde{a})(a) - (\tilde{b})(b), \tag{2.57}$$

since the real part of $(\tilde{b})(a)-(\tilde{a})(b)$ is zero.

From Eqs.(2.57) and (2.52),

$$P = (\tilde{a})(a) - \left((\tilde{a})(\tilde{S})\right) \left((S)(a)\right)$$

$$= (\tilde{a}) \left(1_n - (\tilde{S})(S)\right) \ (a). \tag{2.58}$$

Now if the n-port is passive, $P \geq 0$, and the matrix $\left(1_n - (\tilde{S})(S)\right)$ must be positive semidefinite [4]. If this is true, then

$$1_n - (\tilde{S})(S) \geq 0, \tag{2.59}$$

is a restriction on the scattering matrix for a passive n-port. Furthermore, if the n-port is lossless, then $P = 0$ and Eq.(2.59) reduces to

$$(\tilde{S})(S) = 1_n. \tag{2.60}$$

This result is an important conclusion, and is commonly referred to as the unitary condition for the scattering matrix of an n-port. This condition will be used in the directional coupler work later in the thesis.

Now it is necessary to show that the scattering matrix (S) that has been derived does indeed satisfy the definition (2.50). In deriving Eq.(2.59) no restrictions have been placed on the R_j in the (A), (B), (C), and (D) matrices other than that they be real, finite, non-zero, and positive. Thus there is no connection

between the r_j in Fig.2.6 and R_j so far. Certain convenient properties arise when the r_j are set equal to the port normalizing numbers R_j, however, and this equivalence will be assumed in the following derivation.

Using Eq.(2.54) (with R_j now replaced by r_j) and the current direction as shown in Fig.2.7,

$$\frac{V_j}{I_j} = r_j \left(\frac{a_j+b_j}{a_j-b_j}\right) = -r_j \ . \tag{2.61}$$

This equation can only be true in general if

$$a_j = 0 \ , \tag{2.62}$$

which is a direct result of setting $R_j = r_j$. Sometimes a_j is referred to as the "incident" wave. In this context, Eq.(2.62) states that there is no incident wave at port j if $V_j = 0$. In low frequency circuitry, it is very difficult to visualize a_j as a "wave". From Eq.(2.57), the average power delivered to r_j (noting the current direction) by V_k with the n-port inserted is

$$P_L = -\left((a_j^*)(a_j)-(b_j^*)(b_j)\right) = b_j^* b_j \ . \tag{2.63}$$

To determine the maximum power delivered to r_j by V_k with an optimizing transformer substituted for the n-port, by the maximum power transfer theorem it is known that the turns ratio of the transformer must be chosen such that it makes the r_j load appear as r_k at the port k. Then, in Fig.2.8, using Eq.(2.54),

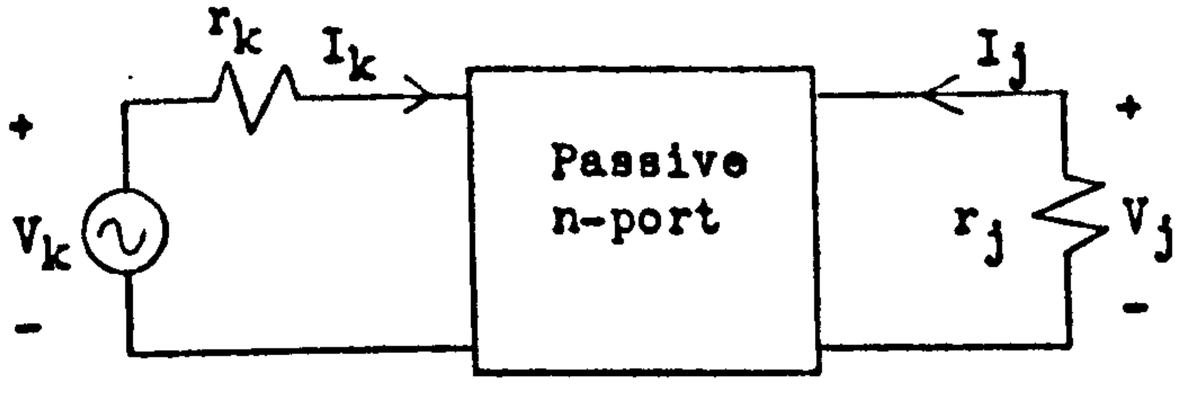

Fig. 2.7. The insertion loss between ports j and k with an n-port network in place.

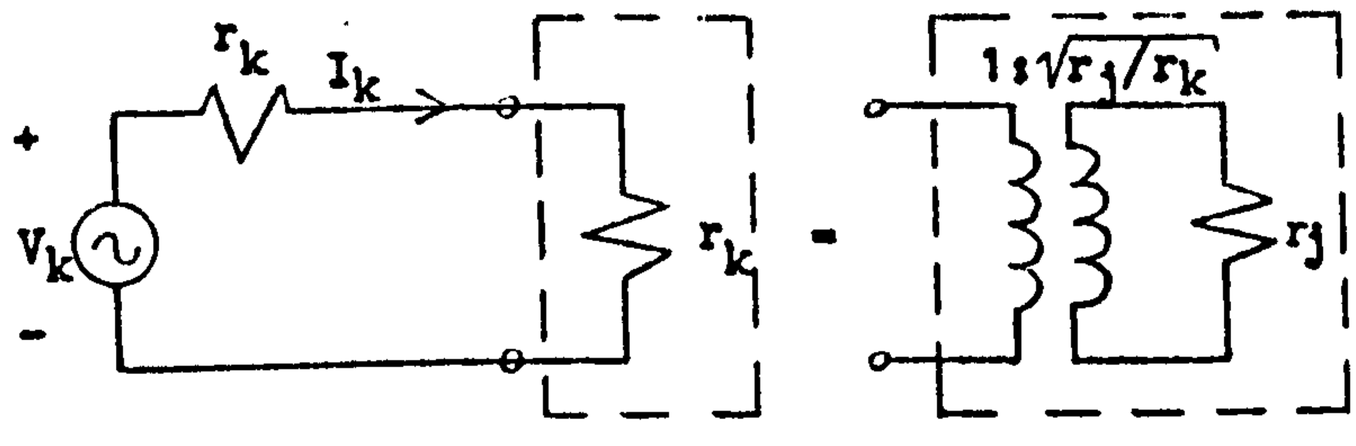

Fig. 2.8. The insertion loss between ports j and k with an optimizing transformer replacing the n-port network.

$$V_1 = \frac{1}{2}V_k = r_k^{\frac{1}{2}} (a_k + b_k) \quad , \tag{2.64}$$

$$\text{and} \quad I_k = \frac{V_k}{2r_k} = r_k^{-\frac{1}{2}} (a_k - b_k) \ .$$

Thus,

$$1 = \frac{a_k + b_k}{a_k - b_k} \ , \qquad \text{or} \quad b_k = 0. \tag{2.65}$$

Historically, b_k has been called the "reflected" wave from port k. Eq.(2.65) shows that there is no reflection at a matched port. Now the power delivered to r_j in Fig.2.8 is

$$P_A = R_e \ (V_1^* \ I_k) = a_k^* a_k \quad . \tag{2.66}$$

Finally, by using Eqs.(2.66), (2.63), and the fact that $b_j = S_{jk} a_k$, it is seen that the definition (2.50) is true, as was asserted.

It will now be instructive to show that the scattering matrix for a passive n-port always exists and is symmetric $(S_{ij} = S_{ji})$[5]. Consider the augmented n-port in Fig.2.9. In general it can be shown that the (Y) matrix for the augmented n-port always exists, although it may not do so for the original network. The idea behind this augmentation is to express (S) for the non-augmented n-port in terms of (Y) of the augmented network, which is known to exist. The R_j are, as usual, chosen as the port normalizing numbers for the non-augmented network. Let (Y_A) be the (Y) matrix for the augmented n-port.

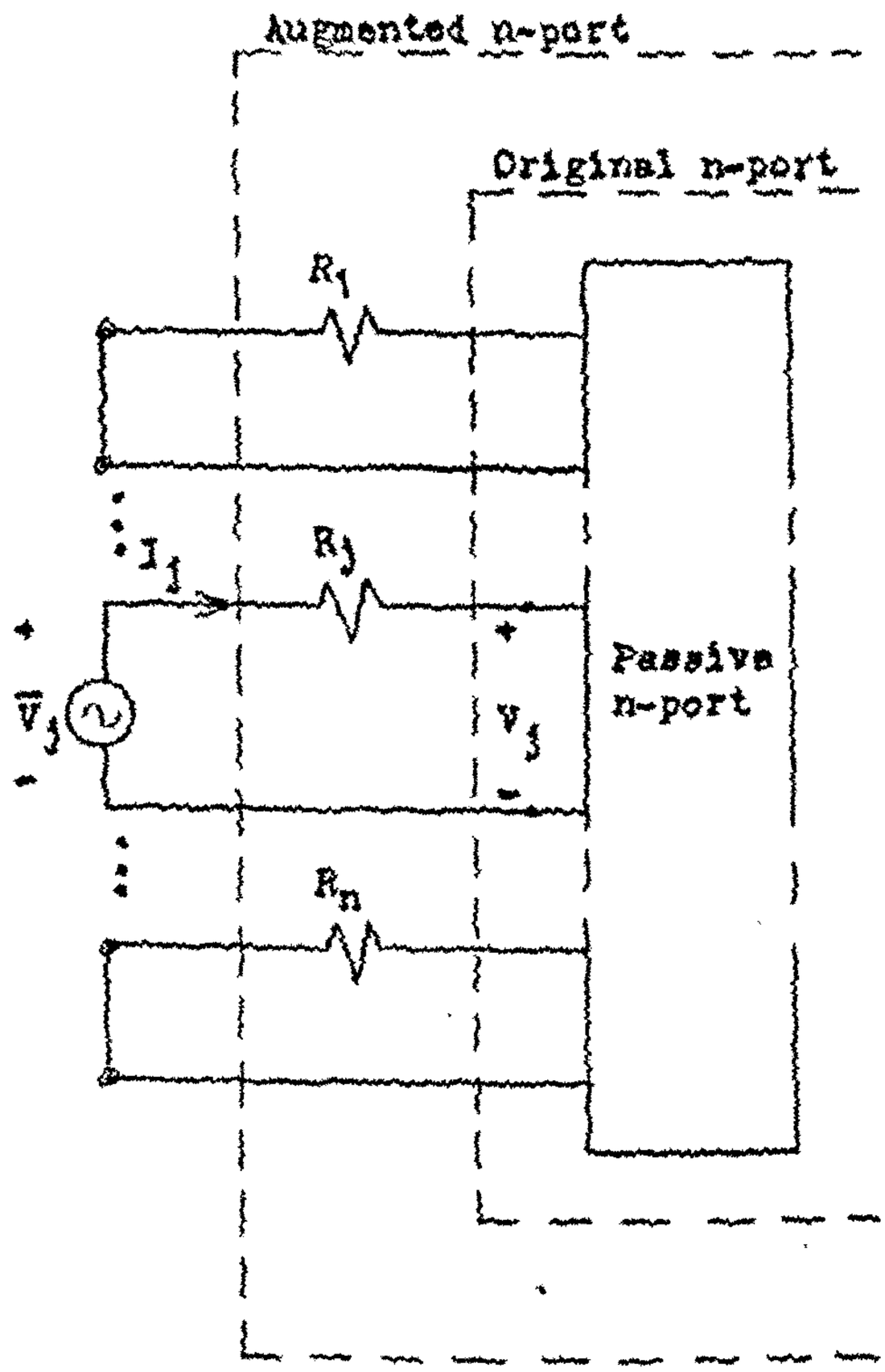

Fig. 2.9. The augmented network used to demonstrate the existence of the scattering matrix.

Then, by definition,

$$(I) = (Y_A)(\bar{V}). \tag{2.67}$$

Inspection of Fig.2.8 gives the relation

$$\bar{V}_j = V_j + I_j R_j \quad , \tag{2.68}$$

or

$$(\bar{V}) = (V) + (\text{diag } R_j)(I).$$

By using Eqs.(2.67), (2.68), and (2.54), it is found that

$$\begin{aligned}(I) &= (Y_A)\left((V) + (\text{diag } R_j)(I)\right) \\ &= (Y_A)\left((\text{diag } R_j^{\frac{1}{2}})\left((a)+(b)\right) + (\text{diag } R_j^{\frac{1}{2}})\left((a)-(b)\right)\right) \\ &= (Y_A)\left(2(\text{diag } R_j^{\frac{1}{2}})\ (a)\right).\end{aligned} \tag{2.69}$$

But also

$$(I) = (\text{diag } R_j^{-\frac{1}{2}})\ \left((a)-(b)\right) \quad , \tag{2.70}$$

from Eq.(2.54). Thus,

$$(\text{diag } R_j^{-\frac{1}{2}})\ (b) = \left((\text{diag } R_j^{-\frac{1}{2}}) - 2(Y_A)(\text{diag } R_j^{\frac{1}{2}})\right)\ (a) \quad , \tag{2.71}$$

which yields

$$\begin{aligned}(b) &= \left(1_n - 2(\text{diag } R_j^{\frac{1}{2}})\ (Y_A)(\text{diag } R_j^{\frac{1}{2}})\right)\ (a) \\ &= (S)(a).\end{aligned} \tag{2.72}$$

Therefore, since (Y_A) exists (by assertion), (S) exists for a passive n-port.

It is also known that if (Y) exists for a passive n-port containing only reciprocal elements, then (Y) is symmetric ($Y_{ij} = Y_{ji}$). From (2.72) it is obvious then that

$$S_{ij} = S_{ji} \quad . \tag{2.73}$$

This symmetry property, the existence theorem, and the unitary condition for a lossless network are the main results which are used in chapter 5.

2.6 Determination of Phase From A Magnitude Specification.

In chapter 5 it will be necessary to determine the phase of an analytic function at one frequency point given the magnitude of the function along the frequency axis. The following discussion is directed towards this end.

An important result from analytic function theory is the Cauchy integral law, which states that

$$\oint_C F(s)ds = 0, \tag{2.74}$$

where C is a simple closed curve in the s-plane, and F(s) is an analytic function of s in and on C. Now assume that F(s) is analytic when $\sigma \geq 0$, and that $F(\infty)$ is finite and single-valued. Let

$$G(s) = \frac{F(s)}{s-jw_1}, \tag{2.75}$$

and consider the curve C shown in Fig.2.10. It is seen that the Cauchy integral law may be invoked for this G and C, and therefore

$$\oint_C G(s)ds = 0. \tag{2.76}$$

The contribution from path ABD to this integral is

$$\int_{ABD} G(s)ds = \int_{-\frac{\pi}{2}}^{\frac{\pi}{2}} \frac{F(R_e{}^{j\theta})\ jR_e{}^{j\theta}}{R_e{}^{j\theta} - jw_1}\, d\theta.$$

As $R \to \infty$,

$$\int_{ABD} G(s)\ ds = jF(\infty) \int_{-\frac{\pi}{2}}^{\frac{\pi}{2}} d\theta = j\pi F(\infty). \tag{2.77}$$

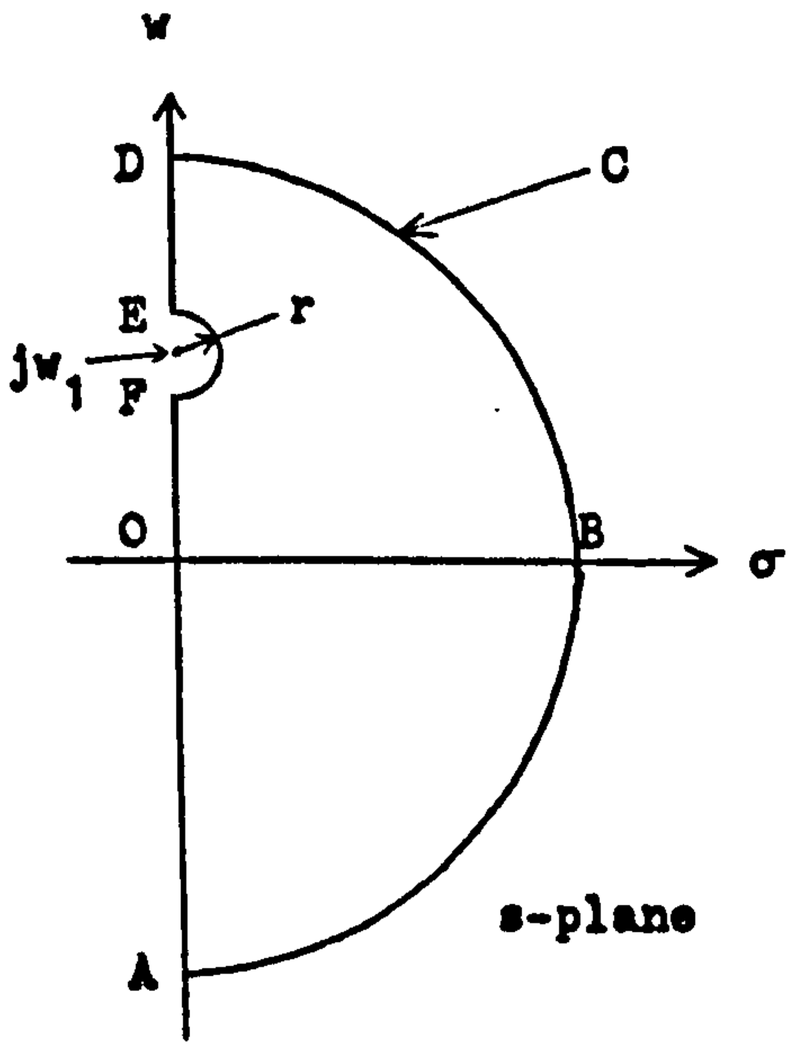

Fig. 2.10. The integration contour used in Eq. (2.76).

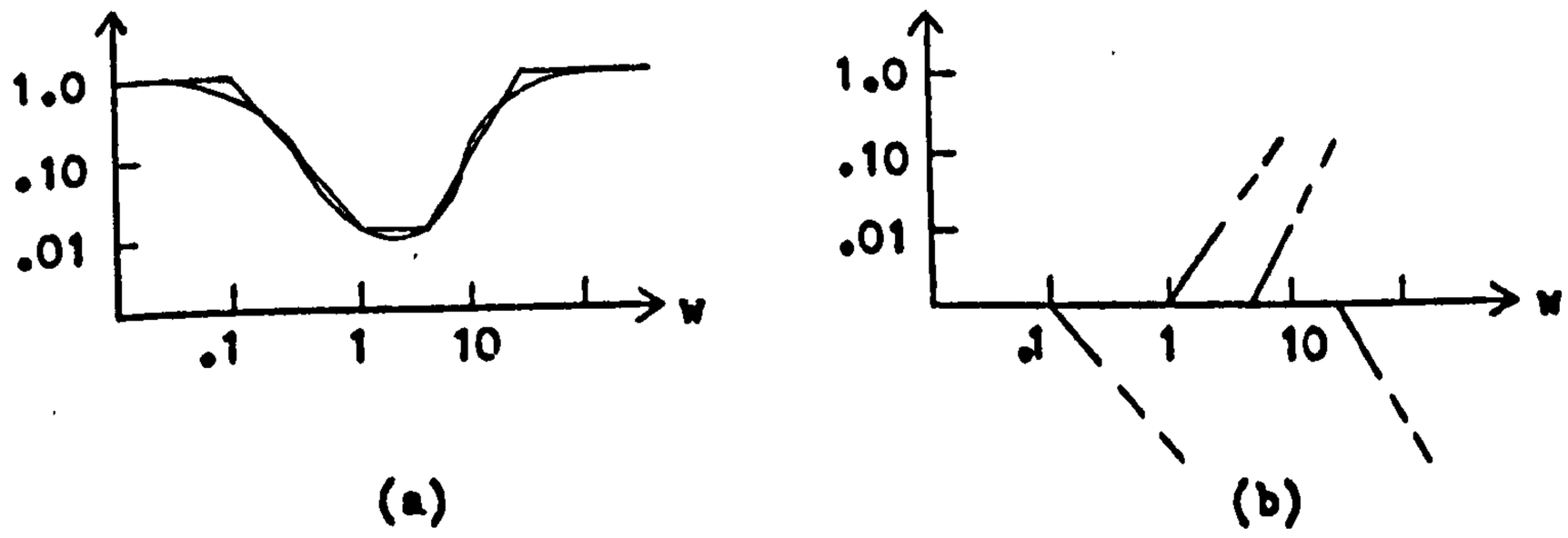

Fig. 2.11. (a) Straight line approximation to $|F(jw)|$ and (b) the decomposition of (a) into semi-infinite segments.

The contribution to Eq.(2.76) from path EF is

$$\int_{EF} G(s)ds = \int_{\frac{\pi}{2}}^{-\frac{\pi}{2}} \frac{F(jw_1 + r_e e^{j\theta}) j r_e e^{j\theta}}{r_e e^{j\theta}} d\theta$$

$$= j \int_{\frac{\pi}{2}}^{-\frac{\pi}{2}} F(jw_1 + r_e e^{j\theta}) d\theta .$$

As $r \to 0$,

$$\int_{EF} G(s)ds = -j\pi F(jw_1). \tag{2.78}$$

Thus Eq.(2.76) becomes

$$\int_{-\infty}^{\infty} \frac{F(jw)}{w-w_1} dw = j\pi \Big(F(\infty) - F(jw_1) \Big) , \tag{2.79}$$

where

$$\int_{-\infty}^{\infty} \frac{F(jw)}{w-w_1} dw \equiv \lim_{r \to 0} \left(\int_{-\infty}^{w_1 - r} \frac{F(jw)}{w-w_1} dw + \int_{w_1 + r}^{\infty} \frac{F(jw)}{w-w_1} dw \right) .$$

Now let

$$F(s) \equiv R(s) + jX(s), \tag{2.80}$$

where R and X are the real and imaginary parts of F. Using this definition, the real part of Eq.(2.79) becomes

$$\frac{1}{\pi} \int_{-\infty}^{\infty} \frac{R(w)}{w-w_1} dw = X(w_1) - X(\infty) . \tag{2.81}$$

Eq.(2.81) shows that once R(w) is specified, X(w) is uniquely determined. It is sometimes referred to as a Hilbert transform.

By algebraic manipulation, it can be shown[6] that Eq.(2.81) is equivalent to

$$X(w_1) = \frac{1}{\pi}\int_{-\infty}^{\infty} \frac{dR}{du} \quad \ln \coth \left|\frac{u}{2}\right| du, \tag{2.82}$$

where

$$u = \ln\left(\frac{w}{w_1}\right) . \tag{2.83}$$

Next, $H(s)$ is defined by $H(s) \equiv \ln F(s) = \ln \left|F(s)\right| + j\beta(s)$, where $\beta = \tan^{-1}\left(\frac{R}{X}\right)$ is the phase of $F(s)$. Then Eq.(2.82) becomes

$$\beta(w_1) = \frac{1}{\pi}\int_{-\infty}^{\infty} \frac{d\ln\left|F(jw)\right|}{du} \ln \coth \left|\frac{u}{2}\right| du. \tag{2.84}$$

Eq.(2.84) is the main result for this section, and shows how the phase of an analytic function can be determined from the magnitude on the w axis.

Unfortunately, the integral in Eq.(2.84) is very difficult to evaluate for most cases of practical interest. An approximation can, however, be made[7], which gives satisfactory results. First, $\left|F(jw)\right|$ is plotted on log-log graph paper, with both the w (horizontal) axis and the $\left|F(jw)\right|$ axis having the same logarithmic scale. The number of logarithmic cycles for both axes is made large enough to show the principal variations in $\left|F(jw)\right|$. Next, $\left|F(jw)\right|$ is approximated by a number of straight line segments (Fig.2.11 (a)). This approximation can be regarded as the superposition of straight lines, each starting on the w axis at w_i (the "break point"), having a slope k_i, and extending to infinity (Fig.2.11 (b)). For each straight line, Eq.(2.84) gives the result

$$\beta_i(w) = k_i \left(\frac{1}{\pi} \int_{u_i}^{\infty} \ln \coth \left| \frac{u}{2} \right| du \right) \equiv k_i F_o \left(\frac{w}{w_i} \right), \qquad (2.85)$$

where

$$u_i = \ln \left(\frac{w}{w_i} \right) .$$

The βi's are then added together on a common w axis to form the overall $\beta(w)$. The function $F_o \left(\frac{w}{w_i} \right)$ is given in table form in Reference (7), which permits the rapid determination of the $\beta_i(w)$ functions.

The overall accuracy of this approximation depends on how closely the $|F(jw)|$ curve (plotted on log-log paper) can be approximated by straight line segments. Usually the maximum percentage error in β is about the same as the maximum percentage error between $|F(jw)|$ and the straight line approximation(7). Obviously, the accuracy improves as more straight line segments are used in the approximation. It is important to remember that the above methods are only valid when F(s) has no singularities in the right half plane or on the imaginary axis.

Chapter 2 REFERENCES

1. Brune, O.: "Synthesis of a finite two terminal network whose driving-point impedance is a prescribed function of frequency", Journal of Maths. & Physics, 1931, 10, p.191.

2. Ragan, G.L.: "Microwave Transmission Circuits". MIT Radiation Laboratories Series, McGraw-Hill, 1948, p.550.

3. Darlington, S.: "Synthesis of reactance four-poles which produce prescribed insertion loss characteristics, including special applications to filter designs", Journal of Maths. and Physics, 1939, 18, p.257.

4. Weinberg, L.: "Network Analysis and Synthesis". McGraw-Hill, 1962, p.258.

5. Carlin, H.J.: "The Scattering Matrix in Network Theory", IEEE Trans., CT-3, June 1956, pp.88-97.

6. Tuttle, D.F.: "Network Synthesis, Volume I". Wiley, 1958, pp.387-391.

7. Tuttle, D.F.: "Network Synthesis, Volume I". Wiley, 1958, Appendix B.

Chapter 3

Transmission Line Network Synthesis

3.1. Introduction.

In the following work a transmission line network will be defined as a network containing only lengths of transmission line and resistors. A transmission line may be realized in many different forms; stripline, microstrip, and a section of waveguide excited in one mode are common examples. If the section of waveguide is propagating energy in more than one mode then each mode may be shown to have its own transmission line analogy[1].

The following restrictions will now be placed on the various transmission lines contained in a transmission line network:

Each line is uniform. (3.1)

Each line is lossless. (3.2)

All lines have the same wavelength vs. frequency variation. (3.3)

All lines are of commensurate length. (3.4)

Restriction (3.1) means that the cross-sectional shape of the transmission line does not change in the direction of propagation. This restriction is necessary if a simple mathematical transfer matrix for the line is desired. Non-uniform lines in general have transfer matrix entries which,

as a function of frequency, are expressible only as an infinite series[2]. Thus a non-uniform line presents formidible mathematical difficulties.

Restriction (3.2) is not strictly true of course, for all metals have a finite conductivity. In addition, at microwave frequencies the skin effect is prevalent, which reduces the effective cross-sectional area that current can flow through. Furthermore, the "hot" line in microstrip is supported by a dielectric which will have some loss at microwave frequencies. The devices to be subsequently considered, however, are compact. In fact, at center frequency, it will be seen that they are at most a few wavelengths long, and thus have very small loss. This loss may be minimized by the usual techniques of plating with silver, gold, etc.

The meaning of restriction (3.3) is that lines with different wavelength vs. frequency relationships (i.e., waveguide and stripline) should not be used in the same network. It would be possible to do this, of course, but leads (once again) to significant mathematical complications, as the different transfer matrices would have different frequency variations.

The most severe restriction is (3.4). It reduces the set of possible transmission line networks satisfying (3.1), (3.2), and (3.3) to a small but important subset. By commensurate it is meant that every line length l_i is an integer multiple of some common length l_o in the network. The reason for imposing (3.4) is again mathematical simplicity. The

frequency behaviour of all lines now have a common frequency variable (ie., a line which has $l_1 = 5l_o$ may be viewed as five lengths of line, each with length l_o, cascaded together). If (3.4) is not met, however, then multi-variable network theory must be used. This theory has been little developed so far, and much work remains to be done in this important field before it can be put to practical use.

3.2 The Tangent Transformation.

In Chapter 2 the transfer matrix for a length l of lossless uniform transmission line was given as

$$\begin{pmatrix} A & B \\ C & D \end{pmatrix} = \begin{pmatrix} \cos\beta\ell & jZ_o\sin\beta\ell \\ jY_o\sin\beta\ell & \cos\beta\ell \end{pmatrix}. \tag{3.5}$$

This equation may be rewritten as

$$\begin{pmatrix} A & B \\ C & D \end{pmatrix} = \cos\beta\ell \begin{pmatrix} 1 & jZ_o\tan\beta\ell \\ jY_o\tan\beta\ell & 1 \end{pmatrix}$$

$$= \frac{1}{(1+\tan^2\beta\ell)^{\frac{1}{2}}} \begin{pmatrix} 1 & jZ_o\tan\beta\ell \\ jY_o\tan\beta\ell & 1 \end{pmatrix}$$

$$= \frac{1}{(1-\tanh^2 j\beta\ell)^{\frac{1}{2}}} \begin{pmatrix} 1 & Z_o\tanh j\beta\ell \\ Y_o\tanh j\beta\ell & 1 \end{pmatrix}.$$

Now an analytic continuation process is performed, similar to the one in the last chapter when jw was extended to the s-plane. Let

$$\gamma(s)\Big|_{s=jw} = j\beta(w).$$

The transfer matrix then becomes

$$\frac{1}{(1-\tanh^2 \gamma\ell)^{\frac{1}{2}}} \begin{pmatrix} 1 & Z_o \tanh \gamma\ell \\ Y_o \tanh \gamma\ell & 1 \end{pmatrix}$$

$$= \frac{1}{(1-t^2)^{\frac{1}{2}}} \begin{pmatrix} 1 & Z_o t \\ Y_o t & 1 \end{pmatrix}. \qquad (3.6)$$

Thus the only (complex) frequency variable involved is t. The process may be viewed as a conformal transformation of the complex variable s to the complex variable t. This transformation was first introduced by Richards[3] for TEM transmission lines. For that case $\beta = \frac{w}{c}$, where c is the velocity of TEM electromagnetic propagation in the dielectric medium of the line, and $\gamma = \frac{s}{c}$. The conformal mapping $t = \tanh s \frac{l}{c}$ is shown[4] in Fig.3.1. It is seen that a semi-infinite strip in the s-plane maps into an entire t-plane. The t-planes corresponding to two adjacent s-plane strips are linked together by the branch cuts[5] as shown. Also it is seen that the right-half s-plane is mapped into the right-half t-plane, that a segment of the imaginary axis of the s-plane is mapped into the imaginary axis of the t-plane, and that the real axis of the s-plane ($k = o$) is mapped into a segment of the real axis in the t-plane. The transfer matrix for a transmission line has entries which are transendental functions in the s-plane and therefore give rise to a zero pattern in the semi-infinite strip in Fig.3.1. which is repeated again and again as k takes on all integer values. In

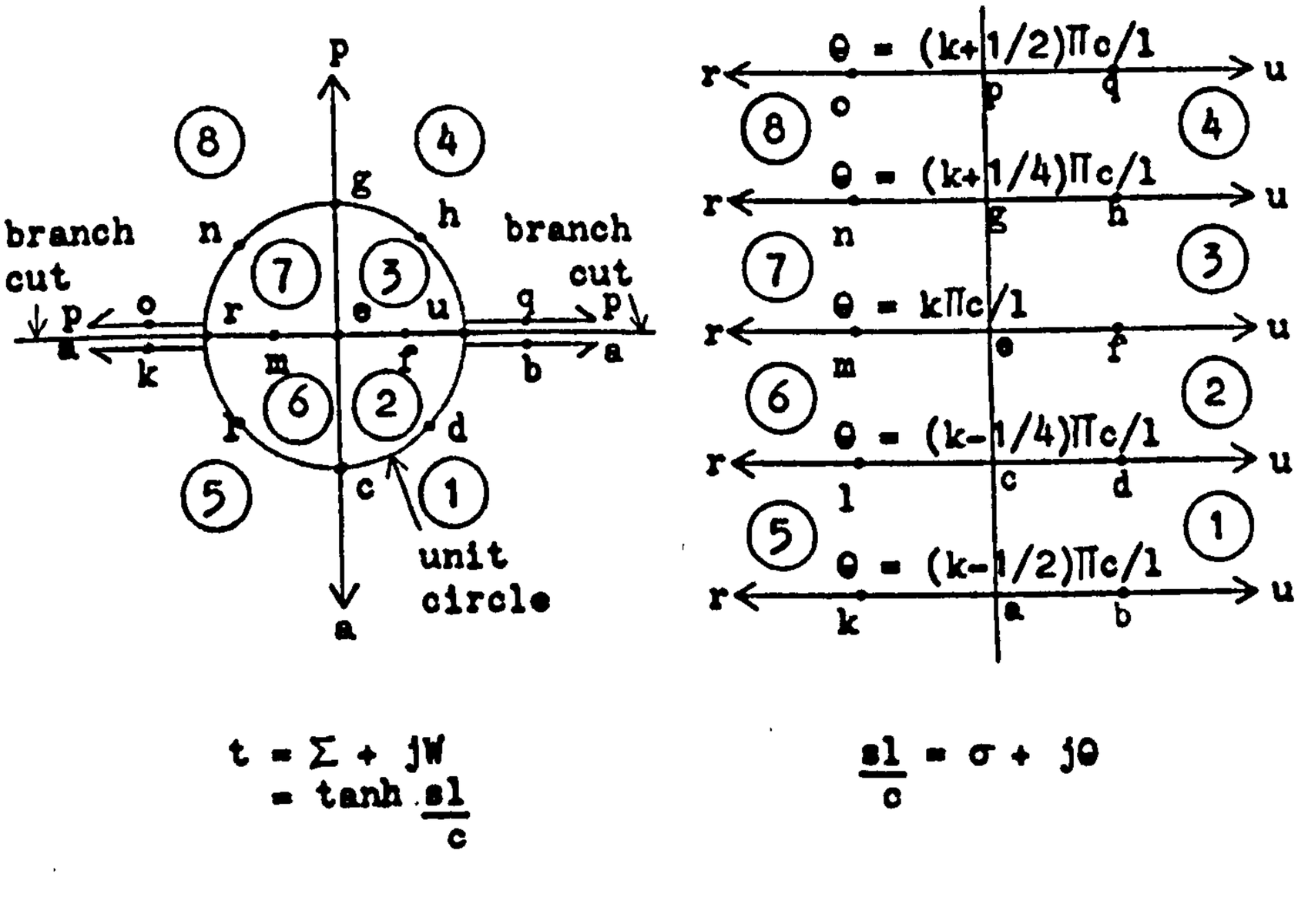

$$t = \Sigma + jW = \tanh \frac{sl}{c} \qquad \frac{sl}{c} = \sigma + j\theta$$

Fig. 3.1. The conformal mapping $t = \tanh \frac{sl}{c}$.

the t-plane, however, these entries are (excepting the common factor $(1-t^2)^{\frac{1}{2}}$) rational functions of t.

3.3 Driving-Point Impedances and Richards' Theorem.

For most theoretical discussions s may be normalized to 1/c to give

$$t = \tanh s. \tag{3.7}$$

From the last chapter it is seen that a necessary and sufficient condition for Z(s) to represent the driving-point impedance for a passive network is that Z(s) be positive real, or that

$$R_e\{Z(s)\} \geq 0 \quad \text{when } R_e\{s\} \geq 0,$$

and $$Im\{Z(s)\} = 0 \quad \text{when } Im\{s\} = 0.$$

Now it is desired to show that Z(t) for a transmission line network is a rational real function of t, and furthermore is p.r.

Suppose a given $Z'(t)$ is a real rational function of t. Then the driving-point impedance of a basic length of transmission line (commonly referred to as a unit element) of impedance Z_o terminated with $Z'(t)$ is therefore

$$Z(t) = \frac{A\,Z'(t)+B}{C\,Z'(t)+D}$$

$$= \frac{Z'(t)+Z_o t}{Y_o t\,Z'(t)+1}, \tag{3.8}$$

which again is obviously a real rational function of t.

Thus this property cannot be destroyed by adding a unit element. But the only basic network elements available (other than unit elements) are open-circuits, short-circuits, and lumped resistors, which are not irrational functions of t (since the network is commensurate), thus by induction all driving-point impedances are rational functions of t. Also, since all matrix operations involved in forming the driving-point impedance consist of addition and multiplication of the real positive resistances and the real positive coefficients of the transmission line transfer matrix, it follows that any driving-point impedance Z will be a rational function of t with real positive coefficients.

Thus

$$\text{Im}\left\{Z(t)\right\} = 0 \quad \text{when Im}\left\{t\right\} = 0. \tag{3.9}$$

It was shown in chapter 2 that a p.r. Z(s) does not have poles or zeros in the region $R_e\{s\}>0$. But the poles and zeros of Z(s) and Z(t) are linked by the mapping shown in Fig.3.1. This implies that Z(t) (and $Z^{-1}(t)$) is analytic in the region $R_e\{t\}>0$. Now since $R_e\{Z(t)\}\geq 0$ when $R_e\{t\}=0$, by a result from complex variable theory (Poisson's integral equations) it is seen that

$$R_e\left\{Z(t)\right\} \geq 0 \quad \text{when } R_e\left\{t\right\} \geq 0. \tag{3.10}$$

Eqs.(3.9) and (3.10) establish that Z(t) is a positive real function of t. This same result can be established through the mapping shown in Fig.3.1.

A lumped-element network containing no coupled coils with an impedance function Z(s) may be converted to a transmission line network of impedance Z(t) by replacing the reactive lumped elements by suitable transmission line stubs. An inductance of reactance jLw is replaced by a short-circuited stub of input impedance $jZ\tan\theta/\tan\theta_o$; a capacitance of susceptance jCw is replaced by an open-circuited stub of input susceptance $jY\tan\theta/\tan\theta_o$, where the factor $\tan\theta_o$ has been included as a scale factor so that the edge of the passband may be fixed at the arbitrary value of electrical length θ_o .

As an example, consider the Butterworth insertion loss function synthesised in section 2.4.2. It is recalled that

$$\frac{P_o}{P_L} = 1 + w^6 \quad . \tag{3.11}$$

The corresponding distributed filter has the insertion loss function

$$\frac{P_o}{P_L} = 1 + \frac{\tan^6\theta}{\tan^6\theta_o} \quad , \tag{3.12}$$

as shown in Fig.3.2. The lumped element network of Fig.2.5 is thus transformed, as shown in Fig.3.3.

The distributed network of Fig.3.3 consists of a number of stubs connected to the same physical point in the network and there is no provision for separation of the stubs for ease

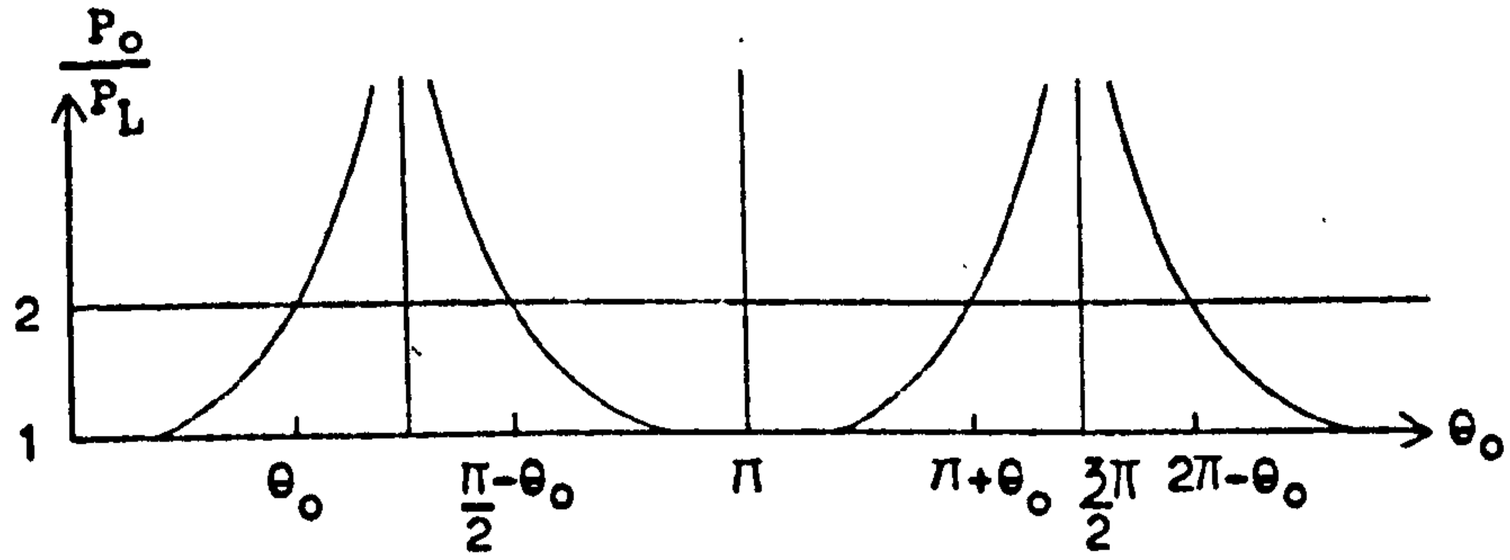

Fig. 3.2. Butterworth insertion loss function of Eq. (3.12).

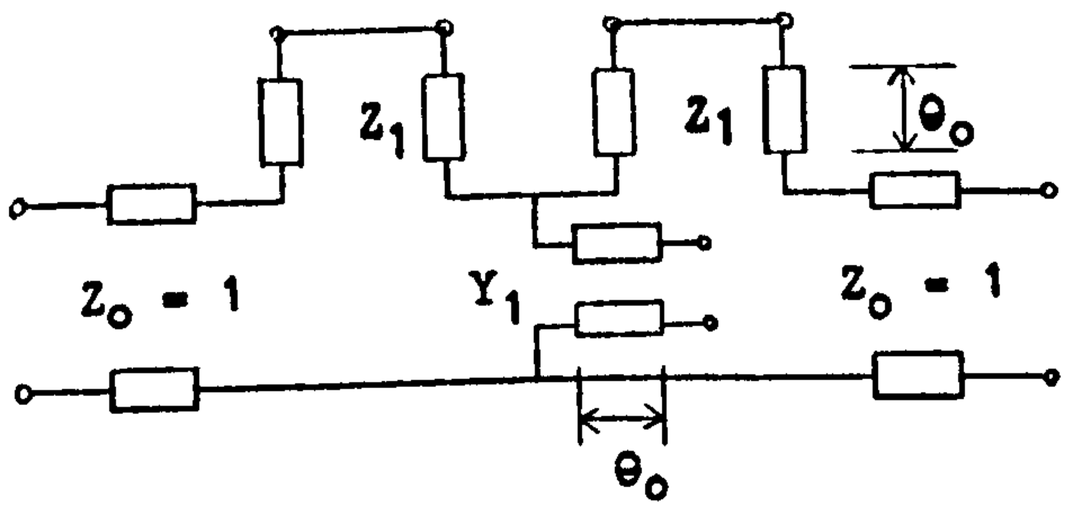

$Z_1 \tan \theta_o = 1$
$Y_1 \tan \theta_o = 2$

(The stubs are all connected to the same physical point)

Fig. 3.3. A transmission line network having the insertion loss of Fig. 3.2.

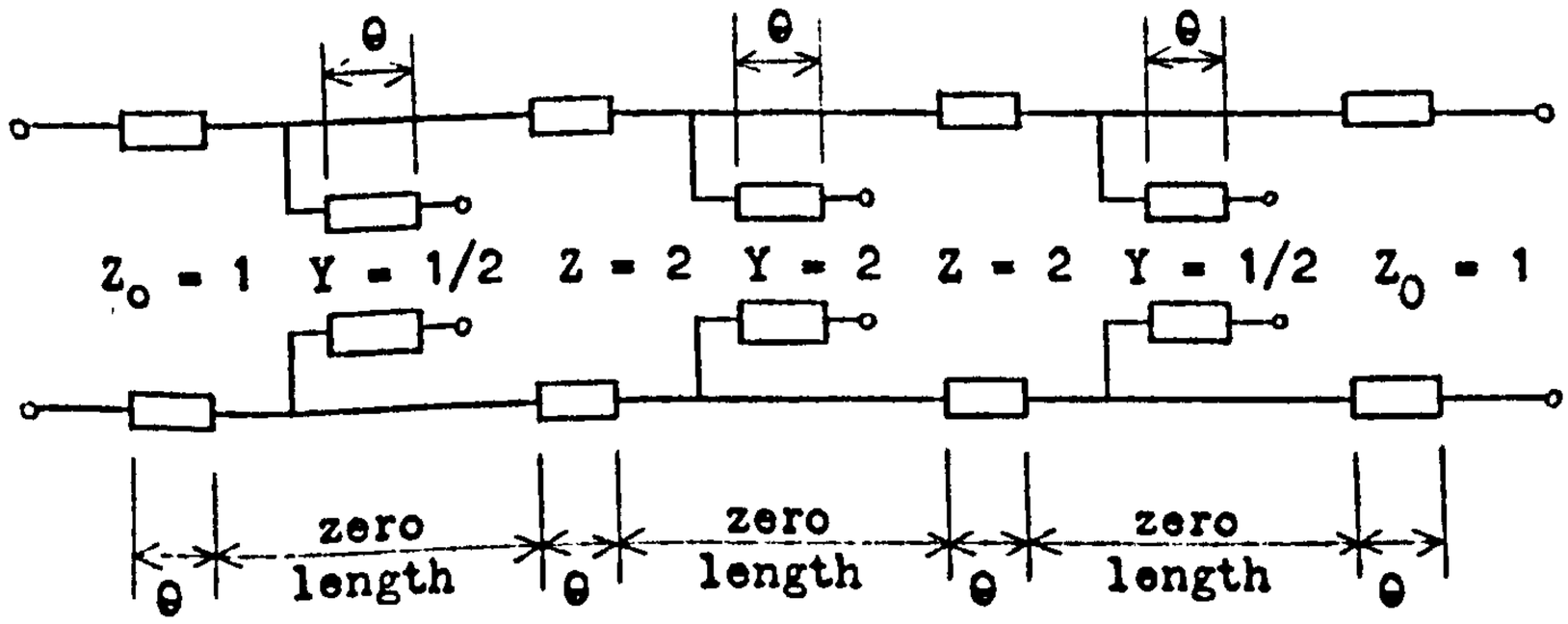

Fig. 3.4. A realizable transmission line network having the insertion loss of Fig. 3.2.

of manufacture, and indeed, of physical realizability in the practical sense. This most important point in the theory of distributed networks must be emphasized, namely that networks resulting from any proposed synthesis procedure must satisfy the elementary condition that it be at least possible to construct them, otherwise the problems are trivial.

The stubs in Fig.3.3 may be separated by using unit elements. Any number of unit elements of characteristic impedance 1 and length θ_0 may be inserted between the last stub and the load $R_L = 1$, since the terminating impedance of the network is still 1 (the line is matched), without affecting the insertion loss. If a means could then be found for interchanging the position of a unit element and a stub, enough unit elements could be "jumped" into the network so that each stub would be separated from its neighbour by a unit element and the construction of the network is then perfectly feasible. The resulting network is shown in Fig.3.4. The method whereby a simple series or shunt stub may be interchanged in position with a unit element has been given by Kuroda [6] who presented a set of identities known as "Kuroda's Identities" which can readily be used with a simple ladder (shunt C's and series L's) prototype network. Levy[7] has extended Kuroda's work to the case where an arbitrary network in t followed by a unit element may be shown to be equivalent to another (realizable) network preceeded by a unit element.

These procedures have, of course, a sound mathematical basis expressed most concisely by Richards' theorem[8]. This theorem states that a unit element of characteristic impedance Z(1) may always be removed from a p.r. impedance Z(t) leaving a remainder Z'(t) which is still p.r. Thus for any network followed by a unit element one computes the driving-point impedance at the port remote from the unit elements and extracts another unit element of characteristic impedance Z (1) leaving a p.r. remainder impedance. Using $Z_0 = Z(1)$ in Eq.(3.8), it is found that

$$Z(t) = Z(1)\ \frac{Z'(t) + t\ Z(1)}{Z(1) + t\ Z'(t)}\ , \tag{3.13}$$

where a unit element of characteristic impedance Z(1) is extracted from Z(t) leaving a remainder Z'(t). Solving for Z'(t),

$$Z'(t) = Z(1)\ \frac{Z(t) - t\ Z(1)}{Z(1) - t\ Z(t)}\ , \tag{3.14}$$

and Richards' theorem states that Z'(t) is positive real if Z(t) is p.r. It is evident from Eq.(3.14) that Z'(t) has a factor (1-t) in numerator and denominator. After cancellation of this factor the degree of Z'(t) will be equal to the degree of Z(t). If, however, $Z(-1) = -Z(1)$ then the factor (1+t) also exists in the numerator and denominator of Z'(t), and hence it will be of lower degree than Z(t).

In order to apply Richards' theorem when it is desired to extract a unit element from a transfer matrix, the follow-

ing procedure is used. The inverse matrix for a unit element can readily be calculated from Eq.(3.6) as

$$\frac{1}{(1-t^2)^{\frac{1}{2}}} \begin{pmatrix} 1 & -Z_o t \\ -Y_o t & 1 \end{pmatrix} . \tag{3.15}$$

Now the transfer matrix for a lossless cascade of stubs and n unit elements will be of the form

$$\frac{1}{(1-t^2)^{\frac{n}{2}}} \begin{pmatrix} A & B \\ C & D \end{pmatrix} . \tag{3.16}$$

Premultiplying the matrix by Eq.(3.15) gives the result

$$\frac{1}{(1-t^2)^{\frac{n-1}{2}}} \times \frac{1}{1-t^2} \begin{pmatrix} 1 & -Z_o t \\ -Y_o t & 1 \end{pmatrix} \begin{pmatrix} A & B \\ C & D \end{pmatrix}$$

$$= \frac{1}{(1-t^2)^{\frac{n-1}{2}}} \begin{pmatrix} \frac{A-Z_o tC}{1-t^2} & \frac{B-Z_o tD}{1-t^2} \\ \frac{C-Y_o tA}{1-t^2} & \frac{D-Y_o tB}{1-t^2} \end{pmatrix}$$

$$= \frac{1}{(1-t^2)^{\frac{n-1}{2}}} \begin{pmatrix} \underline{A} & \underline{B} \\ \underline{C} & \underline{D} \end{pmatrix} . \tag{3.17}$$

It is required that the resulting transfer matrix be of lower degree (since a unit element has been extracted). This means that $\underline{A}$, $\underline{B}$, $\underline{C}$, $\underline{D}$ must all contain the factor $(1-t^2)$, which leads to the equations

$$Z_o = \frac{A(1)}{C(1)} = \frac{-A(-1)}{C(-1)} = \frac{B(1)}{D(1)} = \frac{-B(-1)}{D(-1)} . \tag{3.18}$$

It only remains to show that the reduced degree matrix (3.17) represents a realizable transmission line network. Now Richards' theorem states that from the driving-point impedances A/C and B/D (corresponding to the output open-and short-circuited), an impedance equal to A(1)/C(1) and B(1)/D(1) may be extracted, respectively, with the result that $\underline{A}/\underline{C}$ and $\underline{B}/\underline{D}$ are positive real driving-point impedances. But this impedance value is precisely that given by Eq.(3.18), and so the desired unit element extraction may be carried out.

The proof of Richards' theorem is simple and interesting. The voltage reflection coefficient between Z(t) and a real impedance Z(1) is, by Eq.(2.17),

$$\Gamma = \frac{Z(t) - Z(1)}{Z(t) + Z(1)} \quad , \tag{2.17}$$

and it is easily derived that the reflection coefficient between Z'(t) and Z(1) is

$$\Gamma'(t) = \Gamma(t) \frac{1+t}{1-t} \quad .$$

Now since Z(t) is p.r., $\Gamma(t)$ is bounded real (b.r.) and

$$1 \geq \Gamma(jW)\,\Gamma(-jW) \geq 0,$$

where $t = \sigma + jW$.

But

$$\Gamma'(jW)\;\Gamma'(-jW) = \Gamma(jW)\;\Gamma(-jW).$$

Therefore $\Gamma'(t)$ is b.r. provided $\Gamma(t)$ has a first order zero at $t=1$, which, since Z(1) is the impedance of the extracted unit element, it has. Hence the associated Z'(t) is p.r.

The application of this theorem is straightforward. In simple ladder design a specified Z(t) is realizable with series short-circuited and shunt open-circuited stubs. Now by application of Richards' theorem after extraction of each stub the stubs may be separated by unit elements and a physically realizable design completed. If the transfer matrix approach is used, the starting point is to determine the transfer matrix for the lossless network (which is connected between the source and load resistances R_g and R_L) from the reflection coefficient. This matrix is then premultiplied and/or postmultiplied by the transfer matrix of a unit element with characteristic impedance R_g(for premultiplication) or R_L(for postmultiplication) until n lines are in place, n being the number of unit elements required to separate the stubs. The decomposition of the augmented transfer matrix then proceeds in the customary manner. This approach is computationally longer than the preceeding method, but offers accuracy checks at each stage.

Both of these methods and that of "jumping" unit elements into the prototype network have advantages. The methods using Richards' theorem are best where explicit formulae for the element values are not available, and the network must be synthesized directly anyhow, whereas, if explicit formulae are available for the prototype (as with Chebyshev or maximally flat filters[9]), the alternative method may be most convenient. A drawback to using unit elements as "spacers" between

stubs, however, is that they do not contribute to the insertion loss specification. In fact, in the above design methods the only effect of the unit elements is to give added delay between input and output. It is possible to incorporate these unit elements into the insertion loss specification[10], which will result in superior performance for the same number of network elements.

The Darlington insertion loss method outlined in the last chapter may now be employed in the synthesis of transmission line networks. From a given structure the form of the insertion loss (as a function of t) may be deduced by analysis. The approximation problem then consists of arranging the coefficients in the insertion loss to meet some specification function as closely as possible, within the limitations imposed by the form of the insertion loss. From the insertion loss the voltage reflection coefficient is calculated (by factorization), and the transfer matrix for the lossless transmission line network is established. Next the transfer matrix may be augmented, if necessary, to provide enough unit elements for physical realizability, as discussed previously. Unit elements (and stubs) are then removed by multiplying the overall transfer matrix by the inverse matrix of the desired network element with the requirement that the resulting transfer matrix be of lower degree.

3.4 Cascaded Transmission Line Networks.

A network of cascaded transmission lines is obviously of considerable interest from the point of view of ease of construction, and its properties will be considered in this section.

The transfer matrix of such a network is of the form

$$\frac{1}{(1-t^2)^{n/2}} \prod_{i=1}^{n} \begin{pmatrix} 1 & z_i t \\ y_i t & 1 \end{pmatrix} , \tag{3.19}$$

where n lines are cascaded. Writing the matrix as

$$\frac{1}{(1-t^2)^{n/2}} \begin{pmatrix} \underline{A}(t) & \underline{B}(t) \\ \underline{C}(t) & \underline{D}(t) \end{pmatrix} , \tag{3.20}$$

analysis of a few cases reveals that

(1) $\underline{A}(t)$, $\underline{D}(t)$ are even polynomials in t,

(2) $\underline{B}(t)$, $\underline{C}(t)$ are odd polynomials in t,

(3) Highest degree = n,

(4) Degree $\underline{A}(t)$ = Degree $\underline{D}(t)$,

(5) Degree $\underline{B}(t)$ = Degree $\underline{C}(t)$,

(6) Difference in degrees of $\underline{A}(t)$ and $\underline{C}(t)$ = 1,

(7) All coefficients are positive,

(8) Constant term in $\underline{A}(t)$ and $\underline{D}(t)$ is 1,

and of course,

$$\underline{A}(t)\,\underline{D}(t) - \underline{B}(t)\,\underline{C}(t) = (1-t^2)^n .$$

The insertion loss for a lossless network connected between the source resistance $R_s = 1$ ohm and the load resistance R_L was given in chapter 2 as

$$\frac{P_o}{P_L} = 1 + \frac{1}{4}\left\{\left(\sqrt{R_L}\,A - \sqrt{G_L}\,D\right)^2 + \left(\sqrt{G_L}\,B' - \sqrt{R_L}\,C'\right)^2\right\}, \qquad (2.34)$$

where $B' = jB$, $C' = jC$, and $\begin{pmatrix} A & B \\ C & D \end{pmatrix}$ is the transfer matrix for the lossless network.

Hence it is seen that

$$\frac{P_o}{P_L} = 1 + \frac{P'_{2n}(t)}{(1-t^2)^n}, \qquad (3.21)$$

where P'_{2n} is an even polynomial of degree 2n. When t is on the frequency axis, $t = jW$, $t^2 = -W^2$, and Eq.(3.21) becomes

$$\left.\frac{P_o}{P_L}\right|_{t=jW} = 1 + \frac{Q_n(W^2)}{(1+W^2)^n}. \qquad (3.22)$$

From Eq.(3.7) $W = \tan\theta$. By using basic trignometric identities, $(1+W^2)^{-n} = (\sec^2\theta)^{-n} = \cos^{2n}\theta$, and $W^2 = \frac{\sin^2\theta}{\cos^2\theta}$. Thus Eq.(3.22) is found to be equivalent to

$$\frac{P_o}{P_L} = 1 + P_n(\cos^2\theta), \qquad (3.23)$$

where P_n is an n'th degree polynomial. Since $\cos^2\theta = 1-\sin^2\theta$, $\sin^2\theta$ may replace the $\cos^2\theta$ term in Eq.(3.23). This equation

enables many amplitude approximation problems to be solved directly in terms of sine or cosine functions. It is customary to normalize the $\cos\theta$ variable to the value $\cos\theta_0$, θ_0 being the edge of the passband. Then Eq.(3.23) may be written as

$$\frac{P_0}{P_L} = 1 + P_n\left(\frac{\cos^2\theta}{\cos^2\theta_0}\right) \quad . \tag{3.24}$$

Observe that in this equation P_0/P_L can have no poles for real values of θ.

Since B and C are odd functions of t, when $t = jW = 0$ then $B = C = 0$. It was also seen that $A(0) = D(0) = 1$. Thus at zero frequency the transfer matrix for a cascade of unit elements is

$$\begin{pmatrix} 1 & 0 \\ 0 & 1 \end{pmatrix} \quad , \tag{3.25}$$

i.e., the cascade is transparent at DC. The insertion loss at $t = 0$ is

$$\frac{P_0}{P_L} = 1 + \frac{(R_L-1)^2}{4R_L} \quad . \tag{3.26}$$

In Eq.(3.24) this fact implies that

$$\frac{(R_L-1)^2}{4R_L} = P_n\left(\frac{1}{\cos^2\theta_0}\right) \quad . \tag{3.27}$$

In other words, one degree of freedom in the selection of the coefficients for $P_n\left(\frac{\cos^2\theta}{\cos^2\theta_0}\right)$ must be given up if R_L is specified in advance. This can lead to complications as will be seen in the next chapter.

Chapter 3 REFERENCES

1. Ragan, G.L.: "Microwave Transmission Circuits". (Radiation Laboratory Series, McGraw-Hill, 1948).

2. Protonotarios, E.N. and Wing, O.: "Analysis and intrinsic properties of the general nonuniform transmission line", IEEE Trans., 1956, MTT-15 , pp.142-150.

3. Richards, P.I.: "Resistor-transmission-line circuits", Proc. I.R.E., 1948, 34, p.217.

4. Kober, H.: "Dictionary of Conformal Representations". (Dover Publications, 1947), p.88.

5. Guillemin, E.A.: "The Mathematics of Circuit Analysis". (M.I.T. Press, 1949), pp.310-317.

6. Ozaki, H. and Ishii, J.: "Synthesis of a class of strip-line filters", IRE Trans., 1958, CT5, p.172.

7. Levy, R.: "A general equivalent circuit transformation for distributed networks", IEEE Trans, 1956, CT12, p.457.

8. Richards, P.I.: "General impedance-function theory", Quart. Math., 1948, 6, p.21.

9. Weinberg, L.: "Network Analysis and Synthesis". (McGraw-Hill, Inc., 1962), pp.651-669.

10. Carlin, H.J. and Kohler, W.: "Direct synthesis of band-pass transmission line structures", IEEE Trans., 1965, MTT-13, pp.283-297.

Chapter 4

Synthesis of Low-Pass Lumped and Distributed Filters

4.1 Conventional Chebyshev Design.

Consider the low-pass lumped ladder network in Fig.4.1. The transfer matrix for the lossless network is of the form

$$\prod_{i=1}^{n} \begin{pmatrix} 1 & L_i s \\ C_i s & 1 + L_i C_i s^2 \end{pmatrix} , \qquad (4.1)$$

where L_n is zero if an odd number of elements is desired.

Writing this matrix as

$$\begin{pmatrix} A(s) & B(s) \\ C(s) & D(s) \end{pmatrix} ,$$

analysis of a few cases reveals that

(1) A(s) and D(s) are even polynomials in s,

(2) B(s) and C(s) are odd polynomials in s,

(3) Highest degree =n,

(4) Constant term in A(s) and D(s) is 1,

(5) A(s) D(s) - B(s) C(s) =1.

The associated insertion loss may be written as

$$\frac{P_o}{P_L} = 1 + \frac{1}{4}\left\{ \left(\sqrt{R_L}\, A - \sqrt{G_L}\, D\right)^2 + \left(\sqrt{G_L}\, B' - \sqrt{R_L}\, C'\right)^2 \right\}$$

$$= 1 + P'_{2n}(s), \qquad (2.34)$$

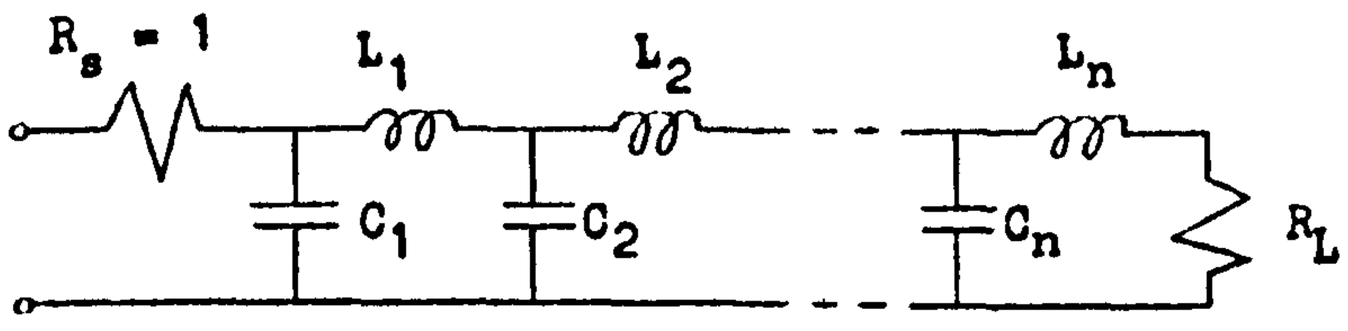

Fig. 4.1. Low-pass lumped ladder network.

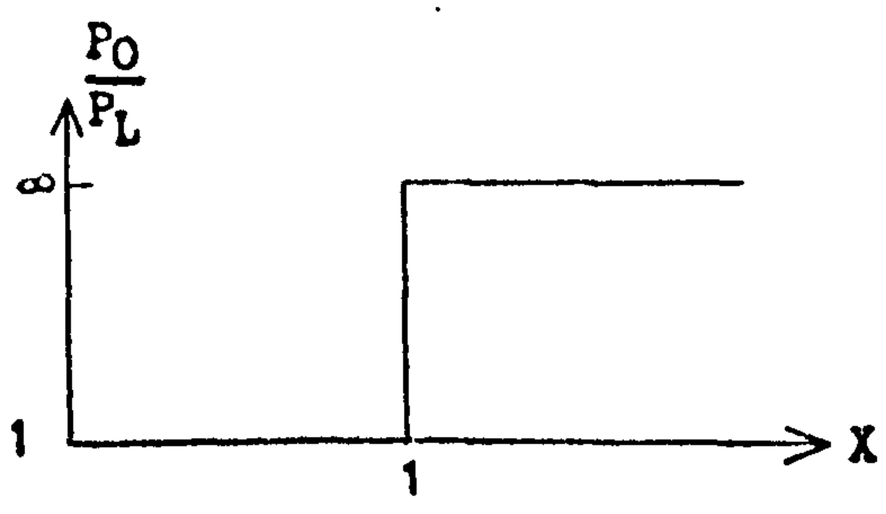

Fig. 4.2. Ideal low-pass insertion loss specification function.

where P'_{2n} is an even polynomial of degree 2n. When $s = jw$,

$$\frac{P_o}{P_L} = 1 + P_n(w^2),$$

where P_n is a polynomial of degree n. Now the form of the insertion loss is just the same for this case as for the cascade of transmission lines in the last chapter, i.e.,

$$\frac{P_o}{P_L} = 1 + P_n(x^2) \quad , \tag{4.2}$$

where $x = w$ for the lumped case and $x = \frac{\cos\theta}{\cos\theta_0}$ or $\frac{\sin\theta}{\sin\theta_0}$ for the distributed case.

An ideal low-pass filter with $R_S = R_L = 1$ would have the insertion loss shown in Fig.4.2, where the passband has been normalized to unity. Since no finite-degree polynomial can represent this "brick wall" response exactly, which polynomial of degree n will approximate it best? The problem of determining such an optimum polynomial can be more precisely stated as follows:

Among all polynomials of degree not exceeding n and not exceeding unity in absolute value over the interval $-1 \leq x \leq 1$, determine the polynomial that exceeds all others outside this interval. The answer to this question turns out to be $T_n(x)$, which is a Chebyshev polynomial of the first kind[1].

$T_n(x)$ may be defined by

$$T_n(x) = \cos(n\cos^{-1}x). \tag{4.3}$$

As x goes from -1 to 1, $\cos^{-1}x$ goes from π to 0 radians (principal value) and so $n\cos^{-1}x$ goes from $n\pi$ to 0 radians. This means that $T_n(x)$ oscillates between -1 and 1 n times as x goes from -1 to 1. If $|x| > 1$, then $\cos^{-1}(x) = j\ \cosh^{-1}(x)$, and $T_n(x) = \cosh(n\ \cosh^{-1}x)$. That $T_n(x)$ is a polynomial in x may be shown as follows.

Let $y = \cos^{-1}(x)$. Then, by use of trignometric identities,

$$T_{n+1}(x) = \cos(n+1)y = \cos\ n\ y\ \cos\ y - \sin\ n\ y\ \sin\ y$$

$$= \cos\ n\ y\ \cos\ y + \frac{1}{2}\cos(n+1)y - \frac{1}{2}\cos(n-1)y,$$

which gives

$$T_{n+1}(x) = \cos(n+1)y = 2\cos\ n\ y\ \cos\ y - \cos\ (n-1)y.$$

Now $\cos\ y = x$. Therefore,

$$T_{n+1}(x) = 2xT_n(x) - T_{n-1}(x). \qquad (4.4)$$

Though Chebyshev polynomials are used only for $n > 0$, the definition also holds for $n = 0$. Thus by inspection it is seen that $T_0(x) = 1$ and $T_1(x) = x$. Eq.(4.4) shows by induction that $T_n(x)$ is indeed a polynomial. T_2, T_3, and T_4 may next be computed from T_0 and T_1 and from the recurrence relation Eq.(4.4) as

$$\begin{aligned} T_1(x) &= x, \\ T_2(x) &= 2x^2 - 1, \\ T_3(x) &= 4x^3 - 3x, \\ T_4(x) &= 8x^4 - 8x^2 + 1. \end{aligned} \qquad (4.5)$$

Some characteristics of these polynomials are immediately evident. They are even and odd functions for n even and odd respectively. Every coefficient is an integer, the coefficient of the term of highest degree being 2^{n-1}. At the origin

$$T_{2n}(0) = \pm 1,$$
$$T_{2n+1}(0) = 0. \qquad (4.6)$$

Since these polynomials take on negative as well as positive values with a maximum value of unity in the passband $-1 \leq x \leq 1$, they are not suitable by themselves to approximate an insertion loss of unity in the passband. Therefore they are first squared and multiplied by a suitable scaling function (called the ripple level e^2), i.e.,

$$\frac{P_o}{P_L} = 1 + e^2 T_n^2 (x). \qquad (4.7)$$

From the trignometric identity $\cos^2(ny) = \frac{1}{2}(\cos 2ny + 1)$, it is seen that

$$T_n^2 (x) = \frac{1}{2}(T_{2n}(x) + 1), \qquad (4.8)$$

and so a Chebyshev polynomial of even degree may be used in a modified form of Eq.(4.7).

An interesting fact emerges from the examination of Eqs.(4.6) and (4.7); namely that

$$\left.\frac{P_o}{P_L}\right|_{x=0} = \begin{cases} 1 & n \text{ odd}, \\ 1+e^2 & n \text{ even}. \end{cases} \tag{4.9}$$

In chapter 3 it was found that

$$\left.\frac{P_o}{P_L}\right|_{x=0} = 1 + \frac{(R-1)^2}{4R}\ , \tag{4.10}$$

where $x = \sin\theta/\sin\theta_o$ and $R = R_L/R_s$. The same is seen to be true for the structure in Fig.4.1, (where now $x=w$), since the lossless network is completely transparent at DC.

Comparison of Eqs.(4.9) and (4.10) reveals that, for the insertion loss specification (4.7), R is also determined, i.e.

$R = 1$ for n odd,

$\frac{(R-1)^2}{4R} = e^2$ for n even.

This specification has been used by Levy[2] in the design of distributed low-pass filter prototypes (where $x = \sin\theta/\sin\theta_o$). A distributed filter is defined as a doubly terminated cascade of commensurate length transmission lines, as discussed in chapter 3.

The insertion loss specification (4.7) may be generalized to accommodate an arbitrary load to source resistance ratio with the addition of another parameter, e.g.

$$\frac{P_o}{P_L} = 1 + k^2 + e^2\, T_n^2(x), \tag{4.11}$$

where now

$$k^2 = \frac{(R-1)^2}{4R} \quad \text{for n odd,} \tag{4.12}$$

and

$$k^2 = \frac{(R-1)^2}{4R} - e^2 \geq 0 \quad \text{for n even.} \tag{4.13}$$

In Eq.(4.11) $k^2 \geq 0$ since $P_o/P_L \geq 1$ for all x, and hence Eq.(4.13) puts a definite limit on the ripple level e^2 when a value of R has been decided upon. The specification (4.11) has been used by Weinberg[3] in the design of lumped, low-pass Chebyshev filter prototypes. Tables for a large variety of ripple levels and resistance ratios for various n are given in this reference. In these tables there are blank spaces which occur whenever Eq.(4.13) is not fulfilled by the input specifications.

In the calculation of Weinberg's tables of Chebyshev filters[3], a set of closed formulae are used to calculate the filter element values, and hence the formal synthesis procedure need not be carried out. These remarkable formulae are due to Takahasi[4], who not only found their general form but also <u>proved</u> that they are correct. In the specification (4.11) it is seen that when $k^2 > 0$ the numerator of $\Gamma(s)\,\Gamma(-s)$ formed from $P_o/P_L - 1$ will have zeros not on the

imaginary axis but in the complex s-plane. Thus many choices are possible for the numerator of $\Gamma(s)$, as discussed in chapter 2. Takahasi's results apply to the case where all the zeros of $\Gamma(s)$ are chosen from the left-half s-plane and to the case where the zeros of $\Gamma(s)$ alternate between the r.h.p. and l.h.p. Closed formulae for the element values for other choices of the zeros of $\Gamma(s)$ have not been discovered yet. It is seen that Takahasi's results will apply to the insertion loss specification (4.7), since this may be viewed as a case where the zeros of $\Gamma(s)$, which are on the imaginary axis, are in the left-half plane.

4.2 Modified Design Theory.

In the insertion loss specification

$$\frac{P_o}{P_L} = 1 + k^2 + e^2 \cdot T_n^2(X) \qquad (4.11)$$

there are three degrees of freedom, k^2, e^2, and n. In most filter design work the resistance ratio $R = R_L/R_s$ is known at the outset, and thus one degree of freedom is used for R. This leaves two degrees of freedom, which are usually determined from either (1) or (2) and either (3) or (4) of the following list:

(1) Maximum passband insertion loss.

(2) Allowable passband ripple level.

(3) Stop band attenuation rate (for large X).

(4) Required attenuation at one or more stopband frequency points. (4.14)

In the design of a microwave distributed filter the input and output resistances are nearly always equal to the system characteristic impedance (which is usually 50Ω). In this case $R=1$. In lumped filter design a doubly terminated filter having a $R=1$ (which gives maximum power transfer when $\frac{P_o}{P_L}=1$) is also frequently met in practice. Thus the $R=1$ case is by far the most important one in low-pass filter design. When $R=1$, it is seen that, for n odd, $k^2=0$ (from Eq.(4.12)) and so

$$\frac{P_o}{P_L} = 1+e^2\,T_n^2(X). \tag{4.7}$$

Since $T_n(X)$ is an optimum polynomial, as seen earlier, this specification is an optimum one for n odd. For n even, Eq.(4.13) states that

$$k^2 = \frac{(R-1)^2}{4R} - e^2 \geq 0, \tag{4.13}$$

which implies that $k^2=e^2=0$ and leaves Eq. (4.11) in the form $\frac{P_o}{P_L}=1$, which is clearly a non-optimum filter specification! This is confirmed in Weinberg's tables[3], where there are blank spaces for n even and $R=1$ in the Chebyshev designs. Since approximately half of all filter design problems should lead to a structure with an even number of sections, it is clear that half of the existing Chebyshev

low-pass filter designs (for R=1) have one more section than is necessary. From a cost standpoint this fact is far from trivial; reducing a five section filter to a four section one represents a 20% saving.

When n is even it appears that a rearrangement of the three degrees of freedom in the specification Eq.(4.11) is desirable. In particular, a Chebyshev-like polynomial is desired which is equiripple in the passband except at the origin, where it assumes the correct level for the specified value of R.

The even degree Chebyshev polynomial will now be examined in greater detail. From Eq.(4.3), $T_{2n}(X)$ is defined as

$$T_{2n}(X) \equiv \cos(2n \cos^{-1} X)$$

$$= \cos(n\cos^{-1}(2X^2-1)) = \cos \theta , \qquad (4.15)$$

since $\cos^{-1}(2X^2-1) = 2\cos^{-1} X$ (or $2X^2-1 = \cos 2 \cos^{-1} X = T_2(X)$). Inspection of this equation is interesting. At $X=\pm 1$, $(2X^2-1)=1$, $\cos^{-1}(1)=0$, and so $\theta_{\pm 1}=0$. At $X=0$, $(2X^2-1)=-1$, $\cos^{-1}(-1)=\pi$, and so $\theta_0 = n\pi$. It is now desired to modify Eq.(4.15), so that $\theta_{\pm 1} = 0$, but $n\pi - \frac{\pi}{2} \leq \theta_0 \leq n\pi$. Then $\cos\theta$ would go from 1 (at $X=\pm 1$), ripple between +1 and -1 in the passband, and finish at a predetermined DC level at $X=0$. Eq.(4.15) may gain two degrees of freedom by letting

$$L_{2n}(X,a,b) = \cos(n \cos^{-1} (ax^2 - b)). \qquad (4.16)$$

At $x=\pm 1$, $\theta_{\pm 1} = 0$, which implies that $a-b=1$, or that $a=1+b$.

Thus Eq.(4.16) loses one degree of freedom and becomes

$$L_{2n}(X,b) = \cos(n \cos^{-1}([1+b]X^2 - b)). \tag{4.17}$$

Notice that $([1+b])X^2 - b)$ goes from 1 to $-b$ as X goes from ± 1 to 0. Assume $|b| < 1$. Then $|L_{2n}| \leq 1$ for $|X| \leq 1$. If this were not true, then $\cos^{-1}([1+b]X^2 - b)$ would become imaginary, and L_{2n} is no longer equiripple when $|X| \leq 1$. In fact, the relationship between the DC level and b may easily be shown to be

$$\theta_L = \sin^{-1} |L_{DC}|, \tag{4.18}$$

and that

$$b = \cos\left[\frac{\pi - 2\theta_L}{2n}\right] < 1. \tag{4.19}$$

In the special case of the even n, R = 1 low-pass filter design, $L_{DC} = 0$,

$$\theta_L = 0, \quad b = \cos\frac{\pi}{2n}, \text{ and}$$

$$L_{2n}(X,b) = \cos\left(n\cos^{-1}\left(\left[1+\cos\frac{\pi}{2n}\right]X^2 - \cos\frac{\pi}{2n}\right)\right)$$

$$= T_n\left(\left[1+\cos\frac{\pi}{2n}\right]X^2 - \cos\frac{\pi}{2n}\right). \tag{4.20}$$

These last four equations have been reported by Lind[5], with Eq.(4.20) then being used for the design of lumped and distributed low-pass filters. Eqs.(4.17), (4.18), and (4.19) have also been found by Jones[6],[7], although no specific mention was made of applying them to even n, equally terminated filter designs. Eq.(4.20) has been reported by Vasil'yev[8],

who obtained this equation through a differential equation solution. He also proved that this function is optimal (for the $R=1$, even n case) and then he used it in computing a table of lumped element low-pass filter prototypes with from two to ten sections. Vasil'yev does not apply the result to the synthesis of distributed filters, however, and he does not state the extension in Eqs.(4.17), (4.18), and (4.19).

In Fqs. (4.18) and (4.19), let $|L_{DC}|=1$ (which should result in the conventional Chebyshev design). Then $\Theta_L = \frac{\pi}{2}$, $b=1$, and Eq.(4.17) becomes

$$L_{2n}(X,1) = \cos(n \cos^{-1}(2X^2-1)),$$

which checks with Eq.(4.15). As the value of b is decreased from unity, it can be shown that the zeros of $L_{2n}(X,b)$ shift towards the origin, and the attenuation rate of L_{2n} in the stopband is decreased. When b reaches the lower limit of $\cos\frac{\pi}{2n}$, the two zeros of L_{2n} closest to the origin coalesce at the origin. L_n is equiripple in the passband(except at the origin) during this entire process, of course.

It is interesting to compare the stopband performance of $L_n(x, \cos\frac{\pi}{n})$ (n even) to that of $T_n(X)$, the optimum polynomial. In Fig. 4.3 is shown the stopband attenuation curves for a number of M (from 2 to 12) section low-pass filter designs. The passband ripple level in each case is .5 dB. The broken lines represent optimum Chebyshev designs,

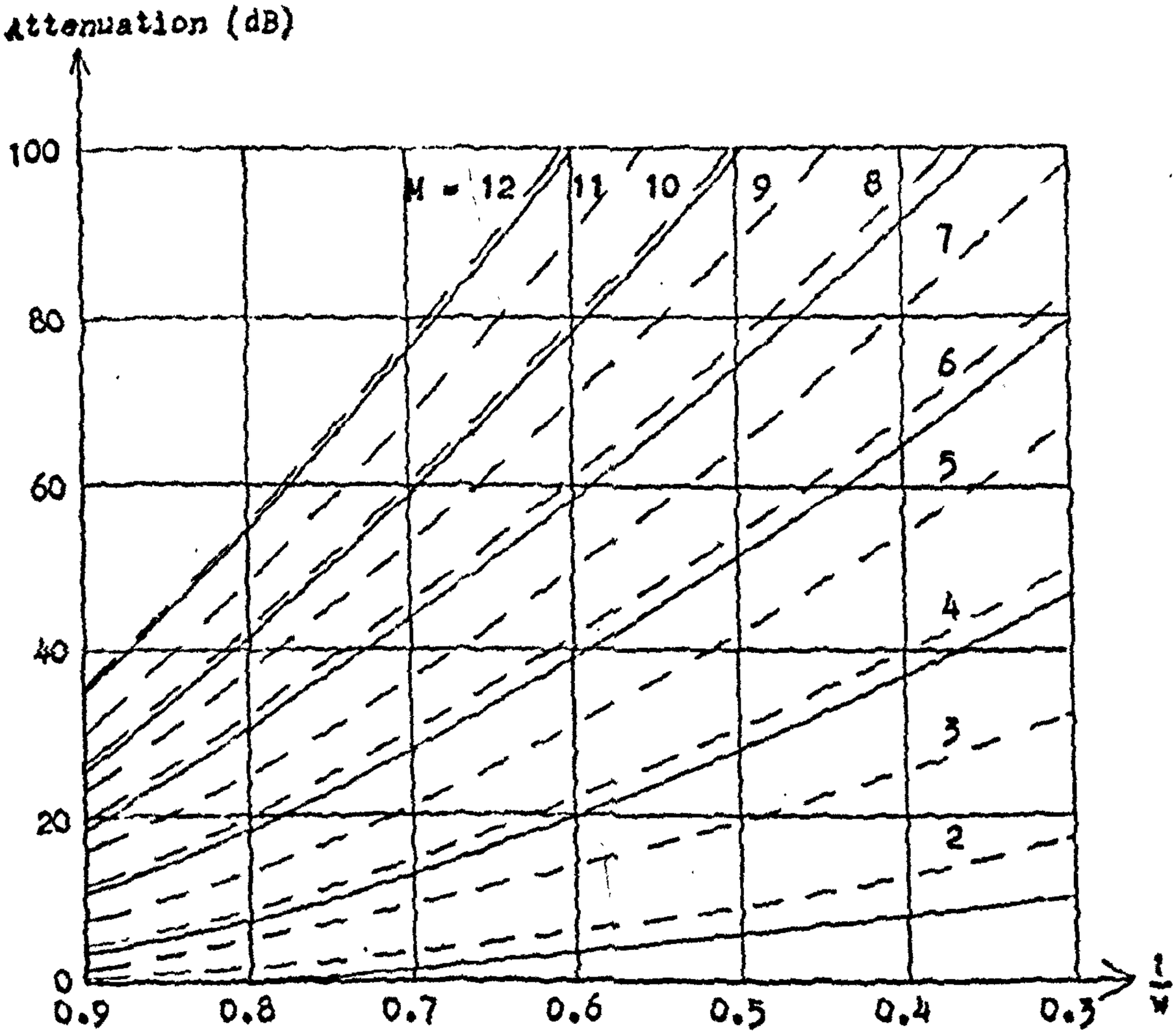

Fig. 4.3. Stopband performance of L_M (——) and T_M (- -) for various M, each having a .5 dB passband ripple level.

which means that for M even, $R \neq 1$. The solid lines represent the results obtained through the specification

$$\frac{P_o}{P_L} = 1 + e^2 L_M^2(X), \qquad (4.21)$$

where M is even and $R = 1$.

It can be seen from these curves that Eq.(4.21) yields filters having a stopband attenuation only slightly inferior to those of the corresponding Chebyshev filters. For a given $w_1 > 1$ the difference between the attenuation levels of the filter types compared vanishes asymtotically with increasing n. A proof that L_M is the optimum polynomial (for a given DC level) is given at the end of this chapter.

4.3 Synthesis of Even N, Equally Terminated, Low-Pass Filters.

4.3.1. Lumped element filters.

The specification function used in this design is

$$\frac{P_o}{P_L} = 1 + e^2 L_{2n}^2 \left(w, \cos \frac{\pi}{2n}\right)$$

$$= 1 + e^2 T_n^2 \left(\left[1 + \cos \frac{\pi}{2n}\right] w^2 - \cos \frac{\pi}{2n} \right), \qquad (4.21)$$

where w is the standard lumped frequency variable. In the Darlington procedure the next step is to find the poles and zeros of $\Gamma(s)$.

The zeros of $\Gamma(s)\,\Gamma(-s)$ in this case are the roots of the polynomial $\frac{P_o}{P_L} - 1$. It is seen that these roots are all at least double roots (there are four roots at the origin) and are on the imaginary axis. Hence a unique factorization results, as discussed in chapter 2.

The zeros of $T_n\left(\left[1 + \cos\frac{\pi}{2n}\right] w^2 - \cos\frac{\pi}{2n}\right)$ occur when

$$n \cos^{-1}\left(\left[1 + \cos\frac{\pi}{2n}\right] w_m^2 - \cos\frac{\pi}{2n}\right) = \left(\frac{\pi}{2} + m\pi\right)$$

$$m = 0, 1, 2, \ldots\ldots, n-1, \qquad (4.22)$$

that is, when

$$\left(1 + \cos\frac{\pi}{2n}\right) w_m^2 - \cos\frac{\pi}{2n} = \cos\left(\frac{\pi}{2n} + \frac{m}{n}\pi\right) ,$$

or
$$w_m = \pm\sqrt{\frac{\cos\left(\frac{\pi}{2n}\right) + \cos\left(\frac{\pi}{2n} + \frac{m}{n}\pi\right)}{\left(1 + \cos\frac{\pi}{2n}\right)}} \; . \qquad (4.23)$$

Thus a pair of conjugate zeros yields the numerator factors

$$\left[s^2 + w_m^2\right] \qquad m = 0, 1, 2, \ldots\ldots, n-1, \qquad (4.24)$$

and it is seen that the numerator has 2n zeros, as it should have. Also it is seen in Eq.(4.23) that $w_{n-1} = 0$, which gives the double root at zero, as expected.

The denominator roots of $\Gamma(s)$ are more complicated in form. Convenient formulae[9] give the roots of

$$1 + e^2 T_n^2(Z) = 0,$$

as

$$Z_m = a_m + jb_m = \sinh \phi_2 \sin \frac{(2m+1)}{2n}\pi + j \cosh \phi_2 \cos\frac{(2m+1)}{2n}\pi,$$

$$m = 0, 1, 2, \ldots . 2n-1, \qquad (4.25)$$

where $\phi_2 = \frac{1}{n}\sinh^{-1}\left(\frac{1}{e}\right)$.

From Eq.(4.21),

$$-\left(1 + \cos \frac{\pi}{2n}\right) s_m^2 - \left(\cos \frac{\pi}{2n}\right) = a_m + jb_m, \qquad (4.26)$$

or

$$s_{m_{1,2}} = \pm\sqrt{\frac{-\cos \frac{\pi}{2n} - a_m - jb_m}{1 + \cos \frac{\pi}{2n}}}, \qquad (4.27)$$

which gives rise to two roots in the s-plane that are 180° apart and equidistant from the origin. Now in Eq.(4.25) there will also be a root of the form $Z_m' = a_m - jb_m$, which gives rise to two roots in the s-plane which are conjugate to the Z_m roots. The four roots from Z_m and Z_m' in the s-plane thus form a quartet of roots which are symmetrical with respect to the real and imaginary axes. The two l.h.p. roots are then selected for the denominator of $\Gamma(s)$. Altogether it is seen that the denominator will have 2n roots.

Now $\Gamma(s)$ may be written as

$$\Gamma(s) = K \frac{\prod_{i=1}^{2n} (s - s_i)}{\prod_{k=1}^{2n} (s - s_k)} . \qquad (4.28)$$

K is determined from the fact that as $s = jw \to \infty$, the insertion loss becomes infinite, and so $\Gamma(jw)\big|_{w\to\infty} = 1$. This implies that $K = 1$ in Eq.(4.28), and so

$$\Gamma(s) = \frac{\prod_{i=1}^{2n} (s-s_i)}{\prod_{k=1}^{2n} (s-s_k)} \quad . \tag{4.29}$$

In chapter 2 it was found that

$$\Gamma(s) = \frac{(A-D) + (B-C)}{(A+D) + (B+C)} \quad , \tag{4.30}$$

where $\begin{pmatrix} A & B \\ C & D \end{pmatrix}$ is the transfer matrix for the lossless network connected between the $R_s = R_L = 1$ loads. It has also been established that for the network in Fig.4.1, B and C are odd polynomials in s, A and D are even polynomials, and the constant term in A and D is 1. Comparing Eqs.(4.29) and (4.30), therefore, $B = C$, and the structure is antimetrical. This means that[10]

$$L_{n-i} = C_{1+i} \quad , \tag{4.31}$$

$$C_{n-i} = L_{1+i} \quad ,$$

in Fig.4.1. Thus the synthesis need only be carried out for half the network, and Eq.(4.31) then gives the remaining element values. So that both A and D have a constant term of unity, both numerator and denominator of Eq.(4.30) are multiplied by a factor which leaves the denominator constant term equal to 2.

The last step is to decompose the $\begin{pmatrix} A & B \\ C & D \end{pmatrix}$ matrix by successive premultiplication by the inverse matrix of the desired element in Fig.4.1, with the requirement that the overall matrix be of lower degree. Recall in chapter two this leads to two independent equations for the element value. Let the two values so found be Z and Z'. If no numerical errors occur in the synthesis process, then $Z = Z'$. In the computer program that was written for the synthesis procedure, however, it was found that serious rounding errors did occur.

When first written, the computer program calculated Z from the A and C polynomials, and then the value was used to reduce the degree of A and C. Similarly, Z' was calculated from B and D, and was then used to reduce the degree of B and D. Next, the computer program printed out the first n digits in Z and Z' that agreed, up to five digits. The computer itself was an English Electric KDF-9 computer, with 11 digit accuracy. It was found that roughly a digit of accuracy was lost for every section in the filter. Since up to 20 element designs were desired, the above method of obtaining element values was not adequate. A slight modification in the program improved the accuracy. This was to reduce the degree of the A and C, and B and D polynomials, not by using Z and Z', but by using

$$Z_1 = k(Z) + (1-k)Z',$$

where k is between 0 and 1. This simple step has the effect of cross-linking the A and C polynomials with the B and D ones. A few numerical experiments indicated that k = .5 (maximum cross-linking) is about optimum. It was found that for the high order filter designs there was still not enough accuracy.

The next numerical experiment was to change the s variable to the Z variable through the mapping

$$Z^2 = 1 + \frac{1}{s^2} \quad .$$

This mapping has the effect of shifting the origin in the s-plane to the region where the poles and zeros of $\Gamma(s)\Gamma(-s)$ are clustered[11]. The computer program first calculated the poles and zeros of Γ in the s-plane, using the previously stated formulae. Then, these poles and zeros were mapped into the Z plane through the above mapping function. Next, $\Gamma(Z)$ was computed. It turns out that this method is much more accurate than first computing $\Gamma(s)$ in polynomial form and then using the mapping function. The reasoning behind this statement is as follows.

If the roots of a polynomial are all clustered in a small region which is distant from the origin, then most of the information in the polynomial coefficients is concerned with describing the location of the region, and there is very little information on the separation of roots in this region.

This means that if a root is displaced a small amount, the coefficients of the new polynomial will be about the same as those of the original polynomial. Conversely, a small change in one of the polynomial coefficients (due to rounding errors, etc., in the computer program) may change the relative root positions by a large amount. If the origin is now shifted into the region containing the roots (i.e., placed at the "centroid" of the roots), then the information in the coefficients will deal mainly with the root separations, and not region location, which will result in much improved numerical accuracy. The mapping presented above does precisely this for the zeros and poles of Γ.

The constant multiplier in Γ is determined from the fact that, at $s = j\infty$, i.e., $Z = 1$, $\Gamma = 1$. After multiplying the appropriate factors together so that $\Gamma(Z)$ is in polynomial form, the final step in the synthesis is the formation of the transfer matrix (as a function of Z) and matrix decomposition.

This mapping experiment proved to be very successful, and it was found that twenty-four section filters could by synthesized without difficulty. The cross-linking feature mentioned previously was retained in the computer program. Results from the computer program are tabulated in Table 4.1, which corresponds to a filter having the structure in Fig.4.1. Eq.(4.31) is used for determining the remaining element values.

ELEMENT VALUES

ELEMENT NUMBER	PASS BAND RIPPLE LEVEL (DB)					
	1/10	1/4	1/2	1	2	3
N=2						
1	0.5525	0.6977	0.8358	1.0088	1.2268	1.4125
N=4						
1	0.9297	1.1183	1.3091	1.5675	1.9430	2.2574
2	1.4346	1.5063	1.5414	1.5537	1.5367	1.4107
N=6						
1	1.0382	1.2454	1.4611	1.7623	2.2156	2.6073
2	1.5163	1.5291	1.5085	1.4528	1.3531	1.2711
3	1.7892	1.8680	1.9332	2.0089	2.1031	2.1729
N=8						
1	1.0880	1.3065	1.5378	1.8642	2.3655	2.8062
2	1.5265	1.5130	1.4679	1.3833	1.2503	1.1473
3	1.9029	2.0042	2.1033	2.2357	2.4248	2.5784
4	1.8301	1.8437	1.8436	1.8319	1.8053	1.7813
N=10						
1	1.1165	1.3425	1.5832	1.9273	2.4611	2.9356
2	1.5249	1.4967	1.4380	1.3374	1.1867	1.0731
3	1.9621	2.0823	2.2072	2.3826	2.6450	2.8661
4	1.8183	1.7993	1.7663	1.7118	1.6291	1.5644
5	1.9346	1.9712	2.0029	2.0410	2.0901	2.1269
N=12						
1	1.1348	1.3662	1.6140	1.9704	2.5275	3.0267
2	1.5209	1.4834	1.4159	1.3053	1.1437	1.0238
3	1.9995	2.1344	2.2791	2.4874	2.8076	3.0834
4	1.8020	1.7630	1.7100	1.6238	1.5147	1.4278
5	1.9930	2.0503	2.1085	2.1878	2.3012	2.3922
6	1.9159	1.9180	1.9131	1.9008	1.8789	1.8602
N=14						
1	1.1475	1.3830	1.6361	2.0017	2.5765	3.0945
2	1.5168	1.4727	1.3932	1.2817	1.1128	0.9887
3	2.0257	2.1721	2.3322	2.5667	2.9332	3.2541
4	1.7873	1.7346	1.6679	1.5706	1.4346	1.3338
5	2.0323	2.1067	2.1864	2.2795	2.4674	2.6060
6	1.8941	1.8739	1.8455	1.8015	1.7366	1.6861
7	1.9723	1.9945	2.0148	2.0392	2.0718	2.0968

ELEMENT NUMBER	PASS BAND RIPPLE LEVEL (DB)					
	1/10	1/4	1/2	1	2	3
N=16						
1	1.1569	1.3955	1.6527	2.0254	2.6140	3.1468
2	1.5130	1.4642	1.3662	1.2637	1.0805	0.9625
3	2.0450	2.2048	2.3733	2.6288	3.0335	3.3920
4	1.7748	1.7122	1.6356	1.5459	1.3752	1.2650
5	2.0613	2.1497	2.2471	2.3883	2.6028	2.7832
6	1.8748	1.8387	1.7937	1.7278	1.6341	1.5631
7	2.0115	2.0509	2.0918	2.1481	2.2288	2.2931
8	1.9482	1.9470	1.9415	1.9306	1.9125	1.8975
N=18						
1	1.1642	1.4053	1.6657	2.0441	2.6438	3.1885
2	1.5097	1.4572	1.3759	1.2495	1.0713	0.9422
3	2.0600	2.2234	2.4061	2.6790	3.1158	3.5057
4	1.7643	1.6941	1.6099	1.4909	1.3295	1.2185
5	2.0837	2.1838	2.2960	2.4611	2.7157	2.9330
6	1.8584	1.8103	1.7529	1.6709	1.5566	1.4713
7	2.0413	2.0952	2.1538	2.2373	2.3605	2.4609
8	1.9267	1.9084	1.8844	1.8483	1.7954	1.7542
9	1.9867	2.0021	2.0164	2.0345	2.0588	2.0773
N=20						
1	1.1699	1.4130	1.6761	2.0591	2.6679	3.2225
2	1.5068	1.4514	1.3674	1.2380	1.0567	0.9259
3	2.0720	2.2418	2.4330	2.7203	3.1836	3.6013
4	1.7555	1.6792	1.5890	1.4609	1.2931	1.1711
5	2.1017	2.2116	2.3364	2.5218	2.8114	3.0616
6	1.8445	1.7871	1.7200	1.6255	1.4958	1.4000
7	2.0649	2.1313	2.2051	2.3122	2.4731	2.6065
8	1.9082	1.8767	1.8387	1.7836	1.7053	1.6457
9	2.0163	2.0462	2.0777	2.1213	2.1838	2.2335
10	1.9641	1.9617	1.9564	1.9469	1.9316	1.9192

TABLE 4.1

It is important to stress the fact that although the above problem has an exact theoretical solution for any (even) number of sections, the accuracy problem becomes quite important for higher order filters, and may well dictate the mechanics necessary for an accurate solution. In this respect the matrix approach outlined above is superior to a continued fraction expansion, as the expansion gives no accuracy data as the synthesis proceeds. In fairness it must be pointed out though that the matrix approach is equivalent to calculating the open and short-circuit continued fraction expansions at the same time and comparing results at each stage.

4.3.2. Distributed Element Filters.

The specification function used in this design is

$$\frac{P_o}{P_L} = 1 + e^2 L_{2n}^2 \left(\frac{\sin\theta}{\sin\theta_o} , \cos \frac{\Pi}{2n} \right)$$

$$= 1 + e^2 T_n^2 \left(\left[1 + \cos \frac{\Pi}{2n} \right] \frac{\sin^2\theta}{\sin^2\theta_o} - \cos \frac{\Pi}{2n} \right) . \qquad (4.32)$$

The passband VSWR and bandwidth are terms often used in conjunction with this filter. The relationship between VSWR and e^2 is

$$e^2 = \frac{(VSWR - 1)^2}{4 \times VSWR} , \qquad (4.33)$$

and the relationship between bandwidth BW and Θ_o is

$$BW = \frac{4\Theta_o}{\pi} \quad . \tag{4.34}$$

In Eq.(4.32) it is seen that the filter offers maximum attenuation when $\Theta = \frac{\pi}{2}(1+2n)$, $n = 0,1,2,\ldots$. The maximum insertion loss is therefore $\frac{P_o}{P_L} = 1 + e^2 L_{2n}^2 \left(\frac{1}{\sin^2 \Theta_o} , \cos \frac{\pi}{2n} \right)$. It is obvious that $0 < \Theta_o < \frac{\pi}{2}$, and hence $0 < BW < 2$.

Having determined a suitable e^2 and Θ_o, the next step in the Darlington procedure is to determine $\Gamma(t)$ from Eq.(4.32), where $t = j \tan\Theta$.

The zeros of $\Gamma(t)$ may be found by use of Eq.(4.24), i.e.

$$\frac{\sin^2 \Theta_M}{\sin^2 \Theta_o} = W_m^2 \quad , \tag{4.35}$$

which implies that

$$\tan^2 \Theta_M = \frac{W_m^2 \sin^2 \Theta_o}{1 - W_m^2 \sin^2 \Theta_o} \quad ,$$

or that the factor

$$\left(t^2 + \frac{W_m^2 \sin^2 \Theta_o}{1 - W_m^2 \sin^2 \Theta_o} \right) \quad , \tag{4.36}$$

where W_m is defined in Eq.(4.23), contains a pair of conjugate zeros of $\Gamma'(t)$. Notice that when $m = n-1$, $W_m = 0$, and thus $\Gamma(t)$ has a pair of zeros at $t = 0$, as it should have.

Similarly, the denominator roots may be found from

$$t_m^2 = \frac{s_m^2 \sin^2\theta_o}{s_m^2 \sin^2\theta_o + 1} , \tag{4.37}$$

where s_m^2 is given in Eq.(4.27). Eq.(4.37) will give one root in the left-half t-plane. Its conjugate mate is found when $Z_{m'}$ is used in Eq.(4.27), as discussed previously.

Now $\Gamma(t)$ may be written as

$$\Gamma(t) = K \frac{\prod_{i=1}^{2n} (t-t_i)}{\prod_{k=1}^{2n} (t-t_k)} . \tag{4.38}$$

K is determined from the fact that, as $t \to 1$, the insertion loss becomes infinite (because a unit element has a transmission zero at $t = 1$) and so $\Gamma(1) = 1$. This implies that

$$K = \frac{\prod_{k=1}^{2n} (1-t_k)}{\prod_{i=1}^{2n} (1-t_i)} . \tag{4.39}$$

In chapter 3 it was found that in the transfer matrix $\begin{pmatrix} A & B \\ C & D \end{pmatrix}$, the A and D entries have a constant term of unity in the numerator. So both numerator and denominator in Eq.(4.38)

are next multiplied by a factor which leaves the constant term in the denominator equal to 2. The $\begin{pmatrix} A & B \\ C & D \end{pmatrix}$ transfer matrix is formed, and then unit elements are extracted as shown in chapter 3. It is easily shown that the lossless network is antimetrical[10] ($B(t) = C(t)$), and so

$$z_{2n-i} = 1/z_i \quad , \tag{4.40}$$

and only the first half of the network need be computed.

In the computer program that was written to implement the above procedure, the mapping

$$z^2 = 1 + \frac{k_1 \tan^2 \theta_o}{t^2} \quad , \tag{4.41}$$

and cross-linking were used to improve the computational accuracy, as discussed earlier. Up to twenty-element filters were synthesized in this manner, with four and five place accuracy being maintained throughout. The results from this computer program are shown in Tables 4.2 to 4.11. The label L(DB) gives the maximum attenuation of the filter, which occurs when $\theta_o = \left(\frac{\pi}{2} + n\pi\right)$, $n = 0, 1, 2, \ldots$. k_1 was adjusted empirically when extreme input specifications were desired to give the required accuracy. It was found that $1 \leq k_1 < 3$ was the best range to use.

To verify the correctness of the tables an experimental distributed filter was built in coaxial form. The design was

STEP IMPEDANCES OF 2-ELEMENT FILTERS

N = 2 VSWR = 1.01

BW	0.01	0.02	0.03	0.04	0.05	0.06	0.07	0.08	0.09	0.10	0.20
L(DB)	38.13	26.10	19.10	14.22	10.58	7.80	5.70	4.14	3.00	2.10	0.18
1	12.7011	6.3526	4.2405	3.1911	2.5704	2.1673	1.8908	1.6947	1.5583	1.4471	1.1068

BW	0.30	0.40	0.50	0.60	0.70	0.80	0.90	1.00	1.10	1.20	1.30
L(DB)	0.04	0.01	0.01	0.00	0.00	0.00	0.00	0.00	0.00	0.00	0.00
1	1.0466	1.0264	1.0171	1.0121	1.0092	1.0072	1.0059	1.0050	1.0043	1.0038	1.0034

N = 2 VSWR = 1.02

BW	0.01	0.02	0.03	0.04	0.05	0.06	0.07	0.08	0.09	0.10	0.20
L(DB)	44.11	32.07	25.04	20.07	16.26	13.20	10.70	8.64	6.94	5.55	0.66
1	17.9177	8.9598	5.9754	4.4856	3.5952	3.0058	2.5899	2.2835	2.0513	1.8715	1.2179

BW	0.30	0.40	0.50	0.60	0.70	0.80	0.90	1.00	1.10	1.20	1.30
L(DB)	0.14	0.05	0.02	0.01	0.01	0.00	0.00	0.00	0.00	0.00	0.00
1	1.0546	1.0331	1.0244	1.0243	1.0183	1.0144	1.0118	1.0100	1.0086	1.0076	1.0068

N = 2 VSWR = 1.05

BW	0.10	0.20	0.30	0.40	0.50	0.60	0.70	0.80	0.90	1.00	1.10
L(DB)	18.23	3.00	0.79	0.27	0.12	0.06	0.03	0.02	0.01	0.01	0.01
1	2.8374	1.5521	1.2423	1.1347	1.0865	1.0608	1.0456	1.0359	1.0293	1.0247	1.0213

N = 2 VSWR = 1.10

BW	0.10	0.20	0.30	0.40	0.50	0.60	0.70	0.80	0.90	1.00	1.10
L(DB)	17.85	6.81	2.47	0.97	0.44	0.23	0.13	0.08	0.06	0.04	0.03
1	3.9437	2.0342	1.4844	1.2716	1.1735	1.1215	1.0908	1.0712	1.0580	1.0488	1.0420

N = 2 VSWR = 1.20

BW	0.10	0.20	0.30	0.40	0.50	0.60	0.70	0.80	0.90	1.00	1.10
L(DB)	23.44	11.74	5.80	3.82	1.43	0.78	0.46	0.29	0.20	0.14	0.11
1	5.4491	2.7554	1.9042	1.5295	1.3423	1.2396	1.1785	1.1395	1.1134	1.0950	1.0819

N = 2 VSWR = 1.50

BW	0.10	0.20	0.30	0.40	0.50	0.60	0.70	0.80	0.90	1.00	1.10
L(DB)	30.83	18.49	11.77	7.46	4.69	2.97	1.93	1.30	0.91	0.67	0.51
1	8.1446	4.0917	2.7609	2.1207	1.7633	1.5485	1.4129	1.3238	1.2629	1.2200	1.1880

N = 2 VSWR = 2.00

BW	0.10	0.20	0.30	0.40	0.50	0.60	0.70	0.80	0.90	1.00	1.10
L(DB)	35.18	23.22	16.34	11.68	8.34	5.96	4.28	3.11	2.31	1.76	1.38
1	10.7180	5.3786	3.6187	2.7455	2.2428	1.9238	1.7121	1.5666	1.4630	1.3899	1.3355

TABLE 4.2

STEP IMPEDANCES OF 4-ELEMENT FILTERS

N = 4 VSWR = 1.01

BW	0.01	0.02	0.03	0.04	0.05	0.06	0.07	0.08	0.09	0.10	0.20
L(DB)	137.64	113.56	99.47	89.47	81.72	75.38	70.03	65.39	61.29	57.63	33.52
1	41.7012	20.8612	13.9193	10.4518	8.3742	6.9914	6.0058	5.2683	4.6862	4.2399	2.2239
2	0.0107	0.0214	0.0321	0.0428	0.0536	0.0645	0.0754	0.0864	0.0975	0.1087	0.2283

BW	0.30	0.40	0.50	0.60	0.70	0.80	0.90	1.00	1.10	1.20	1.30
L(DB)	19.44	9.81	3.82	1.21	0.38	0.13	0.05	0.02	0.01	0.00	0.00
1	1.5940	1.3076	1.1602	1.0857	1.0493	1.0307	1.0206	1.0146	1.0104	1.0085	1.0060
2	0.3686	0.5328	0.7008	0.8290	0.9046	0.9455	0.9670	0.9807	0.9893	0.9940	0.9960

N = 4 VSWR = 1.02

BW	0.01	0.02	0.03	0.04	0.05	0.06	0.07	0.08	0.09	0.10	0.20
L(DB)	143.62	119.54	105.45	95.45	87.70	81.36	76.01	71.37	67.27	63.61	39.50
1	50.2954	25.1565	16.7908	12.5959	10.0873	8.4164	7.2254	6.3332	5.6406	5.0977	2.6309
2	0.0091	0.0183	0.0274	0.0366	0.0458	0.0550	0.0643	0.0736	0.0830	0.0924	0.1919

BW	0.30	0.40	0.50	0.60	0.70	0.80	0.90	1.00	1.10	1.20	1.30
L(DB)	25.38	15.44	8.19	3.56	1.33	0.49	0.19	0.08	0.03	0.02	0.01
1	1.8401	1.4613	1.2798	1.1832	1.0975	1.0614	1.0412	1.0292	1.0219	1.0170	1.0137
2	0.3033	0.4323	0.5763	0.7169	0.8261	0.8961	0.9376	0.9621	0.9769	0.9861	0.9920

N = 4 VSWR = 1.05

BW	0.10	0.20	0.30	0.40	0.50	0.60	0.70	0.80	0.90	1.00	1.10
L(DB)	71.44	47.33	33.20	23.16	15.43	9.40	5.02	2.36	1.04	0.46	0.21
1	6.5451	3.3409	2.3018	1.8026	1.5177	1.3396	1.2237	1.1489	1.1020	1.0729	1.0543
2	0.0757	0.1549	0.2407	0.3361	0.4430	0.5599	0.6778	0.7812	0.8586	0.9107	0.9446

N = 4 VSWR = 1.10

BW	0.10	0.20	0.30	0.40	0.50	0.60	0.70	0.80	0.90	1.00	1.10
L(DB)	77.26	53.15	39.02	28.97	21.16	14.93	9.70	5.75	3.08	1.53	0.75
1	7.9489	4.0561	2.7662	2.1364	1.7745	1.5416	1.3833	1.2726	1.1963	1.1426	1.1073
2	0.0662	0.1345	0.2069	0.2858	0.3715	0.4661	0.5677	0.6706	0.7649	0.8418	0.8978

N = 4 VSWR = 1.20

BW	0.10	0.20	0.30	0.40	0.50	0.60	0.70	0.80	0.90	1.00	1.10
L(DB)	82.40	58.79	44.66	34.61	26.78	20.37	14.99	10.46	6.80	4.07	2.27
1	9.8772	4.9455	3.3754	2.5847	2.1212	1.8406	1.6123	1.4616	1.3408	1.2660	1.2062
2	0.0551	0.1195	0.1825	0.2493	0.3219	0.3990	0.4831	0.5726	0.6640	0.7511	0.8268

N = 4 VSWR = 1.50

BW	0.10	0.20	0.30	0.40	0.50	0.60	0.70	0.80	0.90	1.00	1.10
L(DB)	89.89	65.78	51.65	41.59	33.76	27.33	21.86	17.13	12.99	9.43	6.47
1	13.2755	6.6749	4.4908	3.4104	2.7711	2.3517	2.0574	1.8408	1.6748	1.5466	1.4492
2	0.0531	0.1070	0.1624	0.2200	0.2806	0.3450	0.4136	0.4868	0.5648	0.6452	0.7262

N = 4 VSWR = 2.00

BW	0.10	0.20	0.30	0.40	0.50	0.60	0.70	0.80	0.90	1.00	1.10
L(DB)	94.66	70.56	56.42	46.37	38.53	32.09	26.62	21.84	17.62	13.86	10.54
1	16.7812	8.4229	5.6508	4.2750	3.4573	2.9182	2.5378	2.2562	2.0309	1.8608	1.7316
2	0.0510	0.1026	0.1552	0.2095	0.2661	0.3253	0.3879	0.4541	0.5243	0.5983	0.6753

TABLE 4.3

STEP IMPEDANCES FOR 6-ELEMENT FILTERS

N = 6 VSWR = 1.01

BW	0.05	0.06	0.07	0.08	0.09	0.10	0.20	0.30	0.40	0.50	0.60
L(DB)	150.94	141.44	133.40	126.44	120.30	114.80	78.61	57.38	42.23	30.42	20.71
1	10.6590	8.9935	7.6341	6.6910	5.9589	5.3744	2.7762	1.9490	1.5605	1.3473	1.2194
2	0.0396	0.0476	0.0556	0.0637	0.0717	0.0798	0.1637	0.2547	0.3546	0.4625	0.5754
3	31.2242	26.0099	22.2838	19.4876	17.3119	15.5699	7.6977	5.0294	3.6544	2.7955	2.1957

BW	0.70	0.80	0.90	1.00	1.10	1.20	1.30	1.40	1.50	1.60	1.70
L(DB)	12.59	6.23	2.33	0.72	0.22	0.07	0.02	0.01	0.00	0.00	0.00
1	1.1384	1.0858	1.0522	1.0323	1.0210	1.0145	1.0106	1.0081	1.0065	1.0055	1.0047
2	0.6884	0.7938	0.8777	0.9327	0.9638	0.9807	0.9901	0.9953	0.9984	1.0002	1.0013
3	1.7532	1.4315	1.2235	1.1112	1.0562	1.0294	1.0158	1.0088	1.0050	1.0029	1.0017

N = 6 VSWR = 1.02

BW	0.05	0.06	0.07	0.08	0.09	0.10	0.20	0.30	0.40	0.50	0.60
L(DB)	156.92	147.41	139.38	132.42	126.27	120.78	84.59	63.35	48.21	36.39	26.66
1	12.3764	10.3232	8.8580	7.7604	6.9079	6.2269	3.1905	2.2114	1.7454	1.4934	1.3220
2	0.0356	0.0428	0.0499	0.0571	0.0644	0.0716	0.1460	0.2255	0.3117	0.4044	0.5037
3	34.0840	28.3947	24.3294	21.2793	18.9059	17.0062	8.4293	5.5330	4.0525	3.1358	2.4979

BW	0.70	0.80	0.90	1.00	1.10	1.20	1.30	1.40	1.50	1.60	1.70
L(DB)	18.39	11.36	5.82	2.35	0.80	0.26	0.09	0.03	0.01	0.00	0.00
1	1.2167	1.1458	1.0961	1.0624	1.0417	1.0289	1.0211	1.0162	1.0130	1.0109	1.0096
2	0.6058	0.7072	0.8014	0.8783	0.9309	0.9623	0.9804	0.9908	0.9965	1.0004	1.0025
3	2.0256	1.6632	1.3935	1.2140	1.1118	1.0588	1.0317	1.0175	1.0099	1.0057	1.0035

N = 6 VSWR = 1.05

BW	0.10	0.20	0.30	0.40	0.50	0.60	0.70	0.80	0.90	1.00	1.10
L(DB)	128.61	92.42	71.19	56.05	44.22	34.48	26.17	18.92	12.59	7.29	3.50
1	7.6320	3.9047	2.6748	2.0775	1.7341	1.5168	1.3708	1.2683	1.1982	1.1395	1.0993
2	0.0627	0.1271	0.1947	0.2664	0.3439	0.4261	0.5125	0.6019	0.6918	0.7795	0.8552
3	14.9148	9.4006	6.1989	4.5736	3.5762	2.8912	2.3843	1.9906	1.6790	1.4336	1.2561

N = 6 VSWR = 1.10

BW	0.10	0.20	0.30	0.40	0.50	0.60	0.70	0.80	0.90	1.00	1.10
L(DB)	134.43	98.24	77.01	61.86	50.04	40.30	31.98	24.69	18.22	12.47	7.57
1	9.1714	4.6367	3.1509	2.4239	2.0007	1.7288	1.5428	1.4099	1.3117	1.2371	1.1796
2	0.0575	0.1161	0.1770	0.2411	0.3091	0.3812	0.4573	0.5369	0.6189	0.7019	0.7830
3	20.3321	10.1166	6.6875	4.9530	3.8948	3.1723	2.6414	2.2303	1.9007	1.6526	1.4142

N = 6 VSWR = 1.20

BW	0.10	0.20	0.30	0.40	0.50	0.60	0.70	0.80	0.90	1.00	1.10
L(DB)	140.07	103.89	82.65	67.51	55.68	45.94	37.62	30.33	23.91	17.93	12.63
1	11.1235	5.6061	3.7864	2.8409	2.3646	2.0226	1.7855	1.6135	1.4845	1.3849	1.3063
2	0.0537	0.1083	0.1644	0.2229	0.2843	0.3484	0.4169	0.4893	0.5629	0.6396	0.7177
3	21.6850	10.8005	7.1524	5.3130	4.1932	3.4341	2.8794	2.4521	2.1100	1.8291	1.5962

N = 6 VSWR = 1.50

BW	0.10	0.20	0.30	0.40	0.50	0.60	0.70	0.80	0.90	1.00	1.10
L(DB)	147.06	110.88	89.64	74.50	62.67	52.93	44.61	37.31	30.79	24.86	19.42
1	14.7649	7.4274	4.9902	3.7830	3.0675	2.5977	2.2679	2.0254	1.8408	1.6962	1.5904
2	0.0515	0.1035	0.1566	0.2113	0.2680	0.3272	0.3890	0.4537	0.5213	0.5918	0.6650
3	23.3754	11.6527	7.7289	5.7538	4.5575	3.7495	3.1626	2.7138	2.3563	2.0631	1.8176

N = 6 VSWR = 2.00

BW	0.10	0.20	0.30	0.40	0.50	0.60	0.70	0.80	0.90	1.00	1.10
L(DB)	151.83	115.65	94.41	79.27	67.44	57.70	49.38	42.08	35.55	29.68	24.16
1	18.7288	9.3942	6.2958	4.7562	3.8401	3.2355	2.8087	2.4987	2.2504	2.0598	1.9052
2	0.0528	0.1048	0.1583	0.2131	0.2696	0.3281	0.3889	0.4523	0.5184	0.5875	0.6598
3	24.6841	12.2802	8.1509	6.0746	4.8188	3.9787	3.3601	2.8928	2.5283	2.2195	1.9658

TABLE 4.4

N = 8 VSWR = 1.01

BW	0.05	0.06	0.07	0.08	0.09	0.10	0.20	0.30	0.40	0.50	0.60
L(DB)	219.67	207.00	196.29	187.80	178.81	171.49	123.83	94.29	74.6[illegible]	58.[illegible]9	45.[illegible]6
1	11.6495	9.7182	8.3403	7.3012	6.5068	5.8667	3.0167	2.1023	1.6705	1.4301	1.2939
2	0.0360	0.0432	0.0505	0.0578	0.0651	0.0724	0.1477	0.2[illegible]4	0.3156	0.40[illegible]9	0.5062
3	35.4780	29.5519	25.3220	22.1405	19.6792	17.7028	8.7831	5.7754	4.2427	3.29[illegible]7	2.6501
4	0.0261	0.0314	0.0366	0.0419	0.0471	0.0524	0.1053	0.1595	0.2157	0.2751	0.3398

BW	0.70	0.80	0.90	1.00	1.10	1.20	1.30	1.40	1.50	1.60	1.70
L(DB)	34.72	24.96	16.29	8.82	3.46	0.97	0.24	0.06	0.02	0.00	0.00
1	1.1903	1.1281	1.0858	1.0565	1.0362	1.0231	1.0153	1.010[illegible]	1.00[illegible]1	1.0068	1.0053
2	0.6039	0.6977	0.7835	0.8579	0.9171	0.9567	0.97[illegible]	0.9904	0.[illegible]965	0.9997	1.0014
3	2.1742	1.9110	1.5321	1.3189	1.1687	1.0610	1.03[illegible]3	1.01[illegible]7	1.0096	1.0053	1.0032
4	0.4106	0.4926	0.5896	0.7032	0.8202	0.9087	0.9575	0.9[illegible]89	0.9916	0.9966	0.99[illegible]9

N = 8 VSWR = 1.02

BW	0.05	0.06	0.07	0.08	0.09	0.10	0.20	0.30	0.40	0.50	0.60
L(DB)	225.65	212.98	202.26	192.98	184.79	177.46	129.80	100.[illegible]7	[illegible]0.66	64.[illegible]6	51.[illegible]4
1	13.3434	11.1326	9.5514	8.3666	7.4462	6.7109	3.4284	2.3[illegible]5[illegible]	1.[illegible]570	1.56[illegible]	1.3 [illegible]9
2	0.0329	0.0396	0.0462	0.0528	0.0595	0.0662	0.1345	0.2067	0.2[illegible]81	0.366[illegible]	0.4540
3	37.0848	31.5636	27.0474	23.6592	21.0232	1[illegible].9135	9.3976	6.1963	4.5712	3.5749	2.[illegible]929
4	0.0248	0.0298	0.0347	0.0397	0.0447	0.0496	0.0997	0.150[illegible]	0.2034	0.25[illegible]	0.316[illegible]

BW	0.70	0.80	0.90	1.00	1.10	1.20	1.30	1.40	1.50	1.60	1.70
L(DB)	40.70	30.93	22.19	14.35	7.65	2.99	0.87	0.23	0.06	0.02	0.00
1	1.2722	1.1919	1.1356	1.0953	1.0659	1.0447	1.0304	1.0215	1.0161	1.0127	1.0107
2	0.5435	0.6326	0.7179	0.7966	0.8658	0.9215	0.9593	0.9[illegible]12	0.9930	0.9994	1.002[illegible]
3	2.3922	2.0082	1.7065	1.4678	1.2830	1.1524	1.0756	1.0373	1.0191	1.0105	1.0068
4	0.3603	0.4512	0.5325	0.6277	0.7359	0.8422	0.9197	0.9625	0.9834	0.9932	0.997[illegible]

N = 8 VSWR = 1.05

BW	0.20	0.35	0.50	0.65	0.80	0.95	1.10	1.25	1.40	1.55	1.70
L(DB)	137.04	97.89	72.70	53.90	38.76	25.93	14.81	5.83	1.23	0.1[illegible]	0.03
1	4.1476	2.4635	1.8235	1.5027	1.3196	1.2071	1.1342	1.0[illegible]50	1.0530	1.0353	1.0[illegible]59
2	0.1199	0.2161	0.3210	0.4348	0.5545	0.6743	0.7[illegible]73	0.8[illegible]59	0.9563	0.9919	1.00[illegible]0
3	10.2144	5.7565	3.9364	2.9255	2.2699	1.8076	1.4696	1.229[illegible]	1.0[illegible]04	1.0347	1.0159
4	0.0937	0.1657	0.2408	0.3211	0.4104	0.5144	0.6410	0.7[illegible]95	0.9143	0.973[illegible]	0.9946

N = 8 VSWR = 1.10

BW	0.20	0.35	0.50	0.65	0.80	0.95	1.10	1.25	1.40	1.55	1.70
L(DB)	142.86	103.71	78.52	59.78	44.57	31.74	20.52	10.71	3.52	0.67	0.11
1	4.8669	2.8722	2.0955	1.6982	1.4657	1.3125	1.2201	1.1513	1.1014	1.0697	1.0503
2	0.1115	0.1997	0.2945	0.3970	0.5061	0.6187	0.7301	0.[illegible]352	0.9255	0.9851	1.0137
3	10.8374	6.1238	4.2073	3.1488	2.4654	1.9321	1.6228	1.3527	1.1651	1.067[illegible]	1.0312
4	0.0901	0.1591	0.2305	0.3068	0.3880	0.4804	0.5[illegible]92	0.7195	0.[illegible]572	0.950[illegible]	0.9[illegible]06

N = 8 VSWR = 1.20

BW	0.20	0.35	0.50	0.65	0.80	0.95	1.10	1.25	1.40	1.55	1.70
L(DB)	148.50	109.35	84.16	65.37	50.22	37.34	26.13	16.0[illegible]	7.47	2.0[illegible]	0.[illegible]
1	5.8748	3.4266	2.4703	1.9734	1.6768	1.4844	1.3526	1.25[illegible]	1.1[illegible]9	1.1350	1.10[illegible]2
2	0.1058	0.1885	0.2764	0.3705	0.4710	0.5764	0.6843	0.7[illegible]11	0.[illegible]824	0.9768	1.0067
3	11.4839	6.5021	4.4831	3.3732	2.6602	2.1567	1.7801	1.4902	1.2[illegible]01	1.1965	1.0601
4	0.0875	0.1543	0.2230	0.2990	0.3719	0.4565	0.5529	0.6661	0.7463	0.9150	0.9[illegible]06

N = 8 VSWR = 1.50

BW	0.20	0.35	0.50	0.65	0.80	0.95	1.10	1.25	1.40	1.55	1.70
L(DB)	155.49	116.34	91.15	72.36	57.21	44.37	33.12	22.98	13.79	6.07	1.63
1	7.7823	4.4996	3.2060	2.5240	2.1090	1.8339	1.6406	1.4927	1.3901	1.3037	1.2396
2	0.1038	0.1841	0.2681	0.3570	0.4515	0.5515	0.6562	0.7639	0.[illegible]725	0.9788	1.0641
3	12.4547	7.0647	4.8864	3.6947	2.9333	2.3982	1.9978	1.6961	1.4395	1.2514	1.1338
4	0.0856	0.1508	0.2175	0.2868	0.3598	0.4383	0.5250	0.6234	0.7372	0.8609	0.9617

N = 8 VSWR = 2.00

BW	0.20	0.35	0.50	0.65	0.80	0.95	1.10	1.25	1.40	1.55	1.70
L(DB)	160.26	121.11	95.92	77.13	61.98	49.15	37.89	27.78	18.44	10.05	3.75
1	9.8808	5.6904	4.0307	3.1493	2.6090	2.2458	1.9873	1.7956	1.6473	1.5279	1.4309
2	0.1077	0.1905	0.2766	0.3669	0.4624	0.5635	0.6699	0.7812	0.[illegible]961	1.0133	1.1235
3	13.3727	7.5919	5.2588	3.9852	3.1741	2.6059	2.1816	1.8509	1.5964	1.3761	1.2248
4	0.0854	0.1504	0.2168	0.2854	0.3572	0.4337	0.5168	0.6094	0.7148	0.[illegible]331	0.9475

TABLE 4.5

STEP IMPEDANCES OF 10-ELEMENT FILTERS

N = 10 VSWR = 1.05

BW	0.30	0.40	0.50	0.60	0.70	0.80	0.90	1.00	1.10	1.20	1.30
L(DB)	146.04	120.76	101.00	84.70	70.75	58.50	47.52	37.52	28.30	19.71	11.82
1	2.9134	2.2524	1.8702	1.6267	1.4619	1.3454	1.2616	1.1991	1.1519	1.1157	1.0878
2	0.1784	0.2432	0.3117	0.3839	0.4592	0.5363	0.6135	0.6886	0.7597	0.8249	0.8830
3	6.9658	5.1823	4.0846	3.3391	2.7952	2.3745	2.0490	1.7835	1.5691	1.3936	1.2539
4	0.1363	0.1831	0.2312	0.2811	0.3334	0.3891	0.4493	0.5153	0.5888	0.6710	0.7620
5	7.5646	5.6357	4.4688	3.6821	3.1116	2.6748	2.3254	2.0349	1.7848	1.5635	1.3665

N = 10 VSWR = 1.10

BW	0.30	0.40	0.50	0.60	0.70	0.80	0.90	1.00	1.10	1.20	1.30
L(DB)	151.86	126.58	106.82	90.52	76.57	64.32	53.34	43.34	34.11	25.49	17.42
1	3.4019	2.6091	2.1460	1.8472	1.6420	1.4949	1.3861	1.3038	1.2402	1.1905	1.1507
2	0.1667	0.2262	0.2888	0.3545	0.4233	0.4944	0.5670	0.6397	0.7109	0.7789	0.8425
3	7.3883	5.4918	4.3405	3.5611	2.9940	2.5601	2.2162	1.9372	1.7076	1.5190	1.3617
4	0.1327	0.1781	0.2246	0.2725	0.3224	0.3748	0.4307	0.4911	0.5572	0.6304	0.7117
5	7.7897	5.8041	4.6106	3.8047	3.2217	2.7772	2.4237	2.1322	1.9841	1.6666	1.4721

N = 10 VSWR = 1.20

BW	0.30	0.40	0.50	0.60	0.70	0.80	0.90	1.00	1.10	1.20	1.30
L(DB)	157.50	132.22	112.46	96.16	82.21	69.96	58.99	48.98	39.75	31.13	23.01
1	4.0666	3.0985	2.5283	2.1569	1.8987	1.7110	1.5701	1.4616	1.3765	1.3085	1.2533
2	0.1591	0.2152	0.2737	0.3348	0.3986	0.4650	0.5335	0.6033	0.6734	0.7426	0.8097
3	7.6304	5.8292	4.6170	3.7975	3.2048	2.7515	2.3923	2.1001	1.8590	1.6554	1.4852
4	0.1307	0.1752	0.2207	0.2673	0.3156	0.3660	0.4191	0.4756	0.5366	0.6032	0.6766
5	7.9972	5.9666	4.7405	3.9164	3.3214	2.8690	2.5108	2.2174	1.9697	1.7549	1.5640

N = 10 VSWR = 1.50

BW	0.30	0.40	0.50	0.60	0.70	0.80	0.90	1.00	1.10	1.20	1.30
L(DB)	164.49	139.21	119.45	103.15	89.20	76.95	65.97	55.97	46.74	38.11	29.98
1	5.3620	4.0594	3.2062	2.7777	2.4201	2.1564	1.9563	1.7994	1.6740	1.5722	1.4881
2	0.1579	0.2128	0.2695	0.3284	0.3895	0.4531	0.5191	0.5871	0.6567	0.7274	0.7983
3	8.5621	6.3529	5.0654	4.1782	3.5366	3.0483	2.6622	2.3481	2.0871	1.8669	1.6795
4	0.1310	0.1756	0.2209	0.2672	0.3149	0.3642	0.4157	0.4699	0.5274	0.5891	0.6561
5	8.2570	6.1641	4.9014	4.0536	3.4426	2.9791	2.6136	2.3158	2.0665	1.8525	1.6645

N = 10 VSWR = 2.00

BW	0.30	0.40	0.50	0.60	0.70	0.80	0.90	1.00	1.10	1.20	1.30
L(DB)	169.26	143.98	124.22	107.92	93.97	81.72	70.75	60.75	51.51	42.99	34.75
1	6.8132	5.1414	4.1454	3.4871	3.0218	2.6769	2.4122	2.2034	2.0353	1.8973	1.7828
2	0.1660	0.2233	0.2822	0.3430	0.4059	0.4712	0.5389	0.6086	0.6812	0.7553	0.8307
3	9.3253	6.9564	5.5256	4.5634	3.8687	3.3409	2.9244	2.5859	2.3045	2.0668	1.8635
4	0.1343	0.1798	0.2262	0.2734	0.3219	0.3719	0.4238	0.4780	0.5352	0.5961	0.6614
5	8.4584	6.3161	5.0242	4.1573	3.5329	3.0600	2.6875	2.3849	2.1325	1.9170	1.7289

TABLE 4.6

N = 12 VSWR = 1.05

BW	0.30	0.40	0.50	0.60	0.70	0.80	0.90	1.00	1.10	1.20	1.30
L(DB)	183.89	152.94	129.82	109.64	92.89	78.18	64.98	52.96	41.86	31.48	21.72
1	2.9606	2.2884	1.8981	1.6492	1.4805	1.3614	1.2748	1.2105	1.1620	1.1249	1.0961
2	0.1760	0.2397	0.3070	0.3778	0.4516	0.5272	0.6029	0.6767	0.7465	0.8106	0.8675
3	7.1084	5.2764	4.1623	3.4065	2.8557	2.4342	2.1013	1.8332	1.6159	1.4408	1.2997
4	0.1342	0.1808	0.2273	0.2761	0.3270	0.3809	0.4387	0.5013	0.5699	0.6452	0.7272
5	7.7693	5.7923	4.5974	3.7930	3.2110	2.7669	2.4136	2.1224	1.8746	1.6582	1.4655
6	0.1282	0.1719	0.2165	0.2682	0.3094	0.3586	0.4104	0.4656	0.5257	0.5930	0.6708

N = 12 VSWR = 1.10

BW	0.30	0.40	0.50	0.60	0.70	0.80	0.90	1.00	1.10	1.20	1.30
L(DB)	189.11	158.76	135.04	115.46	98.71	84.00	70.80	58.78	47.68	37.30	27.52
1	3.4555	2.6486	2.1768	1.8723	1.6629	1.5126	1.4013	1.3171	1.2521	1.2012	1.1608
2	0.1652	0.2242	0.2860	0.3508	0.4186	0.4887	0.5602	0.6318	0.7019	0.7688	0.8311
3	7.5044	5.5804	4.4130	3.6234	3.0494	2.6106	2.2833	1.9817	1.7505	1.5598	1.4038
4	0.1316	0.1765	0.2224	0.2697	0.3188	0.3702	0.4246	0.4830	0.5462	0.6151	0.6903
5	7.9791	5.9523	4.7284	3.9055	3.3112	2.8590	2.5007	2.2070	1.9590	1.7480	1.5534
6	0.1260	0.1688	0.2124	0.2571	0.3030	0.3506	0.4004	0.4529	0.5098	0.5707	0.6400

N = 12 VSWR = 1.20

BW	0.30	0.40	0.50	0.60	0.70	0.80	0.90	1.00	1.10	1.20	1.30
L(DB)	194.75	164.41	140.68	121.11	104.35	89.64	76.44	64.42	53.32	42.94	33.15
1	4.1893	3.1449	2.5648	2.1866	1.9236	1.7323	1.5885	1.4778	1.3909	1.3216	1.2656
2	0.1586	0.2144	0.2726	0.3333	0.3966	0.4625	0.5304	0.5995	0.6688	0.7372	0.8038
3	7.9578	5.9857	4.6958	3.8649	3.2629	2.8037	2.4401	2.1447	1.9003	1.6961	1.5253
4	0.1306	0.1751	0.2205	0.2670	0.3150	0.3649	0.4173	0.4729	0.5325	0.5968	0.6666
5	8.2008	6.1202	4.8650	4.0218	3.4137	2.9521	2.5874	2.2897	2.0399	1.8249	1.6356
6	0.1244	0.1667	0.2096	0.2535	0.2985	0.3449	0.3932	0.4438	0.4974	0.5550	0.6184

N = 12 VSWR = 1.50

BW	0.30	0.40	0.50	0.60	0.70	0.80	0.90	1.00	1.10	1.20	1.30
L(DB)	201.74	171.39	147.67	128.10	111.34	96.63	83.43	71.41	60.31	49.93	40.14
1	5.4512	4.1256	3.3385	2.8206	2.4563	2.1879	1.9833	1.8232	1.6953	1.5914	1.5058
2	0.1589	0.2141	0.2710	0.3301	0.3915	0.4552	0.5213	0.5894	0.6590	0.7295	0.8000
3	8.7553	6.5279	5.1817	4.2754	3.6203	3.1220	2.7282	2.4081	2.1424	1.9186	1.7286
4	0.1331	0.1783	0.2242	0.2718	0.3194	0.3693	0.4212	0.4756	0.5332	0.5947	0.6607
5	8.9538	6.6870	5.0808	4.2031	3.5714	3.0927	2.7156	2.4090	2.1532	1.9347	1.7439
6	0.1235	0.1654	0.2079	0.2512	0.2956	0.3412	0.3883	0.4374	0.4889	0.5436	0.6023

N = 12 VSWR = 2.00

BW	0.30	0.40	0.50	0.60	0.70	0.80	0.90	1.00	1.10	1.20	1.30
L(DB)	206.51	176.17	152.44	132.87	116.12	101.40	88.21	76.18	65.08	54.70	44.91
1	6.9438	5.2385	4.2222	3.5503	3.0751	2.7828	2.4523	2.2389	2.0669	1.9259	1.8085
2	0.1686	0.2268	0.2865	0.3481	0.4119	0.4781	0.5466	0.6175	0.6905	0.7653	0.8412
3	9.6332	7.1869	5.7097	4.7165	3.9995	3.4551	3.0256	2.6768	2.3878	2.1426	1.9340
4	0.1387	0.1858	0.2336	0.2824	0.3323	0.3838	0.4378	0.4989	0.5514	0.6134	0.6795
5	8.9104	6.6547	5.2946	4.3823	3.7255	3.2282	2.8370	2.5196	2.2555	2.0306	1.8354
6	0.1238	0.1658	0.2083	0.2517	0.2960	0.3415	0.3884	0.4371	0.4879	0.5415	0.5986

TABLE 4.7

STEP IMPEDANCES OF 14-ELEMENT FILTERS

N = 14 VSWR = 1.05

BW	0.40	0.50	0.60	0.70	0.80	0.90	1.00	1.10	1.20	1.30	1.40
L(DB)	185.08	157.39	134.54	114.99	97.81	82.40	68.36	55.39	43.27	31.83	20.96
1	2.3121	1.9165	1.6639	1.4926	1.3715	1.2834	1.2179	1.1685	1.1306	1.1013	1.0783
2	0.2377	0.3043	0.3743	0.4472	0.5219	0.5967	0.6698	0.7391	0.8027	0.8592	0.9078
3	5.3332	4.2091	3.4469	2.8918	2.4674	2.1322	1.8624	1.6436	1.4666	1.3252	1.2142
4	0.1787	0.2254	0.2736	0.3239	0.3769	0.4334	0.4945	0.5609	0.6333	0.7112	0.7927
5	5.8754	4.6655	3.8515	3.2630	2.8147	2.4587	2.1662	1.9187	1.7040	1.5147	1.3473
6	0.1697	0.2136	0.2586	0.3049	0.3529	0.4031	0.4562	0.5133	0.5760	0.6465	0.7280
7	5.9618	4.7380	3.9158	3.3227	2.8723	2.5164	2.2257	1.9811	1.7690	1.5789	1.4025

N = 14 VSWR = 1.10

BW	0.40	0.50	0.60	0.70	0.80	0.90	1.00	1.10	1.20	1.30	1.40
L(DB)	190.90	163.21	140.36	120.81	103.63	88.82	74.18	61.21	49.09	37.65	26.76
1	2.6750	2.1975	1.8890	1.6768	1.5244	1.4114	1.3258	1.2598	1.2081	1.1671	1.1343
2	0.2230	0.2844	0.3487	0.4160	0.4855	0.5564	0.6274	0.6969	0.7633	0.8251	0.8808
3	5.6359	4.4583	3.6621	3.0837	2.6418	2.2921	2.0088	1.7762	1.5845	1.4272	1.2997
4	0.1754	0.2216	0.2685	0.3172	0.3681	0.4219	0.4793	0.5412	0.6083	0.6809	0.7584
5	6.0337	4.7946	3.9618	3.3608	2.9040	2.5425	2.2468	1.9980	1.7834	1.5946	1.4266
6	0.1678	0.2111	0.2553	0.3007	0.3476	0.3964	0.4477	0.5021	0.5609	0.6258	0.6990
7	6.0575	4.8165	3.9833	3.3828	2.9274	2.5683	2.2760	2.0313	1.8209	1.6347	1.4648

N = 14 VSWR = 1.20

BW	0.40	0.50	0.60	0.70	0.80	0.90	1.00	1.10	1.20	1.30	1.40
L(DB)	196.54	168.85	146.01	126.45	109.27	93.86	79.82	66.85	54.73	43.89	32.39
1	3.1766	2.5897	2.2069	1.9406	1.7468	1.6011	1.4888	1.4007	1.3304	1.2735	1.2271
2	0.2141	0.2721	0.3326	0.3957	0.4613	0.5289	0.5977	0.6667	0.7347	0.8002	0.8621
3	5.9896	4.7469	3.9085	3.3009	2.8377	2.4711	2.1733	1.9271	1.7216	1.5498	1.4071
4	0.1754	0.2208	0.2673	0.3153	0.3651	0.4173	0.4725	0.5315	0.5949	0.6633	0.7369
5	6.2154	4.9418	4.0865	3.4700	3.0022	2.6330	2.3321	2.0802	1.8641	1.6748	1.5065
6	0.1670	0.2100	0.2538	0.2987	0.3450	0.3929	0.4430	0.4957	0.5520	0.6130	0.6805
7	6.1464	4.8891	4.0454	3.4378	2.9775	2.6152	2.3209	2.0755	1.8658	1.6821	1.5167

N = 14 VSWR = 1.50

BW	0.40	0.50	0.60	0.70	0.80	0.90	1.00	1.10	1.20	1.30	1.40
L(DB)	203.53	175.84	153.00	133.44	116.26	100.85	86.81	73.84	61.72	50.28	39.38
1	4.1722	3.3753	2.8507	2.4816	2.2096	2.0022	1.8398	1.7101	1.6047	1.5179	1.4454
2	0.2152	0.2724	0.3317	0.3932	0.4572	0.5234	0.5917	0.6614	0.7320	0.8025	0.8719
3	6.6313	5.2644	4.3445	3.6796	3.1739	2.7746	2.4501	2.1808	1.9541	1.7619	1.5985
4	0.1805	0.2271	0.2746	0.3234	0.3737	0.4261	0.4809	0.5389	0.6005	0.6665	0.7373
5	6.5421	5.2043	4.3066	3.6602	3.1705	2.7850	2.4719	2.2109	1.9884	1.7949	1.6236
6	0.1684	0.2116	0.2557	0.3007	0.3470	0.3947	0.4443	0.4962	0.5509	0.6094	0.6727
7	6.2620	4.9828	4.1249	3.5076	3.0404	2.6731	2.3755	2.1281	1.9178	1.7352	1.5731

N = 14 VSWR = 2.00

BW	0.40	0.50	0.60	0.70	0.80	0.90	1.00	1.10	1.20	1.30	1.40
L(DB)	208.30	180.61	157.77	138.21	121.03	105.63	91.58	78.61	66.49	55.05	44.15
1	5.3081	4.2773	3.5956	3.1133	2.7556	2.4809	2.2641	2.0804	1.9461	1.8269	1.7263
2	0.2295	0.2899	0.3522	0.4167	0.4835	0.5527	0.6243	0.6980	0.7734	0.8499	0.9267
3	7.3574	5.8456	4.8294	4.0960	3.5391	3.0999	2.7434	2.4474	2.1977	1.9847	1.8021
4	0.1905	0.2395	0.2895	0.3407	0.3934	0.4479	0.5048	0.5646	0.6277	0.6949	0.7667
5	6.9042	5.4937	4.5476	3.8667	3.3513	2.9460	2.6174	2.3441	2.1118	1.9105	1.7331
6	0.1719	0.2160	0.2609	0.3067	0.3538	0.4023	0.4525	0.5048	0.5597	0.6179	0.6803
7	6.3566	5.0591	4.1890	3.5631	3.0897	2.7177	2.4167	2.1668	1.9550	1.7718	1.6184

TABLE 4.8

STEP IMPEDANCES OF 16-ELEMENT FILTERS

N = 16 VSWR = 1.05

BW	0.50	0.60	0.70	0.80	0.90	1.00	1.10	1.20	1.30	1.40	1.50
L(DB)	185.58	159.42	137.06	117.42	99.80	83.74	68.91	55.04	41.95	29.49	17.5[illegible]
1	1.9293	1.6743	1.5011	1.3786	1.2694	1.2231	1.1729	1.1346	1.1049	1.0816	1.0631
2	0.3025	0.3720	0.4444	0.5185	0.5929	0.6655	0.7345	0.7979	0.8542	0.9025	0.942[illegible]
3	4.2399	3.4735	2.9156	2.4891	2.1524	1.8813	1.6614	1.4935	1.3412	1.2206	1.1442
4	0.2283	0.2728	0.3221	0.3746	0.4305	0.4906	0.5559	0.6267	0.7025	0.7814	0.[illegible]595
5	4.7072	3.8072	3.2947	2.8436	2.4859	2.1924	1.9445	1.7303	1.5424	1.3773	1.2349
6	0.2193	0.2568	0.3027	0.3501	0.3996	0.4518	0.5075	0.5681	0.6354	0.7116	0.7986
7	4.8006	3.9694	3.3702	2.9157	2.5570	2.2648	2.0199	1.[illegible]089	1.6219	1.4908	1.2[illegible]04
8	0.2086	0.2523	0.2971	0.3433	0.3913	0.4415	0.4947	0.5517	0.6145	0.6860	0.7715

N = 16 VSWR = 1.10

BW	0.50	0.60	0.70	0.80	0.90	1.00	1.10	1.20	1.30	1.40	1.50
L(DB)	191.35	165.23	142.08	123.23	105.62	[illegible]9.56	74.72	60.86	47.77	35.30	23.34
1	2.2121	1.9009	1.6866	1.5327	1.4166	1.3320	1.2652	1.2129	1.1715	1.13[illegible]	1.1114
2	0.2034	0.3475	0.4143	0.4835	0.5541	0.6247	0.6939	0.7601	0.[illegible]216	0.[illegible]770	0.9957
3	4.4892	3.6885	3.1069	2.6628	2.3114	2.0260	1.7932	1.6006	1.4496	1.3147	1.2131
4	0.2212	0.2680	0.3165	0.3671	0.4206	0.4775	0.5387	0.6048	0.6761	0.7517	0.[illegible]294
5	4.6374	3.9982	3.3926	2.9326	2.5689	2.2717	2.0221	1.[illegible]072	1.6189	1.4523	1.3056
6	0.2106	0.2546	0.2998	0.3465	0.3949	0.4456	0.4993	0.5569	0.619[illegible]	0.6[illegible]99	0.7692
7	4.6789	4.0362	3.[illegible]293	2.9693	2.6070	2.3126	2.0667	1.[illegible]563	1.6715	1.[illegible]5047	1.3097
8	0.2065	0.2496	0.2937	0.3392	0.3862	0.4352	0.4867	0.5418	0.6006	0.6665	0.7426

N = 16 VSWR = 1.20

BW	0.50	0.60	0.70	0.80	0.90	1.00	1.10	1.20	1.30	1.40	1.50
L(DB)	197.00	170.88	148.32	129.80	111.26	95.20	80.37	66.50	53.41	40.[illegible]	2[illegible].97
1	2.6077	2.2216	1.9528	1.7572	1.6101	1.4967	1.4076	1.3366	1.2792	1.2323	1.1935
2	0.2719	0.3323	0.3953	0.4607	0.5281	0.5968	0.6656	0.7334	0.[illegible]993	c.[illegible]603	c.9169
3	4.7837	3.9396	3.3279	2.8617	2.4929	2.1934	1.9458	1.7398	1.3665	1.[illegible]232	1.3057
4	0.2213	0.2679	0.3159	0.3657	0.417[illegible]	0.4729	0.5316	0.5946	c.6623	0.7349	c.[illegible]109
5	4.9951	4.1313	3.5087	3.0366	2.6641	2.3608	2.1071	1.[illegible]	1.7000	1.5320	1.3[illegible]25
6	0.2107	0.2546	0.2996	0.3459	0.3938	0.4437	0.4962	c.5519	0.6120	0.6779	c.7513
7	4.9639	4.1083	3.4924	3.0260	2.6591	2.3615	2.1139	1.9027	1.[illegible]	1.5543	1.4936
8	0.2051	0.2478	0.2914	0.3363	0.3[illegible]26	0.4307	0.4[illegible]10	0.5341	0.590[illegible]	c.6527	0.7923

N = 16 VSWR = 1.50

BW	0.50	0.60	0.70	0.80	0.90	1.00	1.10	1.20	1.30	1.40	1.50
L(DB)	203.99	177.[illegible]7	155.51	135.87	11[illegible].25	102.19	87.36	73.49	60.40	47.93	35.96
1	3.4025	2.8730	2.[illegible]004	2.2257	2.0161	1.[illegible]521	1.7210	1.6144	1.5267	1.4535	1.39[illegible]
2	0.2735	0.3330	0.3948	0.4589	0.5253	0.593[illegible]	0.6637	0.7344	0.[illegible]050	0.[illegible]743	c.9812
3	5.3266	4.3963	3.7240	3.2126	2.8092	2.4912	2.2092	1.[illegible]03	1.7[illegible]62	1.6214	1.[illegible]23
4	0.2214	0.2774	0.3266	0.3775	0.4303	0.4855	0.5439	0.6057	0.6719	c.[illegible]42[illegible]	c.[illegible]9[illegible]
5	5.2974	4.3941	3.7265	3.2296	2.8306	2.5104	2.2534	2.03[illegible]5	1.[illegible]315	1.65[illegible]	1.3941
6	0.2140	0.2695	0.3052	0.3521	0.4004	0.4506	0.5030	0.55[illegible]1	0.616[illegible]	c.6[illegible]00	c.[illegible]402
7	5.1069	4.2283	3.5962	3.1174	2.7432	2.437[illegible]	2.1[illegible]32	1.9[illegible]09	1.7[illegible]36	1.6211	1.4[illegible]2[illegible]
8	0.2045	0.2469	0.2903	0.3346	0.3807	0.4281	0.4775	0.5293	0.5[illegible]90	0.6427	0.[illegible]070

N = 16 VSWR = 2.00

BW	0.50	0.60	0.70	0.[illegible]0	0.90	1.00	1.10	1.20	1.30	1.40	1.[illegible]0
L(DB)	208.76	182.64	160.28	140.64	123.02	106.[illegible]6	9[illegible].13	71.26	65.17	52.70	4[illegible].[illegible]3
1	4.3187	3.6296	3.1420	2.7[illegible]02	2.5023	2.2[illegible]30	2.1062	1.9611	1.[illegible]405	1.[illegible]3[illegible]	1.6521
2	0.2[illegible]26	0.3555	0.4205	0.4[illegible]79	0.5577	0.6[illegible]9[illegible]	0.7041	0.7[illegible]00	0.[illegible]570	0.8343	1.[illegible]10[illegible]
3	5.9507	4.9166	4.1703	3.603[illegible]	3.1571	2.7985	2.4936	2.2397	[illegible].0233	1.[illegible]37[illegible]	1.6791
4	0.2443	0.2952	0.3474	0.4011	0.4567	0.5146	0.5758	0.6395	0.7077	0.7[illegible]89	c.[illegible]9[illegible]7
5	5.6486	4.6762	3.9704	3.4468	3.0304	2.6929	2.4123	2.1[illegible]41	1.[illegible]67	1.7[illegible]63	1.6206
6	0.2223	0.2684	0.3156	0.3639	0.4137	0.4653	0.5189	0.5751	c.6346	0.6991	c.[illegible]66[illegible]
7	5.2566	4.3530	3.7031	3.2117	2.8257	2.5134	2.2544	2.0351	1.[illegible]45[illegible]	1.6793	1.5[illegible]00
8	0.2051	0.2477	0.2912	0.3357	0.3815	0.4284	0.4[illegible]50	0.5294	0.5[illegible]35	0.6411	c.7033

TABLE 4.9

STEP IMPEDANCES FOR 18-ELEMENT FILTERS

N = 18 VSWR = 1.05

BW	0.60	0.70	0.80	0.90	1.00	1.10	1.20	1.30	1.40	1.50	1.60
L(DB)	158.27	139.11	137.01	117.18	99.10	82.41	66.80	52.06	38.08	24.55	11.79
1	1.6918	1.5073	1.3858	1.2938	1.2268	1.1782	1.1374	1.1078	1.0859	1.0654	1.0504
2	0.3705	0.4425	0.5162	0.5903	0.6626	0.7314	0.7946	0.8509	0.9992	0.9393	0.9718
3	3.4922	2.9322	2.5043	2.1661	1.8944	1.6737	1.4950	1.3520	1.2398	1.1541	1.0906
4	0.2714	0.3210	0.3732	0.4287	0.4883	0.5528	0.6226	0.6978	0.7786	0.8909	0.9208
5	3.9111	3.3159	2.8629	2.5039	2.2096	1.9615	1.7678	1.5800	1.3959	1.2551	1.1396
6	0.2559	0.3015	0.3496	0.3977	0.4494	0.5044	0.5639	0.6295	0.7029	0.7955	0.8756
7	4.0024	3.3993	2.9421	2.5816	2.2883	2.0409	1.8321	1.6463	1.4780	1.3120	1.1780
8	0.2509	0.2953	0.3410	0.3885	0.4379	0.4901	0.5456	0.6060	0.6736	0.7523	0.8471
9	4.0182	3.4108	2.9537	2.5988	2.3014	2.0576	1.8492	1.6664	1.5010	1.3449	1.1929

N = 18 VSWR = 1.10

BW	0.60	0.70	0.80	0.90	1.00	1.10	1.20	1.30	1.40	1.50	1.60
L(DB)	190.09	164.93	142.82	123.00	104.92	88.22	72.82	57.84	43.96	30.36	17.39
1	1.9097	1.6980	1.5388	1.4233	1.3366	1.2692	1.2165	1.1767	1.1412	1.1142	1.0919
2	0.3466	0.4133	0.4822	0.5525	0.6230	0.6920	0.7580	0.8193	0.8747	0.9231	0.9643
3	3.7074	3.1236	2.6778	2.3252	2.0397	1.8052	1.6120	1.4534	1.3250	1.2232	1.1445
4	0.2678	0.3182	0.3687	0.4199	0.4705	0.5373	0.6029	0.6734	0.7479	0.8241	0.9081
5	4.0237	3.4150	2.9526	2.5873	2.2990	2.0596	1.8634	1.6952	1.5491	1.4235	1.3192
6	0.2545	0.2996	0.3461	0.3943	0.4448	0.4980	0.5550	0.6170	0.6954	0.7619	0.8469
7	4.0711	3.4597	2.9966	2.6320	2.3359	2.0991	1.8782	1.6937	1.5292	1.3761	1.2343
8	0.2492	0.2952	0.3398	0.3951	0.4337	0.4936	0.5585	0.5963	0.6597	0.7216	0.8164
9	4.0570	3.4457	2.9883	2.6262	2.3325	2.0862	1.8801	1.6999	1.5369	1.3870	1.2428

N = 18 VSWR = 1.20

BW	0.60	0.70	0.80	0.90	1.00	1.10	1.20	1.30	1.40	1.50	1.60
L(DB)	195.73	170.57	148.47	128.64	110.57	93.87	78.26	63.52	49.43	36.00	22.97
1	2.2327	1.9821	1.7651	1.6168	1.5026	1.4125	1.3418	1.2833	1.2361	1.1971	1.1644
2	0.3322	0.3951	0.4605	0.5278	0.5963	0.6651	0.7328	0.7980	0.8595	0.9153	0.9662
3	3.9823	3.3481	2.8796	2.5091	2.2082	1.9695	1.7820	1.6286	1.4347	1.3169	1.2224
4	0.2695	0.3165	0.3668	0.4185	0.4736	0.5321	0.5949	0.6623	0.7342	0.8098	0.8955
5	4.1646	3.5375	3.0620	2.6870	2.3818	2.1266	1.9053	1.7179	1.5497	1.4046	1.2700
6	0.2555	0.3006	0.3470	0.3950	0.4449	0.4973	0.5529	0.6125	0.6776	0.7495	0.8295
7	4.1552	3.5311	3.0608	2.6900	2.3998	2.1401	1.9276	1.7429	1.5786	1.4280	1.2957
8	0.2468	0.2926	0.3375	0.3859	0.4319	0.4821	0.5348	0.5939	0.6515	0.7198	0.7981
9	4.0970	3.4890	3.0204	2.6560	2.3608	2.1157	1.9076	1.7273	1.5675	1.4213	1.2983

N = 18 VSWR = 1.50

BW	0.60	0.70	0.80	0.90	1.00	1.10	1.20	1.30	1.40	1.50	1.60
L(DB)	208.72	177.56	155.46	135.63	117.56	100.86	85.25	70.51	56.47	42.99	29.88
1	2.6932	2.5148	2.2380	2.0468	1.8614	1.7190	1.6019	1.5334	1.4596	1.3978	1.3414
2	0.3341	0.3961	0.4604	0.5270	0.5956	0.6657	0.7365	0.8078	0.8766	0.9435	1.0067
3	4.4368	3.7587	3.2431	2.8661	2.5054	2.2312	2.0005	1.8043	1.6388	1.4939	1.3682
4	0.2797	0.3294	0.3806	0.4338	0.4894	0.5461	0.6053	0.6687	0.7376	0.8229	0.9210
5	4.4490	3.7786	3.2740	2.8769	2.5547	2.2963	2.0579	1.8597	1.6889	1.5398	1.4111
6	0.2685	0.3060	0.3564	0.4093	0.4650	0.5239	0.5865	0.6535	0.7269	0.7980	0.8850
7	4.4098	3.6684	3.1776	2.7951	2.4855	2.2289	2.0107	1.8123	1.6466	1.5067	1.3695
8	0.2509	0.2950	0.3401	0.3966	0.4346	0.4836	0.5368	0.5920	0.6504	0.7186	0.7983
9	4.1505	3.5308	3.0825	2.7084	2.3967	2.1499	1.9410	1.7607	1.6059	1.4607	1.3283

N = 18 VSWR = 2.00

BW	0.60	0.70	0.80	0.90	1.00	1.10	1.20	1.30	1.40	1.50	1.60
L(DB)	207.49	182.33	160.83	140.80	122.33	105.63	90.08	75.25	61.24	47.76	34.71
1	3.6568	3.1883	2.7954	2.5190	2.2976	2.1142	1.9788	1.8510	1.7458	1.6609	1.5955
2	0.3581	0.4236	0.4915	0.5617	0.6344	0.7091	0.7855	0.8630	0.9406	1.0178	1.0981
3	4.9861	4.2896	3.6994	3.2026	2.8051	2.5008	2.2750	2.0537	1.8660	1.7053	1.5690
4	0.3000	0.3530	0.4075	0.4639	0.5227	0.5843	0.6493	0.7185	0.7918	0.8700	0.9588
5	5.0798	4.3687	3.7836	3.2983	2.8935	2.4671	2.2838	2.0134	1.8295	1.6640	1.5171
6	0.2787	0.3230	0.3724	0.4233	0.4780	0.5367	0.5991	0.6687	0.7433	0.8269	0.9249
7	5.0883	3.9151	3.3098	2.9118	2.5904	2.3140	2.0985	1.9087	1.7332	1.5905	1.4618
8	0.2552	0.3000	0.3458	0.3929	0.4416	0.4921	0.5448	0.6002	0.6630	0.7321	0.7913
9	5.1960	3.5701	3.0971	2.7257	2.4854	2.1766	1.9663	1.7858	1.6265	1.4868	1.3553

TABLE 4.10

N = 20 VSWR = 1.05

BW / L(DB)	0.60 / 809.11	0.70 / 181.15	0.80 / 156.59	0.90 / 134.55	1.00 / 118.46	1.10 / 95.90	1.20 / 78.55	1.30 / 62.16	1.40 / 46.56	1.50 / 31.57	1.60 / 17.14
1	1.6876	1.5120	1.3877	1.2971	1.2297	1.1756	1.1395	1.1093	1.0857	1.0670	1.0521
2	0.3694	0.4411	0.5146	0.5884	0.6606	0.7292	0.7924	0.8496	0.8969	0.9370	0.9692
3	3.5058	2.9443	2.5153	2.1766	1.9040	1.6826	1.5034	1.3598	1.2471	1.1611	1.0975
4	0.2708	0.3203	0.3723	0.4275	0.4867	0.5507	0.6199	0.6938	0.7703	0.8454	0.9141
5	3.9283	3.3310	2.8766	2.5167	2.2218	1.9734	1.7593	1.5721	1.4085	1.2695	1.1540
6	0.2554	0.3008	0.3478	0.3966	0.4479	0.5025	0.5613	0.6259	0.6978	0.7779	0.8642
7	4.0249	3.4191	2.9800	2.5932	2.3040	2.0581	1.8473	1.6620	1.4950	1.3416	1.2010
8	0.2501	0.2944	0.3399	0.3970	0.4380	0.4876	0.5424	0.6015	0.6670	0.7421	0.8308
9	4.0453	3.4392	2.9796	2.6169	2.3234	2.0789	1.8706	1.6886	1.5254	1.3734	1.2261
10	0.2479	0.2917	0.3366	0.3800	0.4314	0.4920	0.5354	0.5928	0.6557	0.7276	0.8150

N = 20 VSWR = 1.10

BW / L(DB)	0.60 / 814.93	0.70 / 186.97	0.80 / 162.40	0.90 / 140.36	1.00 / 120.28	1.10 / 101.71	1.20 / 84.36	1.30 / 67.98	1.40 / 52.37	1.50 / 37.38	1.60 / 22.90
1	1.9169	1.6996	1.5436	1.4279	1.3401	1.2722	1.2191	1.1771	1.1434	1.1163	1.0960
2	0.3461	0.4126	0.4913	0.5715	0.6518	0.7307	0.7566	0.8178	0.8731	0.9214	0.9624
3	3.7218	3.1382	2.6891	2.3356	2.0495	1.8142	1.6204	1.4614	1.3326	1.2305	1.1518
4	0.2677	0.3180	0.3664	0.4195	0.4780	0.5365	0.6017	0.6717	0.7456	0.8210	0.8938
5	4.0427	3.4315	2.9675	2.6008	2.3016	2.0506	1.8351	1.6468	1.4809	1.3358	1.2185
6	0.2545	0.2996	0.3480	0.3942	0.4445	0.4975	0.5541	0.6155	0.6830	0.7580	0.8403
7	4.0961	3.4515	3.0180	2.6497	2.3524	2.1047	1.8933	1.7088	1.5435	1.3931	1.2540
8	0.2492	0.2932	0.3385	0.3849	0.4333	0.4859	0.5373	0.5944	0.6566	0.7263	0.8070
9	4.0907	3.4781	3.0146	2.6502	2.3549	2.1094	1.9009	1.7197	1.5587	1.4111	1.2707
10	0.2482	0.2897	0.3341	0.3900	0.4276	0.4772	0.5294	0.5850	0.6450	0.7120	0.7903

N = 20 VSWR = 1.20

BW / L(DB)	0.60 / 820.57	0.70 / 192.61	0.80 / 168.04	0.90 / 146.01	1.00 / 125.92	1.10 / 107.36	1.20 / 90.01	1.30 / 73.82	1.40 / 58.02	1.50 / 43.03	1.60 / 28.52
1	2.2414	1.9650	1.7718	1.6281	1.5071	1.4165	1.3447	1.2965	1.2390	1.1998	1.1671
2	0.3328	0.3951	0.4644	0.5276	0.5961	0.6645	0.7329	0.7977	0.8591	0.9153	0.9654
3	3.9509	3.3639	2.8935	2.5216	2.2196	1.9700	1.7618	1.5979	1.4434	1.3253	1.2307
4	0.2690	0.3171	0.3671	0.4192	0.4783	0.5329	0.5955	0.6626	0.7342	0.8090	0.8842
5	4.1906	3.5599	3.0817	2.7047	2.3979	2.1416	1.9224	1.7314	1.5629	1.4137	1.2837
6	0.2564	0.3016	0.3491	0.3961	0.4461	0.4986	0.5541	0.6135	0.6732	0.7428	0.8277
7	4.1874	3.5606	3.0862	2.7133	2.4110	2.1597	1.9461	1.7606	1.5959	1.4465	1.3098
8	0.2498	0.2934	0.3388	0.3853	0.4334	0.4836	0.5368	0.5921	0.6522	0.7183	0.7932
9	4.1414	3.5223	3.0541	2.6863	2.3988	2.1414	1.9319	1.7507	1.5907	1.4459	1.3105
10	0.2443	0.2884	0.3324	0.3779	0.4250	0.4739	0.5252	0.5794	0.6375	0.7009	0.7750

N = 20 VSWR = 1.50

BW / L(DB)	0.60 / 827.56	0.70 / 199.80	0.80 / 175.03	0.90 / 153.00	1.00 / 132.91	1.10 / 114.35	1.20 / 97.00	1.30 / 80.61	1.40 / 65.01	1.50 / 50.08	1.60 / 35.51
1	2.9038	2.5263	2.2478	2.0353	1.8689	1.7359	1.6277	1.5336	1.4584	1.4019	1.3496
2	0.3351	0.3972	0.4617	0.5285	0.5972	0.6674	0.7358	0.8093	0.8783	0.9357	1.0037
3	4.4694	3.7066	3.2675	2.8577	2.5248	2.2487	2.0165	1.8197	1.6526	1.5119	1.3947
4	0.2817	0.3317	0.3853	0.4360	0.4927	0.5517	0.6142	0.6839	0.7530	0.8276	0.9055
5	4.4944	3.8908	3.3108	2.9095	2.5939	2.3129	2.0852	1.8921	1.7081	1.5494	1.4105
6	0.2655	0.3122	0.3601	0.4095	0.4606	0.5140	0.5700	0.6294	0.6932	0.7623	0.8351
7	4.3724	3.7194	3.2255	2.8575	2.5236	2.2631	2.0424	1.8516	1.6857	1.5329	1.3952
8	0.2543	0.2989	0.3447	0.3917	0.4403	0.4908	0.5436	0.5992	0.6588	0.7243	0.7989
9	4.2300	3.5908	3.1815	2.7971	2.4441	2.1909	1.9805	1.7974	1.6363	1.4930	1.3610
10	0.2448	0.2879	0.3318	0.3770	0.4238	0.4782	0.5283	0.5780	0.6324	0.6930	0.7680

N = 20 VSWR = 2.00

BW / L(DB)	0.60 / 838.33	0.70 / 204.37	0.80 / 179.80	0.90 / 157.77	1.00 / 137.68	1.10 / 119.18	1.20 / 101.77	1.30 / 85.39	1.40 / 69.78	1.50 / 54.79	1.60 / 40.29
1	3.8773	3.1882	2.8147	2.5383	2.3098	2.1196	1.9881	1.9593	1.7559	1.6678	1.5920
2	0.3603	0.4282	0.4984	0.5651	0.6358	0.7133	0.7901	0.8679	0.9459	1.0230	1.0979
3	5.0428	4.2780	3.6974	3.2397	2.8688	2.5830	2.3000	2.0785	1.8887	1.7265	1.5889
4	0.3039	0.3576	0.4128	0.4700	0.5295	0.5918	0.6576	0.7274	0.8016	0.8804	0.9632
5	5.0653	4.1376	3.5870	3.1542	2.8035	2.5121	2.2647	2.0508	1.8630	1.6961	1.5478
6	0.2800	0.3298	0.3799	0.4314	0.4850	0.5408	0.5991	0.6607	0.7263	0.7969	0.8733
7	4.9928	3.9076	3.3896	2.9828	2.6538	2.3812	2.1505	1.9516	1.7778	1.6215	1.4820
8	0.2616	0.3075	0.3544	0.4087	0.4585	0.5042	0.5581	0.6146	0.6745	0.7397	0.8136
9	4.3295	3.6806	3.1982	2.8106	2.5013	2.2452	2.0287	1.8425	1.6796	1.5345	1.4083
10	0.2457	0.2888	0.3358	0.3781	0.4248	0.4752	0.5237	0.5765	0.6330	0.6919	0.7568

TABLE 4.11

based on an eight section prototype, with BW = 1.10, VSWR = 1.01 (which therefore has a maximum attenuation of 3.46 dB, from Table 4.5), and a cutoff frequency of 3.0 GHz. In the design, GR-900 14 millimeter precision connectors were used at either end to reduce connector reflections. These connectors also supported the stepped inner conductor of the filter. The entire system was designed on a 50 ohm basis. Referring to Table 4.5, it is seen that the stepped impedances, from left to right, are therefore:

50.00; 51.81; 45.85; 58.43; 41.01; 60.95; 42.71;
54.52; 48.25; 50.00;

To conform with the GR-900 connectors, the inner diameter of the outer conductor of the filter was chosen to be .5625". Standard reference tables[12] were then used to compute the diameter of the inner conductor steps. At 3GH$_z$, $\lambda/4 = .541"$. This should be the length of all the steps. In practice, however, it is found that at each step junction there is fringing capacitance. This capitance causes the pass band VSWR to deviate from its theoretical equiripple shape and, more important, shifts the cutoff frequency of the filter.

A method has been presented[13] however, whereby the junction fringing capacitance is compensated for by changing the length of each step so as to keep the cutoff frequency constant. This method was used in the present design.

It was found by computer analysis that after making the length modifications the maximum passband VSWR should be 1.011.

The final dimensions for the filter are given in Fig.4.4, and the VSWR performance is shown in Fig.4.5. Notice the close agreement at cutoff and the low passband VSWR level. The slight discrepancy in the passband VSWR is thought to be mainly due to the connectors and to mechanical tolerances ($\pm .001^{"}$ for lengths and $.0005^{"}$ for diameters) in the filter itself.

4.4 Concluding Remarks.

Although the function $L_{2n}(X,b)$ has been used thus far in designing filters with an even number of sections, it can also be used to advantage to design filters with an odd number of sections (when $R \neq 1$). Consider the conventional Chebyshev design shown in Fig. 4.6. This $n = 5$ design has the specification

$$\frac{P_o}{P_L} = 1 + \frac{(R-1)^2}{4R} + e^2 T_n^2(X), \text{ n odd.} \qquad (4.42)$$

Now assume that it is desired to modify the form of Eq.(4.42), but that R, n, and the maximum pass-band insertion loss are to remain fixed. Then the modified design in Fig.4.7 may be used, which has the specification

$$\frac{P_o}{P_L} = 1 + e_1^2 \left[\frac{1 + L_{2n}(X,b)}{2}\right] \text{ , n odd} \qquad (4.43)$$

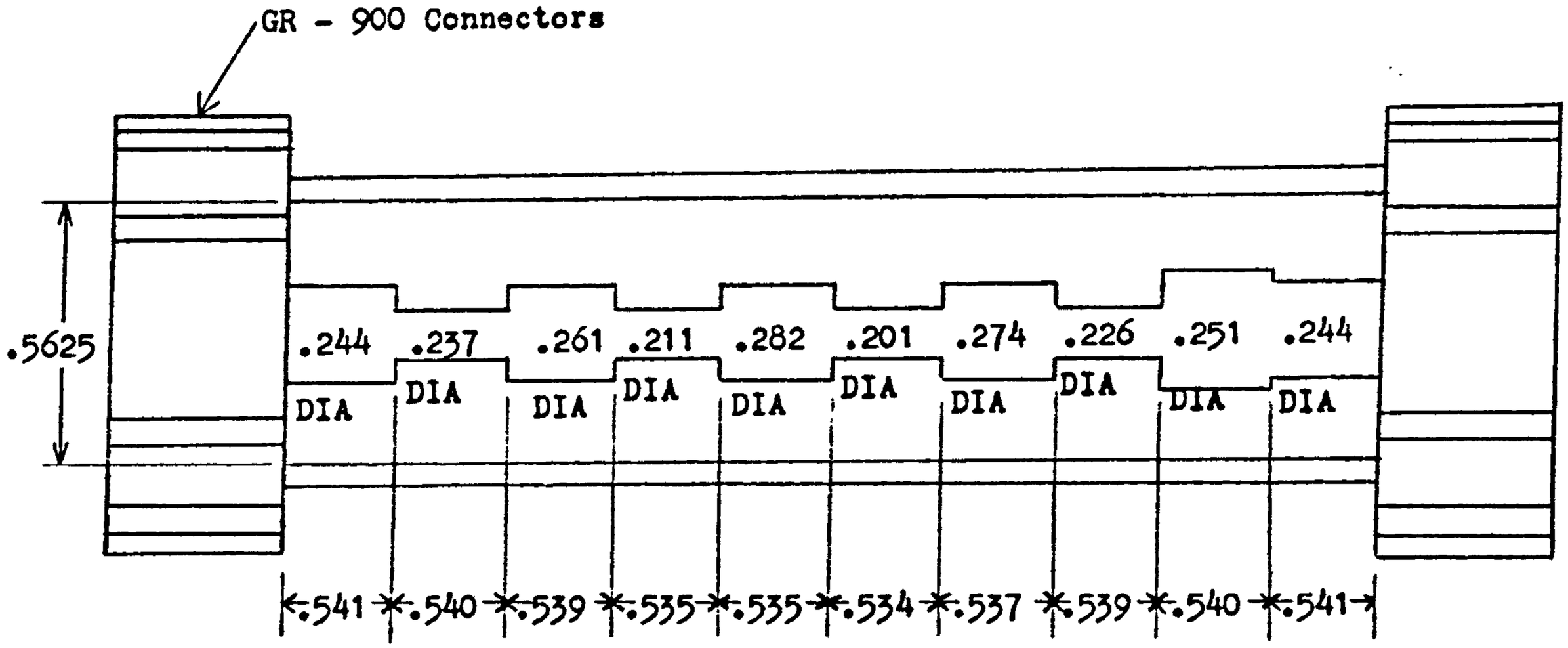

Fig. 4.4. Constructional details of an eight element, low pass distributed coaxial filter which is equally terminated.

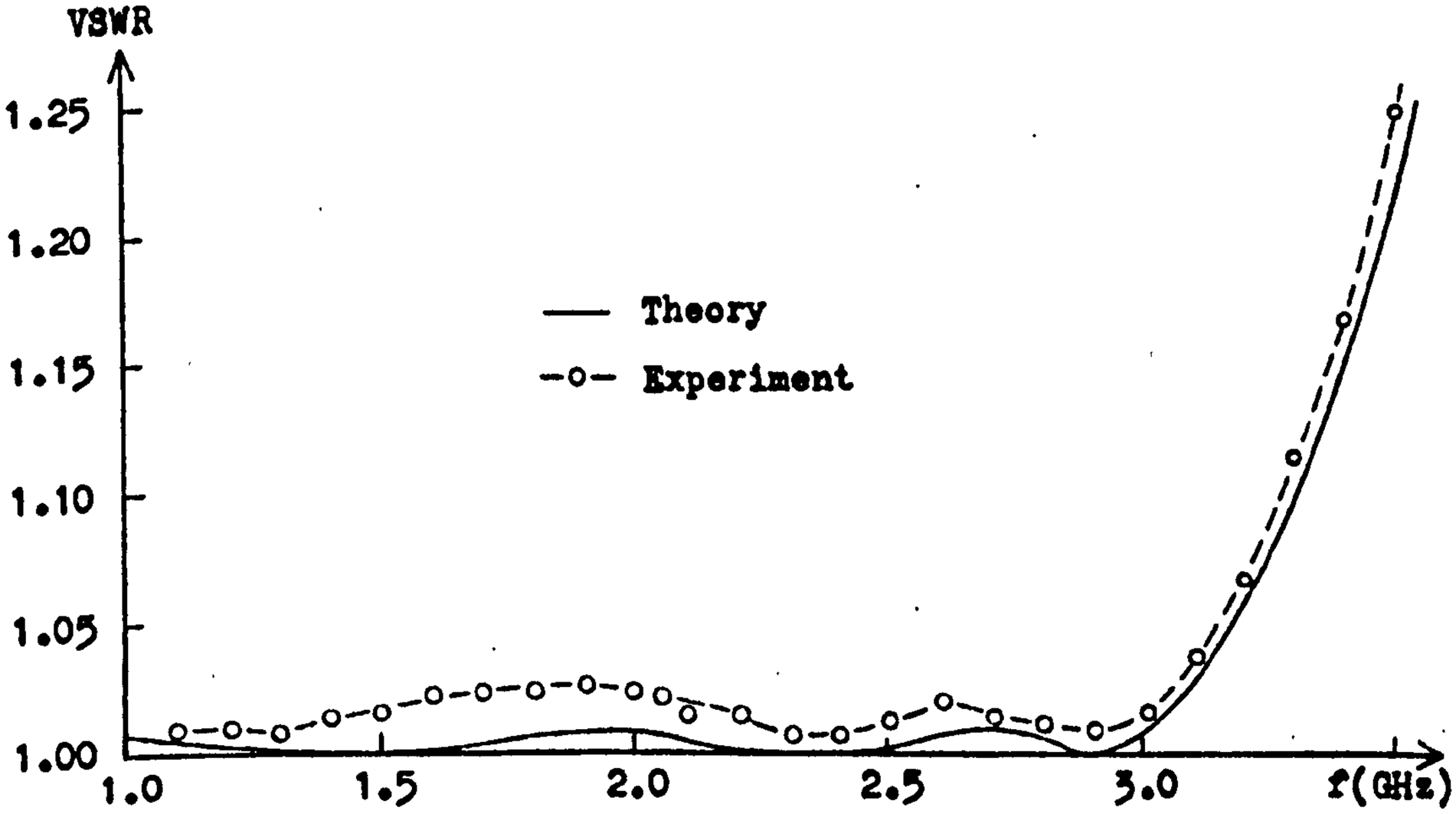

Fig. 4.5. VSWR performance of the filter in Fig. 4.4.

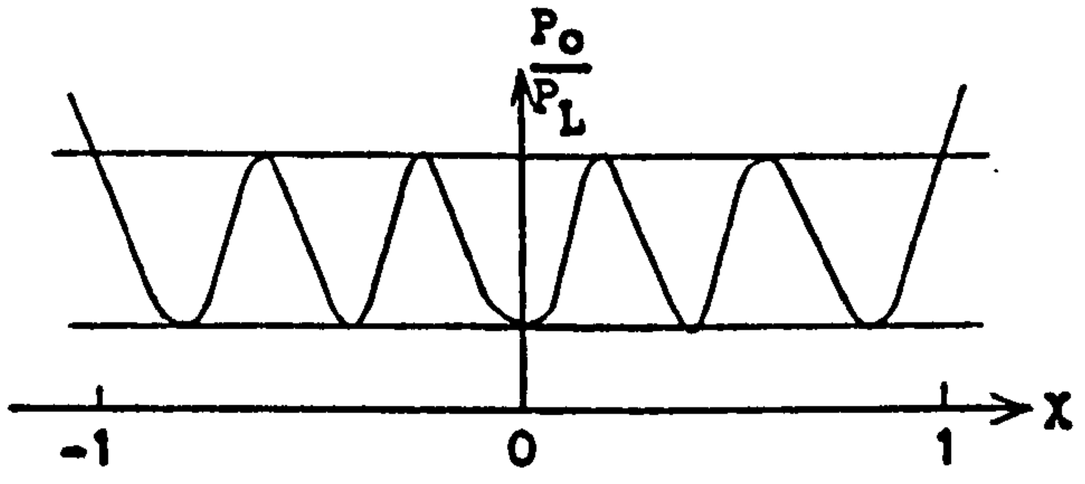

Fig. 4.6. Conventional Chebyshev design for n = 5.

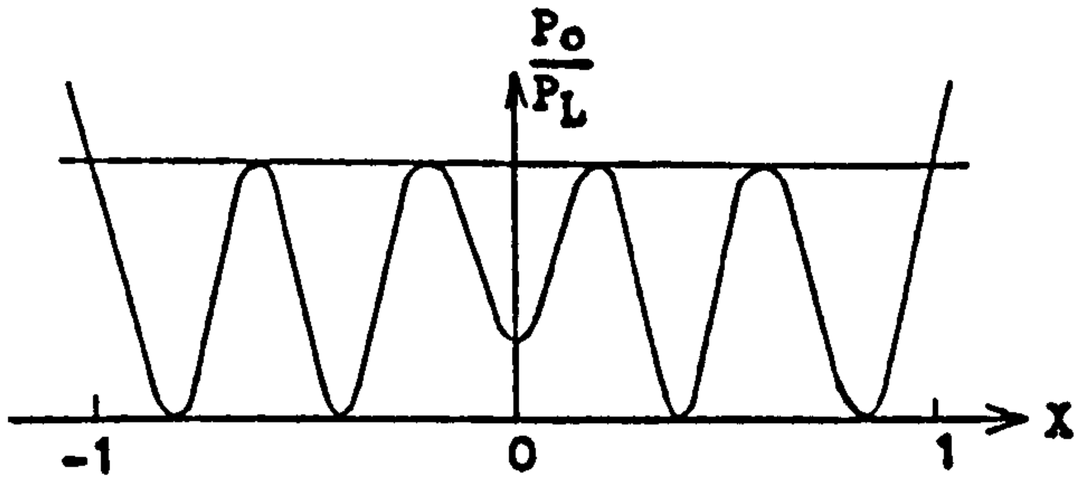

Fig. 4.7. Modified design for n = 5.

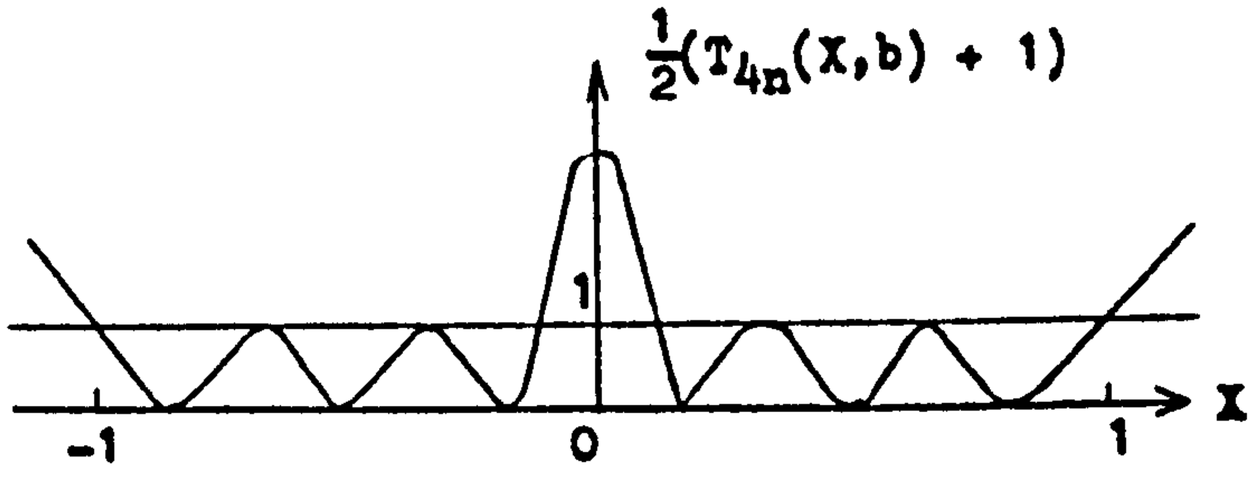

Fig. 4.8. Modified design when b>1.

where

$$e_1^2 = \frac{(R-1)^2}{4R} + e^2 .$$

In the appendix it is proved that Eq.(4.43) has a faster rate of cutoff in the attenuation band than any other polynomial specification, including Eq.(4.42).

There is an interesting comparison between Eqs.(4.42) and (4.43). In Eq.(4.42) the zeros of $\Gamma(s)\Gamma(-s)$, which are the factors of $\frac{P_o}{P_L} - 1$, are not on the imaginary axis but have both real and imaginary parts. As discussed in chapter 2, this fact means that there are many different choices available for the zeros of $\Gamma(s)$, with the number of choices increasing rapidly with n. In a specification of the type of Eq.(4.43), however, it is seen that all except two of the zeros of $\frac{P_o}{P_L} - 1$ are double and on the imaginary axis. The other two zeros are on the positive and negative real axis and equidistant from the origin. This means that there will be only two choices available for the zeros of $\Gamma(s)$.

In the design of even order filters the function $L_{4n}(X,b)$ has an interesting property. When $b > 1$, the argument $2n \cos^{-1}([1+b]X^2 - b)$ becomes pure imaginary as $X \to 0$, resulting in $\frac{1}{2}[T_{4n}(X,b) + 1]$ having the shape depicted in Fig.4.8. This characteristic may either be used in the design of low-pass or band-pass filters. It

is equivalent to a function previously described by Matthaei[14].

There is still much interesting work to be done with the $L_{2n}(X,b)$ function described previously. It would be very rewarding to find closed formulae for the element values in a lumped filter whose insertion loss is described by $\frac{P_o}{P_L} = 1 + e^2 \left[\frac{L_{2n}(X,b) + 1}{2}\right]$. These element values would be functions of e^2, b, and n. When $b = 1$, the element values so determined must agree with Takahasi's results[4], which use "pure" Chebyshev polynomials ($T_n(X)$) in the insertion loss description. Some preliminary work on this problem has already been done. It has been found that whereas the poles of $\Gamma(s)\Gamma(-s)$ lie on an ellipse for the "pure" Chebyshev case, they do not lie on an ellipse for the $L_{2n}(X,b)$ case when $b \neq 1$. A good discussion of Takahasi's proof, which is very suggestive and contains useful information for dealing with the above problem, is given in Weinberg's book[3]. Another useful project would be the compilation of tables to "fill in the blanks" in Weinberg's tables of Chebyshev filters[3] for the cases where n is even and $R \neq 1$. Also, if only R, n, and the maximum passband insertion loss are specified, it was previously seen (Figs.4.6 and 4.7) how the conventional insertion loss can be improved in the stopband. A set of tables for this case would be worthwhile.

4.5 Proof That the L_n Polynomials Are Optimal.

It was stated earlier that, of all polynomials of degree 2n required to be bounded in magnitude by unity in the passband $-1 \leq X \leq 1$ and required to have a given absolute value between 0 and 1 at $X = 0$, the polynomial which exceeds all others in the stopband $|X| > 1$ is $L_{2n}(X,b)$, which is defined through Eqs.(4.17), (4.18), and (4.19). The proof of this statement is shown in two steps.

First, assume $|L_{DC}| > 0$. $L_6(W,b)$ would then have the shape shown in Fig.4.9, for example. Now let there exist another polynomial of degree 2n, $P_{2n}(X)$, which satisfies the above passband conditions, and in addition has the property

$$|P_{2n}(X_o)| > |L_{2n}(X_o,b)| \qquad X_o > 1 \tag{4.44}$$

at least at one point X_o in the stopband interval.

The polynomial

$$Q(X) = L_{2n}(X,b) - \frac{L_{2n}(X_o,b)}{P_{2n}(X_o)} \cdot P_{2n}(X) \tag{4.45}$$

has 2n zeros in the passband $-1 \leq X \leq 1$. To see this fact, refer to Fig.4.9. $|L_{2n}(0,b)| = |P_{2n}(0)| = |C|$, where point C is shown in the Figure. Thus $\left|\frac{L_{2n}(X_o,b)}{P_{2n}(X_o)} P_{2n}(0)\right| = |A| < |C|$, and

hence point A is "trapped" inside the curve DCE. As X varies from $0 \rightarrow \pm 1$, $\frac{L_{2n}(X_o,b)}{P_{2n}(X_o)} P_{2n}(X)$ must intersect $L_n(X,b)$

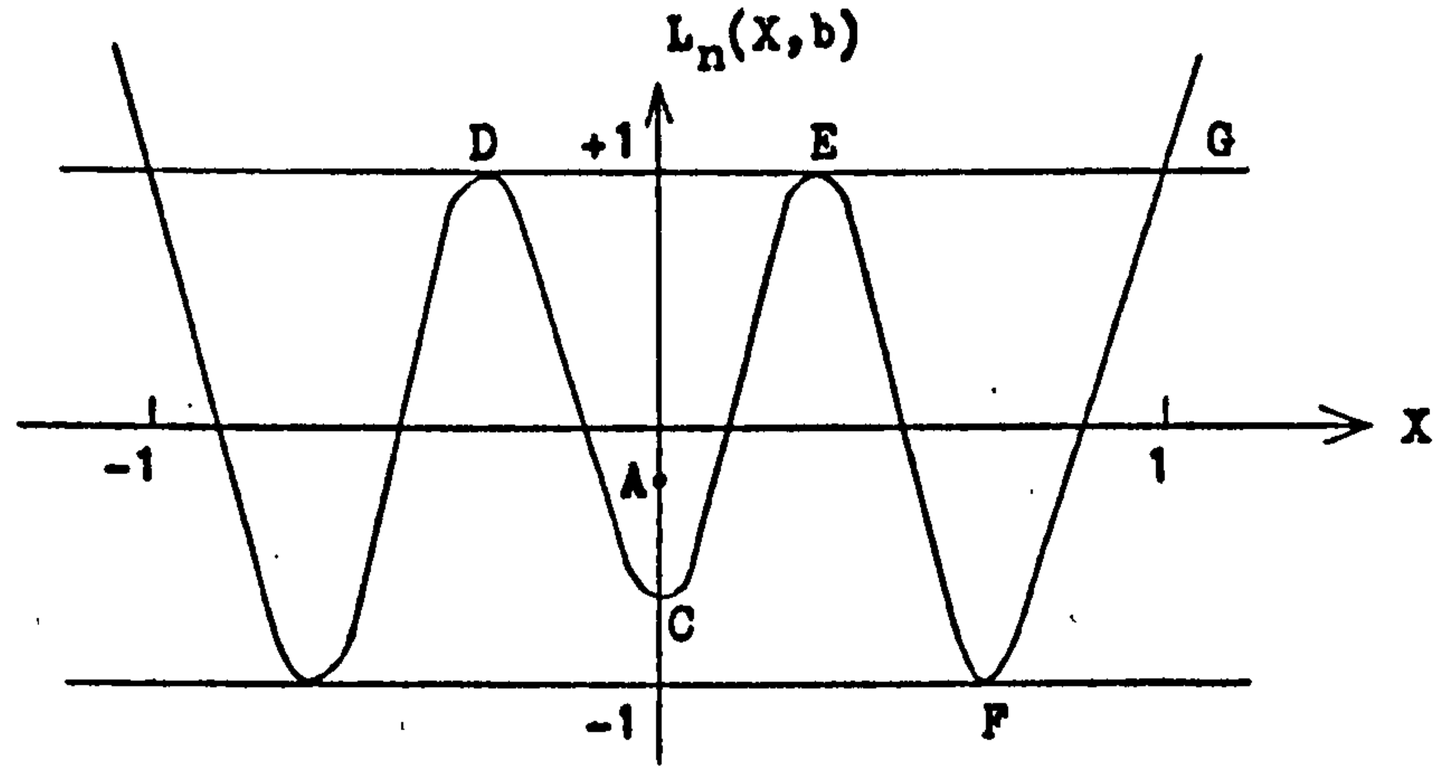

Fig. 4.9. Demonstration of the optimal property of $L_n(X,b)$.

n times, giving rise to 2n zeros of Q(X) in the passband. But Q(X) also has a zero at X_o, which means that Q (X) is at least of (2n + 1) degree, which is impossible, since by construction it is of degree 2n. Thus Eq.(4.44) is false, and $L_{2n}(X,b)$ must be the optimal polynomial.

Next consider the case where $L_{DC} = 0$. Q(X) is again constructed as in Eq.(4.45). Similar to the above method, it is readily seen that Q (X) will have 2n-2 zeros on the range $0 < |X| \leq 1$. Since $P_{2n}(0) = L_{2n}(0,b) = 0$, Q(X) will have at least one more zero at X = 0. Now at $X = \pm 1$, Eq.(4.17) gives

$$L_{2n}(\pm 1,b) = \cos(n \cos^{-1}(1)) = \cos 0 = 1. \tag{4.46}$$

But $\left| \frac{L_{2n}(X_o,b)}{P_{2n}(X_o)} \quad P_{2n}(1) \right| < 1$ and so Q(X) will be positive at $X = \pm 1$. Since the sign of Q(X) is the same at each end of the interval $[-1,1]$, it must possess an even number of real zeros within this interval. Hence the degree of Q(X) is at least 2n. In addition Q (X) also has a zero at X_o, and is therefore of 2n + 1 degree. But by construction Q(X) is of degree 2n, and therefore Eq.(4.44) is false, and $L_{2n}(X,b)$ must be the optimal polynomial.

It is seen that for the above proof to hold, it is necessary for point C to be of opposite sign to D and E.

In Eq.(4.17) it is therefore necessary for $\theta\Big|_{X=0}$ to be in the interval $\left[n\pi - \frac{\pi}{2},\ n\pi\right]$. This is automatically insured by Eqs.(4.18) and (4.19).

Chapter 4 REFERENCES

1. Papoulis, A.: "On the approximation problem in filter design", IRE National Convention Record, Part 2, 1957, pp. 182-183.

2. Levy, R.: "Tables of element values for the distributed low-pass prototype filter", IEEE Trans. MTT, Vol. MTT-13, 1965, pp. 514-536.

3. Weinberg, L.: "Network Analysis and Synthesis". McGraw-Hill, Inc., 1962, Chapter 13.

4. Takahasi, H.: "On the ladder-type filter network with Tchebysheff response", J. Inst. Elec. Commun. Engrs. Japan, February, 1951, Vol. 34, No. 2 (in Japanese).

5. Lind, L.F.: "Synthesis of equally terminated, low-pass, lumped and distributed filters of even order", IEEE Trans. MTT (to be published).

6. Jones, N.B.: "Lowpass filters with approximately equal-ripple modulus error", Electronics Letters,1967, Vol. 3, pp. 516-517.

7. Jones, N.B. and Wood, R.A.: "Generalized Chebyshev lowpass filters", Electronics Letters, Vol. 4, 1968, pp. 158-159.

Chapter 4 REFERENCES (continued)

8. Vasil'yev, V.B.: "Optimum microwave filters with an even number of sections", Telecommunications and Radio Engineering, August, 1966, Vol. 21, No. 8, pp. 85-91. (English edition of Russian Technical journals Elektrosvyaz' and Radiotekhnika.)

9. Weinberg, L.: "Network Analysis and Synthesis". McGraw-Hill, Inc., 1962, pp. 512-513.

10. Weinberg, L.: "Network Analysis and Synthesis". McGraw-Hill, Inc., 1962, pp. 595-597.

11. Bingham, J.A.C.: "A new method of solving the accuracy problem in filter design", IEEE Trans., Sept. 1964, CT-11, pp. 327-341.

12. Saad, T.S.: "Microwave Engineers Technical and Buyers Guide Edition, 1968". Horizon House, p. 44.

13. Levy, R. and Rozzi, T.: "Precise design of coaxial low-pass filters", IEEE Trans. MTT, Vol. MTT-16, March, 1968, pp. 142-147.

14. Matthaei, G.L.: "Tables of Chebyshev impedance-transforming networks of low-pass filter form", Proc. IEEE, 1964, Vol. 52, No. 8, pp. 939-963.

Chapter 5. Branch-Guide Directional Couplers.

5.1 General Directional Coupler Theory[1].

5.1.1 The Scattering Matrix.

In chapter 2 it was shown that the scattering matrix for a lossless, reciprocal network has the properties:

1) $S_{ij} = S_{ji}$, or $S = \widetilde{S}$, (5.1)

i.e., the scattering matrix and its transpose are identical.

Also, the scattering matrix is unitary, or

2) $(S)(\widetilde{S^*}) = 1_n$. (5.2)

From these two properties, it is easily seen that

$$(S)(S^*) = 1_n, \tag{5.3}$$

where * indicates complex conjugate, and 1_n is the unit matrix. It was also shown that the scattering matrix always exists for a passive network.

Consider now a lossless, reciprocal 4-port network having a specified load impedance at each port. The network is defined to be a directional coupler if, at some center frequency, its input ports can be grouped into two pairs having the following properties:

1) Each pair of ports is mutually isolated, (5.4)

2) The ports of one pair are both matched. (5.5)

The 4-port network is shown in Fig.5.1, where ports 1, 2 and 3, 4 are the mutually isolated pairs. In this coupler port 1 delivers coupled power to port 3, and port 2 delivers coupled power to port 4. Coupling between ports j and k is

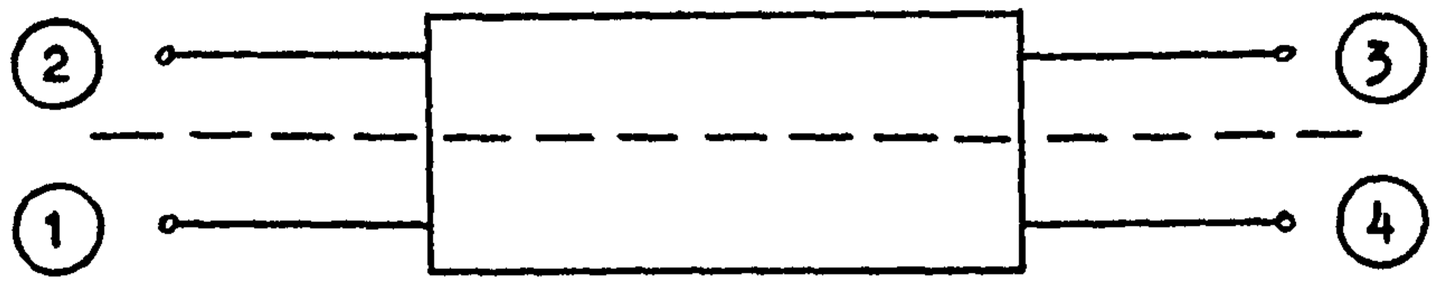

Fig. 5.1. Directional coupler - schematic.

commonly defined as

$$\text{Coupling (in dB)} \equiv -10 \log_{10} |S_{jk}|^2 . \tag{5.6}$$

Perfect isolation between ports 1,2 and ports 3,4, implies that

$$S_{12} = S_{21} = S_{34} = S_{43} = 0. \tag{5.7}$$

If each pair of ports is not perfectly isolated, then the isolation between ports j and k is defined as

$$\text{Isolation (in dB)} \equiv -10 \log_{10} |S_{jk}|^2 . \tag{5.8}$$

A quantity related to the isolation is directivity, which is defined as

$$\text{Directivity (in dB)} = 10 \log_{10} \left(\frac{\text{coupled power}}{\text{isolation power}} \right), \tag{5.9}$$

i.e.,

$$\text{Port 1 Directivity} = 10 \log_{10} \frac{|S_{13}|^2}{|S_{12}|^2} \text{ dB} .$$

It is apparent that perfect isolation implies infinite directivity.

Port j is matched when the voltage reflection coefficient $S_{jj} = 0$. If port j is not perfectly matched, then the VSWR at this port is defined by

$$\text{Port j VSWR} \equiv \frac{1 + |S_{jj}|}{1 - |S_{jj}|} . \tag{5.10}$$

If ports 1 and 2 are the pair which are perfectly matched in Fig. 5.1, then the VSWR =1.0 at these ports, and

$$S_{11} = S_{22} = 0. \tag{5.11}$$

Assuming that conditions (5.4) and (5.5) hold, the scattering matrix of the directional coupler becomes

$$\begin{pmatrix} 0 & 0 & S_{13} & S_{14} \\ 0 & 0 & S_{23} & S_{24} \\ S_{13} & S_{23} & S_{33} & 0 \\ S_{14} & S_{24} & 0 & S_{44} \end{pmatrix}. \tag{5.12}$$

Each entry is in general a complex number. It will now be shown that ports 3 and 4, i.e., all 4 ports of the directional coupler, must be matched. For application of the unitary condition, Eq.(5.3), gives

$$\begin{aligned} |S_{13}|^2 + |S_{14}|^2 &= 1, \\ |S_{23}|^2 + |S_{24}|^2 &= 1, \\ |S_{13}|^2 + |S_{23}|^2 + |S_{33}|^2 &= 1, \\ |S_{14}|^2 + |S_{24}|^2 + |S_{44}|^2 &= 1, \end{aligned} \tag{5.13}$$

which can only be satisfied if

$$|S_{33}| = |S_{44}| = 0. \tag{5.14}$$

Another useful property follows by subtracting pairs of equations in Eqs.(5.13), giving

$$|S_{13}| = |S_{24}| \ ,$$
$$|S_{14}| = |S_{23}| \ . \qquad (5.15)$$

This means that in any 4-port network where all ports are matched the moduli of the elements of the scattering matrix contain only two independent quantities. The phases are arbitrary, but only to that extent allowed by the unitary condition, for applying Eq.(5.3) to the matrix of Eq.(5.12) leads to the following relationships in addition to those of Eqs.(5.13):

$$S_{13}\, S_{23}^{*} + S_{14}\, S_{24}^{*} = 0,$$
$$S_{13}\, S_{14}^{*} + S_{23}\, S_{24}^{*} = 0. \qquad (5.16)$$

It is obvious that the reference planes in the various ports may be chosen to fix the phases of S_{13}, S_{14}, and S_{24} in any way. In particular these planes may be chosen so that S_{13} and S_{24} are pure real, and S_{14} is purely imaginary. Eqs. (5.15) then give

$$S_{13} = S_{24} = a, \qquad S_{14} = jb,$$

which, when inserted in Eqs.(5.16), gives

$$S_{23} = jb.$$

The scattering matrix of Eq.(5.12) then becomes

$$\begin{pmatrix} 0 & 0 & a & jb \\ 0 & 0 & jb & a \\ a & jb & 0 & 0 \\ jb & a & 0 & 0 \end{pmatrix} . \qquad (5.17)$$

Hence, by proper location of the reference planes, the scattering matrix will contain only two arbitrary quantities.

It has been shown that all directional couplers are perfectly matched, and by applying similar methods to those above it is easily proved that the converse is true, that all 4-port junctions which are perfectly matched are directional couplers.

5.1.2 The Symmetric Directional Coupler.

One of the most common and useful classes of directional couplers is completely symmetric, i.e., one where ports 1,2, 3, and 4 of the coupler in Fig.5.1 are physically indistinguishable. Assuming that the coupler is slightly imperfect (that there is finite isolation and slight mismatch, although symmetry is still preserved) then the scattering matrix is restricted by the symmetry properties as follows:

$$S_{11} = S_{22} = S_{33} = S_{44} ,$$

$$S_{12} = S_{21} = S_{34} = S_{43} ,$$

$$S_{13} = S_{31} = S_{24} = S_{42} ,$$

$$S_{14} = S_{41} = S_{23} = S_{32} , \qquad (5.18)$$

so that the scattering matrix becomes

$$\begin{pmatrix} S_{11} & S_{12} & S_{13} & S_{14} \\ S_{12} & S_{11} & S_{14} & S_{13} \\ S_{13} & S_{14} & S_{11} & S_{12} \\ S_{14} & S_{13} & S_{12} & S_{11} \end{pmatrix}, \tag{5.19}$$

and the unitary relationship, Eq.(5.3), gives the following four equations:

$$\begin{aligned} |S_{11}|^2 + |S_{12}|^2 + |S_{13}|^2 + |S_{14}|^2 &= 1, \\ S_{11}S_{12}^* + S_{12}S_{11}^* + S_{13}S_{14}^* + S_{14}S_{13}^* &= 0, \\ S_{11}S_{13}^* + S_{12}S_{14}^* + S_{13}S_{11}^* + S_{14}S_{12}^* &= 0, \\ S_{11}S_{14}^* + S_{12}S_{13}^* + S_{13}S_{12}^* + S_{14}S_{11}^* &= 0. \end{aligned} \tag{5.20}$$

From these equations it is possible to work out some useful general properties of the symmetrical coupler, particularly the phase difference between the waves coupled from port 1 to ports 3 and 4. The last two of Eqs.(5.20) may be rearranged to form the product

$$\begin{aligned} &(S_{11}S_{13}^* + S_{12}S_{14}^*)(S_{11}^*S_{14} + S_{12}^*S_{13}) \\ &= (S_{13}S_{11}^* + S_{14}S_{12}^*)(S_{12}S_{13}^* + S_{14}^*S_{11}), \end{aligned} \tag{5.21}$$

which reduces to

$$\begin{aligned} &(|S_{11}|^2 - |S_{12}|^2)(S_{13}^*S_{14} - S_{13}S_{14}^*) \\ &= (|S_{13}|^2 - |S_{14}|^2)(S_{11}^*S_{12} - S_{11}S_{12}^*). \end{aligned} \tag{5.22}$$

If for the present the condition for perfect isolation between ports 1 and 2 is introduced, i.e., that $S_{12}=0$, Eqs.(5.20) and (5.22) reduce to:

$$|S_{11}|^2 + |S_{13}|^2 + |S_{14}|^2 = 1,$$

$$S_{13}S_{14}^* + S_{14}S_{13}^* = 0,$$

$$S_{11}S_{13}^* + S_{13}S_{11}^* = 0,$$

$$S_{11}S_{14}^* + S_{14}S_{11}^* = 0,$$

$$|S_{11}|^2(S_{13}^*S_{14} - S_{13}S_{14}^*) = 0. \qquad (5.23)$$

Equations (5.23) can be satisfied simultaneously only if $S_{11}=0$, for if $S_{11}\neq 0$ then either S_{13} or S_{14} must vanish, resulting in degenerate cases of no interest. This means that in a symmetric coupler, perfect isolation, $S_{12}=0$, implies perfect match, $S_{11}=0$. Equations (5.23) then reduce still further as follows:

$$|S_{13}|^2 + |S_{14}|^2 = 1. \qquad (5.24)$$

$$S_{13}S_{14}^* + S_{14}S_{13}^* = 0. \qquad (5.25)$$

The phase relationship follows from Eq.(5.25), for putting $S_{13} = |S_{13}|e^{j\theta_3}$ and $S_{14} = |S_{14}|e^{j\theta_4}$, this becomes

$$\cos(\theta_3 - \theta_4) = 0, \qquad (5.26)$$

so that for perfect match and isolation, the symmetric directional coupler possesses a 90^{o} phase difference between the waves in the two output arms.

5.1.3 The Symmetric Hybrid Junction.

A case of particular interest is that of the 3-dB coupler, that is, one giving equal power division between ports 3 and 4. The symmetric 3-dB coupler is, in fact, a hybrid junction. It may be realized in many forms, e.g., in rectangular waveguide as the short-shot (narrow-wall) coupler, the top-wall coupler, and the branch-guide coupler. In quasi-optical guide wave systems it appears as the semireflecting mirror or as a quarter-wave plate ; or in TEM-line systems as the coupled transmission line (proximity) 3-dB coupler, or as a branch-line coupler. The branch-line and branch-guide systems are described in greater detail in subsequent sections of this chapter. At this stage, however, it is convenient to derive properties common to all symmetric 3-dB couplers whatever their physical form. It has already been shown that a perfect symmetric coupler, 3-DB or otherwise, gives a quadrature phase relationship between the waves in the two output ports. It is of interest to find the phase relationship of a slightly imperfect 3-dB coupler, i.e., one with finite isolation and slight mismatch. This gives information about the bandwidth properties of the 3-dB coupler when used as a hybrid.

Eq.(5.22) may be written in terms of the moduli $|S_{1k}|$ and arguments θ_k of the S_{1k} parameters (k=1,2,3,4) to give

$$(|S_{11}|^2 - |S_{12}|^2)\,|S_{13}| \cdot |S_{14}| \sin(\theta_3 - \theta_4)$$

$$(|S_{13}|^2 - |S_{14}|^2)\,|S_{11}| \cdot |S_{12}| \sin(\theta_1 - \theta_2). \qquad (5.27)$$

In the case of a slightly imperfect hybrid,

$$|S_{13}| \simeq |S_{14}| \simeq 2^{-\frac{1}{2}}, \qquad (5.28)$$

$$(\theta_3 - \theta_4) \simeq \frac{\pi}{2}, \qquad (5.29)$$

$$|S_{11}|, |S_{12}| \ll 1, \qquad (5.30)$$

whence Eq.(5.27) reduces to

$$|S_{11}|^2 - |S_{12}|^2 \simeq$$

$$2(|S_{13}|^2 - |S_{14}|^2)\,|S_{11}| \cdot |S_{12}| \sin(\theta_1 - \theta_2), \qquad (5.31)$$

which, by virtue of Eq.(5.28), is very small (i.e., at least an order of magnitude less than either $|S_{11}|^2$ or $|S_{12}|^2$), leading to the final result that

$$|S_{11}| \simeq |S_{12}|. \qquad (5.32)$$

Eq.(5.32) states that the magnitude of the reflected wave at the input port is equal to that of the wave appearing from the "isolated" port, implying the relationship between the input VSWR and the isolation of the hybrid as shown in Fig.5.2. The experimentally determined performance

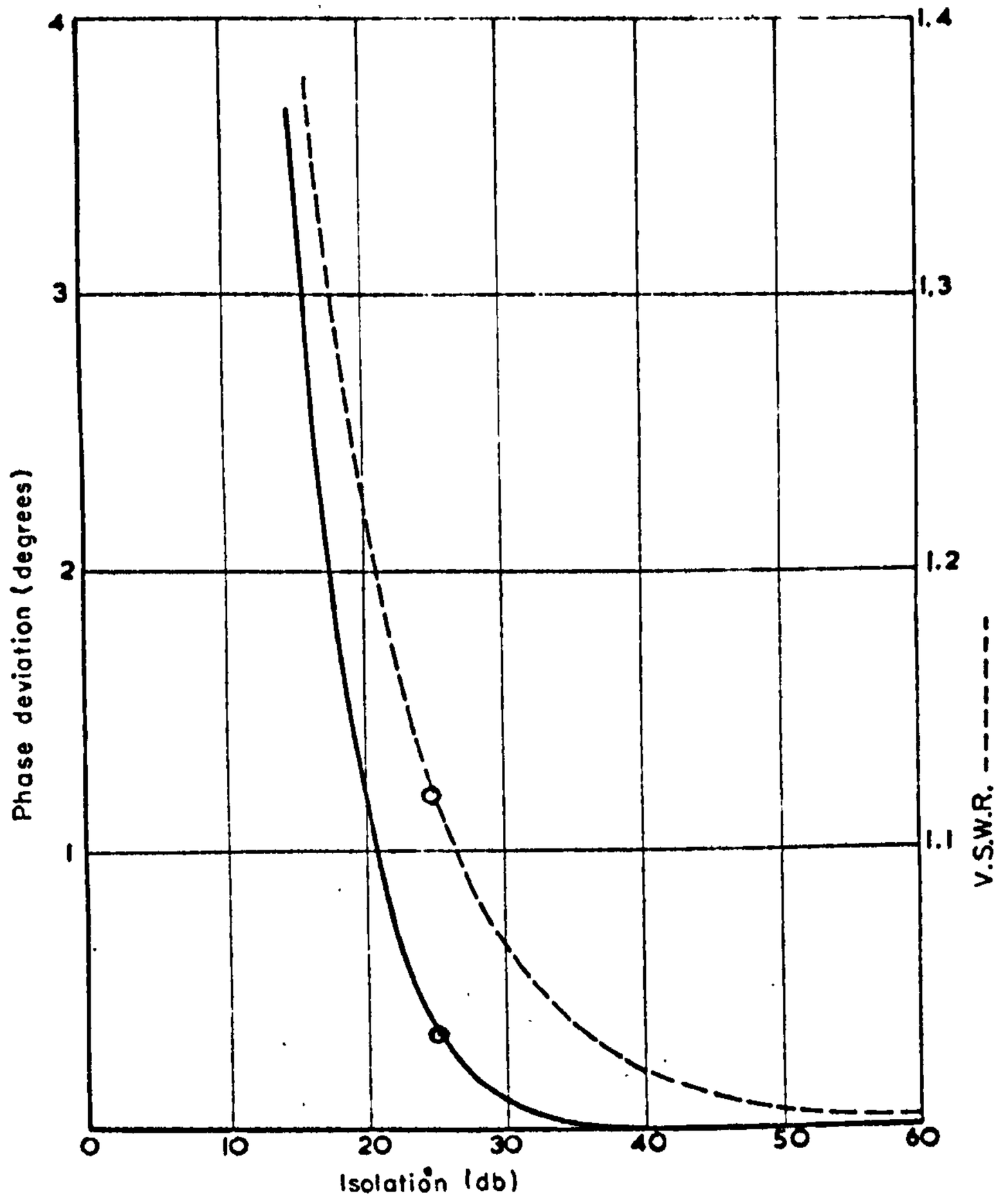

Fig. 5.2. Theoretical phase deviation (—) and VSWR (- -) of an imperfect symmetric 3-dB coupler.

of many symmetric hybrids show that this relationship holds quite closely. An analysis of a branch-guide hybrid yielded the points shown the Figure, showing again the correctness of the approximate equality of Eq.(5.32). Symmetry considerations (i.e., the 3-dB coupling) make this conclusion seem entirely reasonable.

Another useful result is obtained by writing the second of Eqs.(5.20) in the form

$$|S_{11}| \cdot |S_{12}| \cos(\theta_1 - \theta_2) + |S_{13}| \cdot |S_{14}| \cos(\theta_3 - \theta_4) = 0,$$

giving

$$|\cos(\theta_3 - \theta_4)| = \frac{|S_{11}| \cdot |S_{12}|}{|S_{13}| \cdot |S_{14}|} |\cos(\theta_1 - \theta_2)| , \qquad (5.33)$$

which, using Eqs.(5.28) and (5.32) gives in the worst possible case (when $\theta_1 = \theta_2$) the relationship

$$|\cos(\theta_3 - \theta_4)| \simeq 2 |S_{12}|^2$$

$$= 2(10^{-I/10}), \qquad (5.34)$$

where I is the isolation of the hybrid (in dB) when port 1 is the input port. Thus when the isolation is 30dB, $|\cos(\theta_3 - \theta_4)| = 2 \times 10^{-3}$, giving a phase difference which differs from the ideal 90° by only 0.1°. When the isolation has fallen to 20dB, the phase difference has increased to 1.2°. The complete form of Eq.(5.32) is shown in Fig.5.2. Since

3-dB couplers with values of isolation over a broad band of 25 dB or even of 30 dB are quite common, Fig.5.2 shows that the phase deviation property of these devices is extremely good, and equally broad band. Thus, it is possible to construct phase-measuring bridges incorporating 3-dB hybrids which give high accuracy over broad bandwidths. A further result is that when dealing with applications of the hybrid where the output arms may be short-circuited, as in a duplexer or diplexer, it is usually not necessary to take the phase variation into account as it is so small.

5.1.4 Directional Coupler Even and Odd Mode Analysis.

By the adoption of the scattering matrix for the description of a multiport junction, the problem of the solution of Maxwell's equations for the boundary conditions inside the junction has been deliberately relinquished. This is necessary for most practical junctions because of the usually insurmountable mathematical difficulties encountered. The symmetry of the junction can, however, provide some knowledge about the field in the interior. Thus, suppose the directional coupler depicted in Fig.5.1 has a symmetry plane as indicated by the dotted line. Then if two signals of amplitude $\frac{1}{2}$ and in phase are applied to ports 1 and 2, by symmetry a voltage maximum occurs at every point on the line of symmetry. On the symmetry plane then $Z \rightarrow \infty$, i.e.,

the junction may be open-circuited at the plane without affecting the field distribution, or alternatively a "magnetic wall" may be located at this plane (Fig.5.3a). Similarly, if two signals of amplitude $\frac{1}{2}$ and out of phase are applied to ports 1 and 2, a voltage minimum occurs on the line of symmetry. On the symmetry plane Z = 0, i.e., a short circuit (an "electric wall") may be located at the plane without affecting the field distributions, as shown in Fig.5.3b. These two modes of operation of the junction are called the even and odd modes, respectively. They are the so-called normal modes of the junction. For each normal mode, the problem reduces to that of a 2-port network, for which a solution may generally be obtained. By superposition, the sum of the two normal mode field distributions corresponds to that given by a signal of unit amplitude input at port 1. The resultant signals out of each port are also given by the superposition of those obtained in the even and odd modes. For the even mode a reflection coefficient $\Gamma_e = S_{11\,even}$ and a transmission coefficient $T_e = S_{12\,even}$ are determined, and similarly for the odd mode, $\Gamma_o = S_{11\,odd}$ and $T_o = S_{12\,odd}$ are determined. Superposition gives the following vector amplitudes of the signals emerging from the 4 ports:

$$b_1 = \tfrac{1}{2}(\Gamma_e + \Gamma_o), \quad b_3 = \tfrac{1}{2}(T_e - T_o),$$
$$b_2 = \tfrac{1}{2}(\Gamma_e - \Gamma_o), \quad b_4 = \tfrac{1}{2}(T_e + T_o). \tag{5.35}$$

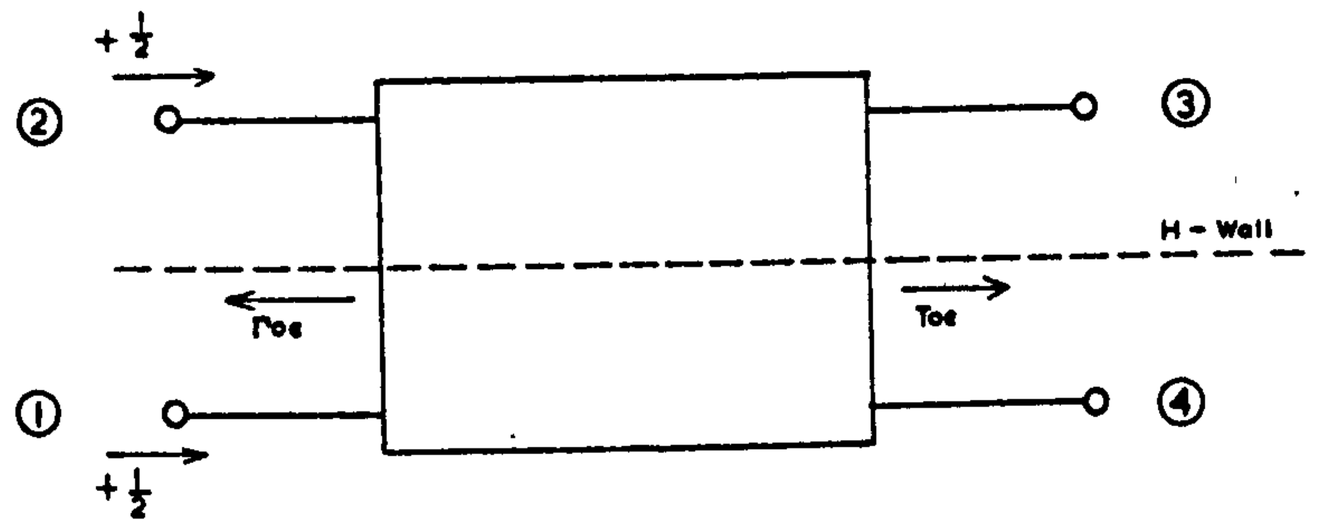

Fig. 5.3. (a) Even mode excitation and (b) odd mode excitation.

In chapter 2 it was found that the reflection coefficient Γ for a lossless network having a transfer matrix $\begin{pmatrix} A & B \\ C & D \end{pmatrix}$, an input source resistance $R_s = 1$ ohm, and a load resistance R_L (normalized to R_s), is given by

$$\Gamma = \frac{(A - G_L D) + (G_L B - C)}{(A + G_L D) + (G_L B + C)} , \tag{5.36}$$

where $G_L = 1/R_L$. For this network the associated transmission coefficient $T = S_{12}$ can easily be shown to be[2]

$$T = \frac{2\sqrt{G_L}}{(A + G_L D) + (G_L B + C)} . \tag{5.37}$$

The analysis of the two networks for the even and odd modes is frequently possible, whence Eqs.(5.36) and (5.37) are then used in conjunction with Eq.(5.35) to determine the four port behaviour of the coupler. An additional relationship between Γ and T for a two port network can be derived through use of the unitary condition, Eq.(5.3). This relationship is

$$|\Gamma|^2 + |T|^2 = 1. \tag{5.38}$$

In words, this equation states that the sum of the transmitted power plus the reflected power equals the incident power. This must be true, since a lossless network cannot absorb power.

The above discussion of the various properties of directional couplers is general and is found to apply to many different types of couplers. The discussion will be become more specialized and will deal exclusively with branch-guide directional couplers.

5.2 Development of Symmetric Branch-Guide Directional Couplers.

5.2.1 Basic Description.

Branch-guide couplers may be constructed using many types of waveguides or transmission lines. In the branch-guide coupler using rectangular waveguides, the coupling region consists of a number of series branch-guides, each $\lambda g_o/4$ in length at the mid-band frequency, connecting the two waveguides. These branch guides are themselves spaced at intervals of $\lambda go/4$, as shown in Fig.5.4. To obtain an optimum broadband performance it is necessary to specify the impedances of both the branch guides and the connecting or main line waveguide sections, as will be shown later. In the case of TEM-mode transmission lines, the branch lines are in shunt rather than in series with the main lines, representing the dual of the waveguide case.

Some of the properties of branch-guide couplers which make them particularly useful in several applications have been summarized by Young(3). Probably the most significant are as follows:

1) The coupling between the two lines is through joining branch-lines of finite length, and not through apertures. This gives additional flexibility in design; e.g.,

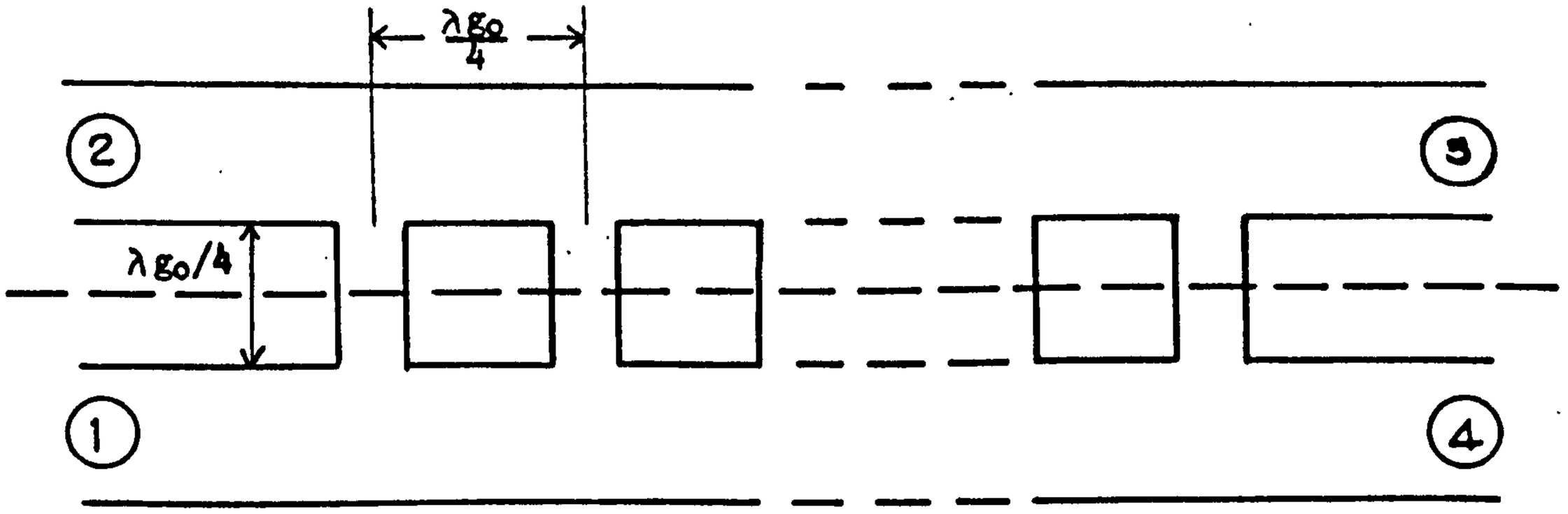

Fig. 5.4. Cross section of a multibranch waveguide coupler.

special-purpose chokes or filters can be placed in the branches.

2) The coupler is better suited for strong coupling (stronger than 20 dB) than weak coupling; 0-dB couplers are feasible over large bandwidths.

3) In waveguide, the coupler E-plane cross-section is constant. It can therefore be milled in two blocks and assembled by the "split-block" construction. Other components can also be milled into the same block.

4) Branch-guide couplers are capable of handling high RF powers.

5.2.2 Analysis of the Branch-Guide Coupler.[4]

The analysis of the coupler is in terms of the even and odd modes, as described in section 5.1.4. The plane of symmetry between the two waveguides bisects the branch guides transversely. The even-mode 2-port circuit comprises a number of open-circuited stubs, and the odd-mode 2-port circuit a number of short-circuited stubs, connected to the main waveguide. At the midband frequency the branch stubs will be $\lambda g_o/8$ ($\theta=45^o$) long, and spaced by $\lambda g_o/4$ ($\theta=90^o$) along the main waveguide. The transfer matrices for the lossless even and odd mode configurations are obtained by multiplication of the individual matrices of the open or short-circuited stubs, and connecting line sections. The values of Γ_e and

T_e, Γ_o and T_o are obtained by application of Eqs.(5.36) and (5.37) to the appropriate matrices, and the values of the wave amplitudes and phases emerging from the four arms are given by Eq.(5.35).

5.2.3 Early Developments.

The earlier papers[4] on branch-guide couplers concentrated on the development of the above even and odd mode analysis, and no attempts at a synthesis technique were described. The assumption normally made in these designs was that the main line impedances were not varied, i.e., they were all equal to the characteristic impedance of the output and input lines of the coupler. Then the design problem was to find a suitable "taper" for the characteristic impedances of the branch lines. Multibranch couplers with tapered branch line impedances were in use during the early 1950's, and the first paper on a binomially taper was published by Lomer and Crompton[5]. The extension to give a Chebyshev distribution was described by Levy[6], and a marked improvement in match and isolation over a specified bandwidth resulted. In both of these methods the stub impedances are made proportional to the desired impedance taper at midband. Then the structure is analyzed (by the even and odd mode method described above) and the constant of proportionality is determined by the center frequency

coupling requirement. Having established the branch line impedance values, the coupler performance over a band of frequencies is found by repetitive analysis. The main line sections may be included in this analysis. This technique is very empirical, i.e., it is difficult to predict what the frequency band performance of a given taper will be.

5.2.4 Patterson's Theory(7).

As in the previous designs, this theory assumes that the main line impedances are all equal to those of the input and output lines. These connecting lines are now regarded as impedance inverters at midband, as they are a quarter wavelength long at this frequency. It is assumed that over a narrow frequency band (centered at midband) the main lines will remain frequency invariant, and thus continue to act as ideal transformers. Therefore it is possible to draw an equivalence between the even and odd mode 2-port networks and prototype high- or low-pass lumped-element networks, as shown in Fig.5.5. The element values in the lumped low-pass network of Fig.5.5b are chosen to give either a maximally flat insertion loss (as discussed in chapter 2) or a Chebyshev insertion loss characteristic (as discussed in chapter 4). Then the network in Fig.5.5a will have a corresponding high-pass insertion loss characteristic.

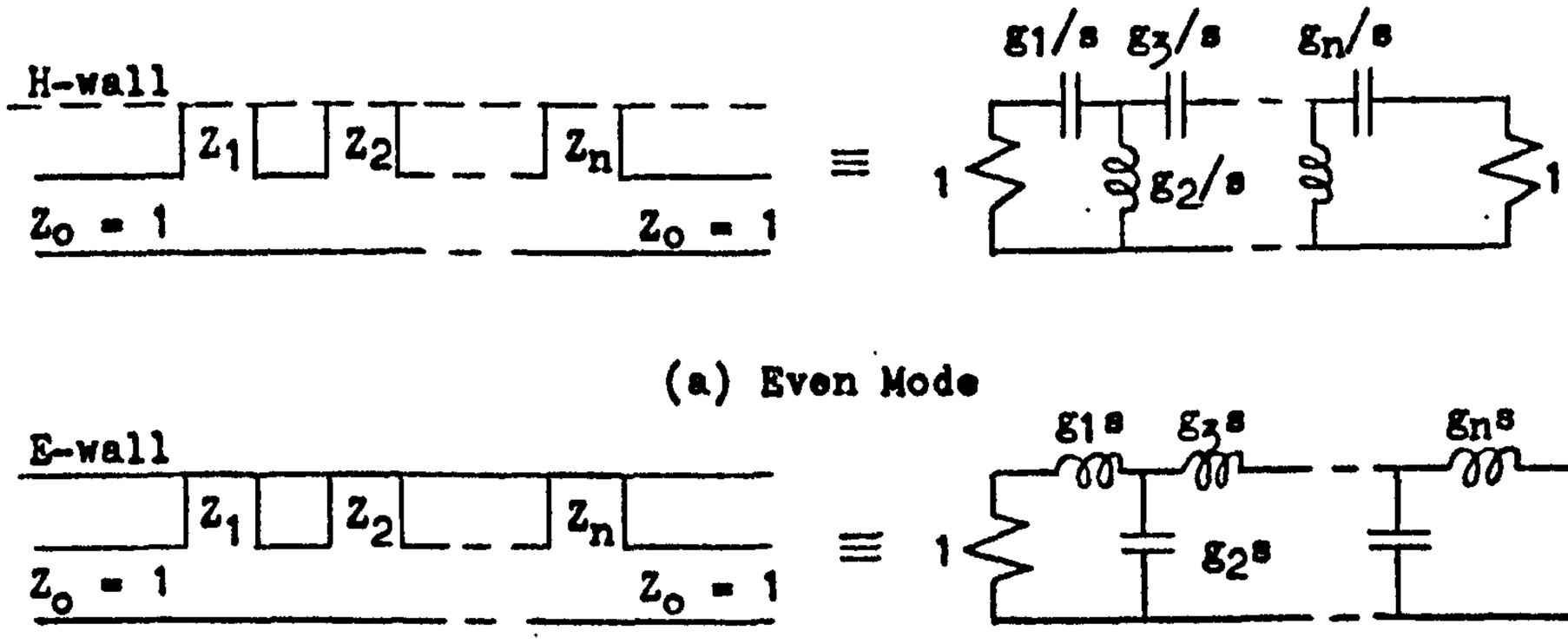

Fig. 5.5. Equivalent circuit representations for even and odd modes in Patterson's Theory: (a) even mode and (b) odd mode.

The equivalence between the distributed and lumped elements is given by making the respective branch line series reactances proportional to those of the prototype filter network. The constant of proportionality is determined by analysis and the center frequency coupling requirement. All branch line reactances are multiplied by this constant. This has the effect of replacing s by $\frac{\tan\theta}{\tan\theta_o}$ in the low-pass network, as discussed in chapter 3. In a five branch maximally flat 3-dB coupler, for example, $\tan\theta_o = 2.08$, or $\theta_o = 63.4^o$. Superposition of the high-pass and low-pass networks (Eq.5.35) gives the "passband" of the coupler as going from $\theta_1 = 26.6^o$ to $\theta_2 = 63.4^o$. The assumption that the main connecting lines act as ideal transformers (90^o in length) over the above passband is a very serious one indeed. Still, this theory gives good results in practice[7]. Also, an attempt has been made to incorporate the frequency behaviour of the branch lines into the design procedure.

5.2.5 Young's Theory[4].

In Patterson's design method, the main line impedance is usually maintained uniformly throughout the coupling region. An approach which requires this impedance to vary between the branch guides has been described by Young[3]. In this approach, the coupler is derived from a prototype

quarter-wave transformer, tables of which have been published[8]. The first step is to choose a suitable quarter-wave transformer prototype having a known bandwidth, passband performance, and output to input resistance ratio R. Usually either a maximally flat or Chebyshev passband characteristic is used. Then the VSWR at each junction of this prototype is calculated, using the relation

$$\text{VSWR} = \frac{1+|\Gamma|}{1-|\Gamma|}, \tag{5.10}$$

where

$$\Gamma = \frac{Z_B - Z_A^*}{Z_B + Z_A}, \tag{5.39}$$

and Z_A and Z_B are the impedances to the left and right of the junction, respectively. The next step is to equate these junction VSWR's to the junction VSWR's of the even (or odd) mode circuit for the coupler. A typical junction is depicted in Fig.5.6. The admittance value for the stub in the even mode circuit is $-jY$, and for the odd mode circuit is $+jY$. For either circuit the junction VSWR in Fig.5.6 may be calculated with the help of Eqs.(5.10) and (5.39) as

$$\text{VSWR} = \frac{((K_1+K_2)^2+Y^2)^{\frac{1}{2}} + ((K_1-K_2)^2+Y^2)^{\frac{1}{2}}}{((K_1+K_2)^2+Y^2)^{\frac{1}{2}} - ((K_1-K_2)^2+Y^2)^{\frac{1}{2}}}, \tag{5.40}$$

where K_1 and K_2 are admittances in Fig.5.6.

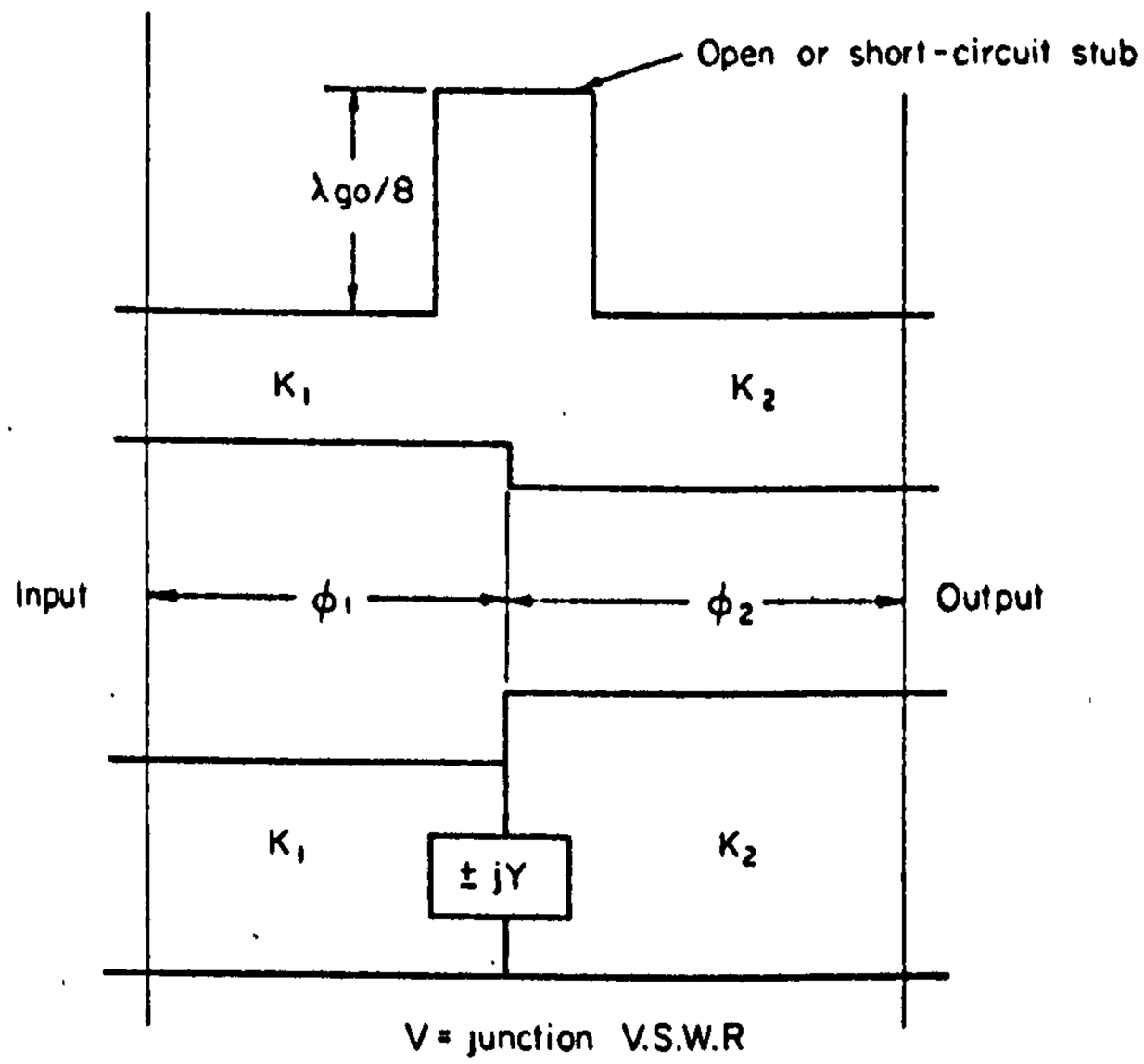

Fig. 5.6. Equivalent circuit of a shunt stub in an even or odd mode excitation.

An important difference between the equivalent circuit of this junction and that in the prototype is that whereas in the latter the junction discontinuity is purely resistive, in the case of the coupler the discontinuity represented by the stub is mainly susceptive or reactive. It is necessary to adjust the distance between the junctions to allow for this effect, i.e., to first establish reference planes on either side of the junction where the reflection coefficient is pure real, and then to have adjacent reference planes touch while keeping the distances between junctions at 90° (electrical length) at midband. This is called the synchronous-tuning condition by Young[3]. In Fig.5.6 it is easily found that

$$\phi_1 = \tfrac{1}{2}\tan^{-1}\left(\frac{2YK_1}{Y^2+K_2^2-K_1^2}\right),$$

$$\phi_2 = \tfrac{1}{2}\tan^{-1}\left(\frac{2YK_2}{Y^2+K_1^2-K_2^2}\right). \qquad (5.41)$$

At each junction only the ratio of impedances is important, and so only two and not three quantities have to be solved for. All of the coupler impedances may be normalized to the input and output system impedances at the end of the design procedure, if desired. But at each junction the two

equations (5.40) and (5.41) are available, and thus the element values in the coupler may be found. In order to apply the synchronous-tuning condition at all steps in the design, the first step is to solve for the junction (s) at which the electrical length is known by symmetry considerations, i.e., in the middle of the symmetrical coupler. Then one "works out" from the center of the coupler until all impedances have been determined. Special design charts have been prepared by Young to facilitate this procedure.

Knowing the coupler specifications of bandwidth, pass-band VSWR amplitude and shape,(i.e., maximally flat or Chebyshev), and center frequency coupling level, a suitable low-pass quarter-wave transformer prototype may be selected as follows. Young has empirically given a bandwidth contraction factor B, which results in equivalent VSWR's for the two structures, i.e.,

$$B = \frac{\text{Bandwidth of coupler}}{\text{Bandwidth of transformer}} .$$

B is found to vary between .5 and .7, and is presented in graphical form in the original paper[3] for a variety of cases. Young has also found that when the coupler is matched at center frequency, then the coupling is related to the output to input resistance ratio R of the transformer by

$$\text{Coupling (in dB)} = 20 \log_{10}\left(\frac{R+1}{R-1}\right).$$

If the coupler is not matched at center frequency, then a factor

$$10 \log_{10} \frac{(V_o + 1)^2}{4V_o}$$

must be subtracted from the coupling in the previous formula, V_o being the center-frequency VSWR. Knowing R, bandwidth, and passband VSWR amplitude and shape for the prototype transformer, the number of sections n may be determined by a table scan.

In the above approach, the frequency behaviour of the main lines has been taken into account, but the stubs have been assumed to be frequency invariant in the even and odd mode circuits, and equal to their midband values. This is a fairly serious restriction for a broadband design, and explains why a "bandwidth contraction factor" is needed in the above development. What is desired is a theory which encorporates the frequency variation of both the main and branch lines in the design. This theory has been developed and will now be discussed.

5.3 New Design Theory[9],[10].

5.3.1 General Considerations.

Thus far in the development of branch-guide directional couplers, only symmetrical couplers (couplers with end-to-end symmetry) have been considered. The design to be presented,

however, allows for asymmetrical couplers as well. These couplers will be shown to have a broader bandwidth than is possible with a corresponding symmetrical coupler. The synthesis technique which follows realizes couplers having a specified reflection coefficient (or VSWR) and isolation, but it is found that in common with the previous design techniques the coupling variation as a function of frequency is not controllable. The coupling becomes progressively tighter as the frequency deviation from midband increases. Another feature of the present synthesis technique (which is common to many synthesis techniques) is that one has no control over the range of element values that result from a design specification. This problem may be overcome to a certain extent by preparing tables for different combinations of input specifications. A scan of the tables quickly reveals which designs may or may not be realized. Many tables have accordingly been prepared using the present synthesis technique.

As was stated previously, this new design theory takes the frequency variations of both the branch lines and the connecting main lines into account. It also allows the main line impedances to be adjusted to optimize performance. It gives exact results for maximally flat characteristics and almost exact results for the Chebyshev cases. In fact, the Chebyshev case yields VSWR and directivity character-

istics which are almost equal ripple, and the exact performance is given by computer analysis. The new theory applied to symmetrical couplers gives designs which have considerably superior performance for a given number of branch lines as compared with previously published results[3],[7].

For convenience in the work that follows, the TEM transmission line coupler has been used as a model (in the even and odd modes the stubs are connected in shunt with the main line), but, on a dual basis, the rectangular waveguide coupler (with the stubs in series with the main line) could equally well be employed.

5.3.2 Coupler Analysis.

The transfer matrix of an open-circuited (even mode) shunt stub of admittance a_1 and length θ was found in chapter 3 to be

$$\begin{pmatrix} 1 & 0 \\ a_1 t & 1 \end{pmatrix} , \tag{5.42}$$

and that of a short-circuited shunt stub of the same admittance and length to be

$$\begin{pmatrix} 1 & 0 \\ \dfrac{a_1}{t} & 1 \end{pmatrix} , \tag{5.43}$$

where, when $s = 0 + j\theta$, $t = j \tan\theta$.

A restriction now imposed on the branch-line coupler is that any main line (between two stubs) of electrical length 2θ should be of uniform impedance, i.e., should consist of a double-length unit element of characteristic admittance b_1 having the transfer matrix

$$\left(\frac{1}{(1-t^2)^{\frac{1}{2}}}\begin{pmatrix}1 & \frac{t}{b_1}\\ b_1 t & 1\end{pmatrix}\right)^2 = \frac{1}{1-t^2}\begin{pmatrix}1+t^2 & \frac{2}{b_1}t\\ 2b_1 t & 1+t^2\end{pmatrix}. \tag{5.44}$$

The restriction imposed above has a most valuable property, namely that Eq.(5.44) is invariant with respect to the transformation

$$t \to 1/t\ , \tag{5.45}$$

except for a change of sign. Note that Eq.(5.43) may be obtained from Eq.(5.42) by using the same transformation (5.45). Thus, if the transfer matrix of the even-mode circuit is calculated, then the transfer matrix for the odd-mode circuit is obtained using Eq.(5.45). Mathematically, if the even-mode transfer matrix is

$$\begin{pmatrix}A_e(t) & B_e(t)\\ C_e(t) & D_e(t)\end{pmatrix}\ , \tag{5.46}$$

then the odd-mode transfer matrix is

$$\begin{pmatrix}A_o & B_o\\ C_o & D_o\end{pmatrix} = (-1)^{n-1}\begin{pmatrix}A_e\left(\frac{1}{t}\right) & B_e\left(\frac{1}{t}\right)\\ C_e\left(\frac{1}{t}\right) & D_e\left(\frac{1}{t}\right)\end{pmatrix}. \tag{5.47}$$

When the transfer matrices of n stubs and the connecting double-length unit elements are multiplied in the appropriate order, then the overall even mode transfer matrix is found to be of the form

$$\begin{pmatrix} A_e & B_e \\ C_e & D_e \end{pmatrix} = \frac{1}{(1-t^2)^{n-1}} \begin{pmatrix} A_{n-1}(t^2) & tB_{n-2}(t^2) \\ tC_{n-1}(t^2) & D_{n-1}(t^2) \end{pmatrix}, \tag{5.48}$$

where the subscripts indicate the degrees of the polynomials $A(t^2),\ldots,D(t^2)$. Analysis of a few cases reveals that the constant term in A_{n-1} and D_{n-1} is unity, i.e., the even mode structure is transparent at DC. Now, from Eq.(5.47), the odd mode transfer matrix must be

$$\begin{pmatrix} A_o & C_o \\ B_o & D_o \end{pmatrix} = \frac{(-1)^{n+1}\, t^{2(n-1)}}{(1-t^2)^{n-1}} \begin{pmatrix} A_{n-1}\left(\frac{1}{t^2}\right) & \frac{1}{t} B_{n-2}\left(\frac{1}{t^2}\right) \\ \frac{1}{t} C_{n-1}\left(\frac{1}{t^2}\right) & D_{n-1}\left(\frac{1}{t^2}\right) \end{pmatrix}. \tag{5.49}$$

It is now desirable to express these transfer matrices on the imaginary axis and in terms of the variable $\cos 2\theta$. From the relation

$$\cos 2\theta = (1-(j \tan\theta)^2)^{-1},$$

Eqs.(5.48) and (5.49) become

$$\begin{pmatrix} A_e & B_e \\ C_e & D_e \end{pmatrix}\Bigg|_{t=j \tan\theta} = \begin{pmatrix} \underline{A}_{n-1}(-\cos 2\theta) & j \tan\theta \underline{B}(\cos 2\theta) \\ j \tan\theta\, \underline{C}_{n-1}(+\cos 2\theta) & \underline{D}_{n-1}(-\cos 2\theta) \end{pmatrix}, \tag{5.50}$$

$$\begin{pmatrix} A_o & B_o \\ C_o & D_o \end{pmatrix}\Bigg|_{t=j\tan\theta} = \begin{pmatrix} \underline{A}_{n-1}(\cos 2\theta) & -j\cot\theta\,\underline{B}_{n-1}(-\cos 2\theta) \\ -j\cot\theta\,\underline{C}_{n-1}(-\cos 2\theta) & \underline{D}_{n-1}(\cos 2\theta) \end{pmatrix}. \tag{5.51}$$

Note that there are two main differences between Eqs.(5.50) and (5.51). The $\underline{B}$ and $\underline{C}$ polynomials are multiplied by $j\tan\theta$ in (5.50) and by $-j\cot\theta$ in (5.51), and the coefficients of the odd parts of the respective $\underline{A},\underline{B},\underline{C}$, and $\underline{D}$ polynomials differ only in sign.

5.3.3 The Approximation Problem.

As stated previously, it is desirable to prescribe the input reflection coefficient (or the input VSWR) and isolation. Recall that for a unit wave incident on port 1 of the coupler, the port outputs are given by

$$b_1 = \tfrac{1}{2}(\Gamma_e + \Gamma_o), \qquad b_3 = \tfrac{1}{2}(T_e - T_o),$$

$$b_2 = \tfrac{1}{2}(\Gamma_e - \Gamma_o), \qquad b_4 = \tfrac{1}{2}(T_e + T_o), \tag{5.35}$$

where port 2 is the isolated port and port 3 is the coupled port. Recall also that for the even and odd mode networks Γ and T are given by

$$\Gamma = \frac{(A - G_L D) + (G_L B - C)}{(A + G_L D) + (G_L B + C)}. \tag{5.36}$$

and

$$T = \frac{2\sqrt{G_L}}{(A+G_L D)+(G_L B+C)}, \tag{5.37}$$

where A,B,C, and D are elements of the lossless transfer matrix and G_L is the load conductance. Thus, when b_1 and b_2 are formulated, they each consist of ratios of rational numerator and denominator polynomials. Hence it is very difficult to specify b_1 and b_2 in this way since the coefficients of the numerator polynomial are closely related in a complex manner to those of the denominator polynomial.

Consider, however, the function Γ/T. It will be found that the function

$$F = \tfrac{1}{2}\left(\frac{\Gamma_e}{T_e} - \frac{\Gamma_o}{T_o}\right), \tag{5.52}$$

has a much simpler form which may be specified by simple Butterworth or Chebyshev polynomials. Now the important assumption is made that Γ_e/T_e and Γ_o/T_o are to have as many common zeros on the frequency axis as possible, and that in the θ variable these zeros be symmetrical about the midband frequency $\theta = 45^\circ$. This statement is a crucial assumption in the work that follows. On one hand the common zeros of Γ_e/T_e and Γ_o/T_o are also the zeros of F in Eq.(5.52). On the other hand, these zeros are points of infinite isolation and perfect match, according to Eqs.(5.35). Thus, as many

zeros as the polynomials will allow have been used to ensure good performance over a frequency band, with perfect isolation and input match at selected points within this band. In this sense the specification (5.52) is optimal. It has the added advantage of being expressed in simple polynomial form. The assumption that a pair of zeros is symmetric about $\theta=45^{\circ}$ is necessary because, when t is replaced by 1/t, cos $(90^{\circ}-2\theta)$ becomes $\cos(90^{\circ}+2\theta)$ and Γ_e/T_e becomes Γ_o/T_o. Examination of Eqs.(5.50) and (5.51) reveals that if n (the number of branches) is odd, then $\frac{n}{2}$ conjugate pairs of common zeros are possible. When n is even, then there are $\frac{n}{2}-1$ conjugate pairs of common zeros plus one zero at $\theta=45^{\circ}$ possible in F when making the above assumption.

By the use of Eqs.(5.36),(5.37),(5.50), and (5.52), Γ_e/T_e may be written in the form (for an n-branch coupler):

$$\frac{\Gamma_e}{T_e} = \frac{1}{2^{n}R} \cdot \frac{P_{n-1}(\cos 2\theta/\cos 2\theta_c)}{P_{n-1}(1/\cos 2\theta_c)} \cdot \left((R-1) - jK\tan\theta\right). \tag{5.53}$$

In this equation R is the output load resistance (with the input resistance normalized to unity). When R=1, it will be shown later that a symmetrical structure results. θ_c is related to the cutoff frequency. K is a parameter which is introduced to fix the midband coupling value and will be discussed in greater detail in section 5.3.7. By using the

above assumption on the zeros of Γ_e/T_e and Γ_o/T_o being common, it is not difficult to show that the associated Γ_o/T_o must therefore be of the form

$$\frac{\Gamma_o}{T_o} = \frac{1}{2\sqrt{R}} \cdot \frac{P_{n-1}(\cos 2\theta/\cos 2\theta_c)}{P_{n-1}(1/\cos 2\theta_c)} \cdot \left((R-1) + jK\cot\theta\right), \quad (5.54)$$

which means that F is given by

$$F = \frac{-1}{2\sqrt{R}} \cdot \frac{P_{n-1}(\cos 2\theta/\cos 2\theta_c)}{P_{n-1}(1/\cos 2\theta_c)} \cdot \left(jK\ \frac{2}{\sin 2\theta}\right)$$

$$= \frac{-1}{2\sqrt{R}}\ \frac{P_{n-1}(X/X_c)}{P_{n-1}(1/X_c)} \cdot \left(jK\ \frac{2}{\sqrt{1-X^2}}\right), \quad (5.55)$$

where $X = \cos 2\theta$. Now P_{n-1} must be either a pure even (for n odd) or pure odd (for n even) polynomial if the roots are to have symmetry about $X = 0$ ($2\theta = 90^\circ$). Having selected a suitable P_{n-1}, Eqs.(5.55) and (5.53) show how to calculate the associated Γ_e/T_e. Two suitable P_{n-1} polynomial specifications will now be described.

5.3.4 The Butterworth Specification.

The Butterworth or maximally flat specification has all of its zeros located at the center frequency, i.e., $2\theta = 90^\circ$. Therefore in Eq.(5.55),

$$P_{n-1}\left(\frac{X}{X_c}\right) = \left(\frac{X}{X_c}\right)^{n-1} . \quad (5.56)$$

For convenience, X_c is set equal to 1. Thus $P_{n-1}(1/1)=1$, and Eq.(5.55) becomes

$$F = -\frac{X^{n-1}}{2R}\left(jK\ \frac{2}{\sqrt{1-X^2}}\right) . \qquad (5.57)$$

Γ_e/T_e is then given by

$$\frac{\Gamma_e}{T_e} = \frac{(\cos 2\theta)^{n-1}}{2R}\left((R-1) - jK\tan\theta\right). \qquad (5.58)$$

The method for recovering Γ from this equation will be described in section 5.3.6.

5.3.5 The Chebyshev Specification.

Consider the function

$$\frac{P_o}{P_L} = 1 + |F|^2$$

$$= 1 + \frac{1}{4R}\ \frac{P_{n-1}^2(X/X_c)}{P_{n-1}^2(1/X_c)}\left(\frac{4K^2}{1-X^2}\right), \qquad (5.59)$$

where K is used to control the midband coupling and in this case also the ripple level. Eq.(5.59) has the generic form of the insertion loss for a cascade of (n-1) unit elements and one short-circuited shunt stub, all having a commensurate electrical length 2θ, as described by Riblet[11] and Carlin and Kohler[12]. They each showed that in order to give Chebyshev equal ripple response with (n-2) ripples in the

band $-X_c \leq X \leq X_c$ (where $X_c < 1$), $P_{n-1}(X/X_c)$ should be set equal to

$$P_{n-1}\left(\frac{X}{X_c}\right) = \tfrac{1}{2}\left(1 + \sqrt{1-X_c^2}\right) T_{n-1}\left(\frac{X}{X_c}\right)$$

$$-\tfrac{1}{2}\left(1 - \sqrt{1-X_c^2}\right) T_{n-3}\left(\frac{X}{X_c}\right), \qquad (5.60)$$

where $T_n(X)$ is again the Chebyshev polynomial of the first kind of degree n. By inspection Eq.(5.60) is either an even or odd polynomial in X, and so this restriction on $P_{n-1}\left(\frac{X}{X_c}\right)$ has been met. Eq.(5.60) may now be substituted into Eq.(5.53) to give Γ_e/T_e for this case.

The value X_c in Eq.(5.60) is given by

$$X_c = \cos(2\theta_1), \qquad (5.61)$$

where the bandwidth of the coupler is from θ_1 to θ_2, with $\theta_o = 45^\circ$ being the center frequency. If $\theta_1 = 45^\circ - \Delta\theta$, then $\theta_2 = 45^\circ + \Delta\theta$, i.e., θ_o is the arithmetic mean of θ_1 and θ_2. Obviously $\Delta\theta < 45^\circ$. The bandwidth BW of the coupler will now be defined as

$$\frac{BW}{\theta_o = 45^\circ} = \frac{\lambda g_o}{\lambda g_2}, \qquad (5.62)$$

since $\theta = \frac{2\pi\ell}{\lambda g}$. It is easily seen that $1 < BW < 2$. The relationship between the bandwidth BW and the ratio of lower frequency wavelength to upper frequency wavelength

is easily found to be

$$\frac{\lambda g_1}{\lambda g_2} = \frac{BW}{2-BW} \quad . \tag{5.63}$$

Thus BW = 1.4 represents a band-edge guide wavelength ratio $\lambda g_1/\lambda g_2 = 2.333$, i.e., greater than one octave. Given either $\lambda g_1/\lambda g_2$ or BW, X_c in Eq.(5.61) may now be easily calculated, i.e.,

$$BW = \frac{2\ \lambda g_1/\lambda g_2}{1+\lambda g_1/\lambda g_2} \quad ,$$

and

$$X_c = \cos(90^o(2-BW)).$$

It is interesting to note at this point that the function $F = (\Gamma_e/T_e - \Gamma_o/T_o)$ is equiripple, and not the VSWR and isolation functions $\Gamma_e \pm \Gamma_o$ given in Eq.(5.35). However, if $|\Gamma_e|$ and $|\Gamma_o|$ are small over the passband, then, by the unitary condition $|\Gamma|^2 + |T|^2 = 1$, $|T_e|$ and $|T_o|$ are nearly equal to unity, and $|\Gamma_e| - |\Gamma_o|$ is nearly equiripple. Also recall that Γ_e and Γ_o possess the same passband zeros. It can be seen in a general way now that $\Gamma_e \pm \Gamma_o$ will be nearly equiripple, especially as F becomes very small over the passband.

5.3.6 The Synthesis Procedure.

Either of the above specification equations (5.56) or (5.60) may be used in determining Γ_e/T_e as a function of X/X_c. For the recovery of Γ_e from Γ_e/T_e, it is convenient to

change variables so that the valuable properties of t-plane may be utilized, as discussed in chapter 3. The relationship between these variables is easily found to be

$$\frac{X}{X_c} = \frac{\cos 2\theta}{\cos 2\theta_c} = \left(\frac{1+t^2}{1-t^2}\right) \cdot \left(\frac{1-t_c^2}{1+t_c^2}\right), \qquad (5.64)$$

where $t_c^2 = (\cos 2\theta_c - 1)/(\cos 2\theta_c + 1)$, so that now Γ_e/T_e may be written as a function of t.

This function may be realized by a cascade of (n-1) double-length unit elements with n single-length open-circuited shunt stubs at the junctions, with the exception of certain extreme specifications where negative element values occur. This is because the specification functions, in general, always lead to a realization consisting of (2n-2) single-length unit elements with one or more stubs at the junctions, but the realization of interest is the special and unique case of a cascade of double-length unit elements with shunt stubs, which is far more restricted than the general case. In practice, it has been found that negative element values occur only for unreasonable performance specifications, i.e., a small number of branch guides with tight coupling and large bandwidth.

The standard Darlington synthesis procedure is used to recover Γ_e from Γ_e/T_e. From the unitary condition $|\Gamma_e|^2 + |T_e|^2 = 1$,

the modulus squared of the even-mode reflection coefficient is given in terms of $|\Gamma_e/T_e|$ as

$$|\Gamma_e|^2 = \frac{|\Gamma_e/T_e|^2}{1+|\Gamma_e/T_e|^2}, \tag{5.65}$$

on the frequency axis. Definition (5.65) may then be extended to the entire t-plane by analytic continuation. As discussed previously, the poles of Γ_e must be in the left-half plane. Inspection of Eq.(5.53) reveals that for the general case ($R \neq 1$) all of the zeros of $|\Gamma_e/T_e|^2$ except for two will be double and on the imaginary axis. These double zeros are roots of the P_{n-1}^2 function. One zero from each of these double zeros is selected for Γ_e. The remaining pair of roots arise from the factor

$$((R-1)^2 - K^2t^2), \tag{5.66}$$

one of which will go into Γ_e. By trying both possibilities and requiring that Γ_e have the form shown in Eq.(5.36), it can be easily shown that if $R>1$ the right-half plane root should be chosen, and if $R<1$ then the left-half plane root is chosen for a zero of Γ_e. For the special case $R=1$, the factor (5.66) degenerates into a double root at the origin, one of which goes to Γ_e. Thus it is seen that for this case the numerator of Γ_e is an odd polynomial in t. From Eq.(5.36) this means that $A_e = D_e$ in the transfer matrix, and so the network for $R=1$ is a symmetrical one.

The factorization of the denominator of Eq.(5.65) is not expressible in closed form, and hence must be carried out numerically, i.e., by digital computation. A computer subroutine, using Bairstow's factorization method, was explicitly written for this purpose. The constant multiplier for Γ_e is determined from

$$|\Gamma|\Big|_{t \to j\infty} = 1, \tag{5.67}$$

and a comparison with Eq.(5.36). Having found Γ_e, the even mode transfer matrix polynomials are found through the use of Eq.(5.36) and the fact that A_e and D_e are even polynomials in t(with a constant term of unity), and B_e and C_e are odd polynomials. Finally, the transfer matrix so determined must be multiplied by the factor

$$\frac{1}{(1-t^2)^{n-1}},$$

to recover the transmission zeros of the main line unit elements. The even mode transfer matrix is now suitable for decomposition.

The first step is the extraction of a shunt stub of characteristic admittance a_1 of such value that a double-length unit element of uniform characteristic admittance b_1 may then be extracted. It is easily shown that the condition for extraction of a double-length unit element from the open- and short-circuited driving-point admittances (formed from the transfer matrix) is that these admittances have a derivative with respect to t which is <u>zero</u> at $t = \pm 1$.

Using this fact, it is simple to show that when the above condition is not satisfied, it is necessary only to perform first the extraction of a shunt open-circuited stub of characteristic admittance

$$a_1 = Y'_{oc}(1) = Y'_{sc}(1), \tag{5.68}$$

where the prime denotes differentiation with respect to t. After this stub is removed, a double-length unit element of characteristic admittance

$$b_1 = \frac{C(1)}{A(1)} = \frac{D(1)}{B(1)}, \tag{5.69}$$

may be removed (by Richards' theorem), and this cycle is then repeated until all of the elements have been removed.

5.3.7 K Vs. Coupling.

Previously it was stated that in Eq.(5.53) K is a parameter which is used to fix the midband coupling level. The relationship between K and midband coupling is very complex. In a Chebyshev design, for example, to attain a given midband coupling K is found to be a function of n (the number of branches), R, and the bandwidth. In general it has been found that the coupling is a monotonic function of K, with the coupling becoming stronger as K is increased in value. Some typical values are: K = .01, coupling ≃ 20 dB; K = .10, coupling ≃ 12dB; K = 1.0, coupling ≃ 4-5dB.

A computer program was written to carry out the entire synthesis procedure described above. In this program both a starting value for K and a desired midband coupling value C_d were entered as input data. With this initial value for K the program computed the associated midband coupling and compared it to C_d. K was then modified and the process repeated. Five to six iterations were found sufficient to give eight digit agreement between the calculated coupling and C_d. The computer program also contained an analysis routine to calculate the VSWR, directivity, and coupling over the band of interest.

For one not possessing this (lengthy) computer program, however, it is desirable to see if there is not a more direct link between coupling and K, such that having found K the synthesis process need only be carried through one time.

Examination of Eqs.(5.35) reveals that, at midband, if $|\Gamma_e| \ll 1$ and $|\Gamma_o| \ll 1$, then $|T_e| \simeq |T_o| \simeq 1$, and the coupling is given by $b_3 = \frac{1}{2}(T_e - T_o)$. Now from Eqs.(5.50) and (5.51), it is seen that angle $(T_e) =$ -angle (T_o) at midband. Therefore

$$b_3 = \cos(\text{angle } (T_e)). \tag{5.70}$$

This means that once the coupling is known, b_3 is known, and hence the phase angle of T_e is known. Therefore a knowledge of the phase of T_e at one frequency point (midband) is sufficient to specify the coupling. It is easily

found from Eq.(5.65) that $|T_e|$ is given by

$$|T_e| = \frac{1}{\sqrt{1+\left|\frac{\rho_e}{T_e}\right|^2}} \cdot \tag{5.71}$$

In chapter 2 it was seen how the phase of an analytic function at one frequency point could be determined by its magnitude behaviour along the frequency axis. Therefore in this method, starting with an initial guess for K, the corresponding $|T_e|$ is plotted along the frequency axis in the t-plane. It has been found that with reasonable input specifications $|T_e| \simeq 1$ on the line $t = j0$ to $t = j1$, and so the plot may be started at $t = j1$. Then the angle of T_e at $t = j1$ is computed using the methods in chapter 2, and the corresponding b_3 calculated from Eq.(5.70). If this is not the desired value for b_3, K is modified and the process repeated. Using the graphical methods presented in chapter 2, each cycle in this process may be rapidly performed. Finally, a K which yields the proper midband coupling and has three to four place accuracy is established, which is then used in the formal synthesis procedure. If a single coupler design is wanted, the above method of determining K will be found to be much quicker than successive synthesis iteration. It has the added advantage of requiring no polynomial factorizations, whereas the factorization of a (2n-1) degree polynomial must be done in each synthesis cycle.

As a simple example of this method, let it be required to find the midband phase of T_e for a three branch Butterworth design, with R = 1 (a symmetrical coupler) and K = 2. Then the specification (5.53) becomes

$$\frac{\Gamma_e}{T_e} = \frac{t(t^2+1)^2}{(t^2-1)^2} \quad , \tag{5.72}$$

and therefore

$$\left|T_e\right| = \left. \frac{1}{\sqrt{1+\left|t^2\left(\frac{t^2+1}{t^2-1}\right)^4\right|}} \right|_{t^2=-\tan^2\theta} \quad . \tag{5.73}$$

At this point it is observed that $\left|T_e\right|$ in Eq.(5.73) has two (transmission) zeros at $t = \pm 1$. But the phase-magnitude derivation in chapter 2 was established for an analytic function having neither poles nor zeros in the right-half plane. However, if Eq.(5.72) is multiplied by the all-pass factor $(t-1)^2/(t+1)^2$, the resulting function will yield a $\left|T_e'\right|$ which has identical values to $\left|T_e\right|$. Furthermore, T_e' has only left-half plane poles and zeros. At $t = j1$, the phase relationship between T_e and T_e' is given by $(j-1)^2/(j+1)^2 = 180^\circ$. A plot of $\left|T_e'\right| = \left|T_e\right|$ on the $t = j\tan\theta$ axis is shown in Fig. 5.7. The break points and slopes are found to be[13]

1) $\tan\theta_1 = 1.53$, $F_o(\tan\theta_1) = 25.22^\circ$,

2) $\tan\theta_2 = 10.27$, $F_o(\tan\theta_2) = 3.556^\circ$

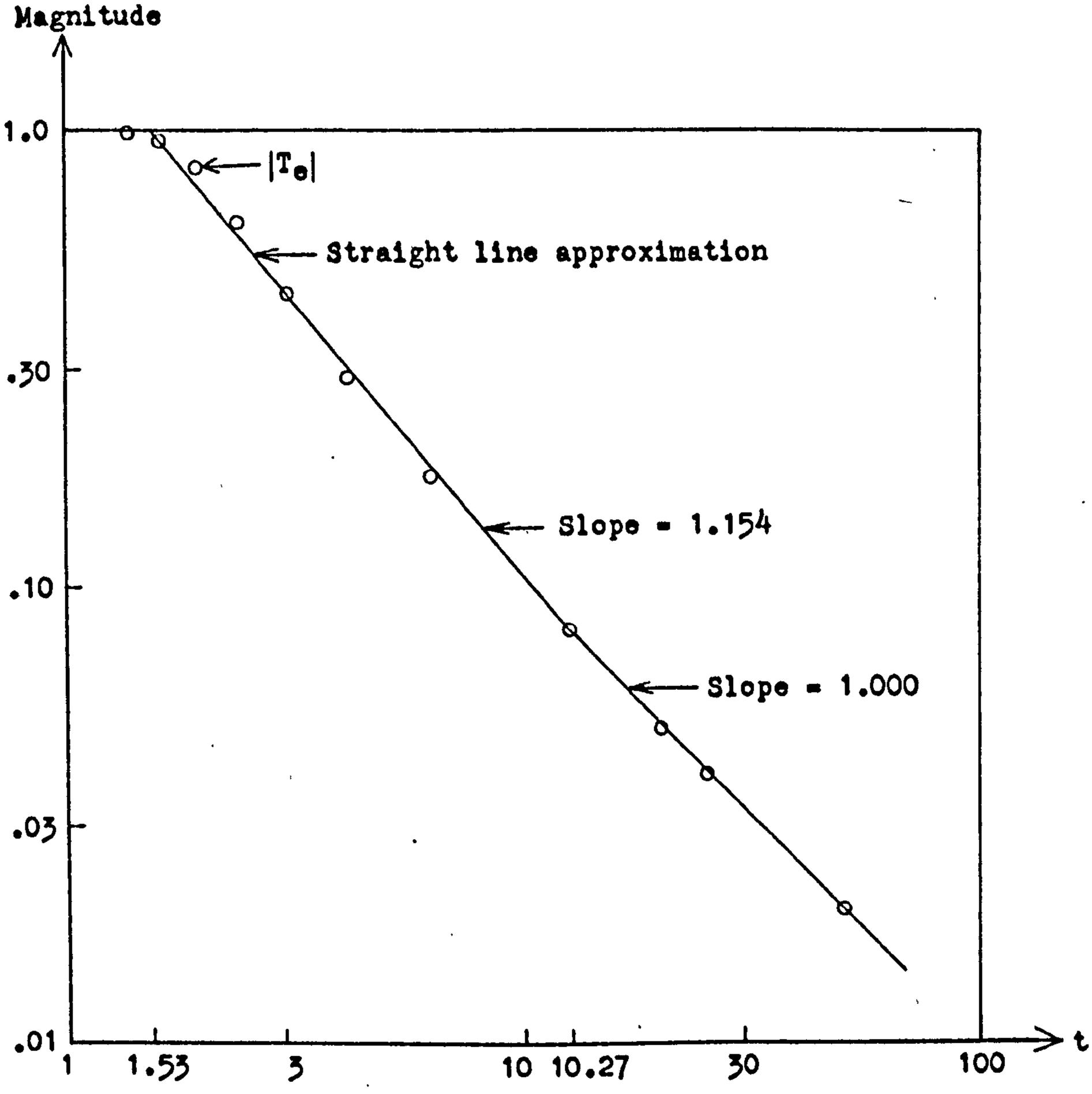

Fig. 5.7. An example of finding the midband phase of an analytic function from its magnitude characteristic.

Net Slope = -1.154, $S_1 = -29.10^\circ$.

Net Slope = -1.000-(-1.154) = .154, $S_2 = +.55^\circ$.

Therefore the net angle of T_e' (j1) is $S_1 + S_2 = -28.55^\circ$. The final angle of T_e(j1) is then given by

$180^\circ - 28.55^\circ$.

The example specifications were next entered into the computer synthesis program. At midband the angle of T_e was eventually computed as

$180^\circ - 28.52^\circ$,

which shows close agreement with the graphical method, and thus justifies the validity of the above method.

5.3.8 Example of the Synthesis Procedure.

Consider the design of a three branch asymmetric Butterworth coupler with the input specifications R = 2 and K = 1. From Eq.(5.58),

$$\frac{\Gamma_e}{T_e} = \frac{1}{2\sqrt{R}} \left(\frac{1+t^2}{1-t^2}\right)\left((R-1) - Kt\right) . \qquad (5.74)$$

Then

$$\left|\frac{\Gamma_e}{T_e}\right|^2 = \left(\frac{1+t^2}{1-t^2}\right)^4 \left(\frac{(R-1)^2}{4R} - \frac{K^2 t^2}{4R}\right) . \qquad (5.75)$$

From Eq.(5.65) $|\Gamma_e|^2$ is given by

$$|\Gamma_e|^2 = \frac{\left|\frac{\Gamma_e}{T_e}\right|^2}{1+\left|\frac{\Gamma_e}{T_e}\right|^2} = \frac{(1+t^2)^4\left((R-1)^2 - K^2t^2\right)}{4R(1-t^2)^4 + (1+t^2)^4\left((R-1)^2 - K^2t^2\right)}$$

$$= \frac{(1+t^2)^4\ (1-t^2)}{8(1-t^2)^4 + (1+t^2)^4\ (1-t^2)}. \qquad (5.76)$$

Recall that when $R > 1$ the right-half t-plane factor of $((R-1)^2 - K^2t^2)$ is chosen as a zero of Γ_e. The numerator of Γ_e thus has the factors

$$(1+t^2)^2\ (1-t) = 1-t+2t^2-2t^3+t^4-t^5. \qquad (5.77)$$

The denominator of (5.76) is factored using the Bairstow method. It is found that when this factorization is performed and the left-half t-plane roots are multiplied back together, Γ_e is given by

$$\Gamma_e \quad K_2\ \frac{1-t+2t^2-2t^3+t^4-t^5}{3.000+12.220t+20.056t^2} \qquad (5.78)$$
$$+15.904t^3+3.068t^4+t^5$$

K_2 may be found by comparing Eqs.(5.76) and (5.78) as $t \to j\infty$. It is seen that $K_2 = 1$. (See Eq.(5.67)).

Now according to Eq.(5.36) Γ_e must be of the form

$$\Gamma_e = \frac{(A_e - G_L D_e) + (G_L B_e - C_e)}{(A_e + G_L D_e) + (G_L B_e + C_e)} . \qquad (5.36)$$

It has previously been shown that the constant term in A_e and D_e is unity. In Eq.(5.36), $G_L = 1/R = .5$. Thus the constant term in the numerator of Eq.(5.78) should be .5, and that in the denominator should be 1.5, i.e., the numerator and denominator of Eq.(5.78) are scaled by .5, resulting in

$$\Gamma_e = \frac{(.500 + 2.000t^2 + (.500)t^4) + (-.500t - 1.000t^3 - .500t^5)}{(1.500 + 10.028t^2 + 3.034t^4) + (6.110t + 7.952t^3 + .500t^5)} . \qquad (5.79)$$

Comparison of Eqs.(5.36) and (5.79) reveals that the elements of the transfer matrix are given by

$$\begin{aligned} A_e &= 1.000 + 5.514t^2 + 1.767t^4, \\ B_e &= 5.610t + 6.952t^3, \\ C_e &= 3.305t + 4.476t^3 + .500t^5, \\ D_e &= 1.000 + 9.029t^2 + 2.533t^4, \end{aligned} \qquad (5.80)$$

and the even mode transfer matrix is therefore

$$\frac{1}{(1-t^2)^2} \begin{pmatrix} A_e & B_e \\ C_e & D_e \end{pmatrix} . \qquad (5.81)$$

Notice that the t^5 term in B_e is missing, as expected by Eq.(5.48).

The final step is the network realization of this transfer matrix. A shunt stub is first removed. By Eq.(5.68),

$$a_1 = \frac{d}{dt}\left(\frac{C_e}{A_e}\right)\Big|_{t=1} = \frac{8.281\times 19.233 - 8.281\times 18.096}{(8.281)^2}$$

$$= .137 = \frac{d}{dt}\left(\frac{D_e}{B_e}\right)\Big|_{t=1} \quad , \tag{5.82}$$

is the admittance of the first stub (branch line). This stub is next removed from Eq.(5.81), i.e.,

$$\frac{1}{(1-t^2)^2}\begin{pmatrix} 1 & 0 \\ -.137t & 1 \end{pmatrix}\begin{pmatrix} A_e & B_e \\ C_e & D_e \end{pmatrix} = \frac{1}{(1-t^2)^2}\begin{pmatrix} A_e & B_e \\ \underline{C}_e & \underline{D}_e \end{pmatrix}, \tag{5.83}$$

where $\underline{C}_e$ and $\underline{D}_e$ are calculated as

$$\underline{C}_e = 3.168t + 3.721t^3 + .258t^5,$$
$$\underline{D}_e = 1.000 + 8.260t^2 + 1.581t^4. \tag{5.84}$$

The first main line admittance is now given from Eq.(5.69) as

$$b_1 = \frac{\underline{C}_e(1)}{A_e(1)} = \frac{7.147}{8.281} = .863 = \frac{\underline{D}_e(1)}{B_e(1)} \quad . \tag{5.85}$$

This main line is now removed from Eq.(5.83), i.e.,

$$\frac{1}{(1-t^2)^3}\begin{pmatrix} 1+t^2 & -.232t \\ -1.725t & 1+t^2 \end{pmatrix}\begin{pmatrix} A_e & B_e \\ \underline{C}_e & \underline{D}_e \end{pmatrix}$$

$$= \frac{1}{(1-t^2)^3}\begin{pmatrix} A_1 & B_1 \\ C_1 & D_1 \end{pmatrix} . \tag{5.86}$$

For the resulting transfer matrix to be of lower degree, it is necessary for A_1, B_1, C_1, and D_1 to contain a factor $(1-t^2)^2$, which they will have, of course. After performing the algebra, it is found that the resulting transfer matrix is

$$\frac{1}{1-t^2}\begin{pmatrix} 1+1.170t^2 & 3.292t \\ 1.442t+.257t^3 & 1+1.579t^2 \end{pmatrix} . \qquad (5.87)$$

The above removal cycle is now repeated until all of the elements have been removed. The admittances for the coupler of the above design are found to be

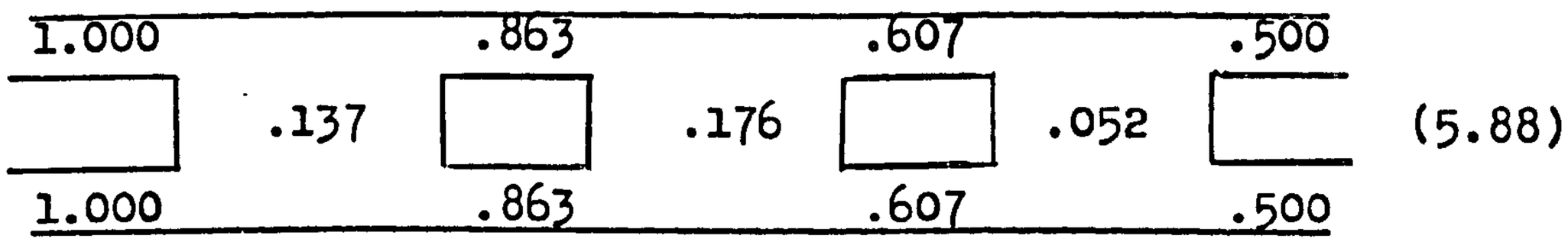

(5.88)

The frequency performance of this design may now be determined by analysis. It is found that the midband coupling value is 9.49 dB in this example. Also at midband the VSWR should be 1.0 and the directivity infinite, as is verified by a midband analysis. At a bandwidth BW= 1.1, the performance is

Coupling = 9.35 dB,

VSWR = 1.013,

Directivity = 30.15 dB,

which shows the degradation in performance from midband for this example.

5.4 Discussion of Computed Results.

5.4.1 The Symmetrical Case[9].

Results have been computed for a large number of cases of practical interest, and the element values are presented in Tables 5.1 and 5.2. Since the couplers are symmetrical, the immittance values tabulated are given as far as the center of the coupler. In Table 5.1 the bandwidth BW $= \lambda g_o / \lambda g_2$ corresponding to points where the directivity falls to 20 dB is given for each case and also the band-edge coupling (B.E. COUP (dB)) and the VSWR at these points. The performance is symmetrical with respect to electrical length θ on each side of midband (where $\theta_o = 45^o$). In Table 5.2 the worst VSWR and lowest directivity over the band are given as well as the band-edge coupling for each case. It is worthwhile noting at this point that for a stripline realization the immittances presented in the Tables correspond to characteristic admittances (normalized to 1 mho). The dual is true for the waveguide case.

The designs in Tables 5.1 and 5.2 have been mainly restricted to cases where the directivity of the couplers is greater than 20 dB. It has been established that the results obtained from the synthesis procedure result in a considerable improvement over existing designs. It is seen also that the new information includes specifications which have previously not been presented, and it is shown possible to design branch-guide couplers with good VSWR and high directivity over large bandwidths, i.e., of the order of one octave or more.

Element Values for Butterworth Branch-Guide Couplers for $n = 3$ to 9 Branches

COUP (DB)	B.E. COUP (DB)	$\frac{\lambda g_0}{\lambda g_2}$	VSWR	Branch Guide Immittances a_1	a_2	a_3	a_4	a_5	Main Line Immittances b_1	b_2	b_3	b_4
n = 3												
20	19.5	1.19	1.01	0.0501	0.1008				1.0039			
15	14.6	1.18	1.01	0.0996	0.1824				1.0128			
10	9.5[illegible]	1.17	1.03	0.1623	0.3450				1.0445			
8	7.60	1.16	1.04	0.2076	0.4607				1.0757			
6	5.64	1.15	1.07	0.2687	0.6448				1.1342			
5	4.70	1.14	1.09	0.3078	0.7874				1.1833			
4	3.70	1.14	1.12	0.3553	0.9974				1.2573			
3	2.69	1.14	1.19	0.4149	1.3432				1.3774			
2.5	2.24	1.13	1.22	0.4513	1.6188				1.4693			
2	1.74	1.13	1.29	0.4941	2.0325				1.5996			
n = 4												
20	19.0	1.29	1.01	0.0253	0.0752				1.0083	1.0053		
15	14.[illegible]	1.28	1.02	0.0454	0.1355				1.0079	1.0176		
10	9.09	1.26	1.04	0.0821	0.2534				1.0281	1.0632		
8	7.15	1.25	1.05	0.1044	0.3357				1.0486	1.1101		
6	5.2[illegible]	1.23	1.08	0.1328	0.4646				1.0875	1.2028		
5	4.24	1.23	1.12	0.1498	0.5635				1.1204	1.2850		
4	3.31	1.22	1.15	0.1688	0.7083				1.1702	1.4165		
3	2.39	1.21	1.20	0.1895	0.9466				1.2510	1.6488		
2.5	1.[illegible]9	1.21	1.23	0.2000	1.1377				1.3125	1.8422		
2	1.4[illegible]	1.20	1.28	0.2102	1.4274				1.3993	2.1411		
n = 5												
20	18.4	1.36	1.02	0.0129	0.0502	0.0749			1.0013	1.0086		
15	13.5	1.34	1.02	0.0233	0.0908	0.1348			1.0044	1.0156		
10	8.63	1.32	1.05	0.0426	0.1665	0.2542			1.0163	1.0373		
8	6.70	1.31	1.07	0.0542	0.2172	0.3411			1.0286	1.1013		
6	4.76	1.30	1.10	0.0687	0.2922	0.4857			1.0523	1.1898		
5	3.92	1.29	1.12	0.0770	0.3460	0.6048			1.0727	1.2696		
4	2.91	1.28	1.16	0.0857	0.4200	0.7931			1.1036	1.3998		
3	2.01	1.27	1.22	0.0941	0.5318	1.1383			1.1541	1.6326		
2.5	1.63	1.26	1.24	0.0976	0.6148	1.4457			1.1926	1.8304		
2	1.18	1.26	1.33	0.0999	0.7323	1.9616			1.2470	2.1417		
n = 6												
20	17.9	1.41	1.02	0.0066	0.0317	0.0683			1.0007	1.0033	1.0094	
15	12.9	1.40	1.03	0.0120	0.0571	0.1119			1.0024	1.0115	1.0185	
10	8.12	1.37	1.06	0.0224	0.1048	0.2096			1.0091	1.0431	1.0694	
8	6.19	1.36	1.08	0.0286	0.1352	0.2798			1.0162	1.0769	1.1046	
6	4.39	1.34	1.11	0.0364	0.1774	0.3957			1.0308	1.1455	1.2399	
5	3.36	1.34	1.14	0.0408	0.2053	0.4905			1.0423	1.2075	1.3480	
4	2.50	1.33	1.19	0.0453	0.2406	0.6403			1.0610	1.3079	1.5311	
3	1.73	1.31	1.22	0.0498	0.2874	0.9168			1.0917	1.4876	1.8832	
2.5	1.31	1.31	1.28	0.0506	0.3179	1.1648			1.1154	1.6386	2.0089	
2	.967	1.30	1.34	0.0510	0.3560	1.5862			1.1493	1.8739	2.7433	

COUP (DB)	B.E. COUP (DB)	$\frac{\lambda g_0}{\lambda g_2}$	VSWR	Branch Guide Immittances a_1	a_2	a_3	a_4	a_5	Main Line Immittances b_1	b_2	b_3	b_4
n = 7												
20	17.3	1.46	1.02	0.0033	0.0193	0.0469	0.0620		1.0004	1.0022	1.0050	
15	12.5	1.44	1.03	0.0062	0.0350	0.0842	0.1111		1.0013	1.0076	1.0171	
10	7.70	1.41	1.06	0.0118	0.0646	0.1564	0.2091		1.0049	1.0293	1.0653	
8	5.77	1.40	1.08	0.0152	0.0830	0.2063	0.2817		1.0090	1.0587	1.1186	
6	4.0[illegible]	1.38	1.12	0.0196	0.1072	0.2846	0.4075		1.0170	1.1000	1.2316	
5	3.11	1.37	1.15	0.0220	0.1222	0.3454	0.5166		1.0241	1.1844	1.3392	
4	2.26	1.36	1.19	0.0244	0.1395	0.4367	0.7001		1.0352	1.2946	1.5239	
3	1.46	1.35	1.25	0.0265	0.1593	0.5942	1.0709		1.0537	1.3391	1.8861	
2.5	1.10	1.34	1.30	0.0271	0.1700	0.7276	1.4365		1.0682	1.4426	2.2214	
2	.9[illegible]	1.33	1.39	0.0272	0.1810	0.9427	2.1198		1.0[illegible]3	1.6[illegible]	2.[illegible]	
n = 8												
20	16.9	1.49	1.02	0.0017	0.0115	0.0332	0.0542		1.0003	1.0018	1.0039	1.0055
15	12.1	1.47	1.04	0.0032	0.0210	0.0598	0.0971		1.0007	1.0048	1.0137	1.0192
10	7.33	1.44	1.06	0.0062	0.0392	0.1104	0.1819		1.0027	1.0188	1.0532	1.0746
8	5.43	1.43	1.09	0.0081	0.0505	0.1440	0.2443		1.0049	1.0342	1.0975	1.1373
6	3.68	1.41	1.13	0.0106	0.0648	0.1935	0.3517		1.0095	1.0662	1.1919	1.2743
5	2.83	1.40	1.16	0.0119	0.0733	0.2291	0.4447		1.0136	1.0951	1.2817	1.4090
4	2.00	1.39	1.20	0.0133	0.0823	0.2785	0.6015		1.0201	1.1414	1.4357	1.6489
3	1.25	1.38	1.29	0.0145	0.0913	0.3548	0.9210		1.0311	1.2045	1.7354	2.1476
2.5	.920	1.37	1.33	0.0149	0.0952	0.4129	1.2401		1.0389	1.2628	2.0105	2.6397
2	.681	1.35	1.34	0.0149	0.0979	0.4978	1.8466		1.0530	1.3477	2.4811	3.5504
n = 9												
20	16.5	1.52	1.02	0.0009	0.0067	0.0248	0.0436	0.0534	1.0001	1.0009	1.0028	1.0052
15	11.7	1.50	1.04	0.0017	0.0124	0.0407	0.0781	0.0964	1.0003	1.0029	1.0100	1.0178
10	6.95	1.47	1.08	0.0033	0.0235	0.0754	0.1455	0.1812	1.0014	1.0110	1.0396	1.0716
8	5.21	1.45	1.09	0.0043	0.0304	0.0976	0.1934	0.2451	1.0027	1.0214	1.0731	1.1330
6	3.33	1.44	1.14	0.0057	0.0392	0.1285	0.2725	0.3601	1.0057	1.0418	1.1448	1.2691
5	2.52	1.43	1.17	0.0065	0.0441	0.1490	0.3301	0.4650	1.0076	1.0606	1.2128	1.4047
4	1.75	1.42	1.24	0.0073	0.0498	0.1750	0.4441	0.6517	1.0113	1.0909	1.3285	1.6495
3	1.09	1.40	1.38	0.0080	0.0537	0.2098	0.6485	1.0663	1.0179	1.1446	1.5503	2.1686
2.5	.800	1.39	1.32	0.0082	0.0553	0.2388	0.8428	1.3180	1.0232	1.1891	1.7505	2.6919
2	.5[illegible]0	1.38	1.35	0.0083	0.0557	0.2680	1.1952	2.4599	1.0313	1.2579	2.0873	3.6839

TABLE 5.1.

Element Values for Chebyshev Branch-Guide Couplers for $n = 3$ to 8 Branches

$\frac{\lambda g_0}{\lambda g_2}$	COUP (DB)	B.E. COUP (DB)	DIR. (DB)	VSWR	Branch Guide Immittances a_1	a_2	a_3	a_4	Main Line Immittances b_1	b_2	b_3	b_4
n = 3												
1.1	20	19.9	36.8	1.000	0.0509	0.0993			1.0039			
	15	14.9	35.9	1.001	0.0911	0.1795			1.0130			
	10	9.86	34.4	1.004	0.1656	0.3385			1.0451			
	8	7.[illegible]5	33.5	1.007	0.2124	0.4512			1.0770			
	6	5.[illegible]4	32.5	1.015	0.2761	0.6301			1.1369			
	5	4.83	31.9	1.021	0.3174	0.7686			1.1874			
	4	3.83	31.2	1.030	0.3681	0.9729			1.2641			
	3	2.83	30.4	1.045	0.4330	1.3103			1.3899			
1.2	20	19.5	24.5	1.004	0.0531	0.0948			1.0041			
	15	14.5	23.5	1.009	0.0957	0.1703			1.0134			
	10	9.42	21.9	1.024	0.1761	0.3177			1.0471			
	8	7.36	21.0	1.040	0.2290	0.4207			1.0808			
	6	5.34	19.9	1.073	0.3008	0.5830			1.1454			
	5	4.32	19.3	1.102	0.3499	0.7087			1.2011			
	4	3.30	18.5	1.150	0.4130	0.8950			1.2880			
	3	2.29	17.7	1.236	0.5007	1.2156			1.4391			
1.3	20	18.9	16.9	1.013	0.0573	0.0864			1.0043			
	15	13.9	15.9	1.029	0.1043	0.1532			1.0148			
	10	[illegible].65	14.2	1.075	0.1962	0.2786			1.0504			

$\frac{\lambda g_0}{\lambda g_2}$	COUP (DB)	B.E. COUP (DB)	DIR. (DB)	VSWR	Branch Guide Immittances a_1	a_2	a_3	a_4	Main Line Immittances b_1	b_2	b_3	b_4
n = 4												
1.1	20	19.9	58.6	1.000	0.0458	0.0747			1.0084	1.0053		
	15	14.9	57.4	1.000	0.0469	0.1344			1.0080	1.0177		
	10	9.87	55.5	1.000	0.0843	0.2513			1.0287	1.0634		
	8	7.96	54.4	1.001	0.1073	0.3328			1.0499	1.1106		
	6	5.06	53.1	1.001	0.1371	0.4607			1.0899	1.2041		
	5	4.[illegible]6	52.3	1.002	0.1550	0.5589			1.1240	1.2873		
	4	3.96	51.8	1.003	0.1753	0.7032			1.1758	1.4207		
	3	2.[illegible]6	50.3	1.004	0.1978	0.9419			1.2606	1.6575		
1.2	20	19.5	40.3	1.000	0.0279	0.0730			1.0085	1.0093		
	15	14.5	39.1	1.001	0.0497	0.1318			1.0083	1.0177		
	10	9.47	37.1	1.004	0.0919	0.2444			1.0307	1.0640		
	8	7.45	35.9	1.007	0.1171	0.3233			1.0535	1.1121		
	6	5.43	34.6	1.013	0.1513	0.4474			1.0977	1.2052		
	5	4.42	33.7	1.019	0.1726	0.5432			1.1357	1.2943		
	4	3.41	32.8	1.027	0.1975	0.6951			1.1944	1.4341		
	3	2.4[illegible]	31.6	1.043	0.2268	0.9235			1.2926	1.6959		
1.3	20	18.9	29.8	1.003	0.0306	0.0699			1.0027	1.0053		
	15	13.9	28.0	1.007	0.0559	0.1850			1.0093	1.0179		
	10	8.76	25.9	1.020	0.1047	0.2310			1.0344	1.0659		
	8	6.72	24.7	1.033	0.1365	0.3043			1.0606	1.1149		
	6	4.67	23.2	1.059	0.1806	0.4193			1.1186	1.2158		
	5	3.66	22.3	1.084	0.2097	0.5096			1.1585	1.3076		
	4	2.66	21.2	1.124	0.2459	0.6422			1.2313	1.4588		
	3	1.71	20.0	1.197	0.2918	0.8705			1.3577	1.7379		
1.4	20	18.6	21.0	1.011	0.0359	0.0646			1.0051	1.0054		
	15	18.9	19.6	1.025	0.0666	0.1143			1.0107	1.0181		
	10	7.71	17.4	1.067	0.1291	0.2067			1.0408	1.0669		
	8	5.63	16.1	1.110	0.1786	0.2683			1.0728	1.1190		
	6	3.61	14.4	1.202	0.2377	0.3683			1.1378	1.2061		
	5	2.66	13.5	1.290	0.2843	0.4335			1.1960	1.3247		

TABLE 5.2.

$\lambda s_0/\lambda s_2$	COUP (DB)	B.B. COUP (DB)	DIR. (DB)	VSWR	BRANCH GUIDE IMMITTANCES a_1	a_2	a_3	a_4	MAIN LINE IMMITTANCES b_1	b_2	b_3	b_4
n = 5												
1.1	20	19.9	80.4	1.000	0.0132	0.0502	0.0742		1.0013	1.0046		
	15	14.9	77.0	1.000	0.0240	0.0902	0.1335		1.0045	1.0157		
	10	9.97	76.8	1.000	0.0439	0.1666	0.2514		1.0168	1.0577		
	8	7.97	75.5	1.000	0.0560	0.2175	0.3371		1.0295	1.1021		
	6	5.97	73.9	1.000	0.0712	0.2929	0.4798		1.0542	1.1917		
	5	4.97	72.9	1.000	0.0800	0.3473	0.5976		1.0753	1.2728		
	4	3.97	71.8	1.000	0.0893	0.4224	0.7841		1.1077	1.4049		
	3	2.97	70.5	1.000	0.0985	0.5370	1.1277		1.1609	1.6440		
1.2	20	19.5	55.9	1.000	0.0143	0.0502	0.0721		1.0014	1.0047		
	15	14.5	54.5	1.000	0.0261	0.0901	0.1294		1.0049	1.0159		
	10	9.49	52.1	1.001	0.0484	0.1665	0.2427		1.0183	1.0588		
	8	7.49	50.8	1.001	0.0621	0.2178	0.3249		1.0324	1.1045		
	6	5.46	49.1	1.002	0.0798	0.2945	0.4519		1.0601	1.1976		
	5	4.46	48.2	1.003	0.0903	0.3504	0.5756		1.0842	1.2828		
	4	3.46	47.0	1.005	0.1017	0.4289	0.7570		1.1215	1.4229		
	3	2.47	45.6	1.008	0.1136	0.5515	1.0960		1.1839	1.6810		
1.3	20	19.9	41.1	1.001	0.0165	0.0438	0.0685		1.0016	1.0048		
	15	13.9	39.6	1.002	0.0303	0.0894	0.1224		1.0056	1.0163		
	10	8.92	37.1	1.005	0.0572	0.1653	0.2280		1.0213	1.0608		
	8	6.79	35.7	1.009	0.0744	0.2165	0.3041		1.0382	1.1089		
	6	4.76	33.9	1.016	0.0975	0.2941	0.4314		1.0720	1.2086		
	5	3.75	32.9	1.023	0.1119	0.3520	0.5380		1.1022	1.3014		
	4	2.76	31.6	1.034	0.1287	0.4351	0.7110		1.1502	1.4574		
	3	1.79	30.1	1.055	0.1481	0.5706	1.0443		1.2337	1.7551		
1.4	20	18.0	30.0	1.004	0.0202	0.0487	0.0634		1.0019	1.0049		
	15	12.9	28.4	1.008	0.0377	0.0871	0.1124		1.0068	1.0168		
	10	7.80	25.8	1.023	0.0735	0.1600	0.2066		1.0266	1.0639		
	8	5.74	24.2	1.039	0.0980	0.2091	0.2738		1.0485	1.1158		
	6	3.70	22.2	1.073	0.1333	0.2843	0.3870		1.0943	1.2267		
	5	2.71	21.1	1.106	0.1575	0.3416	0.4837		1.1369	1.3336		
	4	1.75	19.6	1.163	0.1889	0.4272	0.6466		1.2085	1.5216		
1.5	20	16.8	20.7	1.013	0.0266	0.0456	0.0565		1.0025	1.0051		
	15	11.6	19.0	1.030	0.0511	0.0805	0.0989		1.0088	1.0176		
	10	6.36	16.0	1.086	0.1053	0.1434	0.1776		1.0358	1.0683		
	8	4.29	14.3	1.148	0.1465	0.1835	0.2326		1.0671	1.1265		
	6	2.32	12.1	1.293	0.2150	0.2424	0.3266		1.1375	1.2578		
n = 6												
1.2	20	19.5	72.0	1.000	0.0075	0.0325	0.0605		1.0008	1.0035	1.0054	
	15	14.5	70.1	1.000	0.0138	0.0587	0.1085		1.0027	1.0120	1.0186	
	10	9.50	67.5	1.000	0.0260	0.1081	0.2027		1.0105	1.0452	1.0703	
	8	7.49	66.0	1.000	0.0336	0.1401	0.2705		1.0189	1.0812	1.1270	
	6	5.49	64.1	1.000	0.0432	0.1852	0.3829		1.0356	1.1553	1.2465	
	5	4.49	63.0	1.001	0.0488	0.2157	0.4759		1.0503	1.2233	1.3539	
	4	3.49	61.7	1.001	0.0547	0.2551	0.6249		1.0733	1.3351	1.5546	
	3	2.50	60.0	1.002	0.0603	0.3098	0.9059		1.1121	1.5400	1.9368	
1.3	20	19.9	53.4	1.000	0.0089	0.0334	0.0583		1.0009	1.0036	1.0055	
	15	13.9	51.8	1.000	0.0165	0.0604	0.1041		1.0032	1.0126	1.0188	
	10	8.95	49.0	1.001	0.0317	0.1118	0.1936		1.0127	1.0481	1.0717	
	8	6.83	47.4	1.002	0.0414	0.1456	0.2579		1.0230	1.0872	1.1303	
	6	4.81	45.5	1.004	0.0542	0.1940	0.3656		1.0442	1.1690	1.2560	
	5	3.82	44.3	1.006	0.0619	0.2278	0.4561		1.0632	1.2456	1.3773	
	4	2.83	42.8	1.010	0.0705	0.2728	0.6038		1.0935	1.3745	1.5895	
	3	1.87	41.0	1.016	0.0796	0.3386	0.8923		1.1464	1.6193	2.0194	
1.4	20	18.1	39.7	1.001	0.0114	0.0344	0.0548		1.0012	1.0039	1.0055	
	15	13.0	37.9	1.003	0.0215	0.0621	0.0974		1.0041	1.0135	1.0191	
	10	7.97	34.9	1.008	0.0424	0.1153	0.1797		1.0167	1.0526	1.0738	
	8	5.89	33.2	1.014	0.0566	0.1507	0.2387		1.0308	1.0966	1.1359	
	6	3.82	31.1	1.026	0.0765	0.2027	0.3387		1.0607	1.1915	1.2723	
	5	2.83	29.7	1.038	0.0895	0.2401	0.4248		1.0886	1.2832	1.4078	
	4	1.88	28.1	1.059	0.1053	0.2922	0.5702		1.1349	1.4433	1.6524	
	3	1.00	26.1	1.099	0.1253	0.3739	0.8714		1.2209	1.7663	2.1755	
1.5	20	16.8	28.3	1.006	0.0159	0.0347	0.0500		1.0016	1.0042	1.0056	
	15	11.7	26.4	1.013	0.0308	0.0623	0.0880		1.0058	1.0148	1.0195	
	10	6.68	23.2	1.038	0.0640	0.1143	0.1597		1.0241	1.0591	1.0773	
	8	5.93	21.2	1.066	0.0886	0.1482	0.2106		1.0458	1.1108	1.1450	
	6	2.46	18.8	1.129	0.1272	0.1977	0.2982		1.0942	1.2270	1.2993	
	5	1.96	17.3	1.192	0.1559	0.2332	0.3757		1.1415	1.3439	1.4580	
	4	.817	15.4	1.309	0.1964	0.2825	0.5110		1.2242	1.5561	1.7544	
1.6	20	18.1	18.3	1.021	0.0249	0.0323	0.0434		1.0023	1.0046	1.0057	
	15	9.82	16.1	1.051	0.0502	0.0561	0.0749		1.0088	1.0165	1.0202	
	10	5.60	12.4	1.159	0.1136	0.0936	0.1308		1.0384	1.0679	1.0823	
	8	2.69	10.3	1.286	0.1676	0.1114	0.1682		1.0746	1.1292	1.1562	

$\lambda s_0/\lambda s_2$	COUP (DB)	B.B. COUP (DB)	DIR. (DB)	VSWR	BRANCH GUIDE IMMITTANCES a_1	a_2	a_3	a_4	MAIN LINE IMMITTANCES b_1	b_2	b_3	b_4
n = 7												
1.2	20	19.0	67.4	1.000	0.0048	0.0216	0.0455	0.0573	1.0005	1.0025	1.0051	
	15	13.9	63.6	1.000	0.0090	0.0394	0.0815	0.1032	1.0018	1.0069	1.0177	
	10	8.87	60.6	1.000	0.0176	0.0735	0.1512	0.1906	1.0074	1.0347	1.0686	
	8	6.86	58.8	1.001	0.0232	0.0955	0.1999	0.2561	1.0136	1.0636	1.1263	
	6	4.85	56.6	1.001	0.0307	0.1255	0.2794	0.3711	1.0265	1.1246	1.2521	
	5	3.86	55.3	1.002	0.0350	0.1451	0.3417	0.4734	1.0382	1.1817	1.3756	
	4	2.88	53.7	1.003	0.0398	0.1692	0.4411	0.6513	1.0572	1.2776	1.5953	
	3	1.92	51.7	1.008	0.0446	0.2001	0.6257	1.0330	1.0906	1.4582	2.0512	
1.4	20	18.1	49.0	1.000	0.0064	0.0233	0.0440	0.0536	1.0007	1.0028	1.0052	
	15	13.0	47.1	1.001	0.0123	0.0427	0.0787	0.0950	1.0025	1.0089	1.0181	
	10	7.98	43.9	1.003	0.0236	0.0809	0.1454	0.1757	1.0102	1.0307	1.0716	
	8	5.89	42.0	1.005	0.0331	0.1068	0.1904	0.2354	1.0191	1.0738	1.1335	
	6	3.89	39.6	1.010	0.0449	0.1396	0.2568	0.3417	1.0392	1.1480	1.2722	
	5	2.91	38.1	1.014	0.0523	0.1691	0.3343	0.4523	1.0563	1.2199	1.4124	
	4	1.97	36.4	1.022	0.0611	0.1936	0.4402	0.6139	1.0864	1.3453	1.6704	
	3	1.08	34.1	1.037	0.0716	0.2364	0.6506	1.0149	1.1427	1.5974	2.0422	
1.5	20	16.8	35.5	1.002	0.0095	0.0252	0.0416	0.0485	1.0010	1.0032	1.0053	
	15	11.7	33.4	1.006	0.0176	0.0461	0.0738	0.0852	1.0037	1.0115	1.0188	
	10	6.56	29.8	1.017	0.0392	0.0865	0.1352	0.1555	1.0157	1.0473	1.0762	
	8	4.53	27.7	1.030	0.0545	0.1132	0.1777	0.2073	1.0305	1.0900	1.1450	
	6	2.56	25.1	1.059	0.0779	0.1516	0.2527	0.3021	1.0638	1.1876	1.3064	
	5	1.64	23.4	1.088	0.0949	0.1784	0.3179	0.3929	1.0970	1.2878	1.4787	
	4	.820	21.3	1.144	0.1181	0.2149	0.4337	0.5642	1.1570	1.4759	1.8195	
	3	.295	18.3	1.274	0.1567	0.2708	0.7004	1.0471	1.2886	1.9200	2.7032	
1.6	20	15.1	23.4	1.011	0.0160	0.0259	0.0377	0.0420	1.0016	1.0037	1.0055	
	15	9.89	21.1	1.027	0.0326	0.0464	0.0659	0.0729	1.0081	1.0137	1.0198	
	10	4.67	17.0	1.077	0.0745	0.0927	0.1179	0.1298	1.0220	1.0501	1.0836	
	8	2.69	14.5	1.160	0.1112	0.1034	0.1544	0.1697	1.0505	1.1165	1.1647	
	6	1.08	11.4	1.348	0.1706	0.1268	0.2012	0.2401	1.1261	1.2605	1.3724	
n = 8												
1.4	20	18.1	58.7	1.000	0.0036	0.0154	0.0336	0.0479	1.0004	1.0019	1.0043	1.0056
	15	13.0	56.7	1.000	0.0070	0.0286	0.0605	0.0850	1.0014	1.0069	1.0154	1.0199
	10	7.93	53.2	1.001	0.0144	0.0545	0.1123	0.1574	1.0061	1.0283	1.0622	1.0798
	8	5.93	51.1	1.002	0.0195	0.0715	0.1478	0.2111	1.0116	1.0533	1.1171	1.1508
	6	3.94	48.6	1.003	0.0265	0.0947	0.2035	0.3072	1.0237	1.1081	1.2416	1.3144
	5	2.97	47.0	1.005	0.0310	0.1095	0.2472	0.3958	1.0352	1.1613	1.3682	1.4853
	4	2.03	46.6	1.008	0.0362	0.1275	0.3148	0.5575	1.0546	1.2539	1.6023	1.8121
	3	1.11	42.5	1.014	0.0422	0.1498	0.4392	0.9372	1.0912	1.4384	2.1211	2.5798
1.5	20	16.8	43.1	1.001	0.0057	0.0177	0.0332	0.0440	1.0006	1.0023	1.0046	1.0057
	15	11.7	40.8	1.002	0.0113	0.0330	0.0595	0.0774	1.0023	1.0085	1.0165	1.0204
	10	6.69	38.0	1.007	0.0242	0.0634	0.1099	0.1418	1.0101	1.0359	1.0685	1.0839
	8	4.60	35.7	1.013	0.0338	0.0836	0.1450	0.1898	1.0198	1.0691	1.1318	1.1618
	6	2.63	31.9	1.027	0.0483	0.1119	0.2024	0.2785	1.0421	1.1457	1.2820	1.3496
	5	1.74	30.1	1.040	0.0585	0.1309	0.2504	0.3447	1.0644	1.2242	1.4431	1.5558
	4	.900	27.8	1.066	0.0720	0.1550	0.3309	0.5338	1.1044	1.3697	1.7612	1.9756
	3	.254	24.7	1.124	0.0925	0.1878	0.5013	0.9853	1.1890	1.6954	2.5549	3.0831
1.6	20	15.1	29.5	1.006	0.0103	0.0200	0.0316	0.0387	1.0011	1.0029	1.0049	1.0058
	15	9.93	27.0	1.014	0.0212	0.0368	0.0561	0.0672	1.0042	1.0109	1.0181	1.0211
	10	4.72	22.6	1.047	0.0492	0.0687	0.1020	0.1204	1.0196	1.0483	1.0781	1.0909
	8	2.76	20.0	1.087	0.0730	0.0882	0.1341	0.1601	1.0401	1.0964	1.1556	1.1812
	6	1.07	17.7	1.186	0.1152	0.1125	0.1892	0.2369	1.0907	1.2150	1.3517	1.4129
	5	.477	14.6	1.294	0.1508	0.1252	0.2386	0.3162	1.1448	1.3440	1.5747	1.6816
	4	.305	12.1	1.499	0.2084	0.1340	0.3262	0.4776	1.2460	1.5919	2.0889	2.2434

TABLE 5.2 (Cont'd)

Performance curves for 3 dB Butterworth couplers having 3 to 9 branches are shown in Fig.5.8. In these curves VSWR has been plotted, and the directivity shows similar maximally flat behaviour. The performance of a 3 dB coupler having eight branch guides analyzed from previously published results[3] is also shown for comparison as the dotted line in Fig.5.8. It has been shown by analysis that the reason that the latter is inferior to the present result for $n=8$ is that the zeros of the F function (see Eq.(5.52)) of this previous result are clustered about the midband frequency rather than being exactly coincident with it.

The performance of Chebyshev designs is displayed in Figs.5.9 through 5.12 for a large number of center frequency coupling values and for various numbers of branch guides. Each figure represents a case of constant bandwidth. The curves show the maximum passband VSWR and the minimum passband directivity for a given number of branch guides as the center frequency coupling is varied. The latter values are indicated in decibels by the labelled points on the curves. These figures present an overall picture of performance and are useful in selecting a design for a given specification.

It is evident that it is now feasible to design symmetrical branch-guide couplers to give excellent VSWR and directivity over much broader bandwidths than hitherto thought

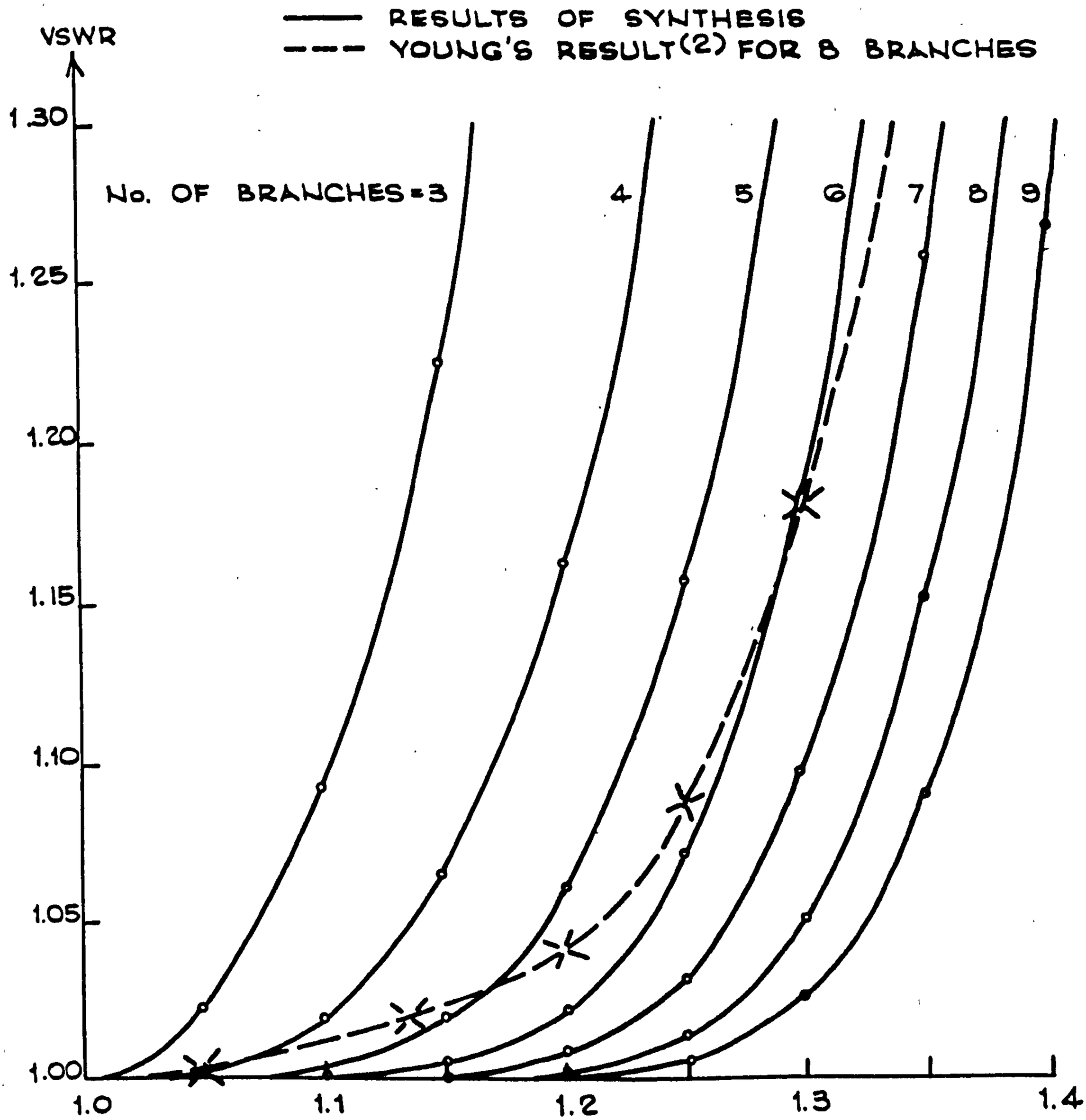

Fig. 5.8. VSWR as a function of frequency for Butterworth branch-guide couplers.

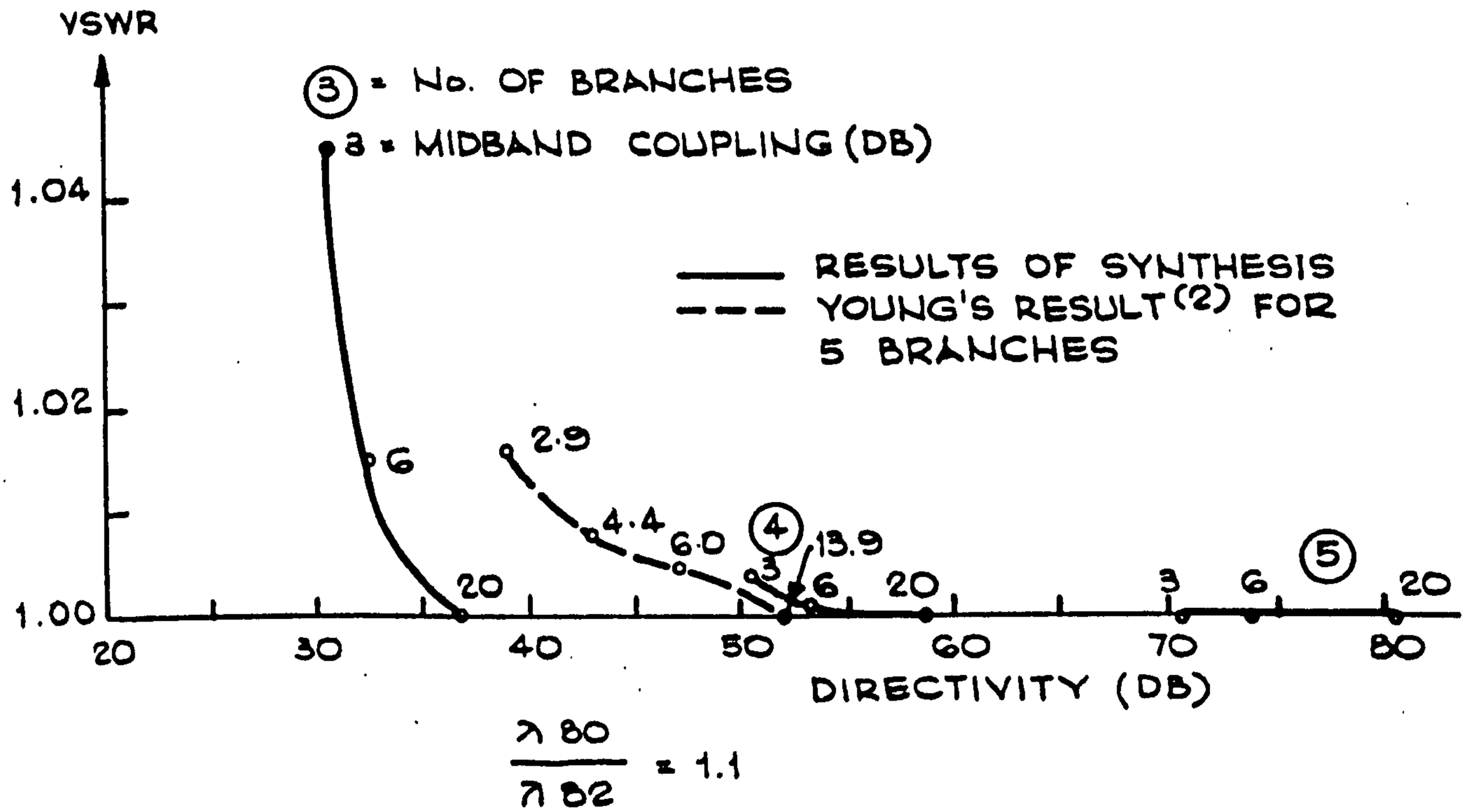

Fig. 5.9. VSWR versus directivity curves for Chebyshev couplers for bandwidth of 1.1.

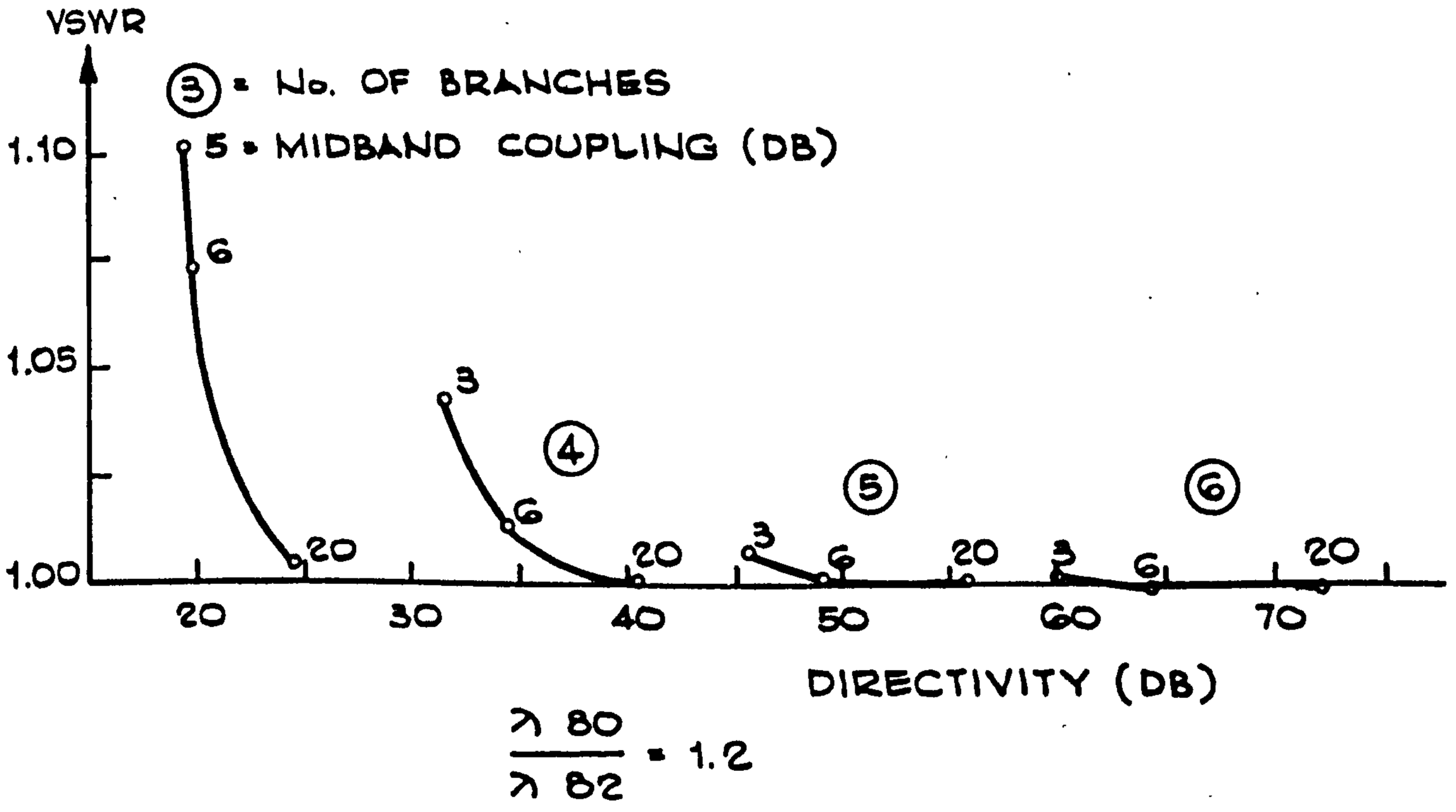

Fig. 5.10. VSWR versus directivity curves for Chebyshev couplers for bandwidth of 1.2.

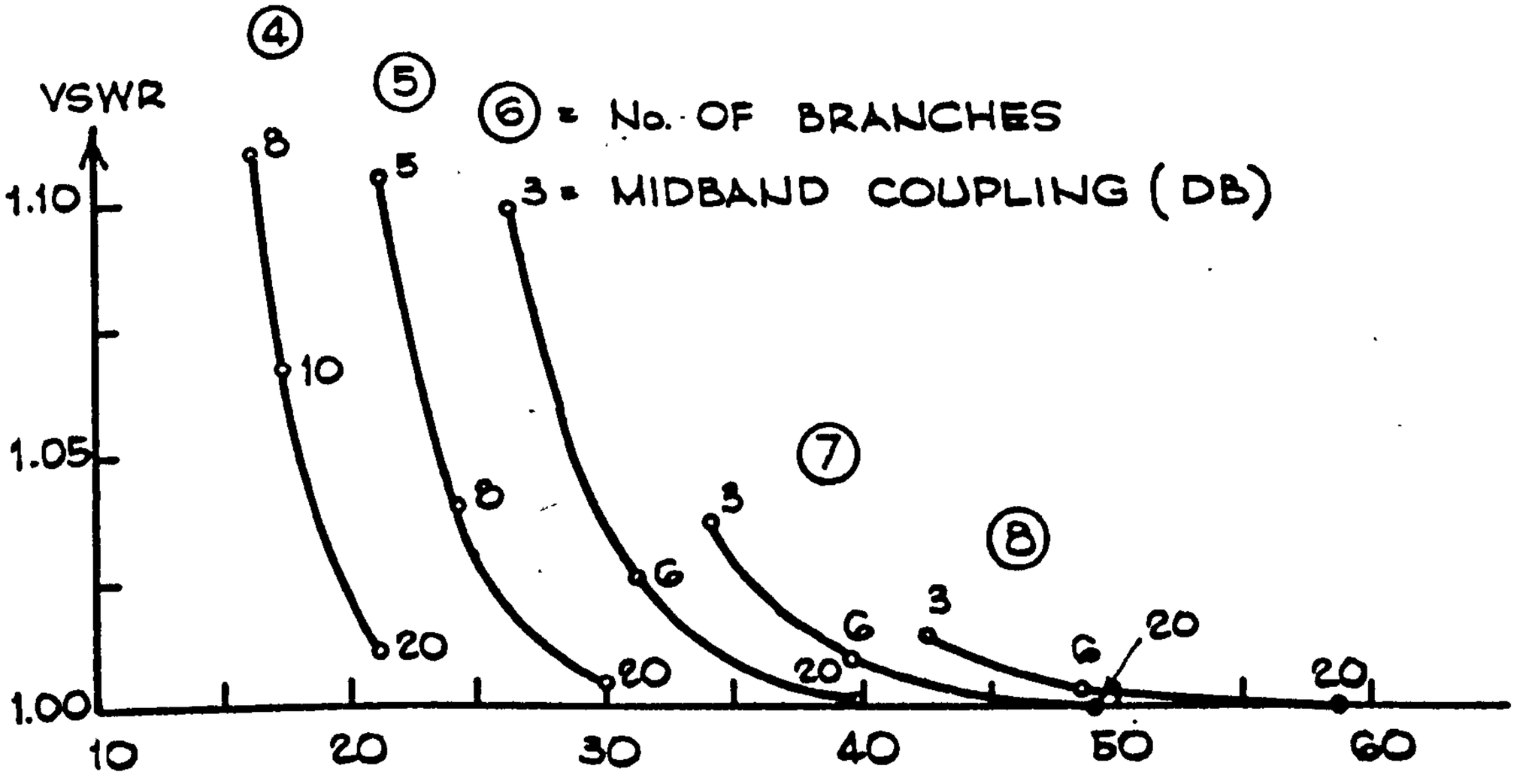

$$\frac{\lambda 80}{\lambda 82} = 1.4$$

Fig. 5.11. VSWR versus directivity curves for Chebyshev couplers for bandwidth of 1.4.

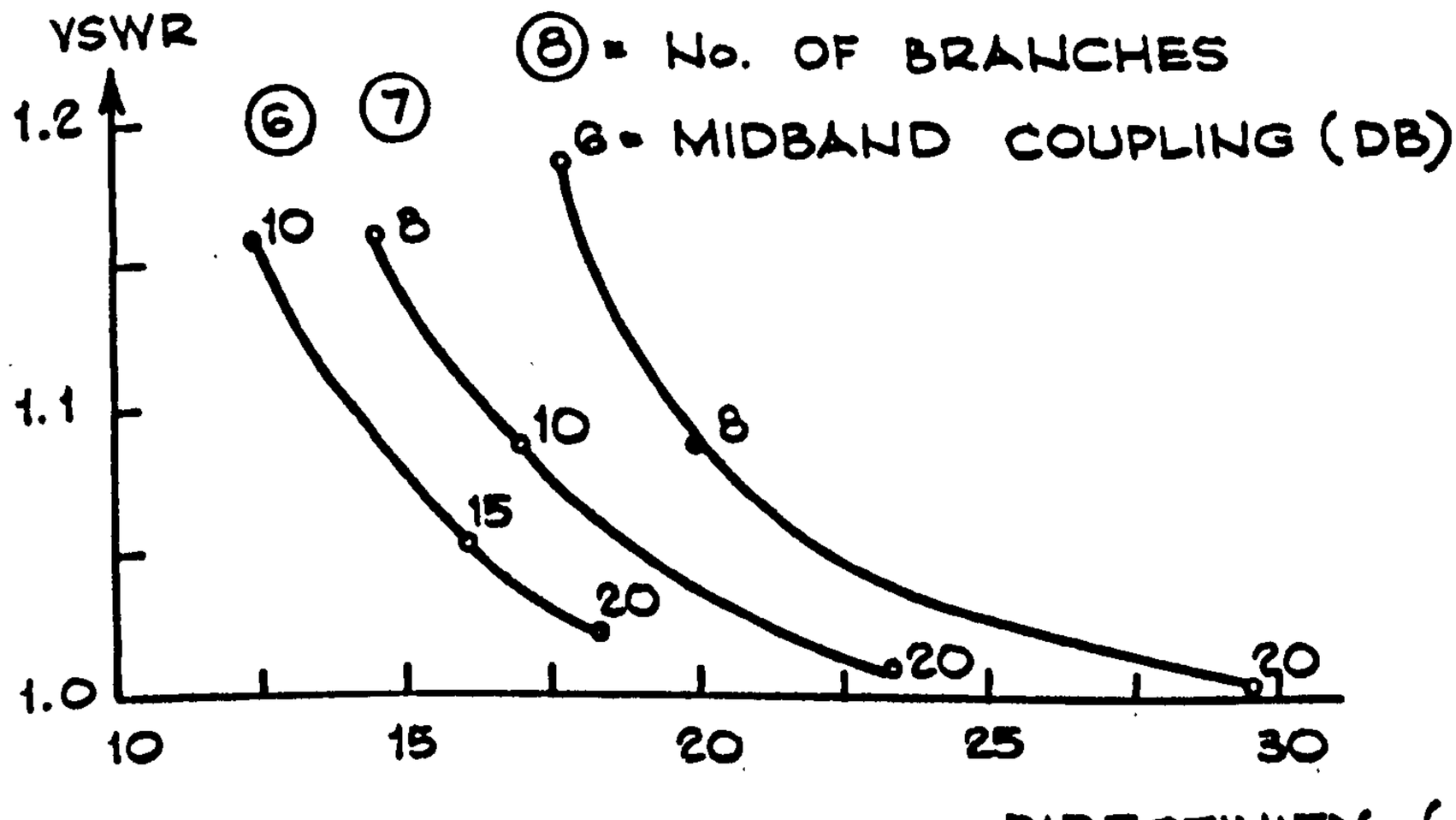

$$\frac{\lambda 80}{\lambda 82} = 1.6$$

Fig. 5.12. VSWR versus directivity curves for Chebyshev couplers for bandwidth of 1.6.

possible. A comparison with previous Chebyshev designs[3] is shown as the dotted curve in Fig.5.9. It is seen that here an even greater improvement is attained than in the Butterworth case.

5.4.2 The Asymmetrical Case[10].

If the output resistance R_L is allowed to be different from the source resistance R_s, then it has been seen previously (i.e., in the numerical example) that an asymmetrical coupler will result. This device is therefore both a branch-guide directional coupler and impedance transformer.

Such an impedance transformer with loose coupling might find application in antenna design work and other fields. Accordingly, Table 5.3 gives the values of branch and main line immittances for the Butterworth specification for 3 to 5 branches, coupling from 40 to 10 dB, and R (the output to input conductance or resistance ratio) from 2 to 10. The bandwidth corresponding to the frequency at which the directivity falls to 20 dB is given for each case and also the coupling and VSWR at this point. Similarly Table 5.4 gives design information for Chebyshev characteristics for 3 to 5 branches. The maximum ripple VSWR and worst ripple directivity are given, as well as the band edge coupling (B.E.C.), for bandwidths of 1.1 and 1.2. As before, the immittances are admittances for a stripline realization (normalized to 1 mho)

ELEMENT VALUES FOR BUTTERWORTH BRANCH-GUIDE COUPLER-TRANSFORMERS
OF RESISTANCE RATIO R AND COUPLING C (IN DB) FOR N=3 TO 5 BRANCHES

R	C	B.E. C	λ_{g_a} / λ_{g_b}	B.E. VSWR	BRANCH GUIDE IMMITTANCES a1	a2	a3	a4	a5	MAIN LINE IMMITTANCES b1	b2	b3	b4
n = 3													
	40	39.55	1.20	1.04	0.0055	0.0150	0.0101			1.1067	1.3555		
1.5	30	29.56	1.20	1.04	0.0175	0.0475	0.0319			1.1073	1.3562		
	20	19.58	1.18	1.04	0.0559	0.1518	0.1005			1.1129	1.3639		
	10	9.65	1.15	1.06	0.1861	0.5442	0.3255			1.1818	1.4561		
	40	39.55	1.20	1.07	0.0059	0.0200	0.0165			1.1893	1.6819		
2	30	29.57	1.20	1.07	0.0187	0.0633	0.0521			1.1900	1.6832		
	20	19.60	1.18	1.06	0.0603	0.2032	0.1637			1.1978	1.6966		
	10	9.69	1.14	1.08	0.2062	0.7665	0.5327			1.3004	1.8640		
	40	39.59	1.20	1.18	0.0070	0.0500	0.0768			1.4956	3.3445		
5	30	29.62	1.18	1.16	0.0227	0.1587	0.2406			1.4977	3.3519		
	20	19.69	1.15	1.11	0.0770	0.5218	0.7487			1.5214	3.4296		
	10	9.83	1.10	1.14	0.2998	3.0130	2.6933			1.9790	4.8146		
	40	39.73	1.16	1.20	0.0078	0.1001	0.2382			1.7788	5.6264		
10	30	29.70	1.16	1.20	0.0261	0.3189	0.7421			1.7836	5.6538		
	20	19.78	1.12	1.12	0.0946	1.0959	2.3143			1.8416	5.9509		
n = 4													
	40	38.96	1.30	1.04	0.0026	0.0096	0.0130	0.0053		1.0521	1.2248	1.4259	
1.5	30	28.97	1.30	1.04	0.0084	0.0305	0.0412	0.0168		1.0523	1.2257	1.4264	
	20	19.03	1.28	1.04	0.0271	0.0975	0.1306	0.0529		1.0555	1.2346	1.4314	
	10	9.19	1.24	1.06	0.0913	0.3448	0.4553	0.1683		1.0973	1.3507	1.4944	
	40	38.96	1.30	1.07	0.0027	0.0115	0.0192	0.0090		1.0907	1.4144	1.8338	
2	30	28.99	1.30	1.07	0.0087	0.0364	0.0607	0.0283		1.0911	1.4157	1.8347	
	20	19.07	1.27	1.06	0.0286	0.1172	0.1925	0.0886		1.0953	1.4296	1.8439	
	10	9.27	1.22	1.08	0.0989	0.4365	0.7003	0.2778		1.1559	1.6244	1.9645	
	40	39.02	1.30	1.18	0.0029	0.0197	0.0649	0.0462		1.2253	2.2366	4.0815	
5	30	29.09	1.28	1.15	0.0096	0.0632	0.2044	0.1437		1.2263	2.2419	4.0876	
	20	19.25	1.24	1.10	0.0344	0.2126	0.6561	0.4361		1.2380	2.3010	4.1518	
	10	9.57	1.17	1.12	0.1299	1.1921	3.5944	1.3379		1.4893	3.6672	5.3055	
	40	39.25	1.26	1.20	0.0030	0.0293	0.1595	0.1535		1.3411	3.1639	7.4606	
10	30	29.21	1.26	1.19	0.0104	0.0959	0.5022	0.4709		1.3432	3.1791	7.4865	
	20	19.43	1.20	1.10	0.0415	0.3447	1.6684	1.3974		1.3703	3.3630	7.7645	
n = 5													
	40	38.36	1.38	1.04	0.0013	0.0058	0.0112	0.0096	0.0027	1.0257	1.1352	1.3215	1.4624
1.5	30	28.39	1.37	1.04	0.0041	0.0184	0.0354	0.0303	0.0086	1.0259	1.1358	1.3224	1.4627
	20	18.47	1.35	1.04	0.0136	0.0593	0.1123	0.0955	0.0275	1.0276	1.1428	1.3311	1.4656
	10	8.72	1.30	1.07	0.0471	0.2061	0.4017	0.3203	0.0881	1.0516	1.2396	1.4495	1.5038
	40	38.37	1.38	1.07	0.0013	0.0064	0.0148	0.0151	0.0047	1.0445	1.2422	1.6104	1.9150
2	30	28.41	1.37	1.07	0.0042	0.0205	0.0469	0.0477	0.0148	1.0447	1.2431	1.6118	1.9155
	20	18.53	1.34	1.06	0.0142	0.0667	0.1494	0.1497	0.0467	1.0469	1.2533	1.6267	1.9209
	10	8.84	1.29	1.08	0.0510	0.2431	0.5679	0.5129	0.1459	1.0816	1.4066	1.8417	1.9961
	40	38.44	1.37	1.18	0.0013	0.0086	0.0356	0.0624	0.0257	1.1081	1.6572	3.0185	4.5130
5	30	28.54	1.35	1.14	0.0045	0.0283	0.1129	0.1948	0.0796	1.1085	1.6601	3.0258	4.5169
	20	18.79	1.30	1.09	0.0171	0.0989	0.3709	0.6066	0.2396	1.1146	1.6953	3.1069	4.5589
	10	9.31	1.22	1.12	0.0658	0.4903	2.4660	2.7692	0.6739	1.2588	2.6110	5.0769	5.3383
	40	38.72	1.34	1.20	0.0013	0.0107	0.0677	0.1760	0.0891	1.1614	2.0658	4.8451	8.6131
10	30	28.72	1.32	1.18	0.0049	0.0364	0.2168	0.5455	0.2712	1.1624	2.0732	4.8703	8.6312
	20	19.05	1.26	1.09	0.0212	0.1397	0.7554	1.7196	0.7855	1.1764	2.1698	5.1695	8.8264

TABLE.5.3

ELEMENT VALUES FOR CHEBYSHEV BRANCH-GUIDE COUPLER-TRANSFORMERS WITH A BANDWIDTH OF 1.1, RESISTANCE RATIO R, AND COUPLING C (IN DB) FOR N=3 TO 5 BRANCHES

R	C	B.E. C	DIR (DB)	VSWR	BRANCH GUIDE IMMITTANCES					MAIN LINE IMMITTANCES			
					a1	a2	a3	a4	a5	b1	b2	b3	b4
n = 3													
2	40	39.89	37.8	1.009	0.0060	0.0197	0.0167			1.1919	1.6782		
	30	29.89	37.3	1.009	0.0190	0.0625	0.0527			1.1927	1.6795		
	20	19.88	35.7	1.009	0.0614	0.2000	0.1659			1.2006	1.6930		
	10	9.44	31.5	1.019	0.2122	0.7492	0.5447			1.3057	1.8626		
5	40	39.89	37.4	1.023	0.0071	0.0492	0.0776			1.5039	3.3259		
	30	29.88	36.1	1.023	0.0232	0.1559	0.2431			1.5061	3.3333		
	20	19.86	32.7	1.024	0.0792	0.5106	0.7590			1.5304	3.4111		
	10	9.81	25.3	1.069	0.3183	2.9233	2.7985			2.0129	4.8272		
10	40	39.89	36.8	1.036	0.0080	0.0979	0.2403			1.7946	5.5768		
	30	29.88	34.4	1.036	0.0269	0.3114	0.7497			1.7996	5.6040		
	20	19.84	29.0	1.041	0.0984	1.0644	2.3511			1.8599	5.9005		
n = 4													
2	40	39.89	59.9	1.001	0.0028	0.0114	0.0191	0.0092		1.0925	1.4144	1.8308	
	30	29.89	59.2	1.001	0.0089	0.0362	0.0602	0.0288		1.0929	1.4157	1.8317	
	20	19.88	57.2	1.001	0.0292	0.1165	0.1908	0.0904		1.0972	1.4296	1.8410	
	10	9.61	52.0	1.002	0.1022	0.4335	0.6927	0.2856		1.1596	1.6255	1.9644	
5	40	39.89	59.4	1.002	0.0029	0.0196	0.0642	0.0470		1.2302	2.2366	4.0653	
	30	29.89	57.7	1.002	0.0098	0.0630	0.2019	0.1461		1.2312	2.2419	4.0714	
	20	19.87	53.6	1.002	0.0354	0.2117	0.6473	0.4449		1.2432	2.3011	4.1364	
	10	9.85	44.6	1.006	0.1372	1.1904	3.5560	1.3913		1.5072	3.6871	5.3273	
10	40	39.89	58.5	1.003	0.0031	0.0292	0.1571	0.1559		1.3492	3.1639	7.4157	
	30	29.88	55.6	1.003	0.0108	0.0956	0.4944	0.4789		1.3514	3.1791	7.4417	
	20	19.86	49.2	1.003	0.0432	0.3434	1.6393	1.4281		1.3796	3.3637	7.7231	
n = 5													
2	40	39.89	81.9	1.000	0.0013	0.0064	0.0147	0.0151	0.0048	1.0456	1.2435	1.6086	1.9129
	30	29.89	81.1	1.000	0.0043	0.0205	0.0464	0.0475	0.0152	1.0458	1.2444	1.6100	1.9134
	20	19.88	78.8	1.000	0.0146	0.0668	0.1479	0.1493	0.0479	1.0481	1.2547	1.6250	1.9190
	10	9.87	72.8	1.000	0.0530	0.2442	0.5609	0.5125	0.1508	1.0841	1.4097	1.8415	1.9965
5	40	39.89	81.3	1.000	0.0014	0.0087	0.0352	0.0621	0.0263	1.1110	1.6615	3.0107	4.5011
	30	29.89	79.4	1.000	0.0047	0.0285	0.1117	0.1937	0.0815	1.1115	1.6645	3.0180	4.5051
	20	19.88	74.7	1.000	0.0177	0.0996	0.3666	0.6033	0.2461	1.1177	1.7000	3.0991	4.5480
	10	9.86	64.3	1.001	0.0694	0.4982	2.4393	2.7803	0.7030	1.2694	2.6376	5.0967	5.3591
10	40	39.89	80.3	1.000	0.0014	0.0107	0.0669	0.1746	0.0911	1.1660	2.0739	4.8262	8.5792
	30	29.88	77.0	1.000	0.0051	0.0367	0.2142	0.5410	0.2778	1.1670	2.0813	4.8514	8.5976
	20	19.87	69.8	1.000	0.0221	0.1410	0.7449	1.7061	0.8080	1.1816	2.1793	5.1506	8.7972

TABLE 5.4

ELEMENT VALUES FOR CHEBYSHEV BRANCH-GUIDE COUPLER-TRANSFORMERS WITH A BANDWIDTH OF 1.2, RESISTANCE RATIO R, AND COUPLING C (IN DB) FOR N=3 TO 5 BRANCHES

R	C	B.E. C	DIR (DB)	VSWR	BRANCH GUIDE IMMITTANCES					MAIN LINE IMMITTANCES			
					a1	a2	a3	a4	a5	b1	b2	b3	b4
n = 3													
2	40	39.56	25.5	1.037	0.0063	0.0189	0.0173			1.2002	1.6667		
	30	29.54	24.9	1.037	0.0199	0.0597	0.0546			1.2009	1.6680		
	20	19.50	23.3	1.039	0.0650	0.1898	0.1727			1.2093	1.6817		
	10	9.36	19.0	1.085	0.2322	0.6940	0.5839			1.3223	1.8584		
5	40	39.55	25.1	1.096	0.0076	0.0466	0.0798			1.5304	3.2685		
	30	29.52	23.7	1.097	0.0249	0.1472	0.2509			1.5327	3.2758		
	20	19.44	20.3	1.104	0.0862	0.4762	0.7916			1.5591	3.3540		
	10	9.25	12.4	1.356	0.3910	2.6816	3.2079			2.1448	4.9183		
10	40	39.54	24.4	1.158	0.0088	0.0914	0.2472			1.8451	5.4243		
	30	29.49	21.9	1.159	0.0296	0.2891	0.7745			1.8506	5.4511		
	20	19.36	16.4	1.179	0.1115	0.9691	2.4717			1.9187	5.7465		
n = 4													
2	40	39.56	41.5	1.006	0.0029	0.0112	0.0186	0.0096		1.0982	1.4144	1.8214	
	30	29.55	40.8	1.006	0.0095	0.0356	0.0586	0.0304		1.0986	1.4157	1.8223	
	20	19.52	39.2	1.006	0.0314	0.1143	0.1852	0.0960		1.1032	1.4297	1.8321	
	10	9.32	33.5	1.014	0.1132	0.4233	0.6682	0.3111		1.1715	1.6290	1.9643	
5	40	39.56	41.0	1.015	0.0032	0.0194	0.0618	0.0493		1.2459	2.2366	4.0143	
	30	29.54	39.8	1.015	0.0106	0.0622	0.1943	0.1538		1.2469	2.2419	4.0206	
	20	19.48	35.6	1.016	0.0390	0.2085	0.6199	0.4729		1.2601	2.3016	4.0881	
	10	9.39	26.2	1.059	0.1631	1.1790	3.4215	1.5757		1.5673	3.7520	5.4008	
10	40	39.55	40.2	1.023	0.0033	0.0289	0.1497	0.1633		1.3754	3.1639	7.2750	
	30	29.52	37.2	1.023	0.0118	0.0946	0.4700	0.5037		1.3777	3.1791	7.3015	
	20	19.43	30.7	1.027	0.0488	0.3388	1.5479	1.5260		1.4094	3.3660	7.5927	
n = 5													
2	40	39.56	57.4	1.001	0.0014	0.0065	0.0143	0.0150	0.0052	1.0493	1.2476	1.6034	1.9062
	30	29.55	56.6	1.001	0.0047	0.0206	0.0452	0.0472	0.0164	1.0495	1.2485	1.6048	1.9068
	20	19.53	54.2	1.001	0.0160	0.0672	0.1434	0.1480	0.0519	1.0520	1.2590	1.6198	1.9128
	10	9.47	48.0	1.002	0.0594	0.2469	0.5398	0.5101	0.1671	1.0921	1.4193	1.8412	1.9979
5	40	39.56	56.8	1.002	0.0015	0.0088	0.0342	0.0610	0.0282	1.1204	1.6746	2.9871	4.4634
	30	29.54	54.9	1.002	0.0051	0.0289	0.1082	0.1902	0.0876	1.1209	1.6777	2.9943	4.4676
	20	19.50	50.1	1.003	0.0198	0.1013	0.3535	0.5921	0.2669	1.1279	1.7144	3.0756	4.5135
	10	9.45	39.3	1.010	0.0823	0.5214	2.3593	2.8060	0.8026	1.3054	2.7231	5.1632	5.4309
10	40	39.55	55.8	1.004	0.0015	0.0110	0.0646	0.1700	0.0976	1.1808	2.0985	4.7697	8.4715
	30	29.53	52.4	1.004	0.0056	0.0376	0.2064	0.5266	0.2986	1.1820	2.1062	4.7946	8.4908
	20	19.46	45.1	1.004	0.0251	0.1450	0.7135	1.6608	0.8805	1.1985	2.2084	5.0939	8.7045

TABLE 5.4 (Cont'd)

and the output conductance of the coupler-transformer is R mhos. The dual is true for the waveguide case.

Another interesting application of the asymmetrical coupler is in the design of hybrids, that is, 3 dB couplers. In Table 5.5 hybrid designs are presented, with the idea of maximizing bandwidth for a given (minimum) directivity specification D over the band. In this case the computer program was given a starting BW, from which it computed the minimum directivity D_1 over the band (after iterating to the correct midband coupling value). If D_1 did not agree with D (to 8 place accuracy), the program modified BW and cycled repeatedly until D_n did agree with D. In Table 5.5, the optimized bandwidth is listed as well as the maximum ripple VSWR and the $\pm\Delta C$ variation in coupling, i.e., the midband coupling is $3.01+\Delta C$ dB, and the band edge coupling is $3.01-\Delta C$ dB. It is hoped that these designs will prove useful in stripline work. Accordingly, the ratio of element values for any given design in Table 5.5 does not exceed 8.5. All hybrid designs with five or more branches have been found to exceed this limit. An interesting property to observe in Table 5.5 is that for a fixed directivity, bandwidth <u>increases</u> as R is reduced, although the element value ratio increases. It was also found that as R is increased beyond unity the bandwidth <u>decreases</u>, with the element value ratio again increasing.

ELEMENT VALUES FOR CHEBYSHEV BRANCH-GUIDE 3 DB COUPLER-TRANSFORMERS WITH A RESISTANCE RATIO R AND DIRECTIVITY D (IN DB) FOR THREE AND FOUR BRANCH DESIGNS

D	R	$\frac{\lambda g_0}{\lambda g_2}$	$\pm\Delta C$	VSWR	BRANCH GUIDE IMMITTANCES				MAIN LINE IMMITTANCES		
					a1	a2	a3	a4	b1	b2	b3
n = 3											
20	1.00	1.179	.283	1.154	0.4540	1.1231	0.4540		1.3729	1.3729	
	0.90	1.186	.302	1.133	0.4277	0.9189	0.3721		1.2767	1.2091	
	0.80	1.193	.320	1.113	0.4018	0.7491	0.2994		1.1885	1.0609	
	0.70	1.200	.340	1.093	0.3758	0.6055	0.2350		1.1057	0.9244	
	0.60	1.208	.362	1.072	0.3494	0.4823	0.1783		1.0260	0.7967	
	0.50	1.216	.384	1.052	0.3220	0.3753	0.1291		0.9471	0.6751	
25	1.00	1.136	.162	1.083	0.4363	1.2105	0.4363		1.3734	1.3734	
	0.90	1.141	.172	1.072	0.4121	0.9921	0.3579		1.2787	1.2094	
	0.80	1.146	.183	1.061	0.3881	0.8102	0.2881		1.1917	1.0605	
	0.70	1.152	.194	1.049	0.3639	0.6560	0.2261		1.1099	0.9233	
	0.60	1.158	.207	1.037	0.3392	0.5236	0.1714		1.0312	0.7947	
	0.50	1.164	.220	1.025	0.3133	0.4084	0.1239		0.9533	0.6723	
30	1.00	1.103	.092	1.046	0.4266	1.2642	0.4266		1.3743	1.3743	
	0.90	1.106	.098	1.040	0.4035	1.0366	0.3501		1.2802	1.2098	
	0.80	1.110	.104	1.033	0.3805	0.8470	0.2818		1.1937	1.0605	
	0.70	1.115	.110	1.027	0.3573	0.6863	0.2211		1.1124	0.9227	
	0.60	1.119	.117	1.020	0.3334	0.5482	0.1676		1.0342	0.7936	
	0.50	1.124	.124	1.013	0.3083	0.4281	0.1210		0.9569	0.6707	
n = 4											
20	1.00	1.309	.704	1.159	0.2652	0.6873	0.6873	0.2652	1.2654	1.5239	1.2654
	0.95	1.314	.729	1.151	0.2600	0.6329	0.6130	0.2424	1.2334	1.4336	1.1881
	0.90	1.319	.754	1.142	0.2546	0.5829	0.5461	0.2206	1.2027	1.3497	1.1143
	0.85	1.323	.780	1.134	0.2492	0.5368	0.4856	0.1997	1.1733	1.2714	1.0435
	0.80	1.328	.805	1.126	0.2436	0.4940	0.4307	0.1797	1.1448	1.1979	0.9755
	0.75	1.333	.832	1.118	0.2378	0.4541	0.3808	0.1607	1.1170	1.1283	0.9098
	0.70	1.338	.858	1.110	0.2319	0.4166	0.3353	0.1426	1.0898	1.0621	0.8462
	0.65	1.344	.886	1.101	0.2259	0.3813	0.2936	0.1254	1.0629	0.9987	0.7844
25	1.00	1.259	.494	1.086	0.2391	0.7631	0.7631	0.2391	1.2610	1.5572	1.2610
	0.95	1.263	.511	1.082	0.2349	0.7037	0.6808	0.2187	1.2302	1.4631	1.1838
	0.90	1.267	.528	1.077	0.2305	0.6491	0.6067	0.1991	1.2007	1.3758	1.1100
	0.85	1.271	.544	1.072	0.2260	0.5987	0.5397	0.1803	1.1724	1.2945	1.0393
	0.80	1.275	.562	1.068	0.2213	0.5519	0.4789	0.1622	1.1451	1.2181	0.9711
	0.75	1.279	.579	1.063	0.2165	0.5082	0.4235	0.1450	1.1185	1.1461	0.9052
	0.70	1.284	.597	1.058	0.2115	0.4672	0.3730	0.1286	1.0924	1.0776	0.8414
30	1.00	1.216	.342	1.047	0.2224	0.8179	0.8179	0.2224	1.2578	1.5828	1.2578
	0.95	1.219	.353	1.045	0.2188	0.7546	0.7296	0.2035	1.2277	1.4856	1.1807
	0.90	1.222	.364	1.042	0.2150	0.6966	0.6502	0.1853	1.1991	1.3957	1.1069
	0.85	1.226	.376	1.039	0.2110	0.6430	0.5783	0.1678	1.1715	1.3119	1.0361
	0.80	1.229	.387	1.037	0.2069	0.5933	0.5131	0.1510	1.1449	1.2334	0.9679
	0.75	1.233	.399	1.034	0.2026	0.5469	0.4538	0.1349	1.1191	1.1594	0.9019

TABLE 5.5

A practical use for Table 5.5 is in the design of hybrids for balanced transistor microwave amplifiers[14]. The amplifier is designed to give the same amplification as one of the transistors by itself. There are practical advantages to using the circuit in Fig.5.13 instead of a single ended design, however. At present, manufacturing techniques for microwave transistors yield devices having substantial performance differences, that is, a high degree of repeatability has not yet been achieved. This is a serious drawback in single ended designs; each amplifier must be "custom made" to obtain the best performance from the transistor chosen for that amplifier. In the balanced amplifier, however, it is only necessary to use a pair of transistors having approximately the same electrical performance. Therefore nearly all of the microwave transistors from a batch production run may be paired and then used in balanced amplifiers. It may also be shown[14] that the balanced amplifier has a 3 dB higher gain compression compared with the single ended design and a 9 dB improvement in third order intermodulation. Furthermore, the couplers in Fig.5.13 improve the input and output match to the transistors. For example, if the transistors each have an input VSWR of 2.0, then the balanced amplifier (using symmetric hybrids) can be designed to have a VSWR of 1.07 over the band of operation[14].

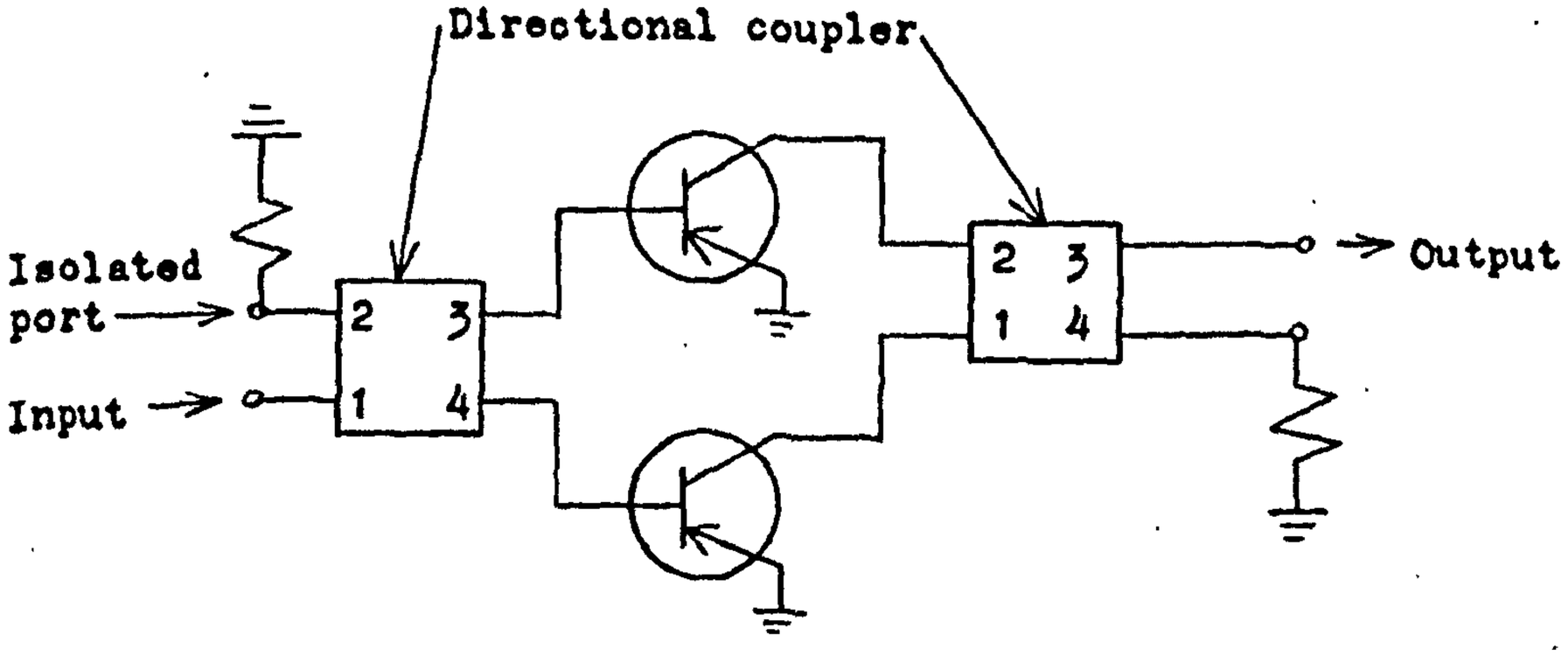

Fig. 5.13. Schematic diagram of a one-stage balanced transistor amplifier.

A further improvement in the design of this structure should be possible by using the asymmetric coupler-transformers described above, for the following reasons:

1) The asymmetric hybrid has a larger bandwidth than the corresponding symmetric one.
2) The asymmetric hybrid, acting as a transformer, provides a better match between the input (or output) line and the transistors.

Thus the asymmetric coupler-transformer is tailored to this type of application.

5.5 Experimental Results.

Several symmetric designs for Butterworth and Chebyshev characteristics have been constructed both in X-band waveguide and in stripline. Due account was taken of corrections to be applied to the branch and main arm lengths and impedances due to discontinuities as explained in Reference (15), which also gives an example of the complete design procedure which was employed. In the waveguide designs, each coupler was constructed in the form of a metal block with slots forming the branch guides. The block was inserted between two waveguides having a section of one side of their broad walls, equal to the length of the block, removed. A photograph of this construction arrangement is shown in Fig.5.14. The arrangement suffered from practical limitations, e.g., the

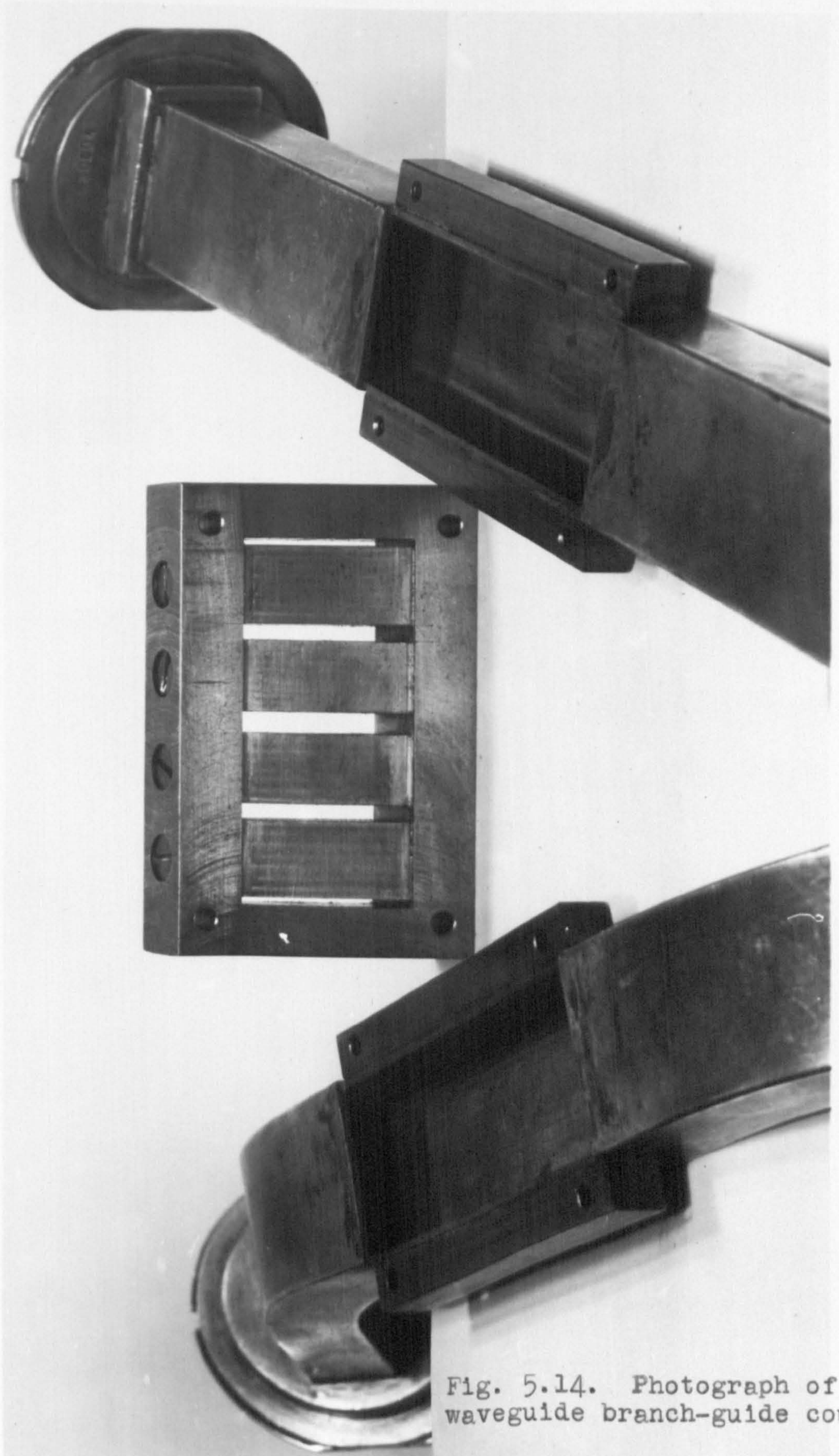

Fig. 5.14. Photograph of a waveguide branch-guide coupler.

difficulty of obtaining good contacts, and the residual VSWR measured using a block without slots was approximately 1.04. Results for couplers constructed by milled block or similar manufacturing techniques might be expected to be somewhat superior to those presented here.

A sketch of a 3-branch Butterworth 10 dB waveguide coupler is given in Fig.5.15, and the measured results are shown in comparison with the theoretical curves in Fig.5.16. Table 5.1 shows that the directivity falls to 20 dB for BW = 1.17, where the band-edge coupling is 9.58 dB and the VSWR is 1.03. With a midband frequency of 9.5 GH_Z, the band-edge frequencies are approximately 8.7 and 10.4 GH_Z, as indicated in Fig.5.16. The results show good agreement with theory within the practical limitations. The error of 0.4 dB in midband coupling was not repeated in other designs, e.g., a 4-branch 6 dB coupler for Butterworth response (Fig.5.17) gave almost perfect agreement between measured and theoretical coupling, and good agreement for directivity and VSWR (Fig.5.18.) The worst deviation from theory occurs at the high-frequency end of the band where the ratio of the waveguide dimensions to the guide wavelength is becoming large. Deviations caused by the use of a narrowband approximation for the equivalent circuit of the T-junction discontinuities may become considerable here.

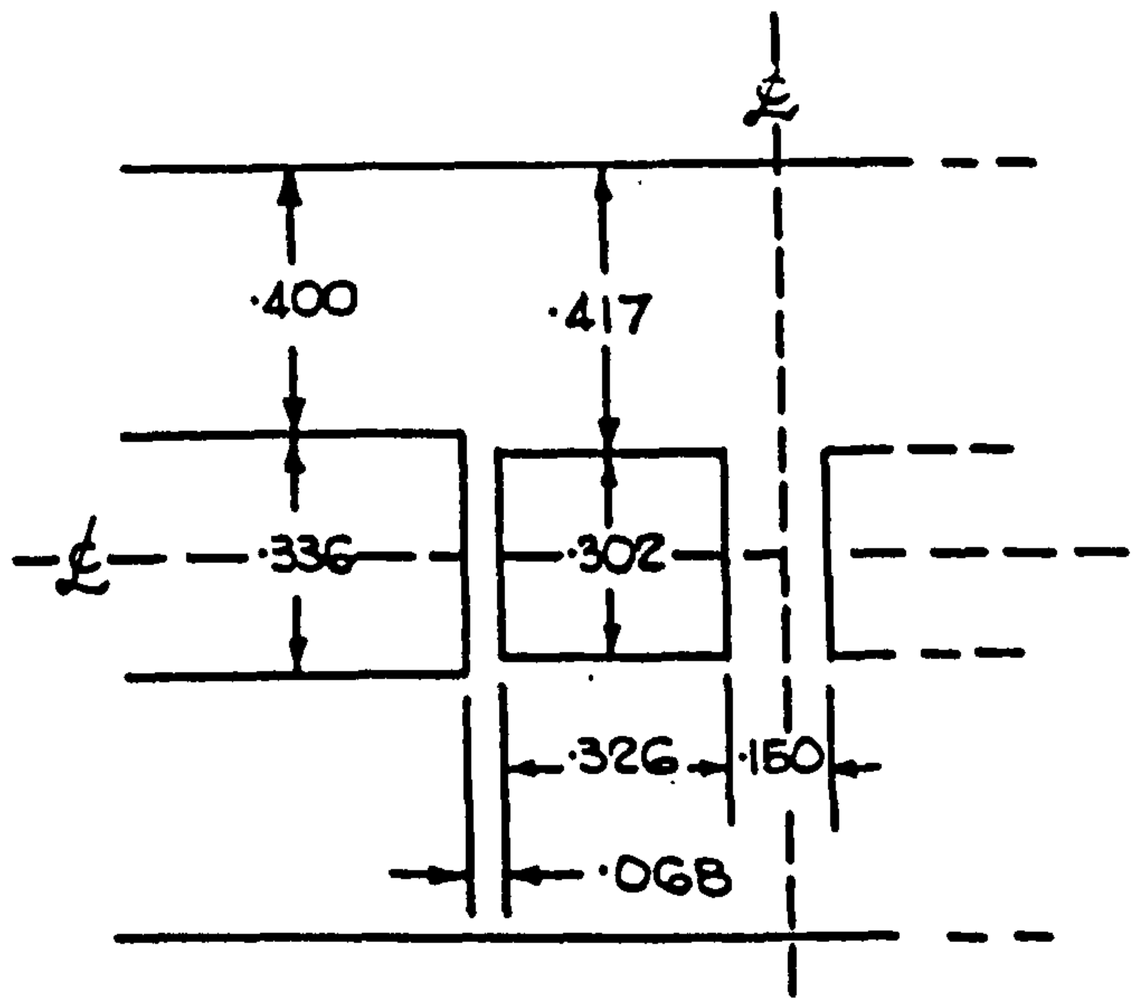

Fig. 5.15. Cross section of Butterworth 3-branch 10 dB coupler in WR90 (WG16) waveguide.

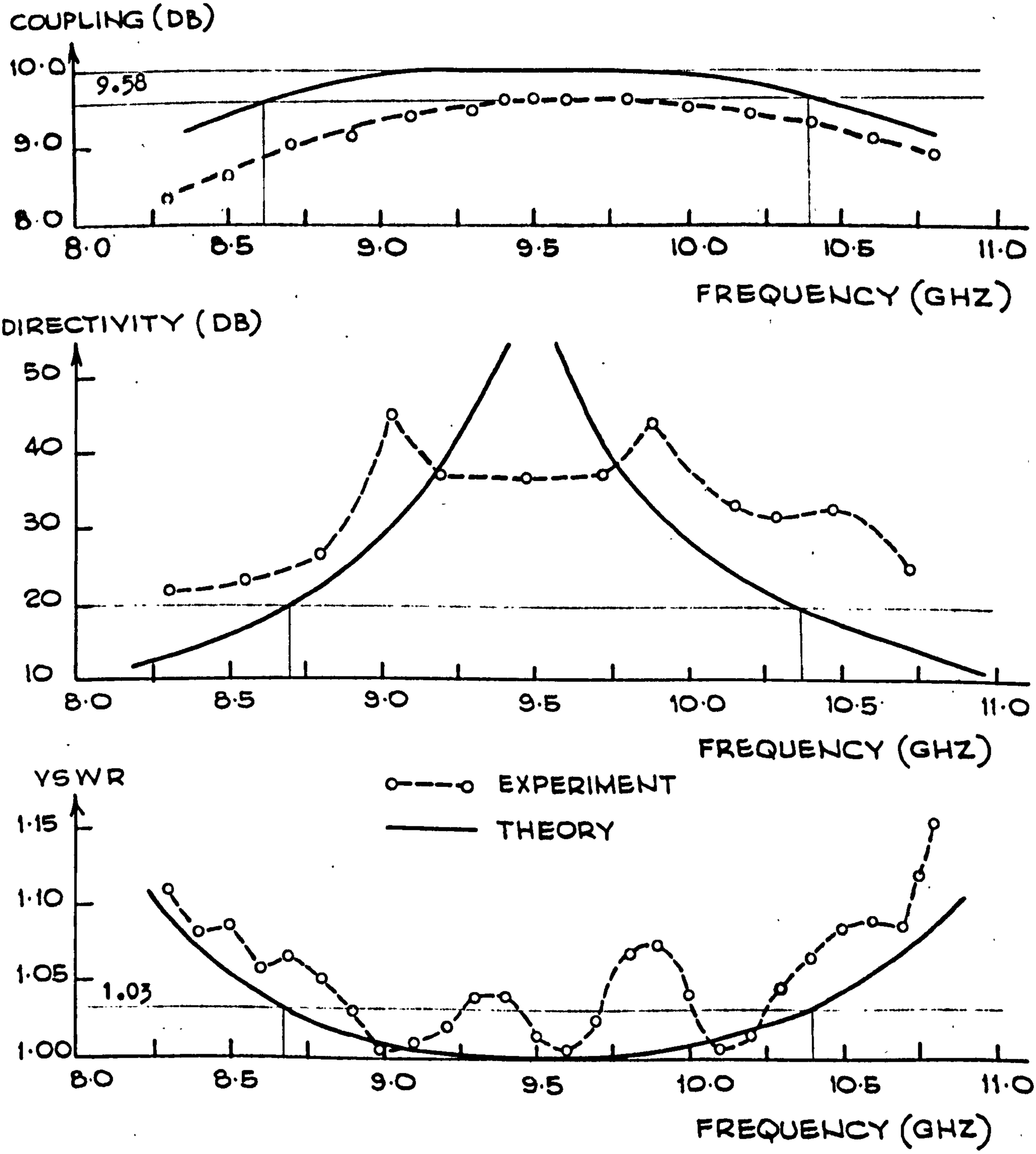

Fig. 5.16. Theoretical curves and experimental results for the coupler of Fig. 5.15.

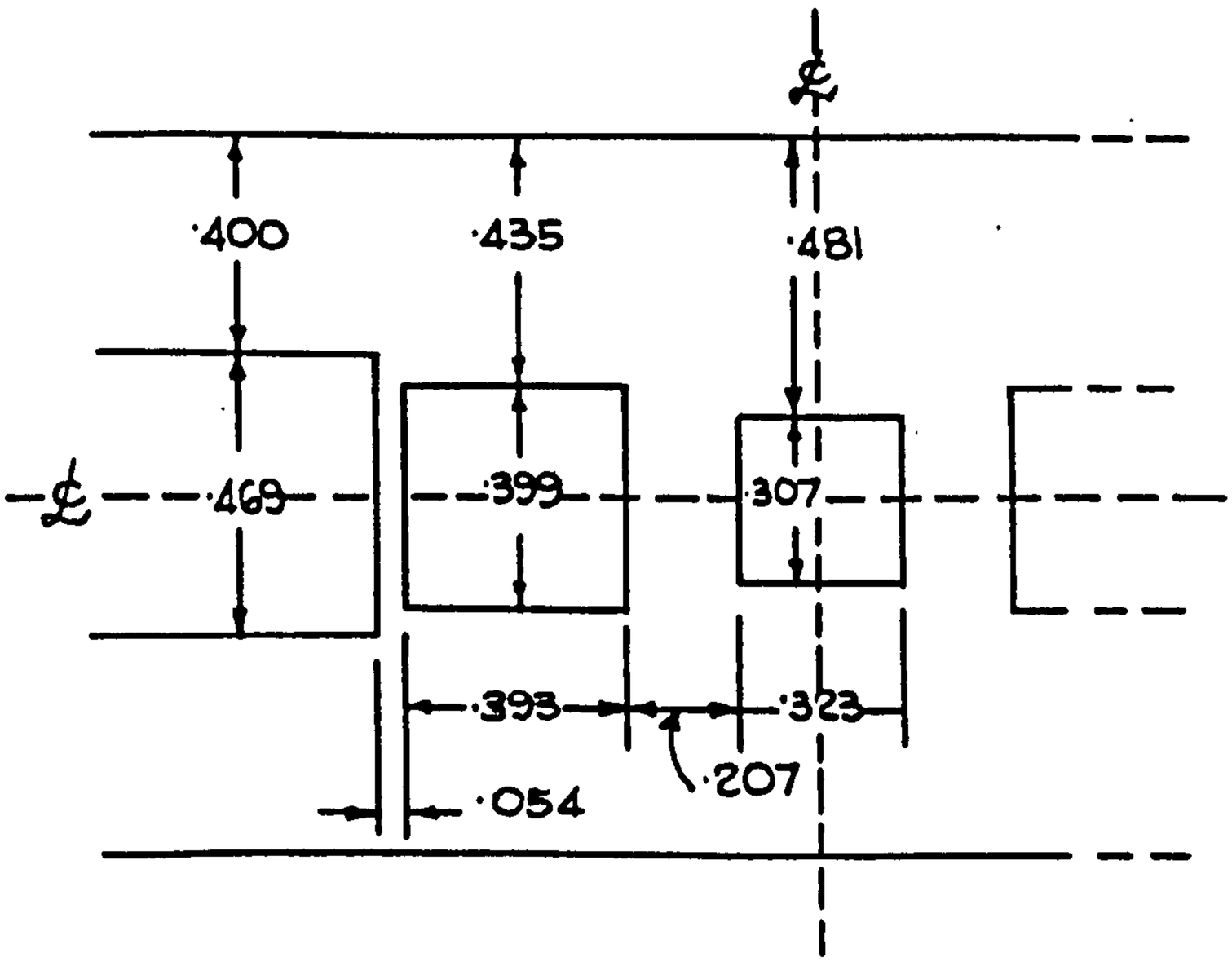

Fig. 5.17. Cross section of Butterworth 4-branch 6 dB coupler in WR90 (WG16) waveguide.

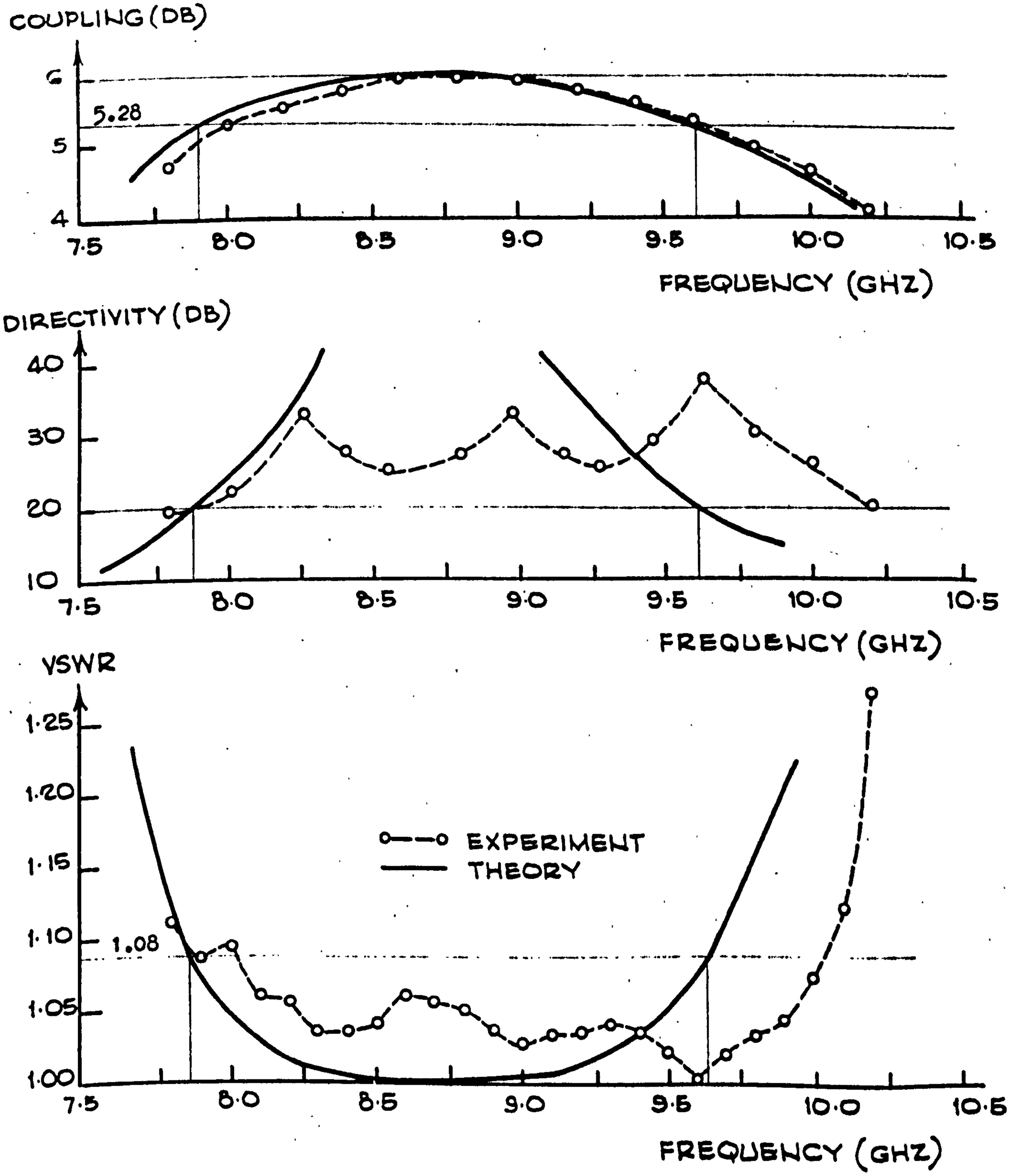

Fig. 5.18. Theoretical curves and experimental results for the coupler of Fig. 5.17.

A 3-branch coupler constructed in stripline for a Butterworth characteristic having 3 dB midband coupling is shown in Fig.5.19. A photograph of this stripline coupler (with the top ground plane removed) is shown in Fig.5.20. Reference (16) explains in detail the discontinuity corrections that should be used in this design procedure. Originally designed for a midband frequency of 1.5 GH_Z, it actually centered at 1.525 GH_Z, ~~and the theoretical curves of Fig.5.21 are drawn accordingly.~~ A similar coupler designed for Chebyshev performance also gave excellent agreement between theory and experiment for VSWR, directivity, and midband coupling, but showed similar coupling deviations at the band edges. In these designs there is a large difference in width between the inner and outer branch lines, and the length correction is different from the two cases. However, a mean length correction is taken in practice. This and other factors could be responsible for deviations from strict theoretical performances at the band edges.

An example of a broadband 5-branch waveguide coupler designed for Chebyshev VSWR and directivity characteristics is shown in Figs.5.22 and 5.23. Here the midband coupling is 8 dB, and for BW = 1.4 Table 5.2 gives a directivity ripple of 24.2 dB, a VSWR ripple level of 1.039, and a coupling which drops to 5.74 dB at the band edges. The slightly nonequal ripple performance is clearly indicated. The experimental results agree quite closely with the theory.

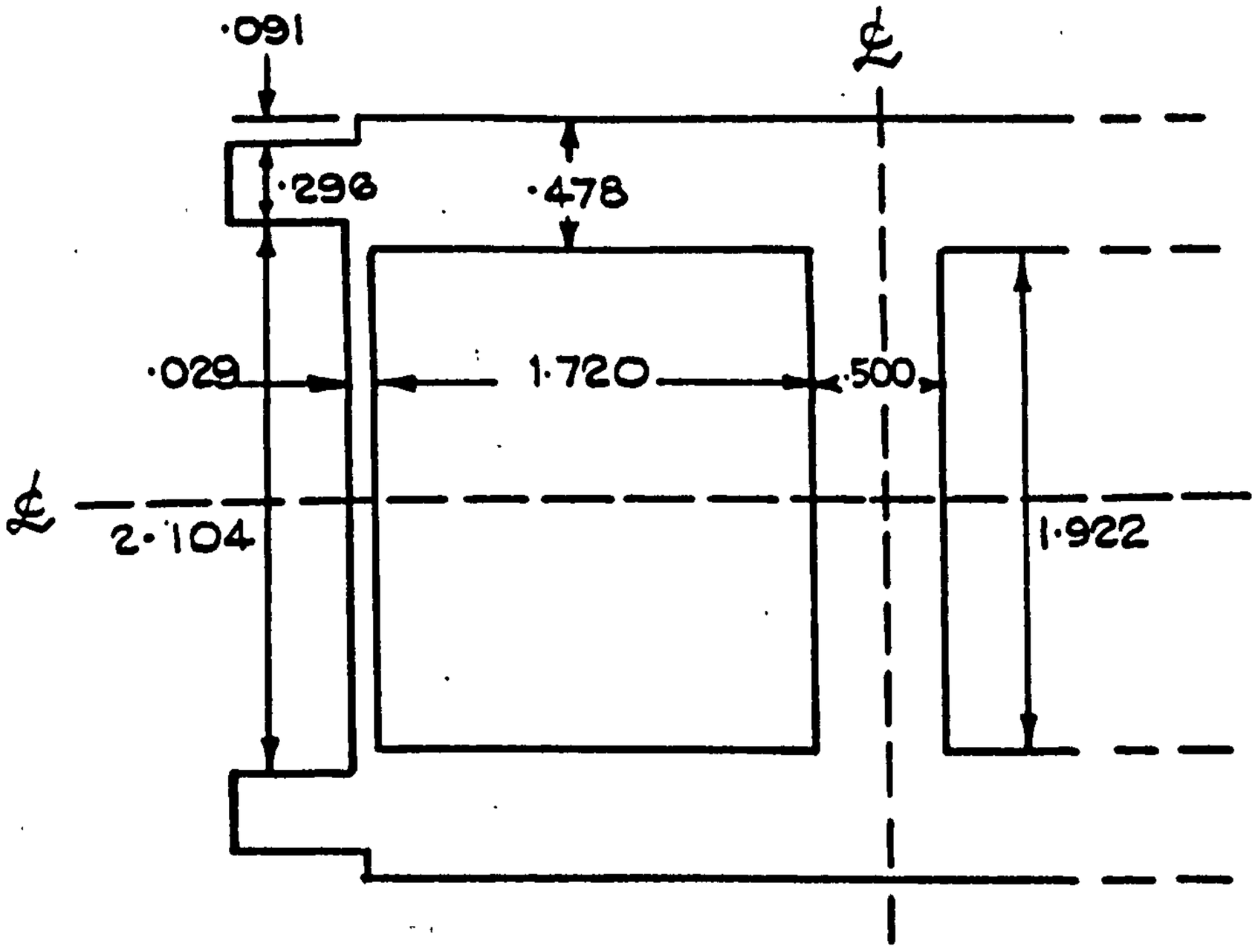

Fig. 5.19. Plan view of Butterworth 3-branch 3 dB coupler in airspaced stripline, with ground-plane spacing 0.3125 inch and strip thickness 0.0625 inch.

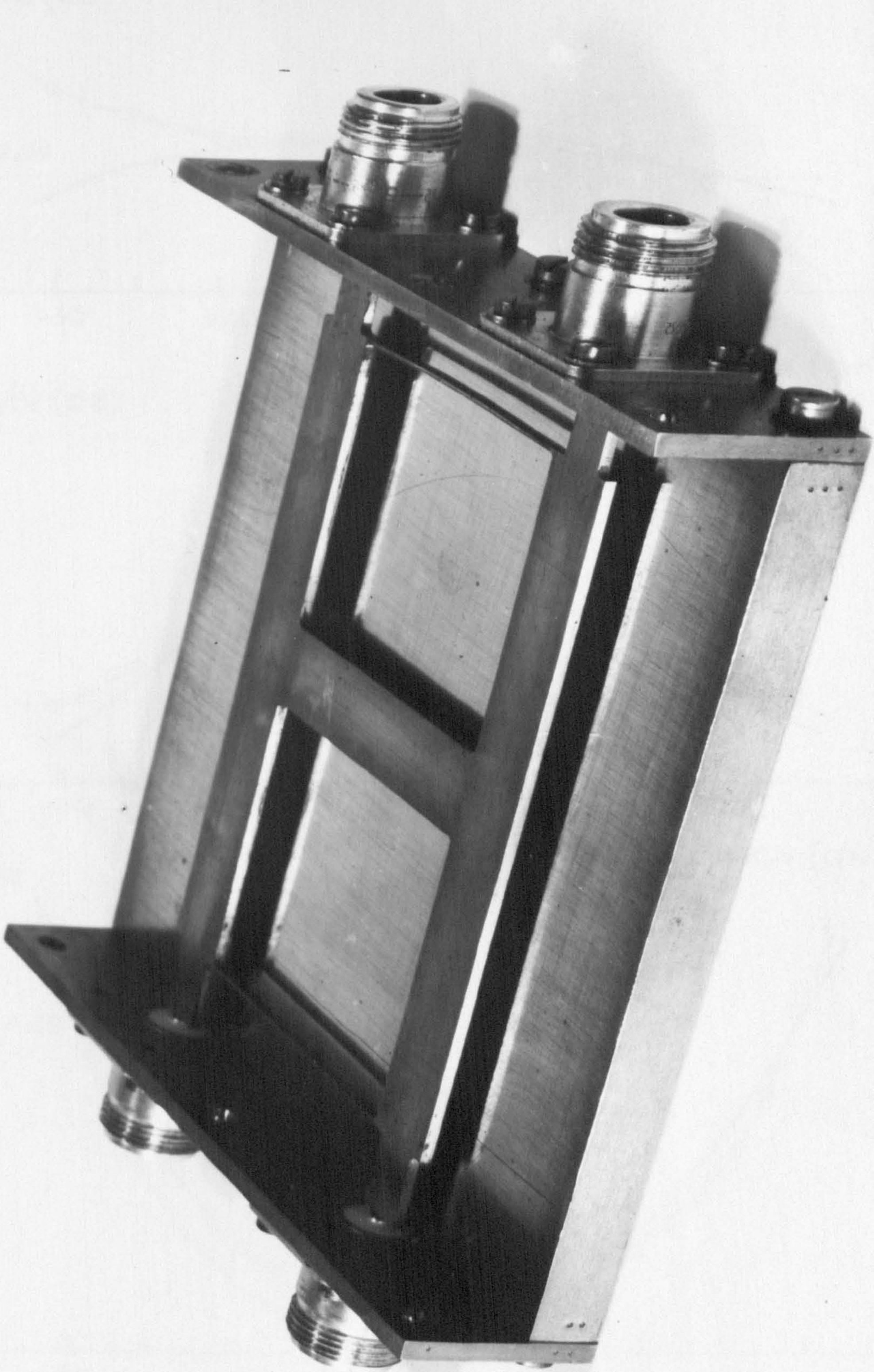

Fig. 5.20. Photograph of a stripline branch-line coupler.

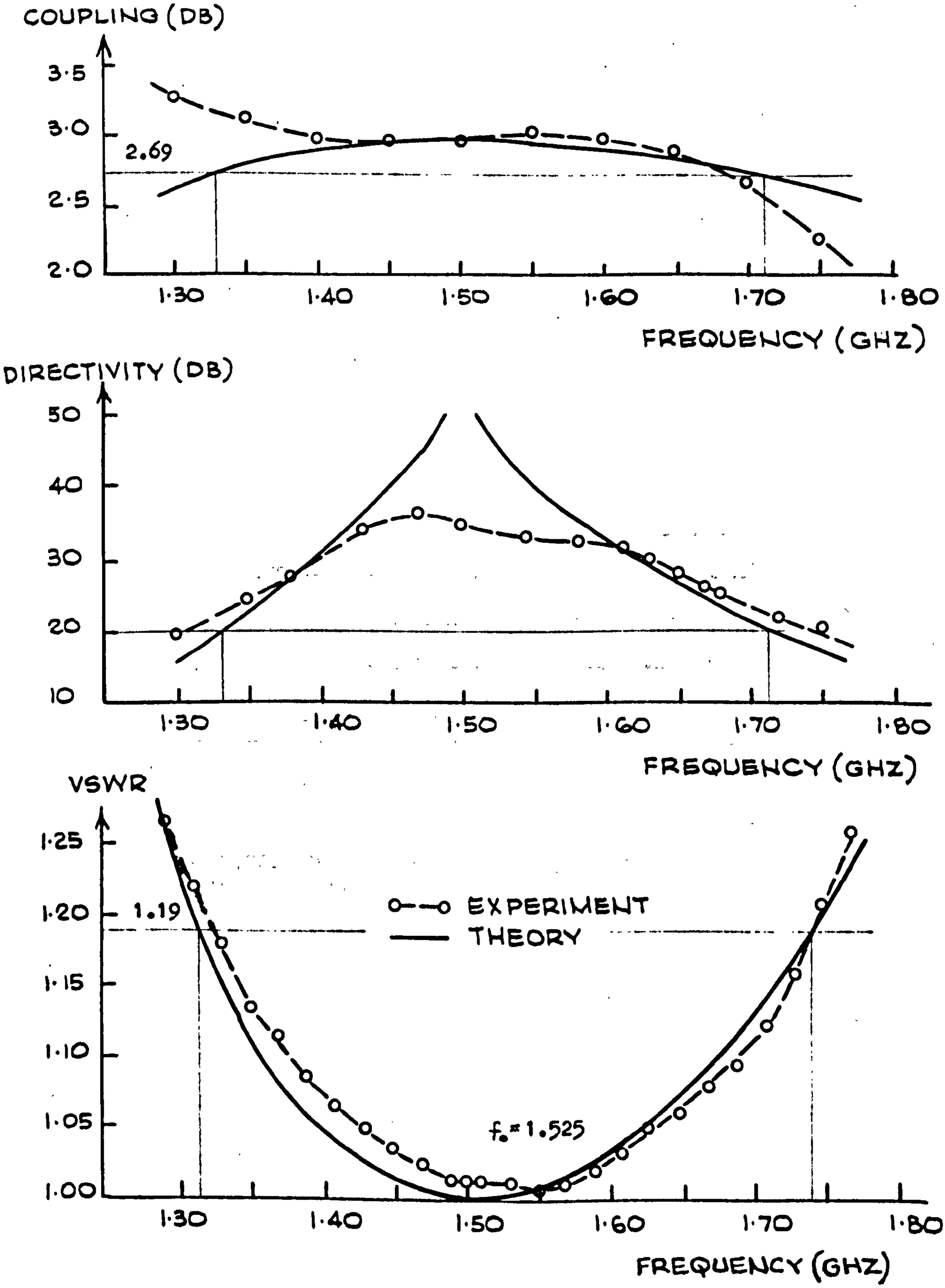

Fig. 5.21. Theoretical curves and experimental results for the coupler of Fig. 5.19.

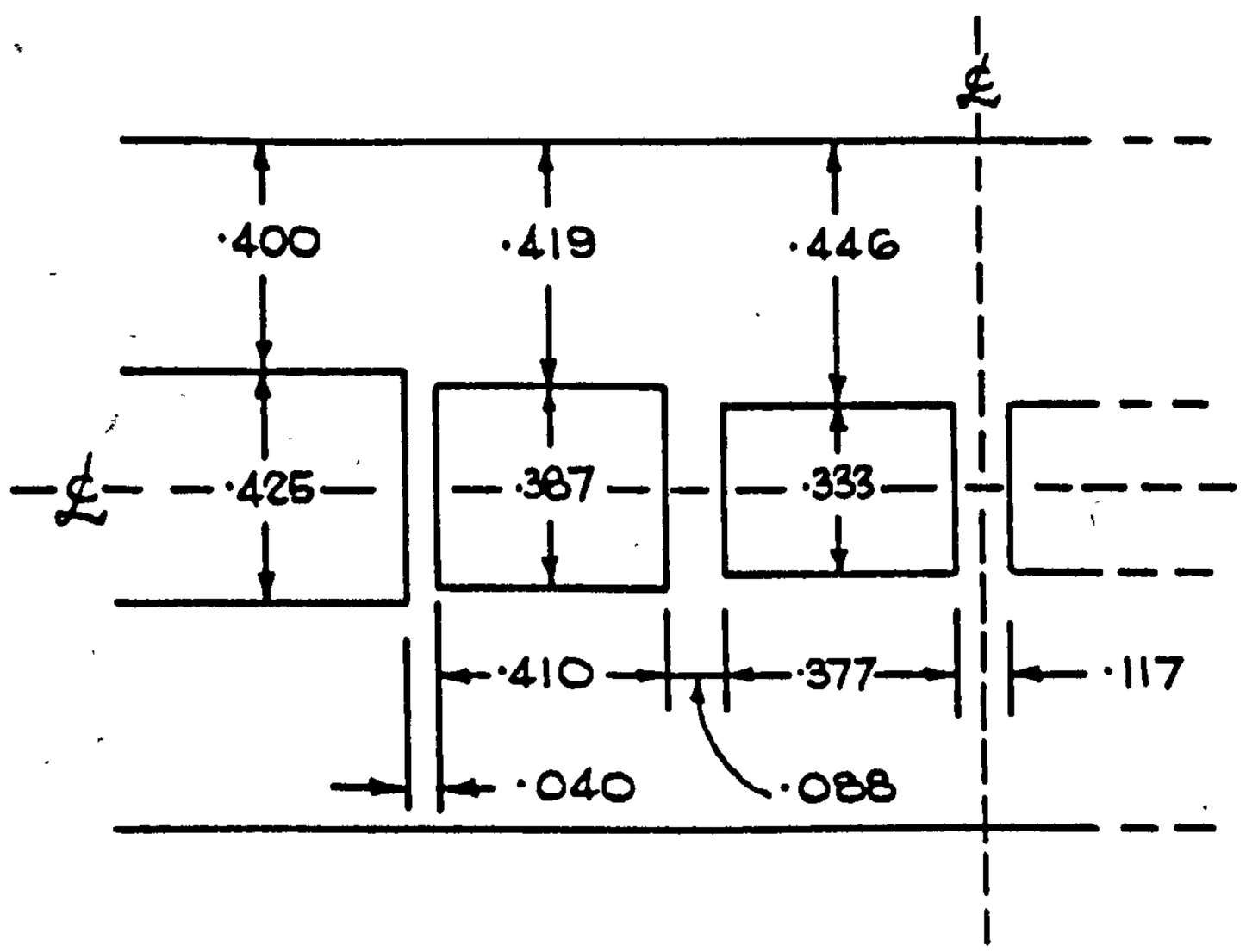

Fig. 5.22. Cross section of Chebyshev 5-branch 8 dB coupler in WR90 (WG16) waveguide.

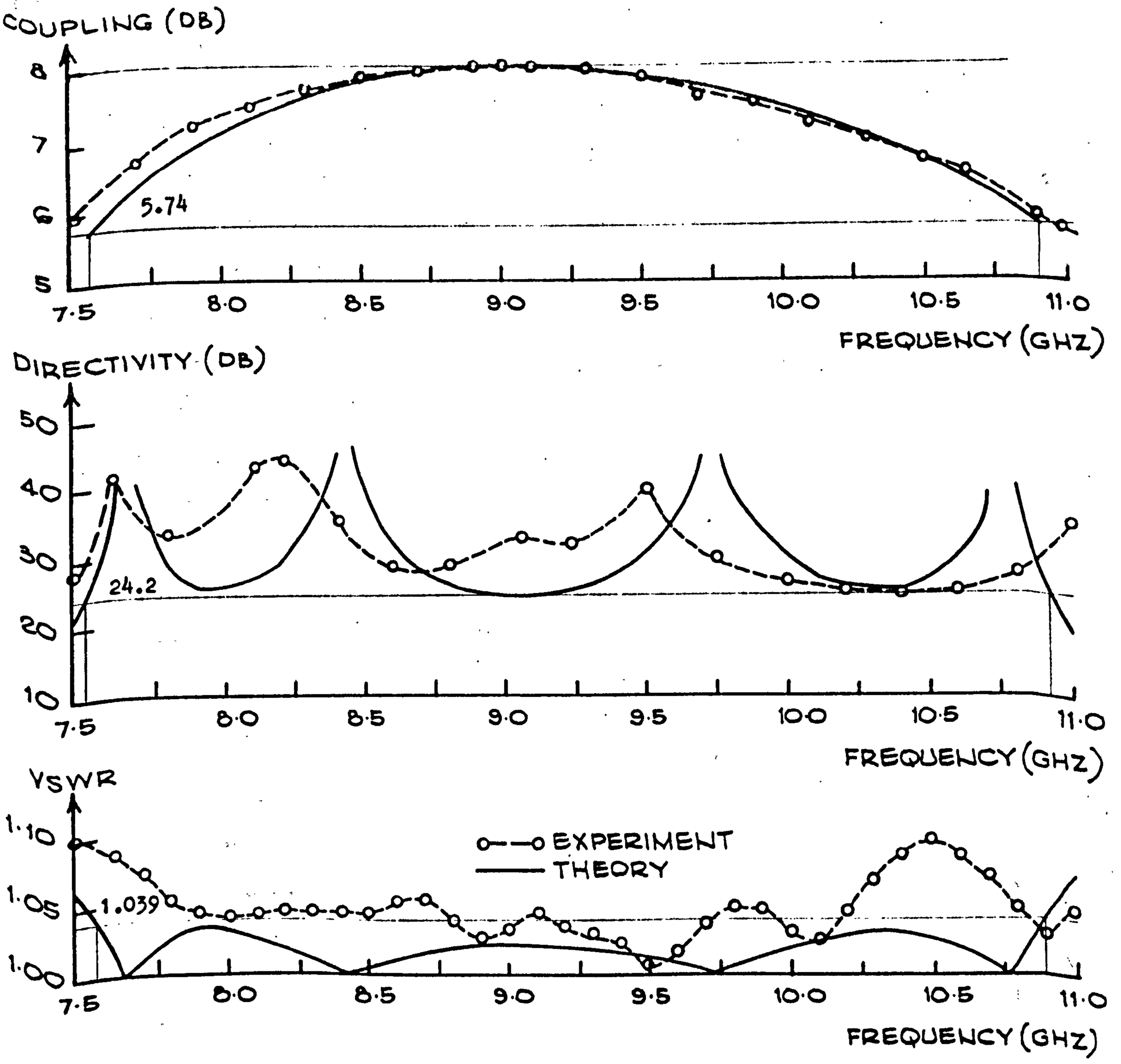

Fig. 5.23. Theoretical curves and experimental results for the coupler of Fig. 5.22.

5.6 Concluding Remarks.

One major restriction that was made in the approximation part of the present design theory was that the functions Γ_e/T_e and Γ_o/T_o had as many common zeros as possible on the imaginary axis of the t-plane. This had the effect of giving the coupler perfect match and infinite directivity at these zero points. As a result, the function $F = \Gamma_e/T_e - \Gamma_o/T_o$ was made equiripple over the passband rather than Γ_e/T_e itself. To see what would happen when Γ_e/T_e was itself equiripple, the following numerical experiment was performed. A three branch symmetrical coupler with a bandwidth BW = 1.1 was used for both prototypes. The Chebyshev design using equiripple F yielded $\Gamma_e/T_e = (1.00t^5 + 2.05t^3 + 1.00t)/(1-t^2)^2$, having the values:

Frequency point	t	Γ_e/T_e
Lower band edge	j.854	.0209
Midband	j1.00	-.0250
Upper band edge	j1.17	.0287

It is seen that Γ_e/T_e is not equiripple over the band. Next, Γ_e/T_e was made equiripple. For this case it was calculated (from an iteration process) that $\Gamma_e'/T_e' = (1.000t^5 + 2.075t^3 + 1.025t)/(1-t^2)^2$. This function has zeros at $t = \pm j.9009$ and $t = \pm j1.124$. Now $.9009^{-1} = 1.110$ and $1.124^{-1} = .8898$, and therefore Γ_o'/T_o' will not have common zeros with Γ_e'/T_e', i.e.,

this design will not have perfect match or perfect isolation at any frequency. The comparison between the two designs is summarized as follows:

Midband Coupling	Type	B.E. COUP	DIR (Min)	VSWR (Max)	a 1	a 2	b 1
20 dB	old	19.88	36.82	1.001	.0509	.0993	1.0039
"	new	19.88	36.87	1.000	.0508	.0995	1.0047
10 dB	old	9.858	34.37	1.005	.1656	.3385	1.0451
"	new	9.859	34.40	1.004	.1655	.3407	1.0486
3 dB	old	2.826	30.41	1.045	.4330	1.3103	1.3899
"	new	2.829	30.35	1.046	.4332	1.3554	1.4138

In this chart the "old" type refers to the coupler designed from the F function, whereas the "new" type refers to the case where Γ_e/T_e was made equiripple. It is seen that there is very little difference between these two designs. Mathematically speaking, however, much more work was done in adjusting roots or coefficients until Γ'_e/T'_e was equiripple (as no closed form solution is known for this problem) than simply in using the specification function Eq.(5.60), which is given in closed form. For ease of computation then, Eq.(5.60) was used in designing Chebyshev couplers.

For both the Chebyshev and Butterworth couplers the coupling shows monotonic variation with frequency (with the coupling becoming tighter away from center frequency), in

common with the previous theories. It was found that it was possible to get some ripple in the coupling characteristic with extreme input specifications, i.e., a directivity of 5-6 dB, BW= 1.4, and n=3. For this same set of conditions it was found that some of the branch lines were calculated to have negative values. All reasonable input specifications (such as appear in the Tables) resulted in the coupling vs. frequency curve having a parabolic shape. In general it was observed that to have the coupling as flat as possible over the band it was necessary to use a Chebyshev design with as large a bandwidth as possible. Recall from the design curves (Figs.5.8 to 5.11) that as bandwidth becomes larger so does the ripple VSWR, with the minimum directivity falling in value. To achieve as flat a coupling as possible therefore, the bandwidth should be increased until either the VSWR or directivity reaches the allowable design specification limit.

In many synthesis techniques there is no control over the resulting element values; such is the case also with the new coupler design theory. In fact with this theory there is no assurance that the branch-line element values will even turn out to be positive, due to the structural realization demanded. A numerical experiment was performed to see if, by changing the structure slightly, a lower element value ratio could be achieved. It was decided to relax the double-length re-

quirement for the main line unit elements, and allow them to become two single-length unit elements of different impedances. A maximally flat three branch symmetrical design was used. It was arranged that the first branch line stub was increased in value, while keeping the even mode Γ/T characteristic maximally flat (two zeros at midband). This did result in the main line unit elements becoming stepped, and it also resulted in a lower element value ratio. Upon analyzing the odd mode Γ/T, however, it was found that the quartet of zeros of Γ_o were now at $t = \pm.447 \pm j1.169$ instead of at $\pm j1$ (double zeros). The VSWR and isolation performance of this design around midband was clearly inferior to the original maximally flat design because of the relatively large value of Γ_o at these frequencies. Thus, the element value ratio cannot be improved in this manner without degrading design performance.

It may be shown that waveguide realizations of Tables 5.1 and 5.2 can only be made for couplings looser than 5 or 6 dB. This is because, for tighter couplers, the branch guides become very large in size with the result that the metal separating two adjacent branch guides becomes a narrow post. Then there is no longer a branch-guide coupler but a waveguide structure which will have a complicated field pattern. Similarly, stripline couplers with a looser coupling than 5 or 6 dB are unrealizable because of the range of element values. In previous designs of waveguide branch-guide couplers, it was

possible to arrive at 3 dB designs. With the new theory, however, the only way to arrive at a 3 dB waveguide coupler is to cascade two 8.34 dB coupler designs together. With this technique, more branches may be necessary than would be required in using an older design technique! It is obvious then that for some input specifications there will be a "tradeoff" between optimum performance and realizability. An important unsolved problem in branch-guide coupler design is to find a method of degrading the frequency performance in such a way as to lower the element value ratio until a waveguide (or stripline) design is realizable. In this context the performance data of couplers described herein may be used as a standard in order to measure the degradation suffered in achieving realizability.

The new synthesis technique for branch-guide directional couplers, in the many cases where a structure is directly realizable, gives superior results compared with previous approximate methods for Butterworth and Chebyshev VSWR and directivity characteristics. The results for practical branch-guide couplers designed using the new theory give good agreement with the computed results, and the design of couplers having a bandwidth greater than one octave appears to be feasible. The design procedure is simplified by the publication of tables of branch guide and main line immit-

tance values for both the symmetric and asymmetric case, which cover most specifications of practical interest. The asymmetric case represents a new structure, which, by combining the properties of a coupler and impedance transformer, will result in a much more economical structure in certain applications.

Branch-guide couplers in stripline are widely used in microwave miniature circuits, and the broadband designs given here could be utilized for such applications.

Chapter 5 REFERENCES

1. Young, L.: "Advances in Microwaves, Vol. 1". Academic Press, 1966, pp. 118-126.

2. Van Valkenburg, M.E.: "Introduction to Modern Network Synthesis". Wiley, 1960, pp. 424-430.

3. Young, L.: "Synchronous branch-guide directional couplers for low and high power applications", IRE Trans. MTT, Vol. 10, Nov. 1962, pp. 459-475.

4. Young, L.: "Advances in Microwaves, Vol. 1". Academic Press, 1966, pp. 155-161.

5. Lomer, P.D. and Crompton, J.W.: "A new form of hybrid junction for microwave frequencies." Proc. Inst. Elec. Engrs. (London), Vol. B104, 1957, pp. 261-264.

6. Levy R.: "A guide to the practical application of Chebyshev functions to the design of microwave components. Proc. Inst. Elec. Engrs. (London), Vol. C106, 1959, pp. 193-199.

7. Patterson, K.G.: "A method for accurate design of a broadband multibranch waveguide coupler." IRE, Trans. MTT, Vol. 7, Oct. 1959, pp. 466-473.

8. Levy, R.: "Tables of element values for the distributed low-pass prototype filter." IEEE, Trans. MTT, Vol. 13, 1965, pp. 514-536.

9. Levy,R. and Lind, L.F.: "Synthesis of symmetrical branch-guide directional couplers," IEEE, Trans. MTT, Vol. 16, Feb. 1968, pp. 80-89.

10. Lind, L.F.: "Synthesis of asymmetrical branch-guide directional coupler-impedance transformers." (Accepted for publication in IEEE Trans. Microwave Theory and Techniques).

11. Riblet, H.J.: "The application of a new class of equal-ripple functions to some familiar transmission-line problems," IEEE Trans. MTT, Vol. MTT-12, July, 1964, pp. 415-421.

12. Carlin, H.J. and Kohler, W.: "Direct synthesis of band-pass transmission line structures," IEEE Trans. MTT, Vol. MTT-13, May, 1965, pp. 283-297.

13. Tuttle, D.F.: "Network Synthesis, Vol. 1." Wiley, 1958, Appendix B.

14. Kurokawa, K.: "Design theory of balanced transistor amplifiers," Bell System Technical Journal, Vol. 44, No. 8, October, 1965, pp. 1675-1698.

15. Matthaei, Young, and Jones: "Microwave Filters,Impedance-Matching Networks, and Coupling Structures." McGraw-Hill, 1964, pp. 835-840.

16. Matthaei, Young, and Jones: "Microwave Filters, Impedance-Matching Networks, and Coupling Structures." McGraw-Hill, 1964, pp. 208-211.

Chapter 6

Conclusions and Possible Developments

In this thesis the following two problems have been investigated:

(1) Synthesis of equally terminated, lumped and distributed filters containing an even number of elements.

(2) Synthesis of symmetrical and asymmetrical branch-guide directional couplers.

The solution of (1) was found to be straightforward once the insertion loss has been specified. The standard Darlington synthesis technique is employed, which leads to a unique solution (since all of the insertion loss zeros are on the frequency axis). It appears likely, however, that there may exist closed formulae for the element values which are direct functions of the input specifications (number of sections and passband ripple level) for the lumped filters. Formulae of this sort have already been determined for lumped filters having a "pure" Chebyshev insertion loss description. The new formulae, if they exist, would simplify design since the Darlington synthesis procedure could then be eliminated. Discovery of these formulae would be a very useful and practical project.

The solution of (2) has also been accomplished for the case where the directivity and VSWR of the coupler are specified. It is found that this new technique gives superior results compared with previous approximate methods both for

Butterworth and Chebyshev specifications. The coupling shows monotonic variation with frequency, in common with previous theories. The coupling variation is an output of the design procedure, rather than an input. Computer results show that when the coupling is made very flat or with ripple over the passband the coupler will have poor directivity and high VSWR. An attempt could be made, however, to arrive at a specification function for the coupler which contains coupling information as well as VSWR and directivity information. Then the "tradeoff" between these three parameters would be brought to light.

Another difficulty with the new design procedure is that one has no control over the element values which will appear at the output of the procedure. In fact it has already been seen that due to the structural form demanded, negative element values might occur. In practice it has been found however that reasonable input specifications result in reasonable element values. Tables have been prepared for a large variety of input specifications. A scan of these tables will quickly reveal which realizations are possible for a given type of transmission line network. An important problem arises here. Assume that certain input specifications for the coupler must be met, and a table scan shows that all such designs meeting or exceeding these specifications are unrealizable. Then the (optimum) design specification function must be degraded

in such a manner as to arrive at realizable element values. The degradation itself should be as small as possible. This problem has not been solved yet, and it is felt that an analytical solution to this problem would be very difficult to find. From a practical viewpoint, however, this problem is very important. A possible numerical solution to this problem might be obtained from a trial and error procedure contained in a computer program.